

Intergovernmental Oceanographic Commission
Workshop Report No. 171



OCEAN CIRCULATION SCIENCE DERIVED FROM THE ATLANTIC, INDIAN AND ARCTIC SEA LEVEL NETWORKS

**Organized in co-operation with the
Observatoire de Midi-Pyrénées**

Toulouse, France
10-11 May 1999

UNESCO

Intergovernmental Oceanographic Commission
Workshop Report No. 171

OCEAN CIRCULATION SCIENCE DERIVED FROM THE ATLANTIC, INDIAN AND ARCTIC SEA LEVEL NETWORKS

**Organized in co-operation with the
Observatoire de Midi-Pyrénées**

Toulouse, France
10-11 May 1999

Editor: Gary Mitchum
University of South Florida

UNESCO 2000

IOC Workshop Report No. 171
Paris, August 2000
English only

Abstract

In May of 1999 a workshop was held concerning the use of sea level data for scientific research, with an emphasis on the Atlantic and Arctic Oceans. This workshop complements earlier workshops focused on the Southern and Pacific Oceans. These workshops are intended to establish the importance of ongoing efforts to improve the global sea level database in order to support research programmes aimed at better understanding of the variability of the Earth's climate. The workshop consisted of 27 talks, all given in plenary, over 1.5 days. After the workshop, 22 papers or abstracts were collected and they comprise this report. The topics covered were wide ranging, spanning from large-scale oceanography, ENSO variations, Arctic and Antarctic sea level variability, the sea level variations of enclosed seas and the Mediterranean, the development of tsunami warning systems, coastally-trapped waves and upwelling, tides, and to the impact of space geodetic techniques on sea level measurements.

TABLE OF CONTENTS

1. INTRODUCTION	1
2. OPENING	1
3. SCIENTIFIC PRESENTATIONS	1
4. CLOSING.....	1

ANNEXES

- I. PROGRAMME OF THE WORKSHOP
- II. LIST OF PARTICIPANTS
- III. SCIENTIFIC PAPERS

LOW FREQUENCY VARIABILITY AT TIDE GAUGES: WHAT CAN WIND-FORCED MODELS EXPLAIN?

W. Sturges and B. Hong

LARGE-SCALE PHENOMENA ON INTERANNUAL TO INTERDECADAL TIME SCALES DETECTED FROM TIDE GAUGES AND ATMOSPHERIC DATA

H.-P. Plag

ENSO RELATED SEA LEVEL VARIATIONS ALONG WESTERN AUSTRALIA

M. Merrifield

COHERENCE OF BOTTOM AND SUB-SURFACE PRESSURES AROUND ANTARCTICA

P.L.Woodworth, C.W.Hughes, J.M.Vassie, R.Spencer, T. Whitworth and R.G.Peterson

SELECTION OF TIDAL CONSTITUENTS ALONG THE COASTLINES OF THE WORLD OCEAN

F. Lefèvre, C. Le Provost and F. Lyard

LONG-TERM TREND OF THE SEA LEVEL AT THE ROMANIAN LITTORAL

V. Malciu and V. Diaconu

SEA LEVEL PROPAGATING COASTAL-TRAPPED WAVES, CIRCULATION FORCING INFLUENCE ALONG CENTRAL CHILE, 1991-1995

C. Valenzuela

ON THE SEA LEVEL NETWORK AND CIRCULATION IN THE SOUTHEASTERN BRAZILIAN COAST

A. de Mesquita and J. Harari

AN EVALUATION OF THE SEA LEVEL OBSERVING NETWORK IN THE WESTERN INDIAN OCEAN

M. Odido and J. Francis

REPORT ON THE PROPOSAL FOR ESTABLISHMENT OF SEA LEVEL OBSERVING NETWORK AND STORM SURGE PREDICTION SYSTEM IN THE NORTHERN INDIAN OCEAN

S. Somasundar and B.N. Krishnamurthy

THE NEED FOR A REGIONAL SEA LEVEL DATA BASE

A. Adekoya

ATLANTIC OCEAN TSUNAMI HAZARDS: CALL FOR AN INTRA-AMERICAS SEA TSUNAMI SYSTEM

G. Maul

ELEMENTS OF A TSUNAMI WARNING SYSTEM FOR THE INTRA-AMERICAS SEA

G. Maul and D. Martin

TIDE GAUGE NETWORK IN THE REPUBLICA ORIENTAL DEL URUGUAY: CURRENT STATE AND FUTURE PERSPECTIVES

E. Forbes

A MULTI-DATA APPROACH TO ASSESS THE SPATIO-TEMPORAL VARIABILITY OF THE IVOIRO-GHANAIAAN COASTAL UPWELLING

A. Aman and H. Demarcq

SEA-LEVEL FLUCTUATIONS AS AN INDEX OF UPWELLING

G. Brundrit and H. Waldron

NON-LINEAR TIDAL ANALYSIS: TRANSFERRING ENERGY FROM THE ASTRONOMICAL TIDE TO THE MEAN SEA LEVEL

E. Marone

SEA LEVEL CHANGES IN THE BLACK SEA (1923-1997)

V. Belokopytov and Y. Goryachkin

MedGLOSS PILOT NETWORK OF SEA LEVEL MONITORING IN MEDITERRANEAN AND BLACK SEAS: PRESENT AND FUTURE ACTIVITIES

D. Rosen

ASCENSION ISLAND: A CENTRAL ATLANTIC NODE FOR SEA LEVEL AND GEODESY

P. Axe

ABSOLUTE CALIBRATION AND VERIFICATION OF MULTIPLE RADAR ALTIMETERS

C.-K. Shum, M.E. Parke and D. Martin

DENSITY AND RESIDUAL TIDAL CIRCULATION AND RELATED MEAN SEA LEVEL OF THE BARENTS SEA

S.K. Popov, G.F. Safarnov, O. Zilberstein, O.V. Tikhonova and O.A. Verbitskaya

1. INTRODUCTION

In May of 1999 a workshop was held in Toulouse, France prior to the biennial meeting of the GLOSS Group of Experts. The meeting was kindly hosted by the Centre National d'Etudes Spatiales and the Observatoire de Midi-Pyrénées with financial support from the IOC. In addition, the National Atmospheric and Oceanic Administration in the United States of America provided travel support for a number of scientists from the United States. The workshop was focused on contributions of sea level to the study of oceanic circulation and its variations.

About 50 scientists from 23 countries attended the workshop, and 27 talks were presented over 1.5 days. The detailed programme of the workshop is attached as Annex I and a list of the workshop participants is provided in Annex II. The speakers were invited to prepare papers based on their presentations, and these are attached as Annex III.

2. OPENING

The workshop opened at 0900 hours on 10 May 1999. Dr. Christian Le Provost made an opening speech on behalf of Dr. Daniel Guedalia, the Director of the Observatoire de Midi-Pyrénées (OMP), in which he welcomed the workshop participants to Toulouse and told them of the interest of the OMP, which comprises five laboratories and more than 400 people, in the topic of the workshop. Dr. Philip Woodworth, the Director of the Permanent Service for Mean Sea Level and the chair of the GLOSS Group of Experts, also made a short speech welcoming the workshop participants and reiterating the importance of the workshop to ongoing efforts to improve the global sea level database and to research programmes aimed at better understanding of the variability of the Earth's climate.

At the end of the first day presentations, the workshop participants were hosted for cocktails by the Centre National d'Etudes Spatiales (CNES). Dr. Philippe Escudier, the CNES project manager for TOPEX/Poseidon and Jason satellite altimetry missions, welcomed the participants and spoke about the exciting new possibilities in sea level science that are now possible with precision satellite altimetry.

3. SCIENTIFIC PRESENTATIONS

The opening remarks were concluded at 0930 hours, and Dr. Gary Mitchum, the workshop convenor, made a few remarks concerning the logistical arrangements for the workshop. The presentations began immediately after and continued until 1800. The presentations resumed at 0930 hours the next day, 11 May 1999.

All of the presentations were given in plenary. The topics covered were wide ranging, spanning large-scale oceanography, ENSO variations, Arctic and Antarctic variability, the variations of enclosed seas and the Mediterranean, the development of tsunami warning systems, coastally-trapped waves and upwelling, tides, as well as the impact of space geodetic techniques on sea level measurements. The materials in Annexes I and III provide a complete description of the scope of the workshop, which gives excellent examples of the vitality of sea level research in the region.

4. CLOSING

The workshop concluded at 1300 hours on 11 May 1999 with a brief thank you to the speakers and the attendees from Drs. Mitchum and Woodworth.

ANNEX I

PROGRAMME OF THE WORKSHOP

10 MAY 1999

0900 – 0930 Opening ceremony

- Opening Address by Dr. Christian Le Provost, Centre National d'Etudes Spatiales
- Welcome Address by Dr. Philip Woodworth, Permanent Service for Mean Sea Level

0930 – 1100 General Session I

- Low frequency variability at tide gauges: What can wind-forced models explain? (W. Sturges and B. Hong)
- Large-scale phenomena on interannual to interdecadal time scales detected from tide gauges and atmospheric data (H.-P. Plag)
- ENSO related sea level variations along western Australia (M. Merrifield)
- Oceanic and atmospheric circulation in the archipelago of Cape Verde (A. Barbosa)

1100 -1130 Break

1130 – 1300 General Session I (continued)

- Coherence of bottom and sub-surface pressures around Antarctica (P. Woodworth et al.)
- Selection of tidal constants from the world coastlines: Focus on the Arctic, Atlantic and Indian Oceans (F. Levebre)
- Long-term trend of the sea level at the Romanian littoral (V. Malciu and V. Diaconu)
- Sea level propagating coastal-trapped waves, circulation forcing influence along central Chile, 1991-1995 (C. Valenzuela)
- Sea level network and circulation in the southern Brazilian shelf (A. de Mesquita)

1300 – 1420 Lunch

1420 – 1610 General Session II

- An evaluation of the sea level observing network in the western Indian Ocean (M. Odido)
- Regional cooperation for establishment of sea level network and storm surge prediction system in the northern Indian Ocean (S. Krothapalli)
- The Needs for Regional Sea Level Data Base (A. Adekoya)
- Atlantic Ocean Tsunami Hazards : Call for an Intra-Americas Sea Tsunami System (G. Maul)
- Elements of a Tsunami Warning System for the Intra-Americas Sea (G. Maul and D. Martin)

- Tide Gauge Network in the Republica Oriental del Uruguay : Current State and Future Perspectives (E. Forbes)

1610 – 1630 Break

1630 – 1800 General Session II (continued)

- A multi-data approach to assess the spatio-temporal variability of the Ivoir-Ghanaian coastal upwelling (A. Aman and H. Demarcq)
- Sea-level fluctuations as an index of upwelling (G. Brundrit and H. Waldron)
- Asymptotic trend evaluation (W. Scherer, W. Mitchell and J. Chittleborough)
- Non-linear tidal analysis: transferring energy from the astronomical tide to the mean sea level (E. Marone)
- Sea level changes in the Black Sea (1923-1997) (V. Belokopytov and Y. Goryachkin)

11 MAY 1999

0930 – 1100 General Session III

- MedGLOSS pilot network of sea level monitoring in Mediterranean and Black Seas : Present and future activities (D. Rosen)
- Monitoring sea level fluctuations in the Mediterranean - Results from the SELF II project (S. Zerbini, A. Cazenave and B. Richter)
- Comparison between gravity, sea level measurements and ocean loading prediction in Brittany (M. Llubes and N. Florsch)
- Ascension Island : A central Atlantic node for sea level and geodesy (P. Axe)

1100 – 1120 Break

1120 – 1300 General Session III (continued)

- Absolute Calibration and Verification of Multiple Radar Altimeters (C.-K. Shum)
- Sea level from satellite altimetry and tide gauges, and vertical crustal motions from DORIS space geodesy system (A. Cazenave)
- Continuous GPS positioning of tide gauges: Some case studies (M. Bevis)

ANNEX II

LIST OF PARTICIPANTS

Adeleke ADEKOYA
Nigerian Institute for Oceanography
and Marine Research
P.M.B. 12729
Victoria Island
Lagos
Nigeria
Tel: +234 1 619 517
Fax: +234 1 619 517
E-mail: niomr@linkserve.com.ng

Philip AXE
CCMS Proudman Oceanographic Laboratory
Bidston Observatory
Birkenhead, Merseyside L43 7RA
United Kingdom
Tel: +44 151 653 86 33
Fax: +44 151 653 6269
E-mail: paxe@pol.ac.uk

T. F. BAKER
CCMS Proudman Oceanographic Laboratory
Bidston Observatory
Birkenhead, Merseyside L43 7RA
United Kingdom
Tel: +44 151 653 86 33
Fax: +44 151 653 6269
E-mail: tfb@pol.ac.uk

Antunio BARBOSA
Director General de Marinha e Portos
P.O. Box 7
San Vicente
Cape Verde
Tel: +238 314 342
Fax: +238 316 519/314271
E-mail: antunio@writeme.com

Victor BELOKOPYTOV
Marine Hydrophysical Institute
2 Kapitanskaya St.
Sebastopol 335000
Ukraine
E-mail: belo@omin.sebastopol.ua

Mike BEVIS
Hawaii Institute of Geophysics and
Planetology
University of Hawaii
1000 Pope Road
Honolulu
Hawaii 96822, USA
Tel: +1 808 956 7864
Fax: +1 808 956 3188
E-mail: bevis@soest.hawaii.edu

R. BINGLEY
Inst.Eng.Surveying and Sp.Geodesy
University Park
Nottingham NG7 2RD
United Kingdom
Tel: +44 115 951 3880
Fax: +44 115 951 3881
E-mail: isxrb@evn1.nott.ac.uk

Claude BOUCHER
Institut Géographique National
ENSG/LAREG
6-8 Avenue Blaise Pascal
Cite Descartes, Champs-sur-Marne
77455 Marne-la-Vallee
France
Tel: +33 1 6415 3250
Fax: +33 1 6415 3253
E-mail: boucher@ensg.ign.fr

G. B. BRUNDRIT
Dept.of Oceanography
University of Cape Town
Rondebosch 7700
South Africa
Tel: +27 21 650 3277
Fax: +27 21 650 3979
E-mail: brundrit@physci.uct.ac.za

Lic. Ernesto A. FORBES
Division Oceanografia Fisica
SOHMA
Casilla de Correos 15209
Montevideo
Uruguay
Tel: +598 2 377369
Fax: +598 2 399220
E-mail: aforbes@sohma.gov.uy
eforbes@ei.edu.uy

C. LE PROVOST
Laboratoire d'Océanographie et
de Géophysique Spatiale
GRGS/Observatoire Midi-Pyrénées
14, Avenue Edouard Belin
31400 Toulouse
France
Tel: +33 5 61 33 29 23
Fax: +33 5 61 25 32 05
E-mail: leprovos@pontos.cst.cnes.fr

Viorel MALCIU
Romanian Marine Research Institute
Bd. Mamaia 300
Constantza 8700
Romania
Fax: +40 41 83 12 74
E-mail: malciuv@alpha.rmri.ro

Eduardo MARONE
Laboratorio de Fisica Marinha
Centro de Estudos do Mar
Universidade Federal do Parana
Av. Beira mar s/n - cep 83255-000
Ponta do Sul - pr
Brazil
E-mail: maroneed@iguacu.cce.ufpr.br
maroneed@cem.ufpr.br

G. MAUL
Division of Marine & Env. Sciences
Florida Institute of Technology
150 West University Boulevard
Melbourne, Florida 32901-6988
U.S.A
Tel: +1 407 674 7453
Fax: +1 407 674 7212
E-mail: gmaul@marine.fit.edu

Mark MERRIFIELD
Dept. of Oceanography
University of Hawaii
1000 Pope Road, MSB 307
Honolulu
Hawaii 96822
USA
Tel: +1 808 956 6161
Fax: +1 808 956 2352
E-mail: markm@soest.hawaii.edu

A. R. de MESQUITA
Instituto Oceanografico
Da Universidade de Sao Paulo
Praca do Oceanografico 191
Cidade Universitaria
Sao Paulo
Brazil
Tel: +55 11 818 6564 - (home 815 0299)
Fax: +55 11 210 3092
E-mail: ardmesqu@usp.br

G. T. MITCHUM
Department of Marine Sciences
University of South Florida
140 Seventh Ave. South
St. Petersburg, FL 33701
Tel: +1 813-553-3941
E-mail: mitchum@marine.usf.edu

Ruth NEILAN
Jet Propulsion Laboratory
4800 Oak Grove Drive
Pasadena, CA 91103
U.S.A.
Tel: +1 818 354 83 30
Fax: +1 818 393 66 86
E-mail: rneilan@pop.jpl.nasa.gov

Rodrigo H. NUNEZ
Servicio Hidrografico y Oceanografico de la
Armada de Chile
P.O. Box 324
Valparaiso
Chile
Tel: +56 32 282704
Fax: +56 32 283537
E-mail: rnunez@shoa.cl

M. ODIDO
Kenya Marine & Fisheries Research Institute
P. O. Box 81651
Mombasa
Kenya
Tel: +254 11 47 1129
Fax: +254 11 47 22 15
E-mail: modido@hotmail.com

Hans-Peter PLAG
Geodetic Institute
Norwegian Mapping Authority
(Statens Kartverk)
118474),Kartverksveien
N-3500 Honefoss
Norway
Tel: +47-32-118100
Fax: +47-32-118101
E-mail: hans.peter.plag@gdiv.statkart.no

D. T. PUGH
Southampton Oceanography Centre
Empress Dock
Southampton SO14 3ZH
United Kingdom
Tel: +44 1703 59 6611
Fax: +44 1703 596 395
E-mail: d.pugh@soc.soton.ac.uk

Bernd RICHTER
IfAG
Richard-Strauss-Allee 11
D-60598 Frankfurt am Main 70
Germany
E-mail: richter@ifag.de

L. J. RICKARDS
British Oceanographic Data Centre
CCMS Proudman Oceanographic Laboratory
Bidston Observatory
Birkenhead, Merseyside L43 7RA
United Kingdom
Tel: +44 151 653 86 33
Fax: +44 151 653 6269
E-mail: ljr@pol.ac.uk

H. P. ROHDE
International Hydrographic Organization
4 Quai Antoine 1er
B.P. 445
MC 98011 Monaco Cedex
Principality of Monaco
Tel: +377 93 10 81 00
Fax: +377 93 10 81 40
E-mail: pah@ihb.mc

Dov. S. ROSEN
Israel Oceanographic and
Limnological Research Ltd.
Tel Shikmona, P.O.B. 8030,
Haifa 31080
Israel
Tel: +972 485 15202
Fax: +972 48511911
E-mail: rosen@ocean.org.il

W. SCHERER
National Tidal Facility
Flinders University
GPO Box 2100
Adelaide
South Australia 5001
Tel: +61 8201 7524
Fax: +61 8201 7523
E-mail: wscherer@pacific.ntf.flinders.edu.au

C. K. SHUM
Civil and Environmental Engineering
and Geodetic Science
Ohio State University
2070 Neil Avenue
Colombus, Ohio 43210
U.S.A

K. SOMASUNDAR
Dept of Ocean Development, GOI
Mahasagar Bharan, Block 12, GCO Complex
Lodi Rad
New Delhi-110 003
India
Fax: +91 11 4360 336

Vladimir UDOVIK
Marine Hydrophysical Institute
2 Kapitanskaya St.
Sebastopol 335000
Ukraine
Fax: +380 692 444 253
E-mail: vaivanov@alpha.mhi.iuf.net

Javier A. VALLADARES
Armada Argentina
Servicio de Hidrografia Naval
Av. Montes de Oca 2124
Buenos Aires 1271
Argentina
Tel: +54 1 301 2918
Fax: +54 1 301 3883
E-mail: shn@oceanar.mil.ar

M. L. VIANNA
MCT/INPE
Av. Dos Astronautas 1758
C. Postal 5/5
12201 - Sao Jose dos Campos
SP - Brasil
E-mail: mvianna@ltid.inpe.br

Philip L. WOODWORTH (Chairman)
Proudman Oceanographic Laboratory
Bidston Observatory
Birkenhead, Merseyside L43 7RA
United Kingdom
Tel: +44 151 653 86 33
Fax: +44 151 653 6269
E-mail: plw@pol.ac.uk

Susanna ZERBINI
Dept. of Physics
University of Bologna
Viale Bertini Pichat, 8
40127 Bologna
Italy
Tel: +39 51 118 100 (direct 118474)
Fax: +39 51 250 106
E-mail: zerbini@astbo1.bo.cnr.it

Serge ALLAIN
SHOM
Brest (France)
E-mail: allain@shom.fr

Cécile CABANES
CNES/GRGS
Toulouse (France)
E-mail: cabanes@cst.pontos.cnes.fr

A. CAZENAVE
CNES/GRGS
Toulouse (France)
E-mail: anny.cazenave@cnes.fr

Kien DOMINH
LEGOS
Toulouse (France)
E-mail: kien.dominh@cnes.fr

Nicolas FLORSCH
CLDG
La Rochelle (France)
E-mail: nflorsch@univ-lr.fr

Fabrice HERNANDEZ
CLS/DOS
31526 Ramonville St Agne (France)
E-mail: fabrice.hernandez@cls.fr

Fabien LEFEVRE
LEGOS
Toulouse (France)
E-mail: Fabien.lefevre@cnes.fr

Muriel LLUBES
CLDG
La Rochelle (France)
E-mail: mllubes@univ-lr.fr

Sylvain MANGIAROTTI
LEGOS
Toulouse (France)
E-mail: mangia@cst.pontos.cnes.fr

Benjamin MARTINEZ
Universitat politecnica de Catalunya
08034 Barcelona
Spain
E-mail: benjamin@etseccpb.upc.es

Yves MENARD
CNES
Toulouse (France)
E-mail: yves.menard@cnes.fr

Francis OLIVIER
Observatoire Royal de Belgique
E-mail: Francis@oma.be

Delphine ORSEAU
University of La Rochelle
E-mail: dorseau@univ-lr.fr

Frédérique PONCHAUT
LEGOS-OMP
14, avenue Ed. Belin 31400
Toulouse (France)
E-mail: ponchaut@pontos.cst.cnes.fr

IOC SECRETARIAT

Thorkild AARUP
IOC, UNESCO
1 rue Miollis
75732 Paris Cedex 15
France
Tel: +33 1 45 68 40 19
Fax: +33 1 45 68 58 12
E-mail: t.aarup@unesco.org

ANNEX III

SCIENTIFIC PAPERS

	Page
LOW FREQUENCY VARIABILITY AT TIDE GAUGES: WHAT CAN WIND-FORCED MODELS EXPLAIN? <i>W. Sturges and B. Hong</i>	3
LARGE-SCALE PHENOMENA ON INTERANNUAL TO INTERDECADAL TIME SCALES DETECTED FROM TIDE GAUGES AND ATMOSPHERIC DATA <i>H.-P. Plag</i>	4
ENSO RELATED SEA LEVEL VARIATIONS ALONG WESTERN AUSTRALIA <i>M. Merrifield</i>	9
COHERENCE OF BOTTOM AND SUB-SURFACE PRESSURES AROUND ANTARCTICA <i>P.L.Woodworth, C.W.Hughes, J.M.Vassie, R.Spencer, T.Whitworth and R.G.Peterson</i>	10
SELECTION OF TIDAL CONSTITUENTS ALONG THE COASTLINES OF THE WORLD OCEAN <i>F. Levèvre, C. Le Provost and F. Lyard</i>	14
LONG-TERM TREND OF THE SEA LEVEL AT THE ROMANIAN LITTORAL <i>V. Malciu and V. Diaconu</i>	21
SEA LEVEL PROPAGATING COASTAL-TRAPPED WAVES, CIRCULATION FORCING INFLUENCE ALONG CENTRAL CHILE, 1991-1995 <i>C. Valenzuela</i>	28
ON THE SEA LEVEL NETWORK AND CIRCULATION IN THE SOUTHEASTERN BRAZILIAN COAST <i>A. de Mesquita and J. Harari</i>	34
AN EVALUATION OF THE SEA LEVEL OBSERVING NETWORK IN THE WESTERN INDIAN OCEAN <i>M. Odido and J. Francis</i>	52

REPORT ON THE PROPOSAL FOR ESTABLISHMENT OF SEA LEVEL OBSERVING NETWORK AND STORM SURGE PREDICTION SYSTEM IN THE NORTHERN INDIAN OCEAN	62
<i>S. Somasundar and B.N. Krishnamurthy</i>	
THE NEED FOR A REGIONAL SEA LEVEL DATA BASE	69
<i>A. Adekoya</i>	
ATLANTIC OCEAN TSUNAMI HAZARDS : CALL FOR AN INTRA-AMERICAS SEA TSUNAMI SYSTEM	70
<i>G. Maul</i>	
ELEMENTS OF A TSUNAMI WARNING SYSTEM FOR THE INTRA-AMERICAS SEA	71
<i>G. Maul and D. Martin</i>	
TIDE GAUGE NETWORK IN THE REPUBLICA ORIENTAL DEL URUGUAY : CURRENT STATE AND FUTURE PERSPECTIVES	72
<i>E. Forbes</i>	
A MULTI-DATA APPROACH TO ASSESS THE SPATIO- TEMPORAL VARIABILITY OF THE IVOIRO-GHANAIAN COASTAL UPWELLING	76
<i>A. Aman and H. Demarcq</i>	
SEA-LEVEL FLUCTUATIONS AS AN INDEX OF UPWELLING	81
<i>G. Brundrit and H. Waldron</i>	
NON-LINEAR TIDAL ANALYSIS: TRANSFERRING ENERGY FROM THE ASTRONOMICAL TIDE TO THE MEAN SEA LEVEL	82
<i>E. Marone</i>	
SEA LEVEL CHANGES IN THE BLACK SEA (1923-1997)	88
<i>V. Belokopytov and Y. Goryachkin</i>	
MedGLOSS PILOT NETWORK OF SEA LEVEL MONITORING IN MEDITERRANEAN AND BLACK SEAS : PRESENT AND FUTURE ACTIVITIES	93
<i>D. Rosen</i>	
ASCENSION ISLAND : A CENTRAL ATLANTIC NODE FOR SEA LEVEL AND GEODESY	97
<i>P. Axe</i>	
ABSOLUTE CALIBRATION AND VERIFICATION OF MULTIPLE RADAR ALTIMETERS	102
<i>C.-K. Shum, M.E. Parke and D. Martin</i>	
DENSITY AND RESIDUAL TIDAL CIRCULATION AND RELATED MEAN SEA LEVEL OF THE BARENTS SEA	106
<i>S.K. Popov, G.F. Safarnov, O. Zilberstein, O.V. Tikhonova and O.A. Verbitskaya</i>	

**Low frequency variability at tide gauges:
What can wind-forced models explain?**

*W. Sturges and B. Hong
Department of Oceanography
Florida State University
Tallahassee FL 32306 USA*

This talk deals with the application of historical tide gauge data in dealing with long-period oceanographic questions. Two issues that are particularly relevant are (a) variations in the transport of boundary currents such as the Gulf Stream and (b) the rise of sea level problem. At long-term tide gauges, a surprising amount of power is found at periods of order 100-200 months. The fluctuations in this frequency band are particularly troublesome when we are forced to deal with the problem of changes in the rate of sea level rise.

We have found that these fluctuations, at the latitudes of the United States east coast and at periods longer than a few years, are driven by the large-scale wind forcing over the mid-latitude oceans. The signals have peak-to-peak amplitudes of nearly 20 cm, which is the same as the sea-level rise over a century.

We have used a relatively simple, wind-forced, linear numerical model. It is continuously stratified and uses a vertical mode decomposition in which (it turns out that) the first two modes contain all the useful information. The model is forced with COADS winds filtered to remove power at periods shorter than 3 years. When the model output is compared with open ocean tide gauges, such as at Bermuda, the agreement is remarkably good. We then take the output of this model on the offshore side of the Gulf Stream as input to a simple coastal model. The fluctuations in sea level, such as observed along the U.S. east coast, are modeled quite well; roughly 90% of the variance is explained with no free parameters. The ocean's response to this wind forcing appears to be contained within the main thermocline, down to depths of approximately 2000 m. There are obviously many low-frequency fluctuations in the ocean below 2000 m, but they do not appear to contribute to the decadal scale fluctuations in sea level at mid latitudes.

**Large-scale phenomena on interannual to interdecadal time scales detected
from tide gauges and atmospheric data**

H.-P. Plag
Norwegian Mapping Authority
Kartverksveien, N-351
Hønefoss, Norway

Climate variability at decadal to interdecadal time scales may, to a significant part, be associated with variations in the global atmospheric circulation pattern. Interannual to multidecadal sea-level variations at these time scales are partly resulting from mechanical forcing of the atmosphere. Consequently, changes in the atmospheric circulation pattern are recorded in the sea level. Coastal relative sea level (RSL) acts as a low-pass filter of the forcing and therefore it is particularly sensitive to variations of the forcing on longer time scales.

The global data set of monthly mean RSL data available at the Permanent Service for Mean Sea-Level (PSMSL) provides a basis to study the decadal variability of coastal RSL in relation to atmospheric parameters over nearly the last one hundred years. In the present study, the patterns or "finger-prints" found in the RSL data are compared to similar patterns in atmospheric parameters (in particular, air pressure). Global data sets of monthly means of relevant parameters such as air pressure, temperature, precipitation and sea level, covering the last up to 200 years are generally biased towards the Northern Hemisphere and towards recent decades. The best data coverage with long records is found on both sides of the North Atlantic (see Figure 1). Therefore, the analyses reported here are mainly restricted to these regions. The time scales considered are interdecadal time scales and the seasonal cycle.

Climate variability at decadal to interdecadal time scales can be expected to introduce long-period modulations of the seasonal cycle in climatological parameters with characteristic spatial patterns (Plag and Tsimplis, 1999). Sequences of geographic maps of the seasonal cycle are constructed for subsequent time intervals for the different parameters (see Plag and Tsimplis, 1999, for a detailed description of the methodology). These maps reveal distinctive spatial variations of the seasonal cycle. For example, in North Atlantic air pressure the transitions from land to ocean are characterised at the western boundary by smooth variations of the seasonal cycle and at the eastern boundary by phase changes of 180 degrees over a narrow (~100 km wide) zone following approximately the coast line. For each investigated parameter, significant temporal variations of the seasonal cycle are found in both amplitude and phase. These variations are spatially coherent with the largest temporal changes generally close to the boundaries of climate domains. For example, in air pressure the largest variations are found close to the narrow transition, one at the eastern boundary of the North Atlantic. However, detecting temporal variations in such small-scale spatial patterns of the seasonal cycle requires climatological data sets with high spatial resolution.

To derive spatial patterns of interdecadal variations, the time series are low-pass filtered. Due to the presence of gaps in all time series, integration over time is used to strongly reduce shorter period variations. Thus, for each time series $x(t)$, we consider the function

$$y(t) = \int_0^t r(t') dt' \quad (1)$$

where $r(t)$ is the residual after the seasonal cycle and a linear trend have been removed; i.e.,

$$r(t) = x(t) - [A_{Sa} \sin(\omega_{Sa} * t - \phi_{Sa}) + A_{Ssa} \sin(\omega_{Ssa} * t - \phi_{Ssa}) + a + bt] \quad (2)$$

Here, S_a and S_{sa} denote the annual and semiannual harmonic constituents, respectively. The parameters A_{S_a} , ϕ_{S_a} , $A_{S_{sa}}$, $\phi_{S_{sa}}$, a and b are determined in a least squares fit to $x(t)$.

Auto- and cross-correlation functions of these y -functions are used to describe a spatial pattern. Auto-correlation functions of the long RSL records show a high spatial coherency for both the European and the East coast of North America, indicating an 80 year-scale variation. Cross-basin correlation reveals a clear anti-correlation of this long-period variation (see Figure 2). Without further evidence, this pattern might be interpreted as a slow east-west oscillation in RSL.

However, it has to be noted that all long RSL records available from the East coast of North America originate from stations further south than most of the European stations. In fact, all of them have latitudes lower than the Netherlands. The only European station at a comparable latitude is Cascais, and for Cascais we find a good correlation with (for example) New York with only a small time lag of approximately 8 years. Thus, the pattern may also be explained as a slow north-south oscillation.

In air pressure records, the same long-period oscillation is found and a similar spatial pattern is revealed (see Figure 3). Spatial coherency is found for all stations at latitudes higher than Vienna and also for those at lower latitudes. There is a clear anti-correlation in the air pressure of these north and south regions. For both regions, air pressure appears to be anti-correlated with sea level, which is in agreement with an inverted barometer response of sea level to air pressure variations.

Taking into account the definition of $y(t)$, a periodic variation in the original time series will have the form

$$\int a \sin \omega t dt = (a / \omega)(1 - \cos(\omega t)). \quad (3)$$

Therefore, we can interpret the results shown in Figure 2 as a variation with an amplitude of the order of 40 mm. For air pressure in Europe, we find a similar oscillation with an amplitude of 1 to 2 hPa. Assuming an inverted barometer response, then the variation in air pressure could explain about 50 % of the variation found in RSL.

The results presented here indicate the presence of a slow north-south variation in air pressure and sea-level at a time scale of approximately 80 years. It is speculated that this oscillation is related to a variation in temperature on a similar time scale as described in Schlesinger and Ramakutty (1994).

References

- H.-P. Plag and N.M. Tsimplis. Temporal variability of the seasonal sea-level cycle in the North Sea and Baltic Sea in relation to climate variability. *Global and Planetary Change*, **20**:173-203, 1999.
- M. E. Schlesinger and N. Ramakutty. An oscillation in the global climate system of 65-70 years. *Nature*, **367**:723-726, 1994.
- N. E. Spencer and P. L. Woodworth. Data holdings of the Permanent Service for Mean Sea Level. Technical report, Permanent Service for Mean Sea Level, Bidston, UK, 1993. 81pp.

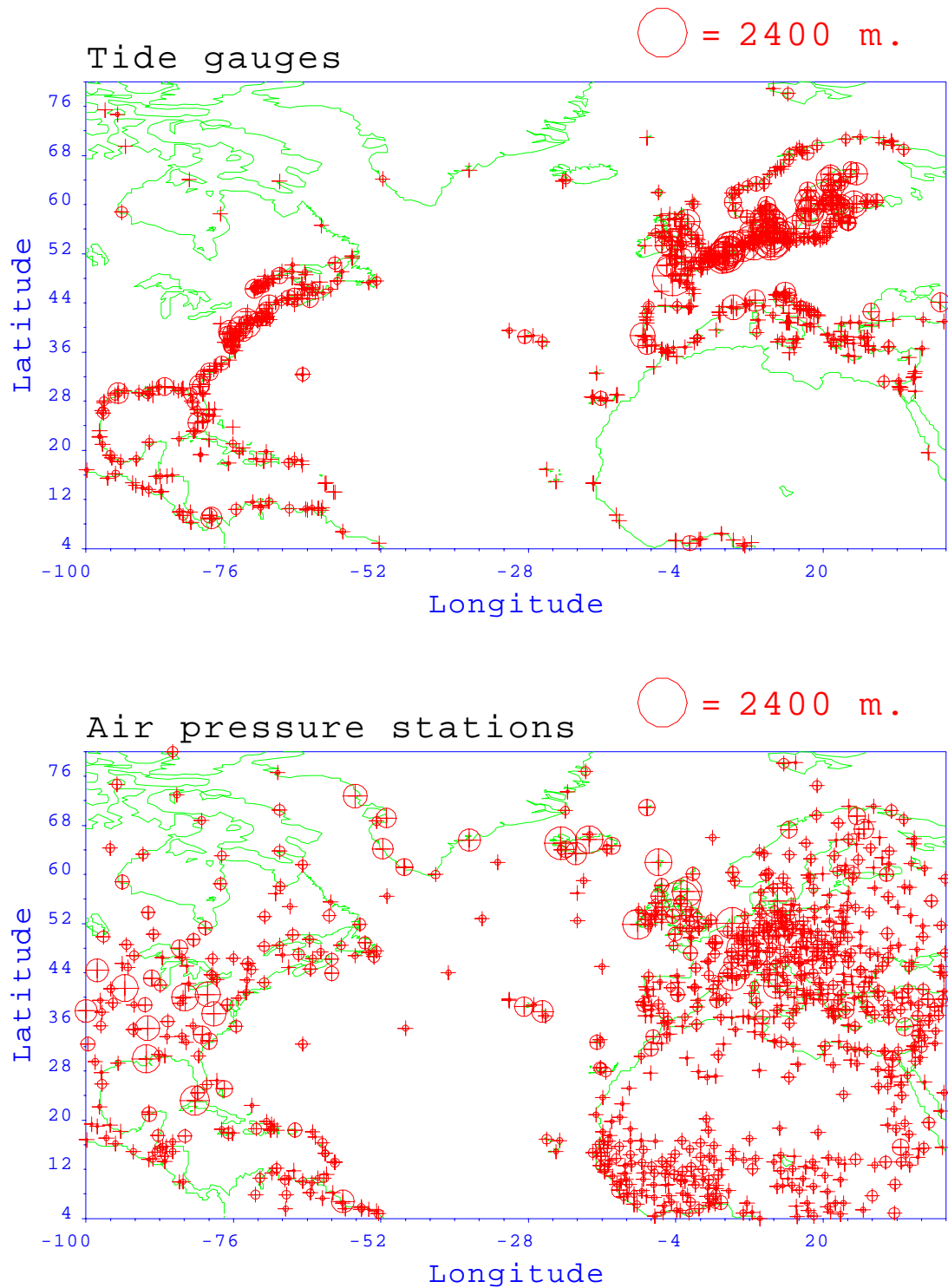


Figure 1: Location of time series. Upper diagram: RSL; Permanent Service for Mean Sea Level data base (Spencer and Woodworth, 1993). Lower diagram: Air pressure; The Global Historical Climatology Network, Carbon Dioxide Information Analysis Center. Note that the size of the circles at each station is proportional to the length of the time series in months.

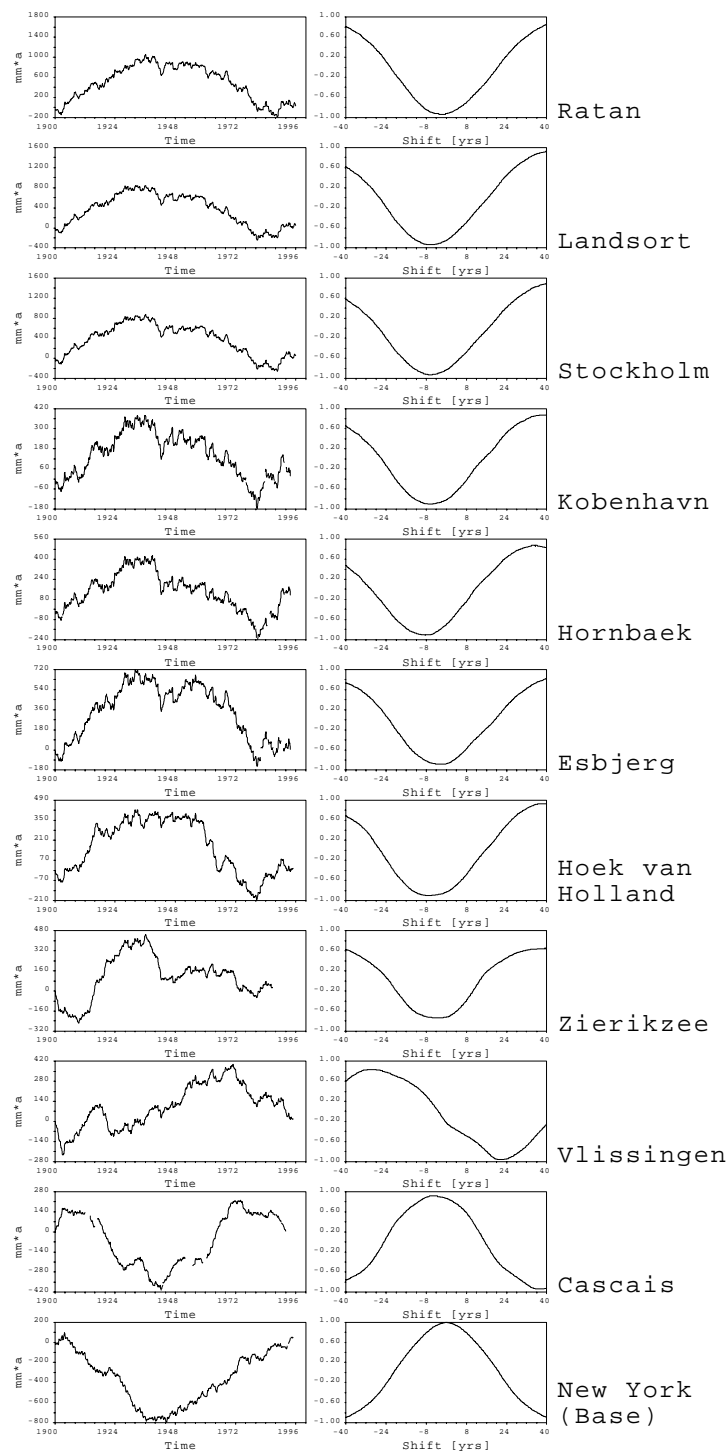


Figure 2: Cross-correlation of RSL time series. Left column: RSL function as defined in eq. 1 for New York and several European stations. European stations are sorted according to latitude with high latitudes on top. Note the high degree of coherency for all series north of Zierikzee. A similar picture is found for stations on the East coast of North America. Right column: Cross-correlation of the RSL function for the European stations with the RSL function for New York. Note that all European stations except for Cascais are anti-correlated with New York. The anti-correlation is found for all other long records from the East coast of North America.

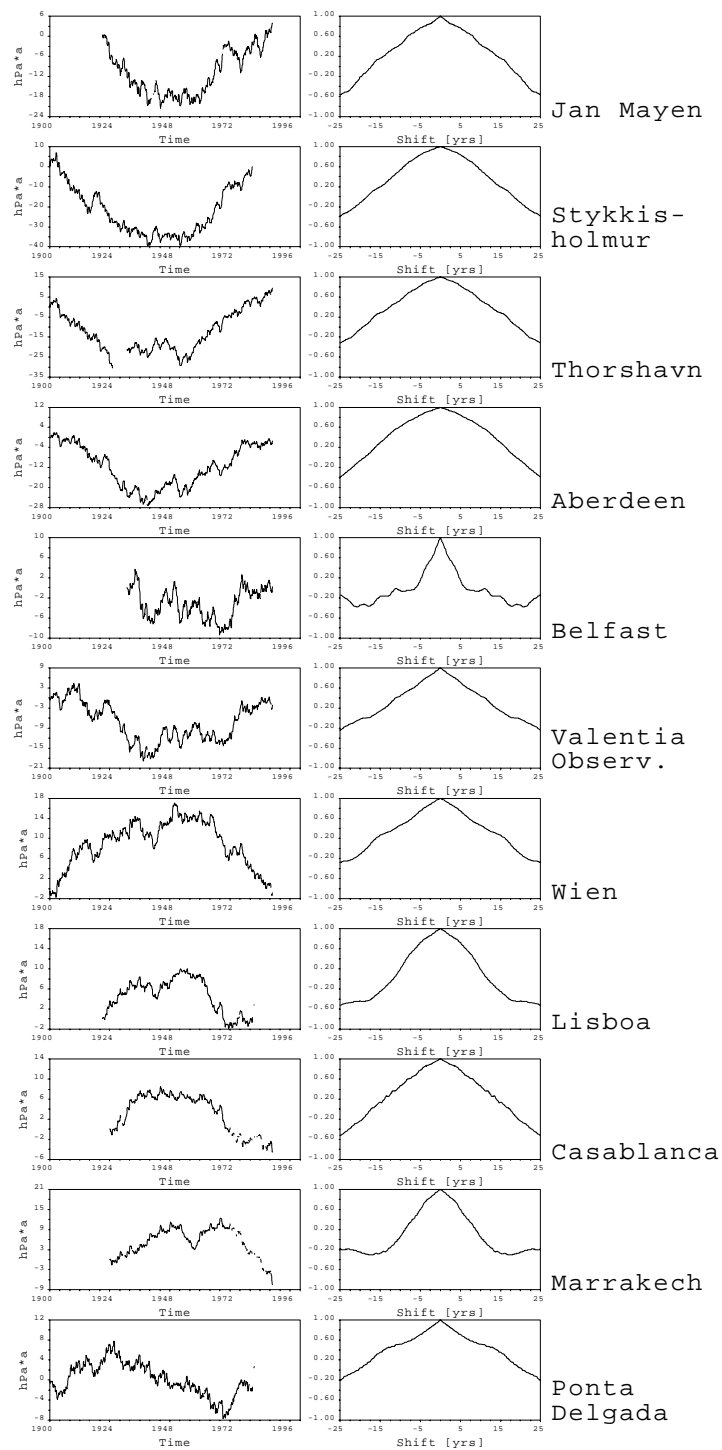


Figure 3: Auto-correlation of air pressure time series. Left column: Air pressure function as defined in eq. 1 for several European stations. Stations are sorted according to latitude with high latitudes on top. Note the high degree of coherency for all series north of Viena (Wien). Right column: Auto-correlation of the air pressure function.

ENSO related sea level variations along western Australia

M. Merrifield
Department of Oceanography
University of Hawaii at Manoa
Honolulu, HI 96822 USA

A combination of tide gauge and Topex-Poseidon altimeter data are used to examine ENSO-related sea surface height (SSH) variability that extends southward from Indonesia along the west coast of Australia. Previous analyses of Australian tide gauge records have documented the occurrence of ENSO variability, particularly along the southern coast (Bye and Gordon, 1982; Pariwono et al., 1986). Here, we examine the propagation characteristics and offshore structure of this signal as seen in the altimeter data. A statistically significant correlation (95% confidence level) is found between the Southern Oscillation Index (SOI), or equivalently the dominant Pacific tide gauge empirical orthogonal mode, and SSH across the wide (400 km) northwest Australian coast. SSH anomalies during the 1997-98 ENSO are 10 cm below normal. The time lag of maximum correlation indicates an alongshelf poleward phase speed of approximately 0.2 m/s, an order of magnitude slower than the fastest baroclinic coastal-trapped wave mode. This slow phase speed cannot be attributed to local wind forcing which shows a poor correspondence with ENSO variations in this region. A regression analysis between the SOI and altimeter SSH shows that the offshore structure of this interannual signal is nearly uniform in amplitude across the wide northwest shelf with offshore decay beginning at the shelf break, indicating that associated geostrophic currents are negligible over the shelf. In addition, regression values in the deep ocean just off the northwest shelf are much larger than expected for a coastally trapped feature, suggesting that energy leakage into Rossby waves is significant. Unresolved issues at this preliminary stage include the extent to which interannual variations in shelf slope currents and isotherm displacements along the west coast of Australia are related to ENSO, the nature of the slow alongshelf phase progression (which was also noted by Pariwono et al. (1986) who saw little evidence of propagation), and the degree to which coastal-trapping occurs at these low frequencies and latitudes.

Bye, J. A. T., and A. H. Gordon, 1982. Speculated cause of interhemispheric oceanic oscillation, *Nature*, **296**, 52-54.

Pariwono, J. I., J. A. T. Bye, and G. W. Lennon, 1986. Long-period variations of sea-level in Australasia, *Geophys. J. R. Astr. Soc.*, **87**, 43-54.

Coherence of bottom and sub-surface pressures around Antarctica

P.L.Woodworth, C.W.Hughes, J.M.Vassie and R.Spencer
Proudman Oceanographic Laboratory
Bidston Observatory, Birkenhead, Merseyside L43 7RA, U.K.

T.Whitworth, R.G. Peterson
U.S. Groups

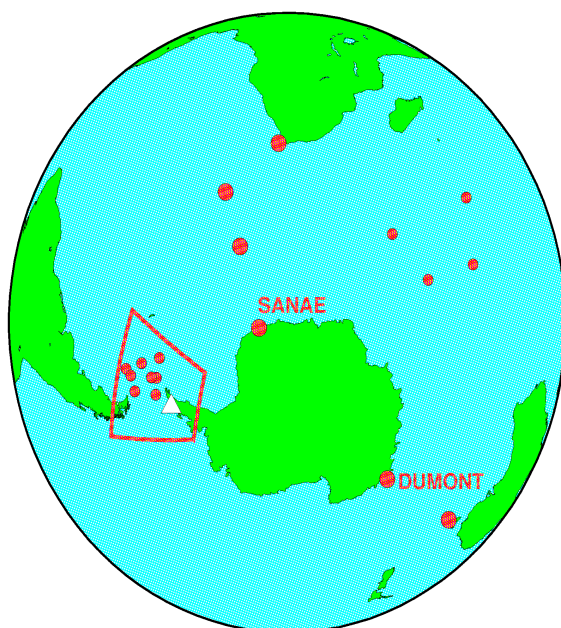
Measurement Programme

Since the late 1980s, the Proudman Oceanographic Laboratory (POL) and Texas A&M University have deployed bottom pressure recorders (BPRs) either side of, and in the middle of, the Antarctic Circumpolar Current (ACC) ‘choke points’ at the Drake Passage and south of South Africa and Australia. POL and French groups have deployed recorders in the Indian Ocean. The object has been to provide information for the World Ocean Circulation Experiment (WOCE) on transport variability for comparison to that obtained from coastal tide gauges, satellite altimetry and numerical models. The maps below show the main locations at which bottom pressure recorders have been deployed for WOCE ACC choke point measurements. Larger circles indicate US deployments.

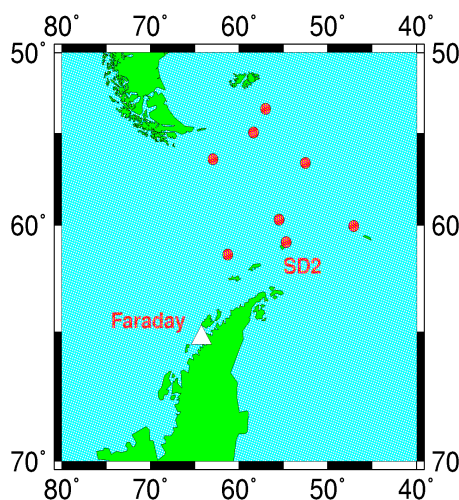
For example, the Multi Year Return Time Level Equipment (MYRTLE) bottom pressure instrument employed by POL in the Drake Passage can be deployed on the sea bed for up to five years (see Spencer and Vassie, *Progress in Oceanography*, Volume 40, 423-435, 1997).

Some Findings of Antarctic Coherence

WOCE ACC Choke Point BPR Positions



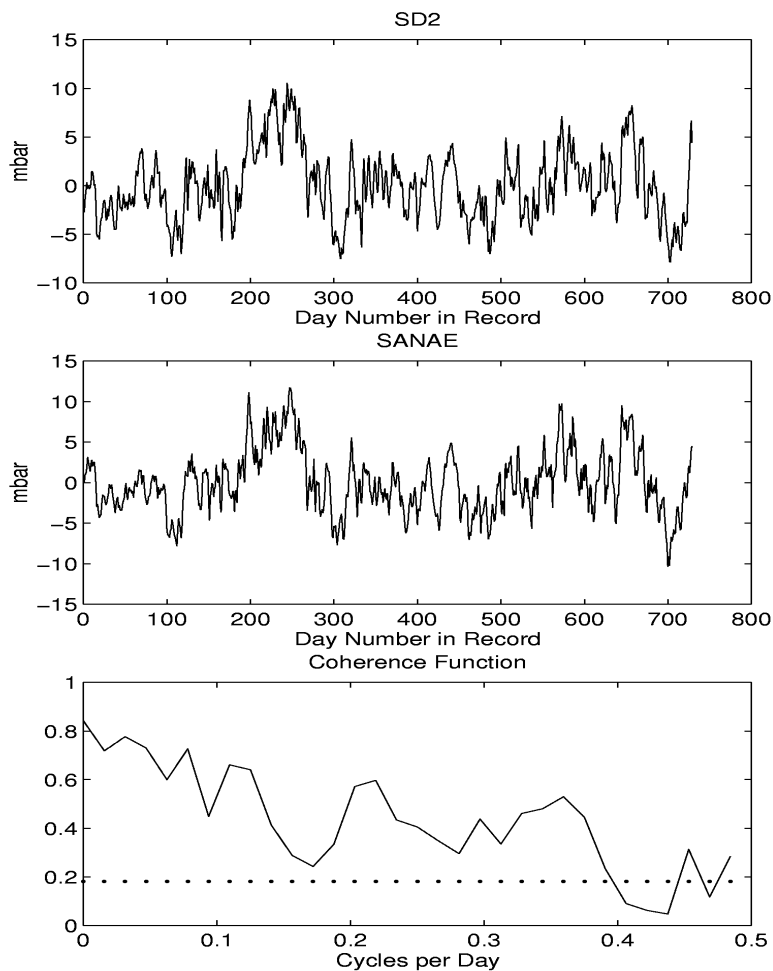
Drake Passage Deployments



This short note presents some of the recent findings from the BPR deployments and from the Faraday tide gauge. One significant feature observed is that large-scale coherence at the several mbar (cm) level does appear to exist between BPR sites and gauges many 1000s of kilometres apart from low frequencies (e.g. annual) to timescales of order 10 days, as suggested by ocean model results. Model results (FRAM and POCM models) also demonstrate coherence between transports and bottom pressures, suggesting a method of measuring proxy-ACC transports in future. The data analysis is continuing, but so far the signals appear to be larger in the real data than those suggested by POCM or FRAM.

For example, the figure below demonstrates the coherence observed between simultaneous 2-year time series from the SD2 BPR at the Drake Passage and from the SANAE BPR (see maps).

Another example demonstrating the large scale Antarctic coherence between simultaneous 2-year time series from the SANAE BPR and DUMONT BPR can be found by inspecting the web page: <http://www.pol.ac.uk/gslc/woceposter2/antcoher.html>



The transfer functions between sets of data in both of the above examples are approximately 1 with roughly zero phase lag across the frequency range shown.

Ongoing BPR deployments will continue to be required beyond WOCE, in order to acquire an extended time series of ACC transport, aided by the constant improvement in technology (e.g. via the use of air-launched ‘expendable’ BPRs). In addition, the availability and suitability of data from the Antarctic coastal sites (e.g. Faraday/Vernadsky, Syowa, Mawson, Dumont d'Urville and several other sites) suggest that they might be appropriate data sources of ACC variability, although perhaps containing a greater degree of near-coastal local ‘noise’.

Time series of Sub-Surface Pressure (SSP = sea level + air pressure load) at the Faraday (now Vernadsky) tide gauge station have previously been shown to be coherent with BPR signals in the southern Drake Passage (Peterson, *Journal of Geophysical Research*, 93 (C10), 12439-12448, 1988) with larger signals observed in the Faraday data than in the BP values.

Faraday/Vernadsky has the longest tide gauge record in Antarctica (1958 onwards) and it would be ideal if (i) its record could be maintained into the future, and (ii) if its SSP time series could be shown to measure similar signals to those from the BP recorders around Antarctica, and (iii) if those signals indeed are of use in providing a measure of ACC transport variability. For example, the figure below demonstrates the coherence observed between simultaneous 2-year time series of SSP from Faraday and of BP from the SANAE BPR.

Another example, which can be seen on the above web page, demonstrates the coherence observed between simultaneous 2-year time series of SSP from Faraday and of BP from the DUMONT BPR.

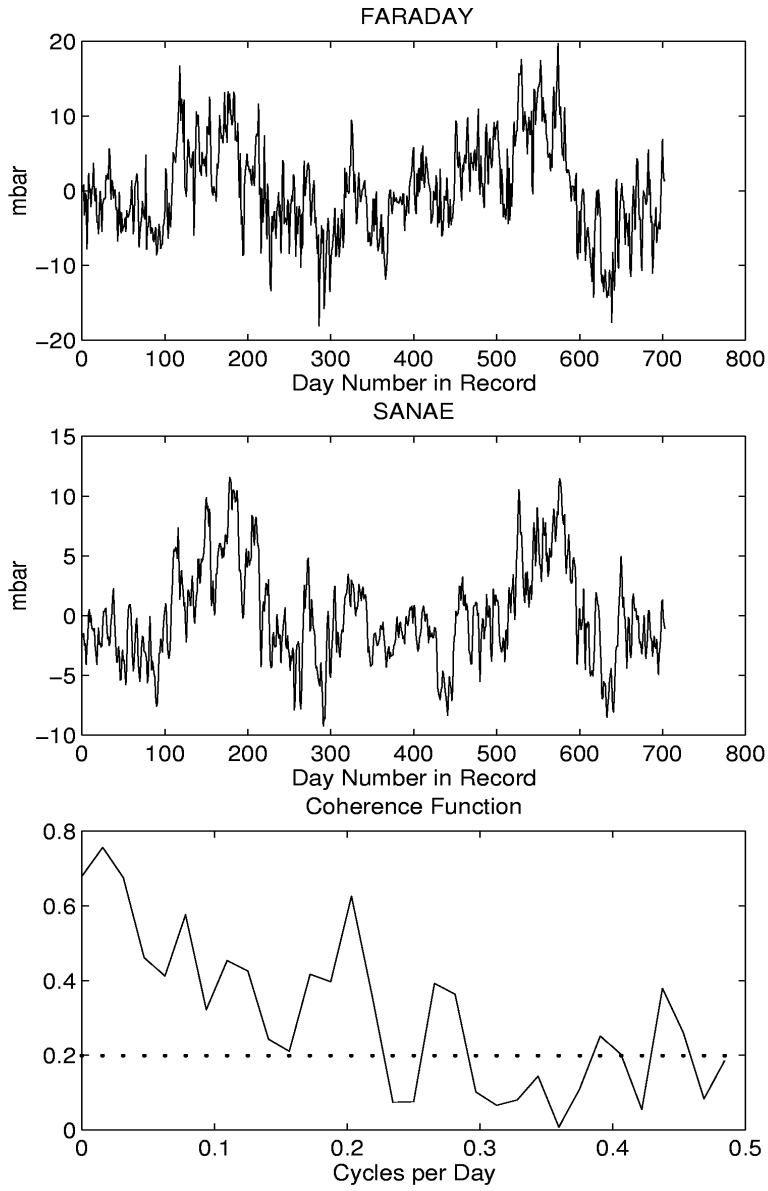
Transfer functions between these sets of data are less than 1, reflecting the larger signals in the Faraday data, with roughly zero phase lag across the frequency range shown.

These examples demonstrate that the continued development of the GLOSS tide gauge network in this part of the world is essential if Antarctic sea level is indeed to prove to be valuable for monitor ocean circulation in the Southern Ocean.

Conclusions

In order to study these kinds of signals in more detail, around the entire Antarctic continent, and over the long term, GLOSS must be developed and maintained in the region. We propose that a subset of coastal stations consisting of, for example, Faraday/Vernadsky, Signy, Syowa, Mawson, Davis, Casey, Dumont D'Urville and Cape Roberts be equipped with tide gauges and/or SSP sensors in addition to the programme of BPR measurements.

The GLOSS Southern Ocean data centre collects and publicises Southern Ocean data (<http://www.ntf.flinders.edu>).



Selection of tidal constituents along the coastlines of the world ocean

*F. Lefèvre, C. Le Provost and F. Lyard
LEGOS, CNES/CNRS/UPS
14, av. E. Belin 31400
Toulouse – France*

INTRODUCTION

The new tide models recently made available to the scientific community, most of them issued from the analysis of satellite altimeter data (TOPEX / POSEIDON and ERS1/2), have shown major improvements by reference to the previous global ocean tide models published in the literature. Over the deep oceans, these new models have reached a high level of accuracy. Indeed, lots of them are very similar (within one centimetre RMS difference, [Shum et al., 1997]). But large differences between these models have been observed over continental shelves and along coastlines, of the order of ten centimetres.

The evaluation of the quality of any global ocean tide model over shallow water areas is a difficult task, because of the complexity of the tidal characteristics over shelves and coastal basins. There, the typical wavelengths are shorter. Regional amplifications, often due to local resonance, result in sharp gradients that are difficult to catch in the models. Besides non-linearities are taking place, which lead to more complex tidal spectra than over the deep oceans. A dedicated effort has been undertaken to build a reference database of harmonic constituents along the coastlines of the world ocean, with the aim to serve as a reference for testing the accuracy of the available or future tidal models over continental shelves and shallow water areas, in the same way as it was done for evaluating the quality of these models over the open ocean ([Cartwright and Ray, 1991; Le Provost, 1994; Shum et al., 1997]).

The reference database basically uses the enormous amount of coastal data available in the International Hydrographic Organisation databank [IHO, 1979]: about 4000 tide gauge harmonic data set. The method followed to select a subset of stations uniformly distributed along the coastlines is based on a careful evaluation of the intrinsic quality of the data, their spatial coherency, and their level of agreement with the ocean tide models themselves.

A first selection of 727 stations is proposed, including at most 41 constituents (8 long period, 12 diurnal, 10 semi-diurnal, 1 ter-diurnal, 5 quarter-diurnal, 5 six-diurnal). By reference to our last global ocean tide solution FES98 [Lefèvre et al., 1999], an estimate of the overall global accuracy (including 8 of the major constituents of the tidal spectrum) of the new generation of tidal models is 7.8 cm.

However difficulties remain to be solved. The main needs for setting a more complete and better qualified “sea truth database”, are:

1. to collect all the available data not in the IHO bank,
2. to get a set of more complete harmonic constituents for each of the stations,
3. to compute not only the harmonic constituents, but also the error bars to be associated with these harmonic constituent data sets.

A COASTAL TIDE GAUGES DATABANK: ST727

Selection of the coastlines

In order to facilitate the selection of the tide gauge data included in the IHO data base, we have distributed them along the coastlines of the six oceans:

1. the Atlantic Ocean;
2. the Indian Ocean;
3. the Pacific Ocean;
4. the Antarctic Ocean;
5. the Arctic Seas;
6. Mediterranean Sea

Also, to avoid very long coastlines (about 10,000 km), they have been divided into 26 segments, allowing an easier visualisation of the distribution and regional properties of the tidal characteristics. Besides, these segments were selected so that the tides that occur along these coastlines are quite homogeneous, with variances of the same order. The distribution of these 26 segments is given in Figure 1. Coastlines were digitalised with elementary steps 5 to 20 km long, which allow to localise the tide gauge positions with a curvilinear abscissa.

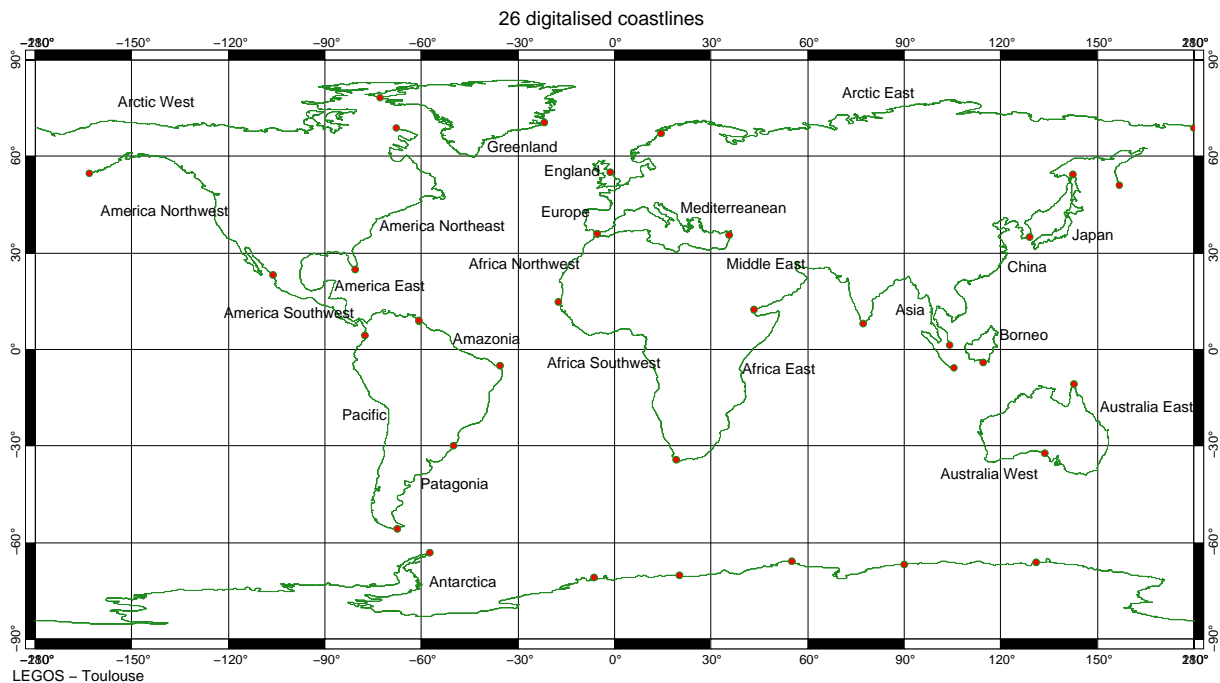


Figure 1: Coastlines selection
IHO database

The tide gauges were extracted from the 3985 IHO tide gauge database. 727 of them were selected to build the databank (hereinafter called ST727 databank) thanks to criteria presented in the following.

SELECTION OF THE ST727 DATABANK

Spatial coherence

Several criteria based on the tide gauge locations were applied to select them or not. First of all, they were dismissed if located far from the digitalised coastline (till 10 km). Then, they were dismissed too if located:

- in a small bay (of lower size than the local increment of the digitalised coastlines),
- in an estuary,
- on the coastal side of an island too close to the coast itself,
- in a river mouth.

This selection acts to exclude tide gauges which measure local phenomena such as resonance, long slacks and extreme non-linear effects. Tide gauges names were also very helpful in providing information on the localisation of IHO tide gauges.

Lastly, only one of several very close or co-located stations was selected. Generally, the tide gauge data set with the longest record was kept.

Selection compared to CSR3.0 and FES94.1 tide models

The IHO database is based on various origins. Measurements date from the last century till the present, and the harmonic decomposition calculations were done with many different algorithms and by different people. This is the reason why the IHO database is not homogeneous in quality. In order to get some homogeneity, we have chosen to refer to two global tide models: CSR3.0 and FES94.1, and to eliminate stations with harmonic constituents too far from the ones given by these model solutions. The scientific community considered CSR3.0 [Eanes and Bettadpur, 1996] as the best altimetric global tide model and FES94.1 [Le Provost et al., 1994] as the best hydrodynamic global tide model. These two models are based on two very different methods. Even if CSR3.0 used FES94.1 as first guess, these two models can be considered as complementary to give a good estimation of modelled tides along the coasts.

Indeed, this criterion of selection is controversial. For stations in disagreement with the models, are the tide gauge measurements and the harmonic decomposition not accurate enough? Or, are the tide models not accurate? The answer needs further investigation. So, for these cases, we have made the choice to dismiss the tide gauge, but this selection must be considered a first step. Borneo and Patagonia are typical areas where some tide gauges were dismissed because of their great differences with the two tide models. For these areas, further investigations are definitively needed, hopefully with recent hourly records.

The selected tide gauge dataset

From the initial 3985 IHO tide gauges, and following the above rational, a 727 tide gauge databank was built. Figure 2 shows the spatial distribution of these 727 selected tide gauges. The distribution is good enough to consider that the main coastlines of the world are studied. However, a lot of islands and areas with sparse tide gauges data are not included in this selection (such as Malaysian seas) because of the initial aim has been to consider the coasts of the continent and areas of large tide amplitudes.

CHARACTERISTICS OF ST727

Root Mean Square of the selected tide gauges

Tides are very different along the coasts. To quantify the tidal characteristics, a root mean square (RMS) is introduced. For N tide gauges, the RMS is equal to:

$$RMS_{TG_N} = \sqrt{\frac{1}{N} \sum_N \frac{1}{2} [(H_{TG} \cos G_{TG})^2 + (H_{TG} \sin G_{TG})^2]} \quad 1$$

where H_{TG} is the tide gauge amplitude, G_{TG} is the tide gauge Greenwich phase lag.

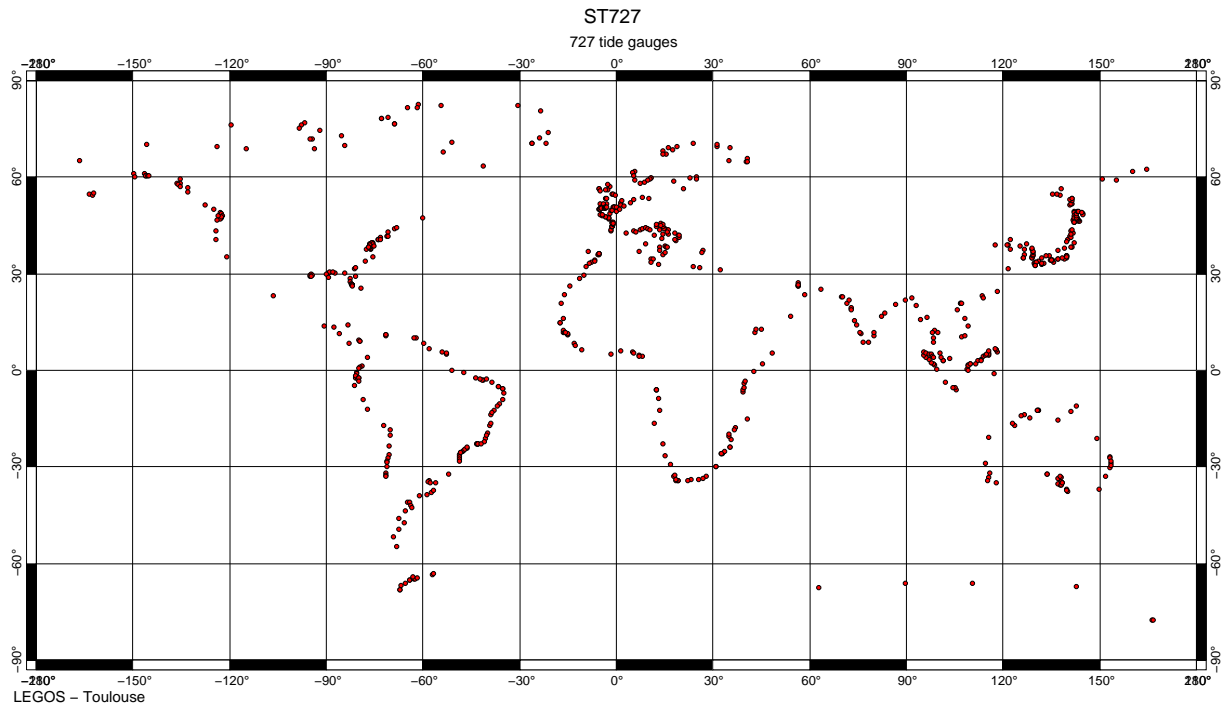


Figure 2: Selected tide gauges

Harmonic characteristics

Figure 3 gives an average estimation of the amplitude of the main tidal constituents based on these 727 tide gauges. It provides a global view of the tides over the coastal areas. M2 and S2 are the two main semi-diurnal constituents. K1 and O1 are the two main diurnal constituents of the tide spectrum along coastlines according to our selection. But this figure is instructive on the detailed content of our selected database in term of harmonic constituents.

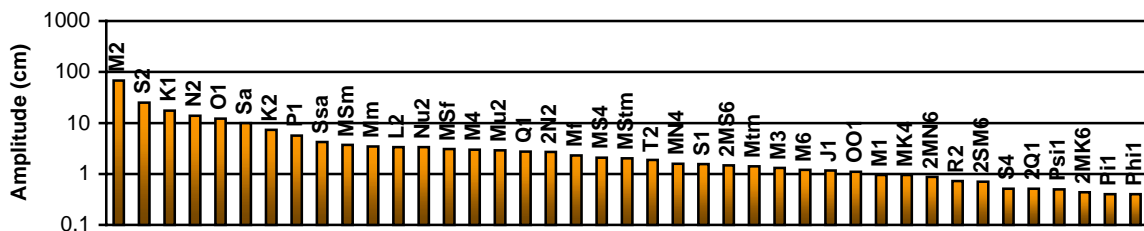


Figure 3: Harmonic decomposition of the 727 selected coastal tide gauges

Diurnal and semi-diurnal tides along coastlines

Large differences in amplitude exist between the 6 areas defined above. For instance, semi-diurnal tide waves amplitudes are higher along the coasts of the Atlantic Ocean than along the coasts of the Pacific or the Indian Oceans (Figure 4). This shows the necessity to take into account the tide height in global RMS difference estimates between tidal solutions or between in situ and numerical solutions, in order to prevent these statistics from being dominated by these areas (such as typically European shelf or Patagonian shelf for M2).

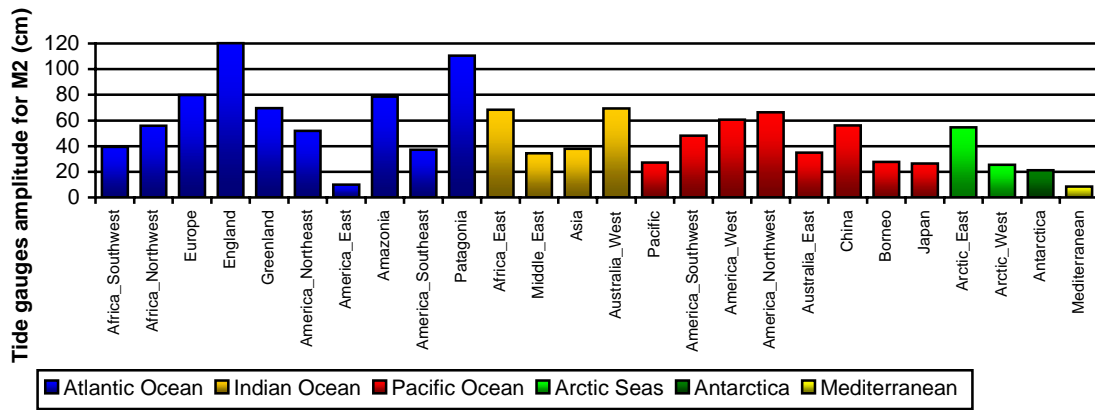


Figure 4: M2 amplitude of the 26 selected coastlines and associated tide gauges

Figure 5 illustrates that, on the contrary, the diurnal waves are higher in the Pacific Ocean than in other parts of the world ocean. This is well known, but emphasises the importance to take into account the tide height in global RMS statistics.

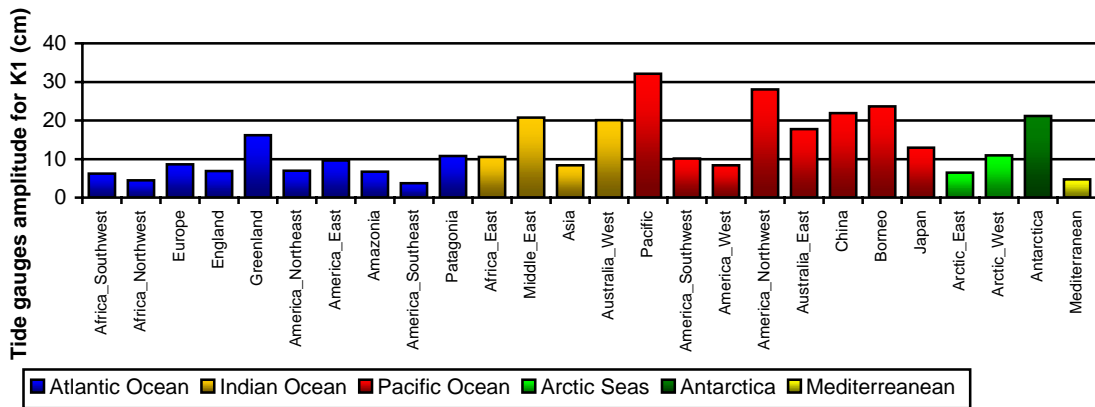


Figure 5: K1 amplitude of the 26 selected coastlines and associated tide gauges

NEEDS TO IMPROVE THE ST727 DATABASE

NEW TIDE GAUGES DATA

Even if the IHO databank contains an important amount of tide gauge data, it remains spatially inhomogeneous. Indeed, if there are lots of data along the coasts the Atlantic and the Pacific oceans, elsewhere it lacks data. This remark is underlined by the Figure 6, which shows the number of IHO sea level stations per 1000 km for each of the 26 areas. The Polar Regions, the Indian Ocean and the South Pacific Oceans lacks dramatically data along the coasts. Collecting new data from other sources would be a major benefit to complete the IHO database.

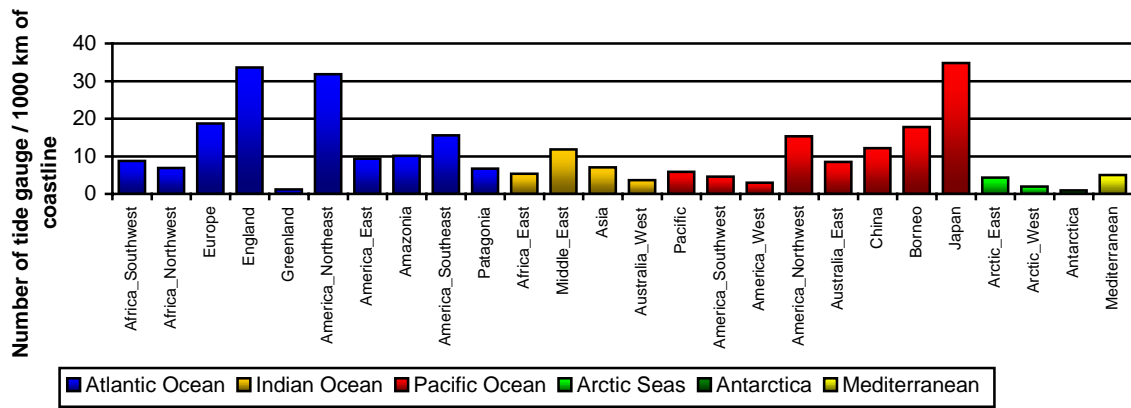


Figure 6: Number of tide gauges per 1000 km of coastlines

MORE ACCURATE DATA

Figure 7 shows the number of constituents available from the ST727 stations. The waves are classified in descending order of amplitude.

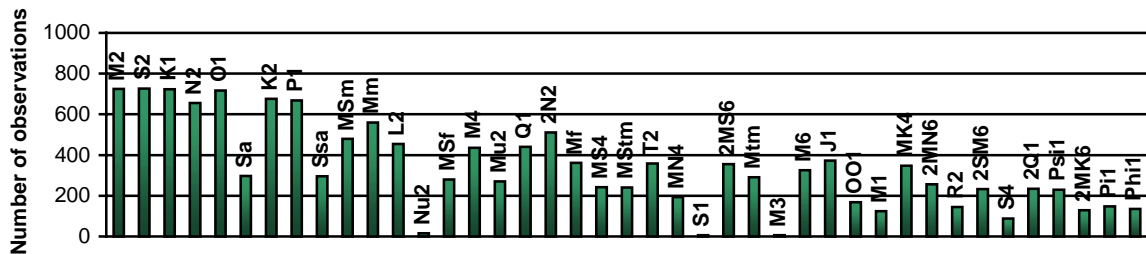


Figure 7: Number of constituents supplied by the analysis of the 727 selected coastal tide gauges

The long waves, the ter-diurnal and four diurnal waves are less documented (or not analysed) despite their important amplitude in the tide spectrum (cf. Figure 3). But, these waves occur in shallow water. Better analyses with longer time series are needed. Obtaining better non-linear constituents is a necessity to test the validity of tide models in coastal areas.

HOURLY TIME SERIES

IHO databank only provides the harmonic constituent of each tide wave without any idea of the precision of the analysed constituents. An error bar for each value would provide a new and important information. This would allow a better interpretation of the comparison between in situ and model solutions.

To calculate the error bar on each value, a methodology has been developed ([Ponchaut et al., 1999]), based on a least-squared method applied on sea level hourly long time series. This method has been applied to the WOCE sea level data set, using very long time series (generally more than 13 years). The work could be extended to coastal stations if the hourly time series were available. Many IHO stations certainly have in their archive long enough records (several years) to allow to compute these error bars.

CONCLUSION

727 tide gauges were extracted and selected from the IHO database to provide a coastal databank (called ST727) with the aim to supply tidal characteristics along the coasts of the world ocean. This database is of major interest to evaluate the accuracy of tide models in coastal areas. The

tide gauges were carefully selected thanks to different criteria of spatial coherence, spatial location and in accordance to CSR3.0 and FES94.1. Doubtful tide gauges were dismissed, but clearly need further investigations.

Let us give an idea of the accuracy of the present global tide models. Following Andersen [Andersen, 1995] who used 3 of the main diurnal (K1, O1, Q1) and 5 of the main semi-diurnal waves (M2, S2, N2, K2, 2N2) to characterise this accuracy, the average combined RMS difference between models and in situ data (based on a set of nearly 5000 individual data) is 6.78 cm for FES94 and 5.55 cm for FES98.

This ST727 database needs to be improved, by:

- collecting new data in areas which lacks dramatically information (Polar Regions, some coasts of the Indian Ocean, Sea of Okhostk, etc.);
- computing again better harmonic constituents, by analysing not only diurnal and semi-diurnal waves but also quarter-diurnal, ter-diurnal and long period waves;
- obtaining sea level hourly time series to re-analyse tide data and to provide a new information (error bars) useful both for validation and assimilation methods.

Thus, this work represents only a first effort to provide to the scientific community a database, extracted only from the IHO databank, to allow the validation and comparison of tide models along the coasts of the world ocean and to supply better estimates for data assimilation models.

Besides, this work underscores the necessity to maintain the existing sea level stations presently operating, to improve the analysis of sea level record applied to tides, and to extend the world sea level station network to areas which lack data.

References

- Andersen, O.B., Global ocean tides from ERS1 and TOPEX/POSEIDON, *J. Geophys. Res.*, 100 (C12), 25261-25282, 1995.
- Cartwright, R.E., and R.D. Ray, Energetics of global ocean tides from Geosat altimetry, *J. Geophys. Res.*, 96, 16897-16912, 1991.
- Eanes, R.J., and S.V. Bettadpur, The CSR3.0 global ocean tide model, Center for Space Research Univ. Of Texas, Austin, 1996.
- IHO, *Tidal Constituent Bank Station Catalogue*, Ocean Aquat. Sci., Dep. Of Fish and Oceans, Ottawa, 1979.
- Le Provost, C., A new in situ reference data set for ocean tides, in: *AVISO Newsletter*, 1994.
- Le Provost, C., M.L. Genco, F. Lyard, P. Vincent, and P. Canceil, Spectroscopy of the world ocean tides from a finite element hydrodynamic model, *J. Geophys. Res.*, 99 (C12), 24777-24797, 1994.
- Lefèvre, F., C. Le Provost, and F. Lyard, A new tide finite element solution (FES98) independent of altimetry, in *EGS, 24th General Assembly*, The Hague, 1999.
- Ponchaut, F., F.H. Lyard, and C. Le Provost, The WSLA98 : A comprehensive analysis of the tidal signal in the WOCE Sea Level data and its application, submitted to: *Journ. of Atm. and Ocean. Technics*, 1999.
- Shum, C.K., P.L. Woodworth, O.B. Andersen, G. Egbert, O. Francis, C. King, S. Klosko, C. Le Provost, X. Li, J.M. Molines, M. Parke, R. Ray, M. Schlax, D. Stammer, C. Thierney, P. Vincent, and C. Wunsch, Accuracy Assessment of recent Ocean Tide Models, *J. Geophys. Res.*, 102 (C11), 25173-25194, 1997.

Long-term trend of the sea level at the Romanian littoral

*Viorel Malciu
Vasile Diaconu
Romanian Marine Research Institute
Bd. Mamaia
Constantza 8700, Romania*

Abstract

The analysis of the longest sea level record at Constantza reveals a significant rising trend. Also, the interdecadal changes, as related to the variations of the river discharge, are investigated.

Introduction

Sea level recording in Romania dates back to 1859, when the European Commission of the Danube, in order to improve the navigation conditions at the Danube mouths, initiated the observation of the sea level by setting up a visual tide staff (VTS) where three readings were made daily. These values were afterwards used for the entire Danube leveling.

In 1933 a float-type gauge was placed at Constantza and it is still operational in the same place. Different institutions were in charge with the exploitation of this tide gauge such as Maritime Harbour Service or Military Hydrographic Service. The Romanian Marine Research Institute as being subordinated to the Ministry of Waters, Forests and Environment Protection, was assigned to carry on this activity since 1970, the year of its foundation, and this work is ongoing. After 1974, three other tide gauges were put into function for a better coverage of the entire Romanian littoral.

Tide gauge network at the Romanian littoral

RMRI tide gauges that are operational are located in the following points: Constantza, Tomis, Sulina and Mangalia (Fig. 1).

Description of the tide gauges:

Constantza: (Fig. 1, Fig. 2, Picture 1, Fig 3a, Fig 3b);

Geographical position: 44°10'21.0" N, 28°39'34.0" E. Float operating tide gauge, OTT type, functional in Constantza Port since 1933, recordings on paper chart, changed once a week. Two VTS are used, one of them for control, and three readings are made daily.

Tomis: (Fig. 1, Picture 2), situated in a small marina, about 1.5 km north from Constantza Port. Float operating and VTS. Three VTS readings are made daily.

Sulina: (Fig. 1, Picture 3), situated at the northern limit of the Romanian littoral. Geographical position: 45°09'45.6" N, 29°43'37.2" E. Float operating tide gauge, type SUM, functional since 1977, daily charts. It is placed near the meteorological station 6 km downstream Sulina locality, on the southern side of the jetty. A horizontal pipe connects the stilling well with the open sea. Violent storms damaged the VTS and a new one is to be installed this year.

Mangalia: (Fig. 1, Picture 4) Situated in the southern area of the Romanian littoral in Mangalia harbour. Geographical coordinates are 43°48'30"N, 28°35'30"E. Float operating, SUM type, daily chart, VTS readings three times a day. Due to sand accumulation that obstructed the stilling well, it was relocated in Dec. 1998 to a new position on the opposite quay of the same port.

Characteristics of the hydrological and meteorological regime of the area

Situated at mid latitudes, the northwestern part of the Black Sea experiences the general conditions imposed by a temperate continental climate, with cold winters and warm summers. Siberian anticyclone influence alternates with the southern Mediterranean circulation. Consequently the rivers which debauch in this area will have an annual high in spring season when the precipitation in their hydrographic basins are in excess, and a minimum in warm seasons when evaporation processes become dominant.

The main components of the water balance in the area of our littoral (Altman, 1990; Bondar et al. 1991) is continental runoff via the Danube discharge, which is 60% of the total fresh water discharged into the sea, and precipitation and evaporation. The high sea levels in the first part of the year occur in the condition of a considerable increase of the river volume and important precipitation quantities (53% in May - August) and a reduced evaporation (37% in the first six months of the year. (Selariu, 1971). Analysis of our data regarding Danube's annual regime indicates a maximum mean discharge in May of 23.74 km³. Maximum discharge of 38.89 km³ occurred in May 1970. The lowest mean discharge, 11.82 km³, was recorded in October, with a minimum of 5.89 km³ in October 1946.

The wind regime at the Romanian littoral is variable, but in certain seasons prevalent frequencies may occur (Climate of Romania). Long-term averages of the wind (1941 - 1997) indicate high frequencies from northern and western directions, 14.9% north and 15% west, where the highest mean speed was recorded as well (north 6.0 m/s). South and southeast winds present a notable frequency, 11.9% and 9.3%, respectively. Due to the coastline orientation, onshore winds produce a sea level rise (northerly and easterly), while offshore wind have an opposite effect (Fig. 4). A significant change of the sea level is induced by strong winds blowing from the same direction for more than 48 hours. Also, short term changes in the sea level are due to the sub-basin seiches (Blatov et al., 1984).

Sea level annual characteristics

As previously mentioned, sea level evolution presents high values in the first part of the year and low ones in the second (Fig. 5). Mean monthly values, which are positive all over the year, range between 6.84 cm in October and 21.24 cm in May. The maximum mean value, 46.40 cm occurred in March 1970, and the Danube discharge reached its maximum mean monthly value in May of the same year, 38.89 km³. The low values in the autumn, -13.20 cm in October and -14.20 cm in November, are exceeded in February 1949, when the volume of the Danube is low (7.16 km³), and severe winter conditions were recorded.

The highest amplitudes, 54.90 cm and 54.40 cm, occurred in February and March, respectively, while lowest amplitude, 35.20 cm, occurred in September and corresponded with the Danube volume's lowest amplitude of 16.27 km³ in September as well.

Sea level long term evolution

A general, preliminary approach of the sea level long-term evolution indicates that a slight rise of the values is evident. Soviet scientist Altman (1990), considering the entire Black Sea basin, indicated a rising tendency between 1875 and 1985, especially in the last 50 years. His estimate is 1.5-2.0 mm/year. Romanian scientists (Banu, 1961; Bondar & Filip, 1963; Selariu, 1971) analyzed the sea level evolution in different periods and they all identified a rising tendency. Using data between 1933 and 1956, Banu (1961) indicated a mean value 12.7 cm and a tendency of 0.425 cm/year. Selariu (1971), for the period 1933 - 1969, found 13.02 cm as mean value and a tendency of 0.256 cm/year. Later on, studies of the Romanian Marine Research Institute (RMRI) found 13.5 cm for 1933 - 1978 and 14.3 cm for the period 1933 - 1983.

Analysis of the data set between 1933 and 1998 reveals the following aspects:

- annual means are positive, with only two exceptions: -2.44 cm in 1943, the lowest annual mean, and -1.22 cm in 1983;
- the highest annual mean (29.70 cm) occurred in 1970, when exceptional runoff was recorded;
- negative values in the entire period represent only 9.7% of the data and these occurred between September and February;
- the mean sea level value, 14.2 cm, is positive relative to the initial reference zero;
- for the entire period, the linear rising trend (Fig. 6) has a value of 0.128 cm/year;
- the Danube's mean water flow at the outlet into the Black Sea during 1858-1988, with an average value of about 191 km³/year, also has an increase trend in time (Bondar);
- the interannual and interdecadal variations have large amplitudes, and a long period oscillation could be detected;
- the averages computed for the 1946-1955 decade is 10.8 cm, while that of the 1966-1975 reaches 18.6 cm;
- spectral analysis reveals strong oscillations with periods of 2.5 years and 4 years, similar to those of the river discharge (Fig. 7);
- the correlation of the variables in the time domain (monthly averages) is significant (Fig. 8);
- the wind regime has only a temporary influence and does not affect the long-term evolution of the sea level.

Conclusions

The analysis of the data measured at the Constantza sea level gauge during 1933-1998 period revealed the existence of a rising trend, in good agreement with the estimates made by other authors for different locations (Gorjachkin, 1995) or for the entire Black Sea basin (Altman et al., 1990). This is also consistent with the contemporary eustatic trend.

Also, significant interannual and interdecadal variations have been observed and estimated through spectral analysis. They are correlated with the changes in the Danube discharge, the main contributor to the river input into the sea. However, the time series are not long enough to allow for the secular oscillations to be accurately assessed.

REFERENCES

- Altman, E. N., A.A. Bezborodov and Y.I. Bogatova, 1990. Practical Ecology of Marine Regions. Black Sea., Naukova Dumka, Kiev, 252 p (in Russian).
- Banu, A. C., 1961. Observations and measurements on the recent and secular oscillations of the Black Sea waters at the Romanian shore. *Hidrobiologia*, vol II., p. 127-160 (in Romanian).
- Blatov, A. S., N.P. Bulgakov, V.A. Ivanov, A.N. Kosarev and V.S. Tuzhilin, 1984. Variability of the hydrophysical fields of the Black Sea, Gidrometeoizdat, Leningrad, 240 p. (in Russian).
- Bondar C., I. State, D. Cernea and E. Harabagiu, 1991. Water Flow and Sediment Transport of the Danube at its Outlet Into the Black Sea. *Meteorology and Hydrology*, vol 21.1, p. 21-25.
- Bondar C., and I. Filip, 1963. Contribution to the study of the Black Sea level. *Studii de hidrologie*, vol IV, (in Romanian).
- Gorjachkin I. N., V.A. Ivanov, 1995. Interannual changes of the sea level in the Northwestern part of the Black Sea. In: *Investigations of the Azov - Black Sea basin / Collected papers*, Eremeev et al. (ed.), Sevastopol, p. 18-21 (in Russian).
- Selariu O., 1971. On the Black Sea level oscillations at Constantza. *Hidrotehnica*, vol. 3, p. 169-176 (in Romanian).
- Stoenescu, S.M., and D. Tastea, 1962, 1966. *Climate of Romania*, 2 vol, 164+277p. (in Romanian).
- RMRI: Study on the Black Sea level, 1973-1985 (unpublished manuscripts).

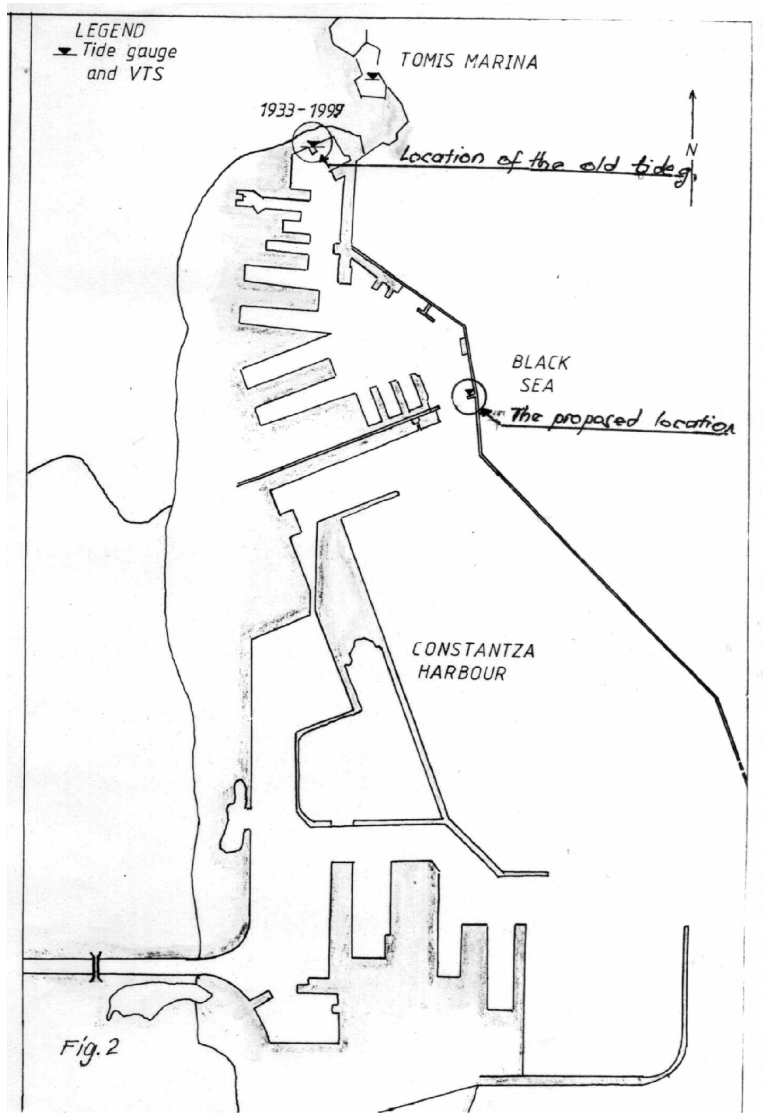


Figure 1. Map of the Constantza area.

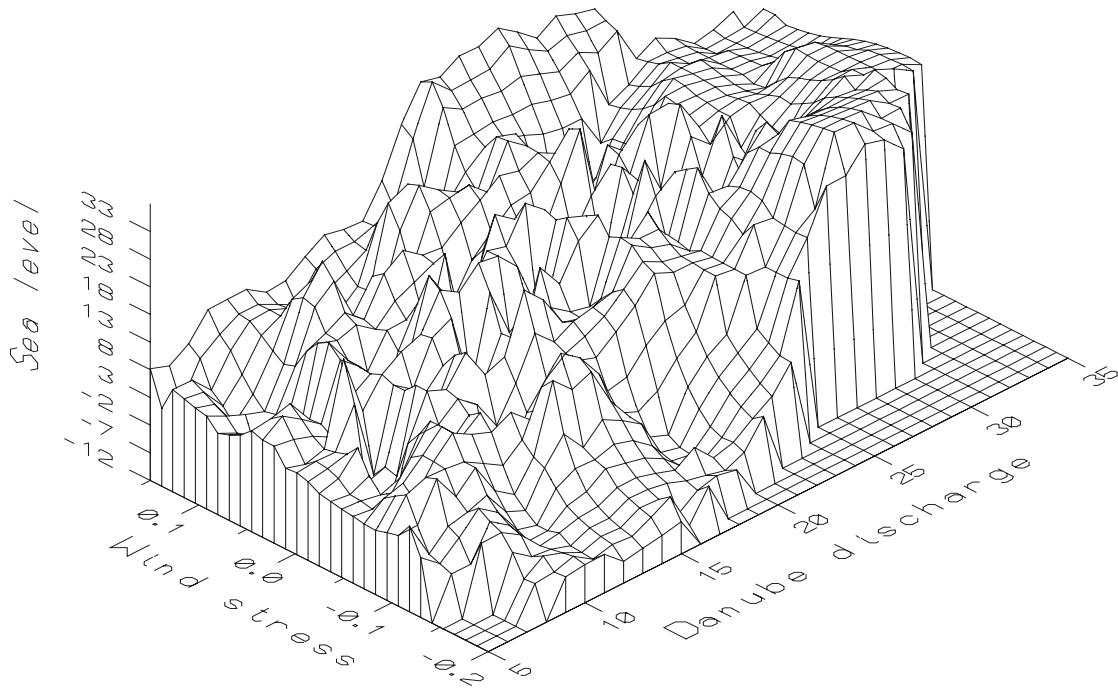


Figure 2 Correlation between sea level and hydro-meteorological parameters

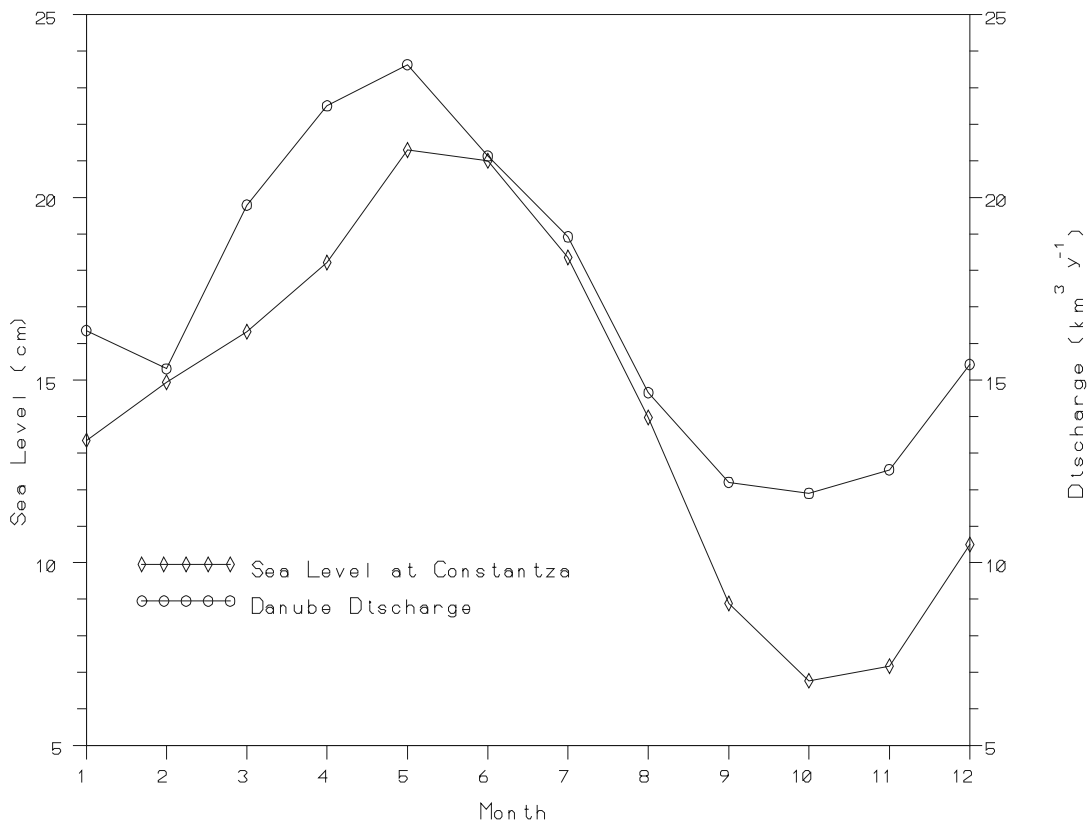


Figure 3 Annual evolution of the sea level at Constantza and Danube Discharge (1933 - 1998)

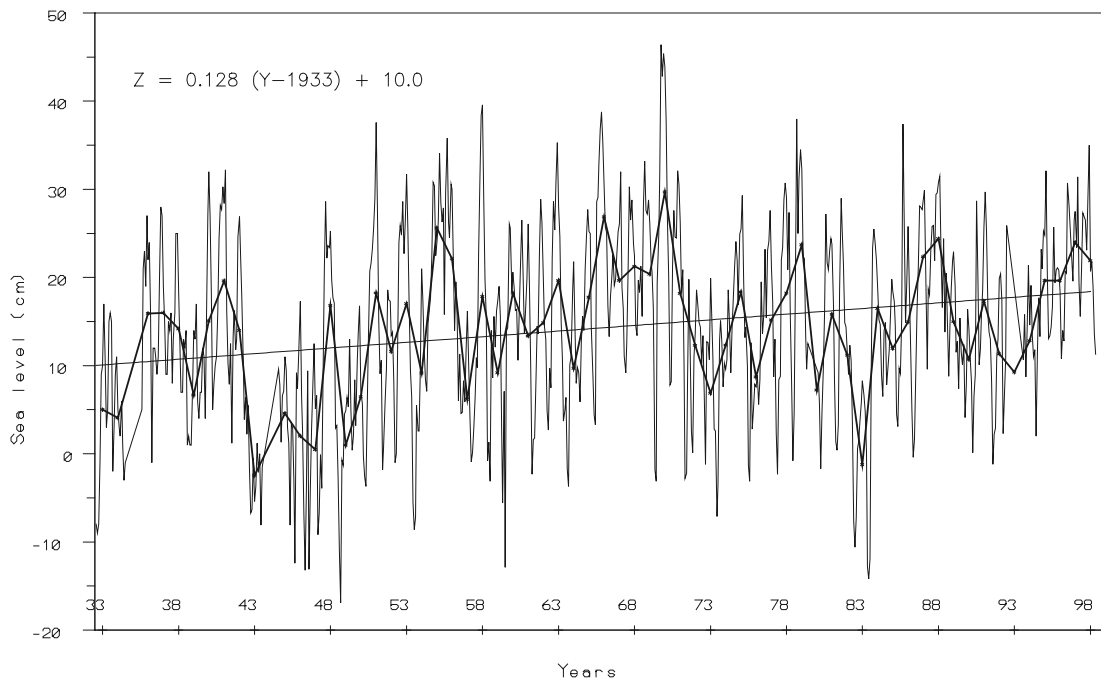


Figure 4 Evolution of the monthly and annual means of the sea level at Constantza and their trend

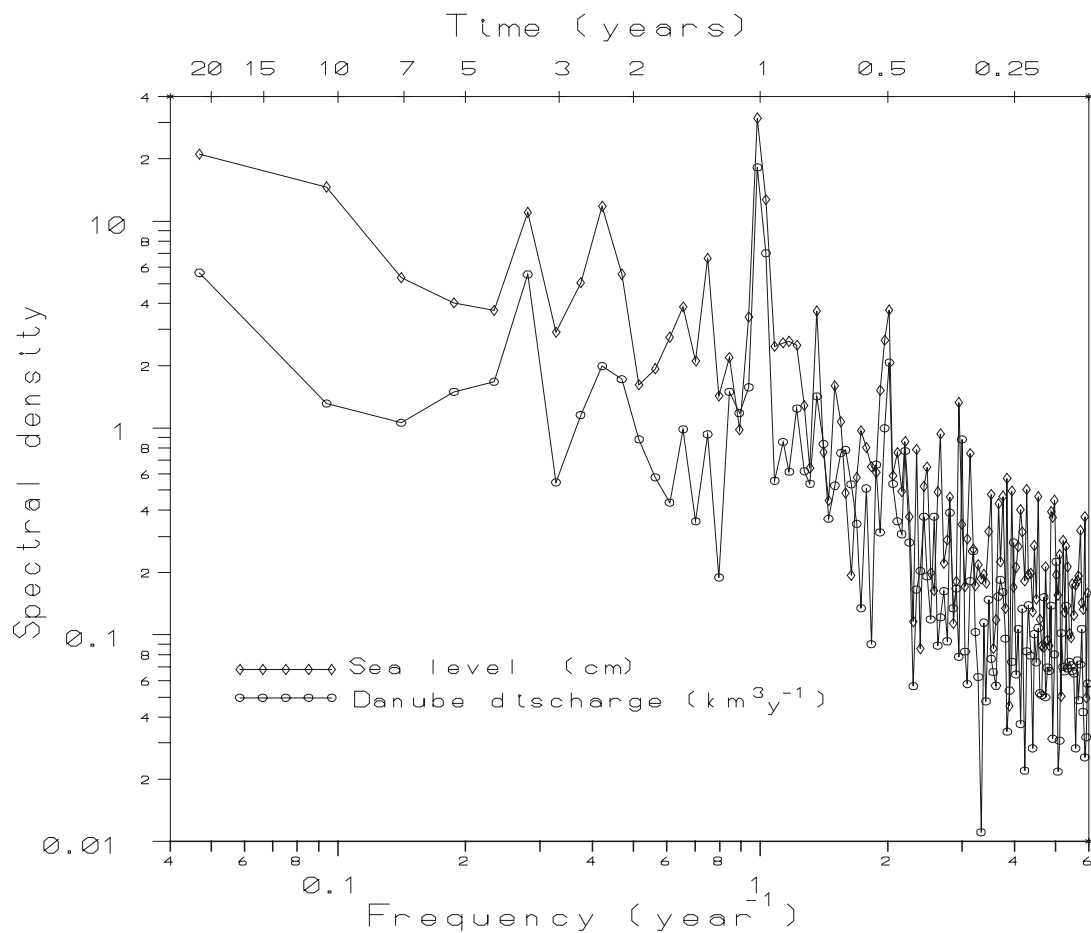


Figure 5 Spectral density of the sea level at Constantza and Danube discharge

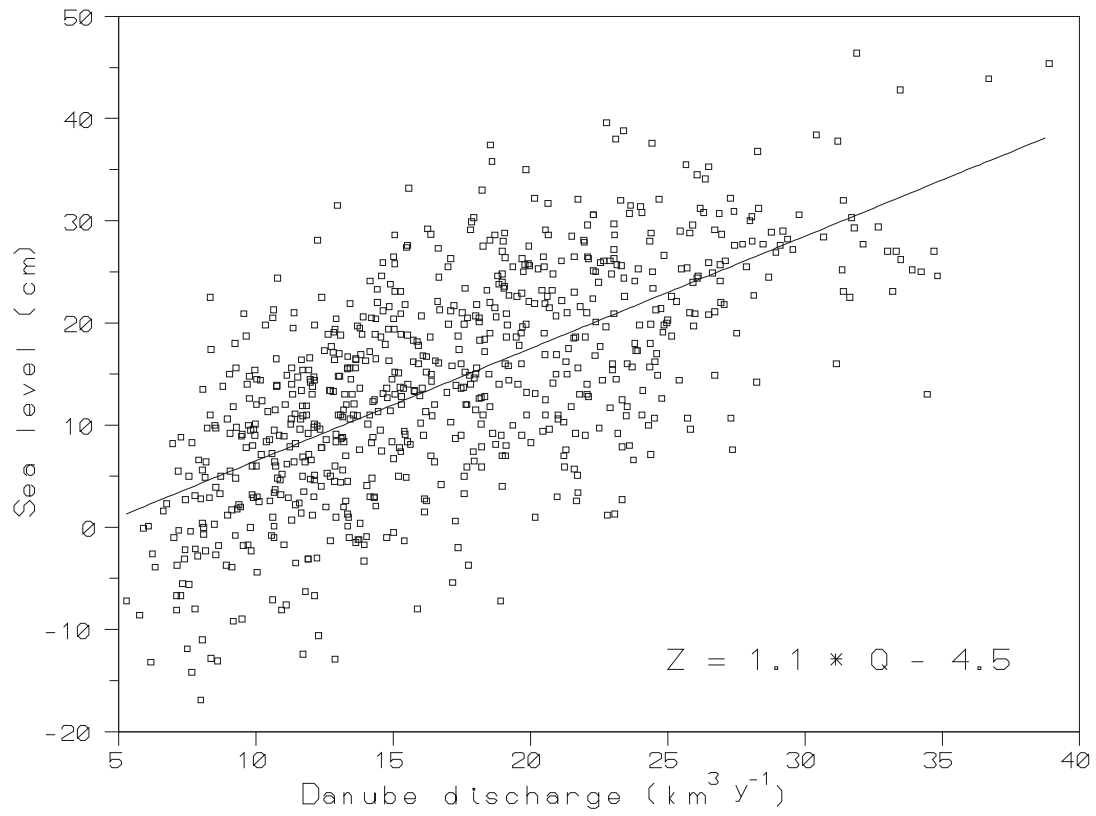


Figure 6 Correlation between sea level monthly means and Danube discharge

**Sea level propagating coastal-trapped waves, circulation forcing influence
along central Chile, 1991-1995**

Claudia Valenzuela-Cuevas
Chilean Navy Hydrographic and Oceanographic Service

Abstract

In this paper, coastal trapped waves (CTW) in sea level are studied, identifying the most energetic frequencies, and determining its influence over shelf circulation in central Chile. CTW propagated southward with phase velocities of 250 km/d, widely modulating the sea level variability. The results presented here are part of the author's Oceanography Thesis, developed at the School of Marine Sciences at Catholic University of Valparaiso, Chile, in 1998.

Observations and methods

The study area (Fig. 1) ranges from 27° S to 36.7° S, and sea level data between November 1991 and August 1995 are analyzed. Sea level was measured at Caldera (27° S), Coquimbo (30° S), Valparaiso (33° S), and Talcahuano (36.7° S).

The preliminary treatment of the time series consisted of eliminating the sea level isostatic effect through atmospheric pressure adjustment. The sea level trend was subtracted through the least squares method, and then the information was low-passed filtered using a Cosine Lanczos filter of 121 points.

In order to analyze the variance distribution in the frequency domain, autospectra were calculated from the hourly sea level for each station through the fast Fourier transform, using 14 degrees of freedom, and a 95% confidence level. Wave propagation was analyzed via coherence and phase functions for sea level between two consecutive tide stations, and phase velocity was calculated by the best linear fit.

Topographic effects on the features of the waves were studied by comparing the Rossby radius and the local shelf-slope scale, the latter being obtained from nautical charts.

Results and discussion

The filtered sea level anomaly (average subtracted from the time series) is shown in Fig. 2. In the sea level signal at Caldera, Coquimbo, Valparaíso, and Talcahuano we observe intense fluctuations between November 1991 and April 1992, each lasting approximately 1 month. These events were in association with the El Niño event 1991/92.

Shaffer et al. (1997), analyzed sea level data in Peru and north and central Chile, and identified these waves as being clearly noticeable until Valparaiso, demonstrating its remote origin. This low frequency fluctuation shows a north to south linked system, since the oscillations that were seen at 27° S were perceptible down to 36.7° S.

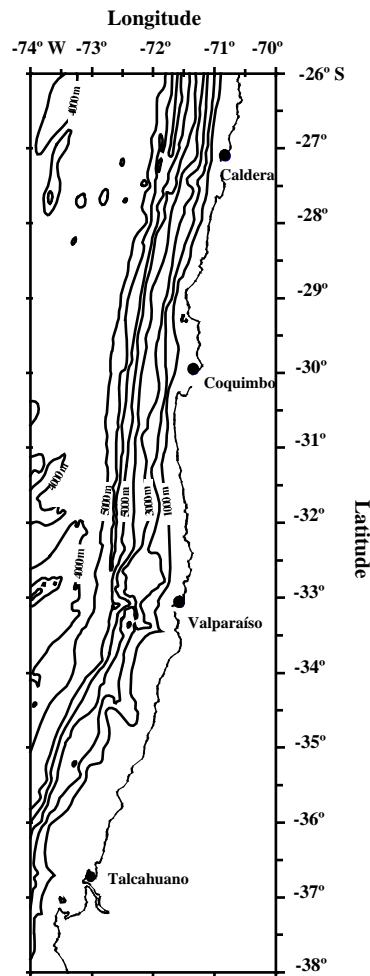


Fig. 1. Study area and location of the tide stations (●).

After these intense fluctuations, since August 1992, sea level showed a smoother behaviour, dominated by the presence of variable intensity fluctuations with periods of 35 to 50 days. From April 1995 at Caldera there appeared two sea level fluctuations as intense as those observed earlier, although this signal did not propagate southward in the study area.

The sea level spectra (Fig. 3) show the highest energy concentrated in the low frequencies, with similar periods over practically all of the study area; that is, 70 days at Caldera, 50 days at Coquimbo, and 45 days at Valparaíso and Talcahuano. There was also significant energy remaining in periods of 10 and 5 days at all the stations.

Pizarro (1991), using sea level from a normal year, observed high variability in periods between 3 to 5 days from Antofagasta to Valparaíso, and Bilbao (1992) found significant evidence of strong sea level fluctuations in the 8 to 12 days band during El Niño 1982-83.

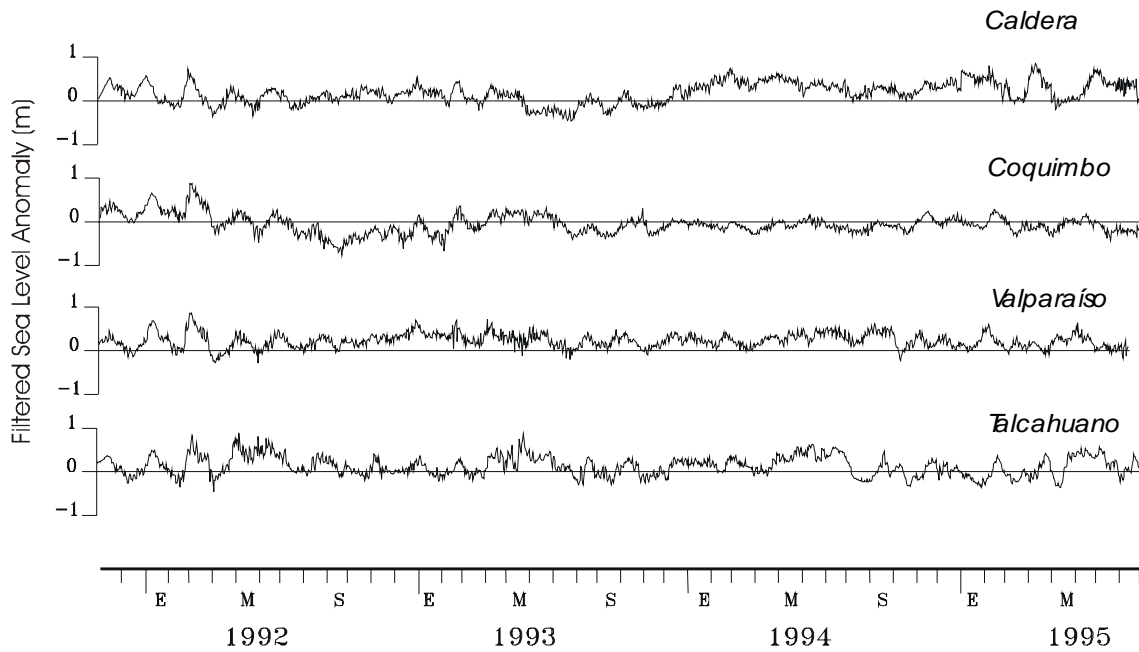


Fig. 2. Sea level signal from Caldera, Coquimbo, Valparaíso, and Talcahuano. The graph was built with daily averages of low-pass filtered sea level and atmospheric pressure adjusted.

Coastal trapped waves, forcing and propagation

Analyzing directly the forcing of circulation due to sea level variations, we calculated the coherence between currents from 170, 400, and 700 m at 30° S and 34° S and sea level at both places (not shown here).

There was a linear relationship in similar periods at 30° S and 34° S. Sea level fluctuations with periods of 70, 50, and 25 days had phases ranging from -90° to -180°, meaning that if sea level rises, a poleward flow in the three depths is developed, from which we deduce that such sea level fluctuations represented a *barotropic forcing*. There was also a significant coherence at 10 days, where at 170 m phases ranged from -90° to -180°, and at 400 and 700 m from 0° to -90°. For propagating waves in sea level of 10 days period, flow developed the same direction in 400 and 700 m, but opposite to that in 170 m; this situation clearly shows a *baroclinic forcing* of such oscillations.

To study this wave propagation, we used coherence between sea level at the pairs of tide stations Caldera-Coquimbo, Coquimbo-Valparaíso, and Valparaíso-Talcahuano, and the phases of the significant coherences were plotted.

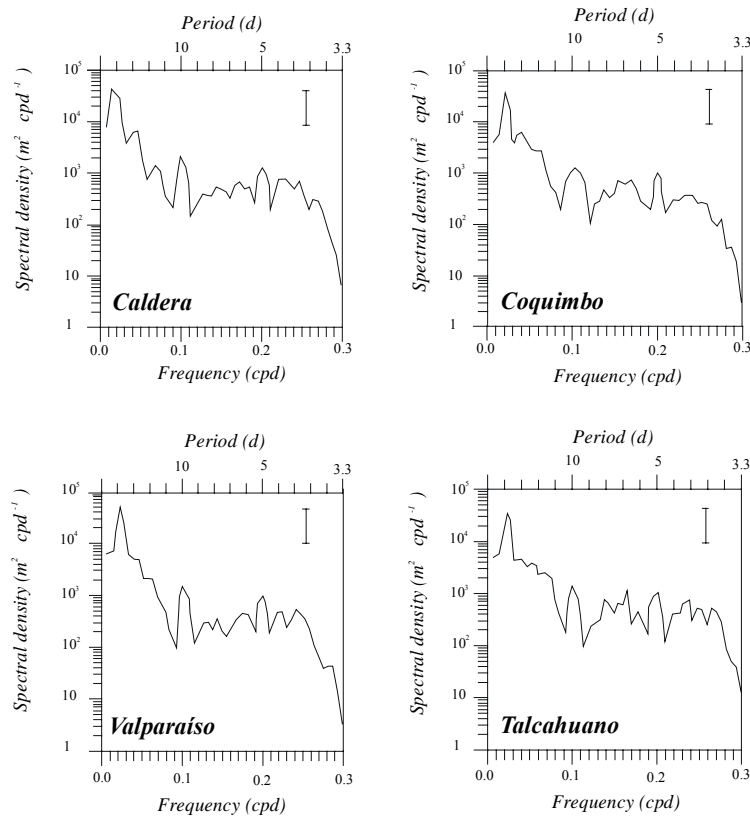


Fig. 3. Sea level autospectras (adjusted and low-pass filtered) from Caldera, Coquimbo, Valparaíso, and Talcahuano.

The phase increased linearly for each pair of stations towards the high frequencies, which means sea level fluctuations were caused by non dispersive CTW, where the wave's phase velocity is not dependent on frequency. Due to this behavior, a linear fit to the phase is done, and since the slope is the ratio D/C was possible to calculate the phase velocity through the following expression:

$$\theta = 360^\circ (D/C) \omega$$

where, D is the distance between stations (km), θ is the phase (degrees), ω is the frequency (cpd), and C is the phase velocity.

According to this, between Caldera and Coquimbo, 323.49 km distant from each other, the poleward phase velocity was 239 km/d, between Coquimbo and Valparaíso 246 km/d ($D=345.98$ km), and between Valparaíso and Talcahuano 251 km/d ($D=434.53$ km). From these values, the average poleward phase velocity is 245 km/d for the study area, which is consistent with the phase velocity for the first baroclinic mode.

This value fits with the results from Pizarro (1991) and Bilbao (1992) on the Chilean coast and Cornejo and Enfield's (1987) for the Peruvian coast, where the values range from 230 to 330 km/d.

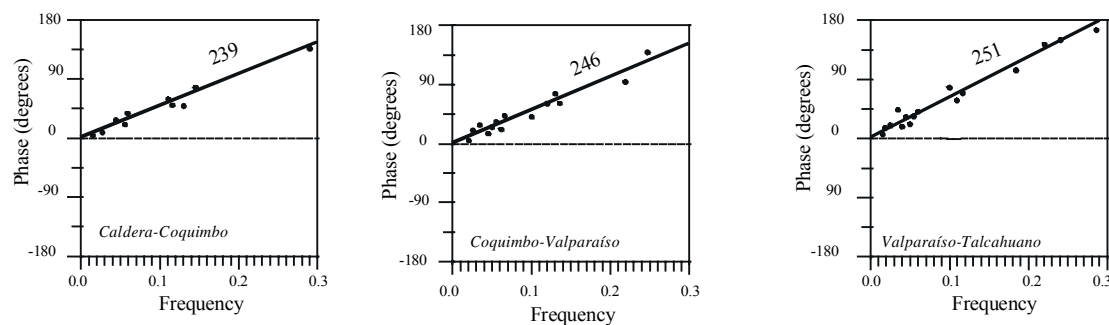


Fig. 4. Phase linear fit (as a function of frequency) and phase velocity (in km/d) for sea level propagating non dispersive waves for contiguous tide stations. The linear fit was performed with phases for significant coherences at 95% confidence level.

Topographic effects

To examine the nature of the waves propagating along the Chilean coasts, the Rossby radius, R , and the topographic length scales were compared at 30° S and 34° S (see Fig. 1).

At 30° S, the shelf and slope are narrow, and the shelf-slope length scale (γ , also referred to as simply the topographic scale) is 46.3 km. At 34° S, the shelf is wider, the shape of the slope is more variable, and γ is 124.1 km, which is three times wider than at 30° S. On the other hand, the Rossby radius, R , is 39 km at 30° S and 34 km at 34° S (using $C=250$ km/d for the calculation of R). If these values are compared, it is easy to see that for the study area $R < \gamma$, which is the usual relation for mid and higher latitudes.

At the equator, the Rossby radius is infinite, the topographic scale is small compared to it, so at low latitudes coastal trapped waves do not experience any changes in vertical structure due to topography, being pure *Kelvin waves*. With increasing latitude the Coriolis parameter, f , increases, and R gets smaller since it is inversely proportional to f . Thus R becomes more and more comparable to γ , until $R < \gamma$. In this way the waves would be affected by topography (Brink and Allen, 1978; Le Blond and Mysak, 1978; Smith, 1978; Brink, 1982; Chapman, 1987; Brink, 1991) through friction associated with the ocean bottom and become *shelf waves*, which would be the type identified in this research. The changes in the CTW can be either attenuation in its modal amplitude, or in other cases dispersion from one mode to another.

At Coquimbo (30° S) the relationship is still $R < \gamma$, but the difference between R and γ is relatively small, so the latitude of the 30° S could be a transition zone to define if the waves are Kelvin or shelf waves.

Conclusions

With the preceding observations and discussions, for the area from the 30° to 36.7° S and the period November 1991 to August 1995, the main conclusions are:

- In Caldera, Coquimbo, Valparaíso and Talcahuano, sea level showed high energy fluctuations at low frequencies, with the most energetic periods concentrated between 40 and 80 days.
- Between 30° and 34° S, 70, 50, and 25-day period sea level fluctuations constituted a barotropic forcing for the alongshore flow. On the other hand, 10-day period sea level fluctuations represented a baroclinic forcing for the alongshore flow.
- Coastal sea level was modulated by shelf waves propagating poleward with an average phase velocity of 245 km/d (2.84 m/s).

Acknowledgments

I wish to thank Lt. Cmdr. Mr Rodrigo Nuñez (Chilean Navy Hydrographic and Oceanographic Service) for representing me and presenting this work at the Toulouse Sea Level Workshop, to Mr Sergio Salinas (School of Marine Sciences, Catholic University of Valparaíso), Mr Ricardo Rojas (Chilean Navy Hydrographic and Oceanographic Service, and School of Marine Sciences, Catholic University of Valparaíso), and Mr Oscar Pizarro (School of Marine Sciences, Catholic University of Valparaíso, and Institute of Oceanography, University of Göteborg) for their support, and to the Chilean Navy Hydrographic and Oceanographic Service for having provided the sea level data necessary for this investigation.

References

- Bilbao, P. 1992. Características físicas del fenómeno de “El Niño” 1982-1983 en la costa de Chile. Tesis para optar al título de Oceanógrafo. Universidad Católica de Valparaíso, 140 pp.
- Brink, K. and J. Allen. 1978. On the effect of bottom friction on barotropic motion over the continental shelf. *J. Phys. Oceanogr.*, 8: 919-922.
- Brink, K. 1982. The effect of bottom friction on low frequency coastal trapped waves. *J. Phys. Oceanogr.*, 12: 127-133.
- Brink, K. 1991. Coastal trapped waves and wind driven currents over the continental shelf. *Ann. Rev. Fluid Mech.*, 23: 389-412.
- Chapman, D. 1987. Application of wind-forced, long, coastal-trapped wave theory along the California coast. *J. Geophys. Res.*, 92(C2): 1798-1816.
- Cornejo-Rodriguez, M. and D. Enfield. 1987. Propagation and forcing of high-frequency sea level variability along the west coast of South America. *J. Geophys. Res.*, 92(C2): 14323-14334.
- Le Blond, P. and L. Mysak. 1978. *Waves in the ocean*. Elsevier, New York, 602 pp.
- Pizarro, O. 1991. Propagación y forzamiento de perturbaciones de baja frecuencia del nivel del mar en la costa norte de Chile. Tesis para optar al Título de Oceanógrafo. Universidad Católica de Valparaíso, 105 pp.
- Shaffer, G., O. Pizarro, L. Djurfeldt, S. Salinas and J. Rutllant. 1997. Circulation and low frequency variability near the chilean coast: remotely forced fluctuations during the 1991-92 El Niño. *J. Phys. Oceanogr.*, 27(2): 217-235.
- Smith, R. 1978. Poleward propagating perturbations in currents and sea level along the Peru Coast. *J. Geophys. Res.*, 83: 6083-6092.

On the sea level network and circulation in the southeastern Brazilian coast

*A. de Mesquita
J. Harari
Institute of Oceanography
University of São Paulo, Brazil*

Abstract

This is an account on the propagation of the principal constituents of tides stemming from the tidal network and the circulation of tidal bands of measured currents of the Shelf, via a rotary spectral analysis, against the background knowledge of the general circulation of the area. Tidal heights seem to propagate in the Southeastern Brazilian coast according to the directions determined by tidal amphidromes in the South Atlantic. The rotary spectral analyses of currents indicate that the long term (3 to 5 days) spectral band, the tidally generated diurnal (24h), semi-diurnal (12h), ter-diurnal (8h) and the non linear tidally induced fourth-diurnal (6h) bands exhibited different responses in the layers that are occupied by the Coastal, Shelf and Brazil Current waters. The long term band of Shelf Water, that generally propagates towards SW, increases in volume in the western part of the area and then tends to propagate, at the surface, towards NNE, with a stronger counter-clockwise spectral component. The Brazil Current water, which intrudes in the mid depths of the water column, has almost equal amplitudes for the counter-clockwise and clockwise bands, while in the western bottom layers the Subtropical Water has similar clockwise and counter-clockwise amplitudes and, in the eastern part of the area the long term band has shifted clockwise and counter-clockwise frequency bands. Diurnal bands are all counter-clockwise, have the greatest amplitudes at surface, and tend to not be significantly determined at bottom layers. In Paranaguá the semi-diurnal bands are also all counter-clockwise and have nearly the same amplitude all along the depths. In Rio de Janeiro, frequency shifting of significant counter-clockwise and clockwise bands of semi-diurnal currents, with corresponding statistically non significant total spectral band, may indicate high values of wave celerity. The ter-diurnal bands are all clockwise only in Paranaguá and have a nearly barotropic response to the tidal forcing all over the area. The fourth-diurnal bands responses to the induced forcing are differentiated along the water column and especially have smaller total spectra in the western part of the area.

Introduction.

The sea level network of the Southeastern Brazilian Coast has been developed since the 1950s and it comprises (Fig 1), the main permanent stations of Cananeia, Ubatuba, Rio de Janeiro and Paranaguá. During 1976-1981 short-term time series measurements of pelagic tides were also added to the local non-permanent sea level network. Analyses of the main aspects of the coastal tides of the area were first described by Franco and Rock (1971) and later in Mesquita and Harari (1983). Franco and Mesquita (1981), Mesquita and Leite (1986) examined the daily, seasonal and long-term sea level variability. The general circulation of the southeastern area (PST, Santos Platform, PPR, Paranaguá Platform, and PRJ, Rio de Janeiro Platform) was first assessed from distributions of temperature, salinity and density by Emilson (1961) and Mesquita, Leite and Rizzo (1979). The first direct measurements of currents were made by Johannessen (1968) with Eckman current meters at four fixed stations along the continental shelf for short periods (2 days time series) on board the *NOc. Alte. Saldanha* of the Brazilian Navy. During 1976-1981 several time series of oceanographic (currents, temperature, salinity) and meteorological variables (wind speed and direction, air temperature and atmospheric pressure) were taken (Table 1) by the *NOc Prof W Besnard* of the University of Sao Paulo. Preliminary results from these efforts are described in the cruise reports by Mesquita et al. (1976a, 1976b and 1977). Other contributions were made by Mesquita, Leite and Rizzo (1979) on the general circulation and the occurrence of shelf break upwelling in the area; Leite (1983) on the winds and circulation of the Cabo Frio upwelling region; and Harari (1977, 1984, 1991) and Camargo (1998) on the circulation, tides and storm surges via a three-dimensional numerical model. General accounts

of the above results were presented in Mesquita (1983 and 1994). This is an account on the propagation of the principal constituents of tides stemming from the tidal network and the circulation of tidal bands of measured currents of the shelf, via a rotary spectral analysis considered against the background knowledge of the general circulation of the area.

Material and methods

The sea level network of the southeastern region of the Brazilian shelf comprises the permanent stations of Rio de Janeiro, Ubatuba, Santos and Cananeia, where sea level has been recorded since the 1950s. Short term time series were taken at pelagic non-permanent stations on the Continental Shelf in the years 1970 and were named PRJ (Platform of Rio de Janeiro), PST (Platform of Santos), PPR (Platform of Paranaguá), and only for sea level in PSC (Platform of Santa Catarina). The analysis of the tidal data was made via the harmonic method (Franco and Rock, 1971) and the response method (Munk and Cartwright, 1966). Table 2 gives the tidal constants of the tidal heights for the permanent stations of the main ports of the area, such as Rio de Janeiro, Ubatuba, Santos, Cananeia, Paranaguá, São Francisco do Sul and Imbituba, which are denoted, RIO, UBA, SAN, CAN, PRG, IMB and SFS, respectively.

The vertical distribution of the main water masses occupying the southeastern region are the Tropical Water that carries the waters of Brazil Current SW, the Subtropical Water that flows underneath the Brazil Current towards NE, the Shelf Water that flows SW and the Coastal Water flowing to the NE as shown in Figure 2. Prominent features are the upwelling of Subtropical Waters along the bottom depths to mix with the local Coastal Waters and the shelf break upwelling of the same water just above the break of the continental platform. The surface circulation of the area is shown schematically in Figure 4, where one can see a shaded area indicating where there is the possibility of occurrence of shelf break upwelling of Subtropical Water; an area (dashed) indicating the occurrence of upwelling mostly due to the continental bottom features; the predominant SW flow of Shelf Water over the platform; the occurrence of NE current flow of Coastal Water near the continental borders and curvilinear arrows, indicating the tidally dominant counter-clockwise sense of propagation in the area. Progressive vector diagrams of wind and currents from PPR were used to visualize their time and space distribution and are shown in Figure 5 for wind, and currents at 5 m, 40 m and 60 m depths. The intrusion of Tropical Waters in the mid column is indicated by the repeated CTD profiles in Figure 6. Also shown in the figure is the water with characteristics of Sub Tropical Water occupying the bottom homogeneous layer. The clockwise and anticlockwise rotary spectra of currents (Figures 3a, 3b and 3c) were estimated by Fourier transforming the smoothed auto-covariance of currents components according to Jenkins and Watts (1968) and following Gonela (1972) for the interpretation of the rotary spectra.

Results

Inspection of the phases in Table 2 shows that semidiurnal height constituents M_2 and S_2 have an anticlockwise propagation from PRJ to PST and a clockwise one between PRJ and PST. Their amplitudes show a general increase from east to west, being higher near the port of Paranaguá. Among the diurnals, the Q_1 and O_1 propagate from IMB to RIO in a west to east clockwise propagation, while the K_1 propagation follows approximately the semidiurnal components, and also has higher amplitude near Paranaguá/Cananéia. The propagation is clockwise from IMB to PPR and anti-clockwise from RIO to PPR. The M_3 have the highest amplitudes along the Paranaguá Shelf, similar to the semidiurnal components. The phases of M_3 in the area progress from the south and east merging nearly at the PPR station, but interpretation of the propagation behavior of higher order components such as M_4 , MS_4 and others is not so clear.

The circulation rotary spectra of all sites, PPR, PST and PRJ, have as prominent common features the long-term band, (3 to 5 days), and the diurnal, (24 h), semidiurnal (12 h), ter-diurnal (8 h) and fourth-diurnal (6 h) tidal bands. The amplitudes of each band were determined with a 95 % confidence interval for PPR (Fig 3a) and PST (Fig 3b), and with an 80 % confidence interval for PRJ (Fig 3c).

The long-term band circulation (3 to 5 days), is mainly an anticlockwise circulation band and is mostly due, but not always, to the atmospheric forcing over the area (Mesquita et al., 1977). However, surface and bottom layers of PBR showed slightly greater amplitudes of the clockwise than the counter-clockwise components while the layer at 40 m had nearly similar clockwise and counter-clockwise components. All the other major circulation bands of Fig. 3 are, in general, tidally-induced anticlockwise bands, except for the ter-diurnal band in PPR, which has a clockwise rotation opposed to the counter-clockwise propagation of the M_3 heights, and the fourth - diurnals, which intermix clockwise and counter-clockwise shifted bands along the depths, showing other aspects of the hydrodynamics in the area.

The vertical distribution of the diurnal circulation band of PPR shows a prominent counter-clockwise rotation that includes the inertial period for the area (27 h) at the surface (5 m) and diminishes with depth, being almost non-existent in the bottom layer (60 m). This is also true for the PRJ shelf, where the diurnal band is well-defined at the surface (5 m) and at 40 m, but in the bottom layer (90 m) has an unclear signature, so that it is difficult to identify a significant peak in the band spectra with clockwise or counter-clockwise circulation.

The distribution of the semidiurnal circulation bands of PPR shows clear counter-clockwise values from the surface layer (5 m) to the bottom (60 m), with a stronger contribution to the total spectra of the clockwise amplitude from the mid depths and less at the (60 m) bottom layer. In PST the semidiurnal circulation band is prominent, keeping the counter-clockwise rotation at the 5 m and 40 m depths. In PRJ, it is almost non-existent, either with clockwise or counter-clockwise rotation, from surface (5 m) to bottom (90 m). The two counter-clockwise and clockwise significant bands seem generally shifted in frequency, making the corresponding band of the total spectra not significant at 80% confidence interval.

The ter-diurnal circulation band with smaller amplitudes is determined in PPR with a clockwise rotation from the surface, which decreases slightly in amplitude along the column to the bottom (60 m). It cannot be detected significantly in PST, but appears in the clockwise and counter-clockwise spectra of PRJ throughout the column from the surface (counter-clockwise) to the bottom (90 m), clockwise.

The fourth-diurnal counter-clockwise circulation band also occurs, but with smaller amplitudes than the major bands. The fourth-diurnal circulation band is evident in PPR in the surface layer with a dominant counter-clockwise rotation, which is equally important as the clockwise rotation at mid depth and has clockwise and counter-clockwise circulation bands slightly displaced in frequency at the (60 m) bottom layer. At the surface layer of PRJ, the fourth-diurnal band seems to have a predominant counter-clockwise rotation. It seems to be clockwise and counter-clockwise at mid depths and is mainly clockwise in the bottom (90 m) layer.

Discussion

The propagation of the tidal heights components on the southeastern coast follows the general pattern fixed by the South Atlantic. Particularly the M_2 component has two amphidromic points, one in the middle of the South Atlantic and the other near the port of Rio Grande, with counter-clockwise and clockwise propagation of the M_2 heights, respectively, that merge in the PPR area (Mesquita and França, 1998). The semidiurnal height constituents M_2 and S_2 have counter-clockwise phase propagation from PRJ to PST and clockwise propagation between PRJ and PST. Their amplitudes show a general increase from east to west, being higher near the port of Paranaguá (Table 2), seeming also to follow the patterns of propagation defined by their amphidromes in the South Atlantic.

However, the highest values of the tidal height constituents do not always correspond to the highest values of the current band components at all levels, indicating some intervention of other factors in their dynamics. Only at the bottom do the currents of PPR and PRJ seem to be following

accordingly; i.e., higher values of current bands are associated with higher values of the corresponding components of tidal heights. This seems to be due to the fact that the diurnal amplitudes of the current bands decrease towards the bottom and the semi-diurnals and the ter-diurnals bands tend to preserve their surface values along the depth, consequent to the barotropic and baroclinic aspects of the tidal propagation in the area.

The circulation rotary spectra produced for the *u* (east-west) and *v* (north-south) components typically include long-term, and tidal (diurnal, semi-diurnal, ter-diurnal, fourth-diurnal) bands of currents, plus other circulation spectral bands not specifically covered by this account. The sense of rotation of each of these bands, which ultimately reflects the *u* and *v* phase relationships, is also variable, seeming to be indicative of the aspects of non-tidal forcing in the circulation.

Examples of these aspects are the non-tidal spectral bands of the circulation of PST, which barely passed the 95 % significance interval, such as the ones in the interval 1.3 to 1.6 cy/day (15 to 18 hours) with a counter-clockwise rotation in the 5 m layer and a clockwise rotation at 40 m, and the band of 2.3 to 2.7 cy/day (10.4 to 8.8 hours) with clockwise circulation at both depths.

The low frequency circulation band 0.15 to 0.4 cy/day (3 to 5 days) of PST has a mainly anticlockwise circulation at 5 m and 40 m depths. In PPR the low frequency band (not forming clear peaks) shows slightly higher clockwise rotation at 5 m and nearly equally valued clockwise and counter-clockwise circulations at 40 m, while for the 60 m layer it has a stronger clockwise and a less pronounced counter-clockwise band circulation. That description is similar to the 5 m and 40 m depths of PRJ, but the opposite to what was observed in the bottom layer (90 m), where there are two long-term bands that are equally important, but displaced in frequency, one counter-clockwise and the other clockwise. The phase relationships of *u* and *v* for the long term of PPR can also be inferred in the time domain (Fig. 5) where the progressive vector diagrams for the wind and currents at 5m, 40m and 60m depths are shown. Current vectors at the surface largely diverted from the corresponding values of the surface winds. There was a period from 26/11 to 5/12 when the wind direction changed abruptly from the south to the north direction. From this day the currents also changed the direction of propagation from nearly towards southwest to north, and at the end of the period of measurements they propagated towards east. The surface waters (0 – 15 m) in the period of 5/12 to 10/12 (Fig. 5b) had T and S characteristics between 25.3 degrees centigrade and 34.5 parts per thousand, which is within the limits of the Shelf Water in the area. From the directions of the vector diagram of the current, one can infer that an increased volume of this water was advected from the south, or climbed the shelf from depths occupied by the Sub Tropical Water (Fig 2). They did not follow the direction of the winds, and because of that the wind forcing can not be entirely taken as responsible for their variability in the period. This is typified by a slightly greater long-term clockwise spectral rotary component relative to the counter-clockwise component at the 5 m depth of PPR, which seems to also be the case for PRJ long-term bands at the same depth.

In the 40 m layer of PPR the progressive vector diagram (Fig. 5c) cannot have a similar description as for the long-term variability. The propagation of currents there, although nearly following the aspects of the surface wind variability (Fig. 5a) cannot be physically put into correspondence to the wind propagation, because the upper surface layers have a strong bias with the (0 – 15 m) depth intrusion of waters and this prevents the variability to be transferred from the surface to the currents at 40 m. They seem more to be driven by the Brazil Current that carries the Tropical Water to the southwest and infiltrates at mid depths over the shelf during the period. This can also be inferred from the salinity values greater than 36 parts per thousand and the temperature values above 20 degrees centigrade observed at 40 m depth in the repeated T, S vertical profiles (Fig. 6) that are typical of the Tropical Water. Therefore, it seems that the waters of the Brazil Current that infiltrate the shelf have counter-clockwise and clockwise rotation components with equal importance. That is also apparent, but not so pronounced, in the PST spectra and in the 40 m depth rotary spectra of PRJ.

At the bottom layer (60 m) of PPR the progressive vector diagram of currents does not seem to be related to the one at the 40 m depth (Fig. 5c), or even to the surface or the wind progressive vector

diagrams (Figs. 5a and 5b). The circulation seems at this level to be more related to the Subtropical Water that occupies the bottom layer. The characteristics of this water mass are clearly observable in the repeated CTD profiles shown in Fig 6 in the nearly homogeneous values of T and S in the 5 m thick bottom layer. Values of temperature remained during the period of measurements below 15 degrees centigrade and the salinity values remained below 35.5 parts per thousand, which are within the limits of the Subtropical Water in the area. This independent behavior of the bottom layers (60 m and 90 m) is clearly shown by the long-term rotary spectra of currents of PPR (Fig 3a) and PRJ (Fig 3c) that have a clockwise band stronger than the counter-clockwise spectral band. Particularly in PRJ the counter-clockwise and clockwise bands are shifted in frequency. All these features were not shown by the long-term rotary spectra of other layers (surface and 40 m depths) and it can be said with some assurance that the long-term bands of the spectra show aspects of the different dynamically forcing. They act in the long-term (3 to 5 days) variability of currents in the Southeastern Brazilian coast in the surface layer, at mid-depths and in the bottom layer, levels occupied by the Shelf Water, Tropical Water and Subtropical Water, respectively (Fig. 2 and Fig 6).

This level composition and circulation of the different water masses in the area seems also to produce different responses to the diurnal tidal forcing. A general characteristic of the structure of the tidal currents is that the diurnal bands of currents have greater amplitudes in the surface layers down to the 40m layer and tend to become smaller with depth. At the surface and 40 m depths of PPR, PST and PRJ, the rotary diurnal band spectra are predominantly counter-clockwise and have zero amplitudes in the clockwise circulation. This characteristic is clearly shown by the corresponding progressive vectors diagrams of PPR (Fig. 5b and Fig. 5c), with daily counter-clockwise loops of diurnal period being carried away by the circulating waters undergoing the long-term variability of each particular layer. The vector diagram for surface winds (Fig. 5a) also has two clockwise loops that are the result of surface wind action associated with two atmospheric cold fronts that passed over the area during the measurements, but these loops do not seem to have any corresponding action on the diurnal tidal currents. The diurnal bands have an average of 15 cm/s to 25 cm/s amplitude, in a total current value of the order of 40 cm/s, where these values are taken from the measurements Mesquita et al (1989), and not from the amplitudes shown in the spectra, which tend to be augmented by filtering, by smoothing of the autocovariances and by truncation of the original series. Another aspect of the diurnal currents that is not understood is the counter-clockwise circulation that is produced by tidal forcing that has clockwise propagating height components such as O_1 and Q_1 . Only the height component K_1 has a double sense of propagation in the area (Table 2) and may be taken as accelerating the diurnal currents in that direction. The corresponding values of the K_1 currents, however, are not identifiable in the vector diagrams. But the diurnal currents are the most pronounced of all current bands on the Southeastern shelf and it seems rather difficult to understand that they may be produced by Kelvin waves with such conflicting propagating heights. This is a point that, perhaps, cannot be settled with the present data set. At the bottom layer, (60 m) of PPR and (90 m) of PRJ, the diurnals do not show any peaks, but have a flat set of amplitudes with counter-clockwise rotation, that do not form a clear peak. Compared to the diurnal bands of the layers above, it can be said that counter-clockwise diurnal currents at the bottom (90 m) layer are not significantly determined even at 80% amplitude interval of significance from the present measurements. This aspect differs from what was observed in the upper layers and seems to indicate that it is related to the characteristics of the response of the Subtropical Water to the diurnal tidal forcing, which occupies the bottom layer in the area, and which differs from the responses of the other layers, which are occupied by the Tropical Water and Shelf Water.

The semidiurnal counter-clockwise currents spectral rotary bands of PPR have approximately constant amplitudes (about 10 cm/s, taken from the measurements) at all depths. At the 40 m depth the clockwise band is much higher than in the surface and 60 m depths, but has equal amplitudes in the counter-clockwise band. These aspects are not seen in the progressive vectors diagram at any of the depths, but the barotropic response of currents to the tidal semi-diurnal forcing is clearly recognizable from the rotary spectra. The semidiurnal currents seem to be accelerated by the tidal heights, as M_2 and S_2 Kelvin waves, that have a double sense of propagation and merge in the PPR area (Table 2), as already pointed out. The fact that both rotary bands have equal amplitude only at the 40 m depth

clearly seems to indicate that the Tropical Water has an equal response to the two opposing propagations of height around the two amphidromes in the South Atlantic. This aspect, however, is not clear at PST, which shows a semi-diurnal clockwise band dominating the much smaller diurnal bands at the surface and 40 m depths, and a nearly zero band for the counter-clockwise circulation. At PRJ the tidal currents are much weaker and are not dominant (Johanenssen 1968) and are represented in Fig. 4 by dashed counter-clockwise circular arrows. The total semi-diurnal spectral bands are mostly not significant, but the splitting of frequencies of the semi-diurnal counter-clockwise and clockwise spectral bands results in significance at 80% statistical levels at the surface, 40 m and 60 m depths, and this is a revision of an earlier description by Mesquita and Harari (1999) that seems to indicate double propagation of the semi-diurnal heights in the area.

This description can also be made for the ter-diurnal circulation band that is determined in PPR (except at 5 m depth) and PRJ from the total spectra to be not significant, but has in PPR a significant spectral clockwise rotation at 95% (except at 60 m depth) and in PRJ a significant spectral counter-clockwise band at 80 % confidence interval throughout the water column. The amplitude of the ter-diurnal bands are almost equal in PRJ and PPR and this does not seem to be consistent with Huthnance (1980), who predicts from an idealized shelf model an increase, from the south and the east, of the ter-diurnal heights near Paranaguá (PPR), a fact that is also seen in Table 2. The increased volume of Shelf Water that invaded the PPR area from the south may have determined the overall clockwise rotary ter-diurnal band from the surface to 40 m, and the higher values of amplitude in the 40 m depth layers of the counter-clockwise rotary band of the water column in PRJ seem to be further indication of different responses to the tidal forcing of the water masses that occupy the Southeastern area.

The fourth-diurnal bands of PPR and PRJ are the only non-linear bands induced by the tidal forcing that are not in the Tables of Tide Generating Potential (TGP) of Cartwright and Edden (1973, see their Figs. 5). Their PRJ counter-clockwise at surface, clockwise and counter-clockwise at 40 m depth and clockwise at 90 m rotary bands, added to their PPR clockwise at surface and equally-valued clockwise and counter-clockwise amplitudes at 40 m depth and shifted frequency of clockwise and counter-clockwise bands at the bottom 60 m seem also to be clear indication of the different responses of the circulation of water masses carried by the coastal currents, the Brazil Current and the Intermediate Current of the area (Fig. 2) to the tidal forces from the TGP, as well as from non-linear processes that appear to occur differently in each of them. These findings of course require further research to confirm.

Concluding remarks

The propagation of the semidiurnal tidal heights on the Southeastern coast of Brazil occurs from Imbituba towards Paranaguá and from Rio de Janeiro towards Paranaguá where they merge. The diurnal components propagate from Imbituba towards Rio de Janeiro except for K_1 , which follows the semidiurnal propagation. The ter-diurnal height propagation is also similar to that of the semi-diurnals and the fourth-diurnals are not well defined from the data under analysis. The rotary spectral analyses of currents identified five spectral bands; the long-term band (3 to 5 days), diurnal (24 h), semidiurnal (12 h), ter-diurnal (8 h) and fourth-diurnal (6 h) bands. These bands were separated into clockwise and counter-clockwise bands and we found, by interpreting these features with the progressive vector diagrams, that the long-term band of currents cannot be entirely taken as caused by the wind forcing. This was typified by a slightly greater long-term clockwise spectral rotary component relative to the counter-clockwise at (5 m) depth of PPR and at PRJ. At mid-depths (40 m) it seems that the waters of the Brazil Current that infiltrate the shelf at this level, have counter-clockwise and clockwise rotation with equal importance and at the bottom, particularly in PRJ, the counter-clockwise and clockwise bands are shifted in frequency, features not shown by the long-term rotary spectra of the layers above. These are aspects of different dynamical forcing in the area that act differently in the long-term variability of currents in the surface layer, and at mid-depths and in the bottom layer, which are levels occupied by the Shelf Water, Tropical Water and Subtropical Water, respectively, on the Southeastern Brazilian coast. The analyses of counter-clockwise and clockwise spectral bands for the diurnal

currents also indicate that these are the characteristics of the response to the diurnal tidal forcing of the Subtropical Water, which occupies the bottom layer in the area, that differs from the responses of the other layers, which are occupied by the Tropical Water and Shelf Water. These different responses of the Tropical Water to the tidal forcing are also seen in the semi-diurnal counter-clockwise currents spectral rotary bands of PPR that have approximately constant amplitude with depth, while the clockwise and counter-clockwise bands are much higher through the column, but have equal amplitudes at the 40 m depth, signaling a different response to the tidal forcing of the Brazil Current water that infiltrates the mid column. In PRJ the semidiurnal band has no significant amplitude in the total spectra, but the clockwise and counter-clockwise components are significant and show shifted significant frequency bands in the layer occupied by Subtropical Water. The currents produced total semi-diurnal spectral bands that are mostly not significant, but the splitting of the frequencies of the semi-diurnal counter-clockwise and clockwise spectral bands, which are significant at 80% statistical levels, at the surface, 40 m and 60 m depths (this is a revision of an earlier description by Mesquita and Harari, 1999) seems to indicate a response to the double propagation of the semi-diurnal heights in the area. The increased volume of Shelf Water that invaded the PPR area from the south may have determined the overall clockwise rotary ter-diurnal band from the surface to 40 m, and the higher values of the amplitude in the 40 m depth layers of the counter-clockwise rotary band of the water column in PRJ seem to be further indication of different responses of the water masses that occupy the Southeastern area to the tidal forcing. Amplitudes of the ter-diurnal bands seem to be nearly equal in the area, in either counter or clockwise bands, although this is not seen in the total spectral band. The non-linear fourth-diurnal bands along the depths seem also to give clear indication of the responses of the water masses carried by the coastal currents, the Brazil Current and the Intermediate Current of the area (Fig. 2) to the tidal forces from the TGP, as well as to the non-linear processes that appear to occur differently in each of them.

Acknowledgements. We are grateful to FINEP (Financiadora de Estudos e Projetos), of the Presidency of Republic of Brazil, to FAPESP, (Fundação de Amparo à Pesquisa do Estado de São Paulo) and the British Council, UK.

References

- Cartwright, D. E. & Zetler B. D., (1985). Pelagic Tidal Constants. *IAPSO Scientific Publication*, 33. 1-53.
- Cartwright, D. E. & Edden A. C., (1973) Corrected tables of tidal harmonics, *Geophys. J. R. Astron. Soc.*, 33: 253-264.
- Emilson, I. (1961). The Shelf and coastal waters off southern Brazil. *Bolm. Inst. oceanogr.*, S. Paulo. 11 (2) : 101 - 112.
- França, C. A. S. . (1988). Estudo da Geração das Componentes da Maré de Pequeno Fundo na Costa Sudeste Brasileira. Dissertação de Mestrado. Inst. Oceanogr. Univ. S. Paulo. S P. 159 pp.
- Franco, A. S. & Rock, N. J. . (1971). The fast Fourier transform and its application to tidal oscillation. *Bolm. Inst., oceanogr. Univ. S. Paulo. SP.*
- Franco, A. S. dos & Mesquita A. R. de (1986). On the practical use in Hydrography of Filtered daily values of mean sea level. *Int. HIDRg. Rev.Monaco LXIII(2):133-141.*
- Gonella, J. (1972). A Rotary- component method for analysing meteorological and oceanographic vector time series. *Deep Sea Res.*, 19 : 833 – 846.
- Harari, J. (1977) Modelo tridimensional da região costeira Centro Sul do Brasil. Dissertação de Mestrado. Instituto Oceanográfico da Universidade de São Paulo. SP. 118 pp.
- Harari, J. 1984. Modelo hidrodinâmico tri-dimensional linear da plataforma continental Sudeste do Brasil. Tese de Doutorado. Instituto Astronômico e Geofísico da USP. 203 pp.
- Harari, J. (1991). Modelo hidrodinâmico tridimensional do Oceano Atlântico Sul. Tese de Livre Docência. Instituto Oceanográfico da USP. 350 pp.
- Huthnance, J. M. (1980). On shelf “resonance” with application to Brazilian M_3 tides. *Deep Sea Research*, Vol. 27A: 347-366.
- Jenkins, G M and D G Watts (1968). Spectral Analysis and its applications. Holden- Day. San Francisco London, Panama Toronto. 523 pp.

- Johannessen O. M. 1968. Note on some hydrographical and current observations from three positions on the Brazilian shelf in the region of Cabo Frio - Santos 1966. *Contribuições Inst. oceanogr. Univ. S. Paulo, ser. oceanogr. fis.*, 10 : 1 - 8.
- Leite, J. B. A. (1983). Estudos da variação temporal de temperatura e salinidade do sistema de correntes e sua estabilidade numa área de ressurgência. Tese de Mestrado. Instituto Oceanográfico da USP. 178 pp.
- Mesquita, A R de, Joao Bastista, Weber R. & Tupinambá P. M. (1976a). Variabilidade dos parâmetros físicos durante a realização da Estação 3.099 do *Noc Prof W Besnard*: Cruzeiro 78. Relat. de cruz. *Noc Prof W Besnard*. Inst.oceanogr. Univ. S Paulo, (1) : 1 – 13.
- Mesquita, A. R. de, Souza, J. M. C., Leite, J. B. de A, & Festa, M. 1976b. Variabilidade dos parâmetros físico químicos durante a realização da estação 3.144 do *Noc. Prof W Besnard*. Cruzeiro 80. Relat. Cruz. *Noc Prof W Besnard*. Inst oceanogr. Univ. S. Paulo., SP. (2): 1 – 28.
- Mesquita A. R. de, Souza, J. M. C., Tupinambá, P. M. , Weber, R. , Festa, M. & Leite, J. B. A. (1977). Correntes rotatórias e variabilidade do campo de massa na plataforma do estado de São Paulo (Ponto : 25° S ; 46° W). Relat Cruzeiros sér *NOc Prof W Besnard*. Inst. oceanogr. Univ. s. Paulo. SP 3: 1 - 37.
- Mesquita, Leite & Rizzo (1989), - Patterns of Instability in a Region of Shelf Break Upwelling. Proc. SIUEC (1982: Nov. 21 - 27 : Rio Grande, RS. Brazil). Vol 2 : 425 - 436.
- Mesquita, A. R. de, Pereira, N. F., Leite, J. B. de A & Rizzo, R. 1989. Circulation and evidence of Shelf Break Upwelling, Brazil, near Lat 26° S: Long 47° W. Relat Cruz. sér *NOc Prof W Besnard*. Inst oceanogr. Univ. S.Paulo. N 8 : 1-27.
- Mesquita, A. R. de ,Leite , J. B. A. & Rizzo R. (1983). A Note on the shelf Break Upwelling off the Southeast coast of Brazil (Lat. 21° 50 S ; Long 33° 05 W) Bolm. Inst. oceanogr. Univ. S. Paulo SP. 32 (2) : 193 - 198
- Mesquita, A. R. de & Harari, J. (1983). Tides and Tide auges of Cananéia and Ubatuba. Relat. int. Inst.oceanogr. Univ. S. Paulo. SP. (11) : 1 - 14.
- Mesquita, A. R. de & Leite, J. B. A. (1986). Sobre a Variabilidade do Nível Médio do Mar na costa Sudeste do Brasil. *Rev. bras. de Geofis.* Vol (4): 229
- Mesquita A. R. de (1983) . Contribuição à Oceanografia da Região Costeira Sudeste do Brasil (Lat 24° S) - Sub Projeto Hidrodinâmica Costeira : Execução e Resultados. Thesis of Livre Docência presented to the Instituto Oceanográfico da Universidade de São Paulo. SP. 187
- Mesquita A. R. de (1994).Variação do Nível Médio do Mar de Longo Termo. Inst. est. avanc. Univ. S Paulo. SP. Documentos-Série Ciências Ambientais.Vol(20):47-67.
- Mesquita, A. R. de & Harari, J. (1999). Propagation of Tidal curenets and Circulation of Tidal Currents on the Southeastern Brazilian Shelf. *Afro-America GLOSS News*. Vol 3(2) : 2-8.
- Munk, W. H. & Cartwright , D. E. (1966). Tidal Spectroscopy and prediction. *Phil. trans. Roy. Soc.*, Ser. A, Mathematical and Physical Sciences. n 1105, Vol (259) : 533 - 581.
- Smithson, M J (1992). Pelagic Tidal Constants. IAPSO (International association for the Physical Sciences of the Oceans o the IUGG) 33: 1 191.
- Spencer, R. & Gwiliam, T. J. P. (1974). Sea bed capsule for measuring pressure at depths up to 4000 metres. Proc., of IEEE. Inter. conf. Ing In the Ocean Environment. Vol(1): 339 - 343.

Table 1. Programme of measurements

Station Name	Santos platform (PST)	Rio de Janeiro Platform (PRJ)	Paranaguá Platform (PPR)	Paranaguá Platform (PPR)	Santa Catarina Platform (PSC)
Latitude (S)	25° 1.0'	23° 23.0'	26° 7.4'	26° 18.1'	28° 30'
Longitude (W)	45° 42.0'	43° 17.0'	47° 39.4'	47° 30.4'	47° 31'
Depth (m)	92	100	60	74	170
Beginning and end times of the tidal record	22/07/1977 12:00 to 04/08/1977 10:15 (GMT)	21/07/1978 to 21/08/1978 GMT	NO	18/06/1981 to 17/07/1981 GMT	28/12/1984 to 27/01/84 LOCAL
Extension of the tidal record (days)	12.9	31.2	NO	29.0	77.0
Sampling interval (min)	15	15	NO	15	30
Beginning and end times of the current meter observations	21/07/1977 22:00 to 03/08/1977 02:00 (GMT)	22/07/1978 to 3/08/1978 GMT	29/11/1980 to 12/12/1980 (GMT)	NO	NO
Extension of the current meter observations (days)	12.3	12.5	12.9	NO	NO
Sampling interval (hours)	4	1	1		
Current meter Sampling depths (m)	05, 15, 30, 40	00-10, 20-30, 40-50, 60-70, 80-90	05-10, 20-30, 40-50	NO	NO
Oceanographic and surface meteorological measurements	YES	YES	YES	NO	NO

Table 2. Main tidal constants of the Southeastern Brazilian Shelf (França, 88)

	Q1		O1		K1		M2		S2		M3	
	amp	phase	amp	phase	amp	phase	amp	phase	amp	phase	amp	phase
RIO	3.0	105.2	10.8	127.5	5.9	184.4	31.6	162.0	17.2	166.4	0.6	302.6
UBA	2.4	103.4	11.0	125.6	6.0	185.8	29.8	164.4	17.4	172.9	1.2	325.0
SAN	3.1	92.7	11.2	121.6	6.5	186.3	36.4	171.7	22.6	178.8	5.4	3.3
CAN	2.4	106.5	11.4	125.6	6.5	190.8	36.8	180.2	23.9	184.5	6.7	3.8
PRG	3.6	106.2	11.9	129.9	7.3	189.9	45.9	193.7	30.0	198.6	15.4	52.8
SFS	0.0	0.0	6.8	124.6	3.4	182.7	21.1	136.1	14.4	126.3	5.8	301.7
IMB	0.9	93.9	3.6	113.9	2.1	176.9	4.4	148.9	3.4	145.8	0.0	0.0
PRJ	2.7	102.4	9.4	124.7	6.0	191.0	25.4	160.5	14.3	167.7	0.6	201.3
PST	2.9	101.9	10.7	122.1	4.8	199.5	22.5	162.7	15.2	179.8	2.0	349.6
PPR	3.3	95.9	10.8	114.8	6.6	179.3	24.6	157.3	16.0	158.3	4.1	302.5
PSC	2.6	75.6	10.8	105.0	6.2	166.0	12.1	145.3	8.3	138.8	0.8	262.9

Figure 1. Southeastern Brazilian Shelf

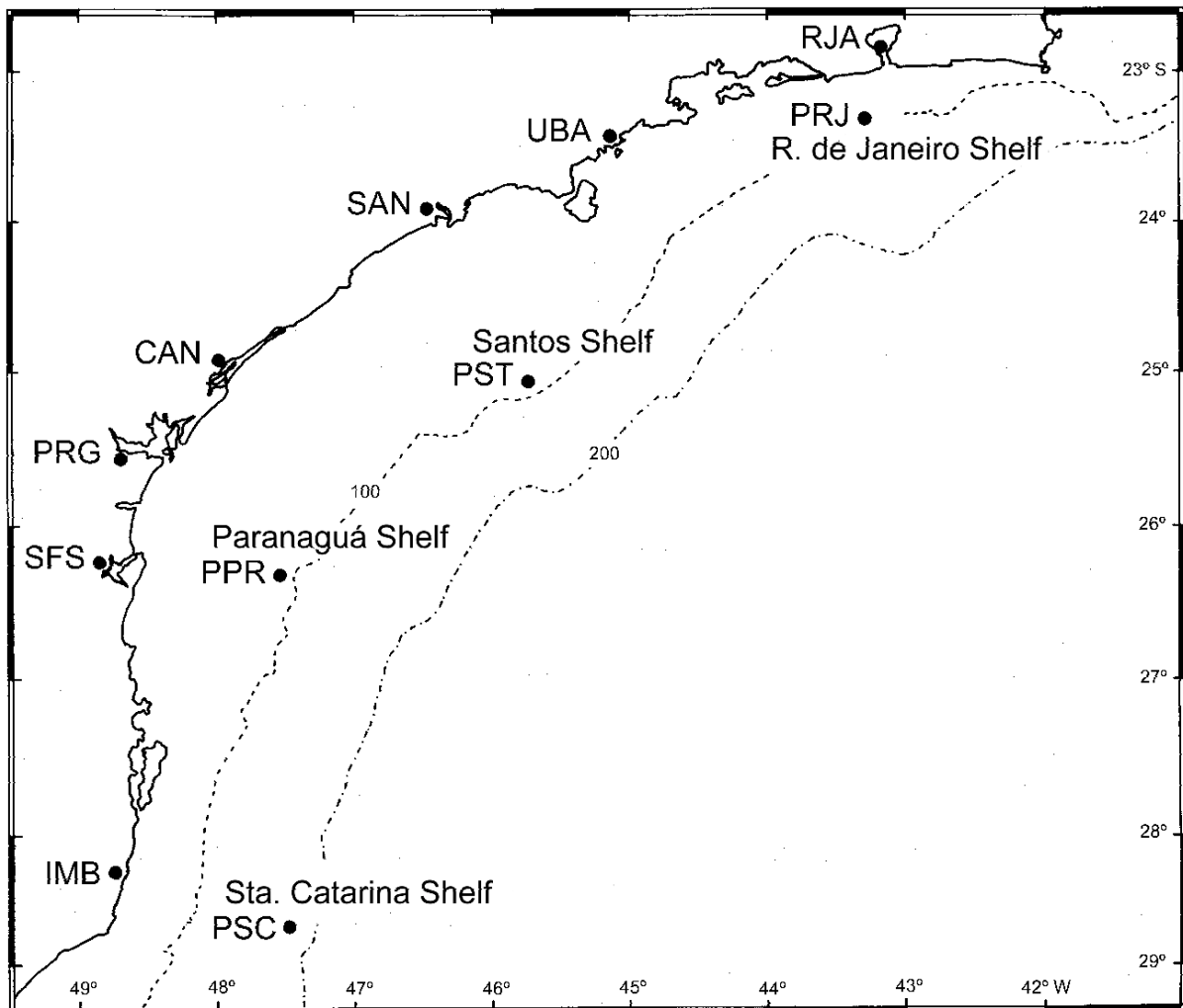


Figure 2. Water masses of the Southeastern Brazilian Shelf, (Emilson, 61 & Mesquita, 83)

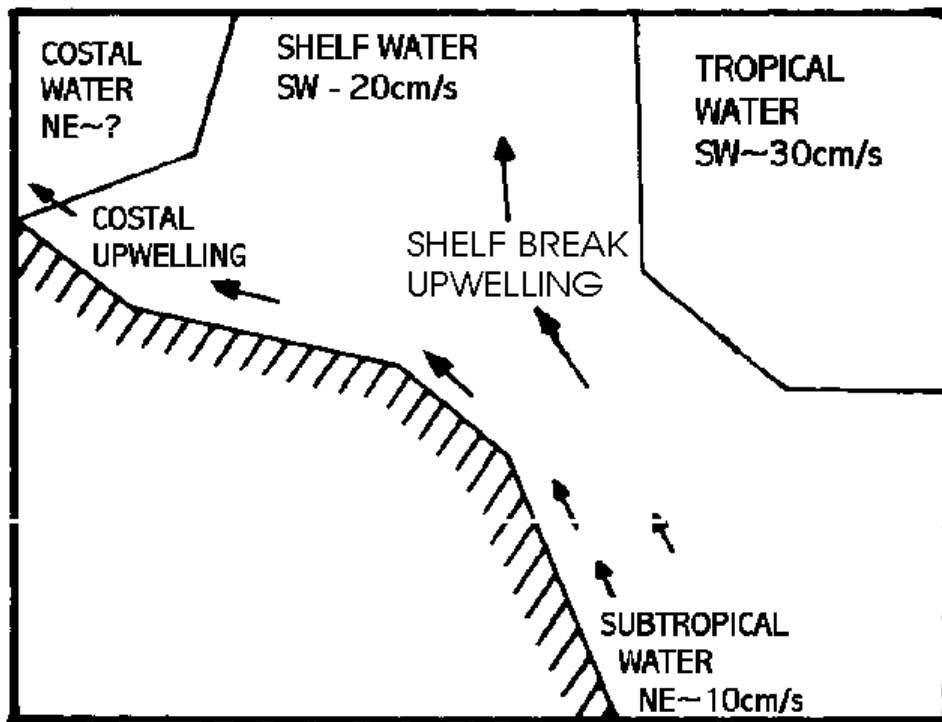


Figure 3a. Current rotary spectra of PPR 0 m, (Mesquita, 83)

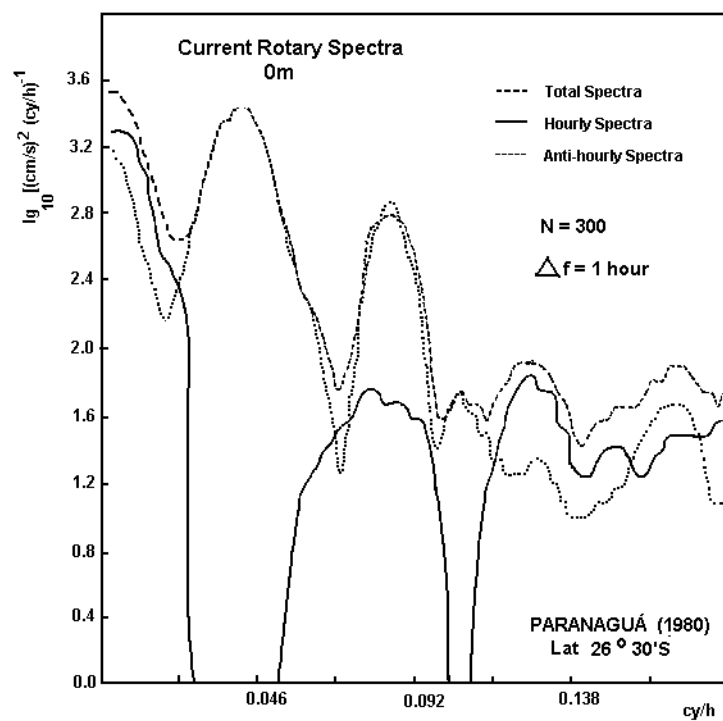


Figure 3a. Current rotary spectra of PPR 40 m, (Mesquita, 83)

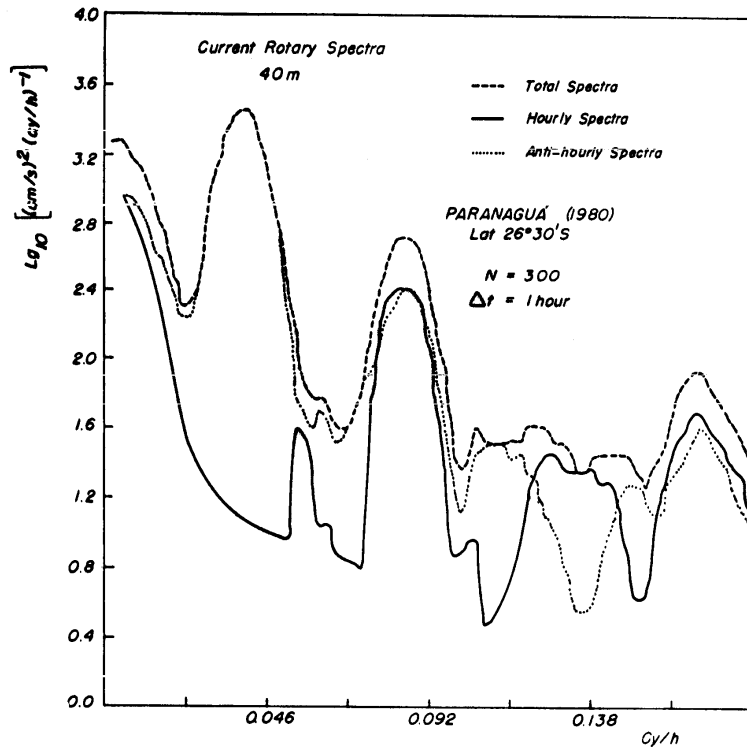


Figure 3a. Current rotary spectra of PPR 60 m, (Mesquita, 83)

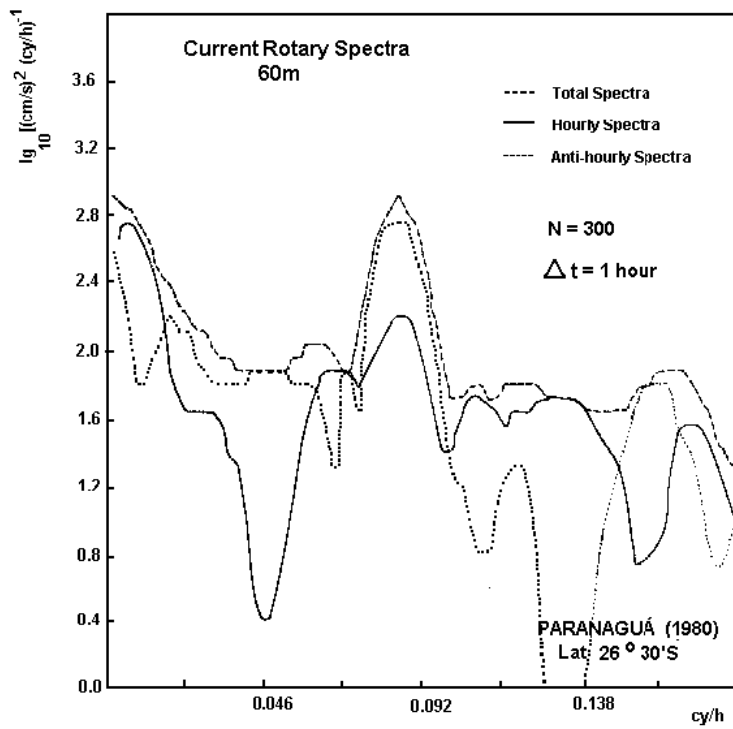


Figure 3b. Current rotary spectra of PST 0 m, (Mesquita et al., 76a)

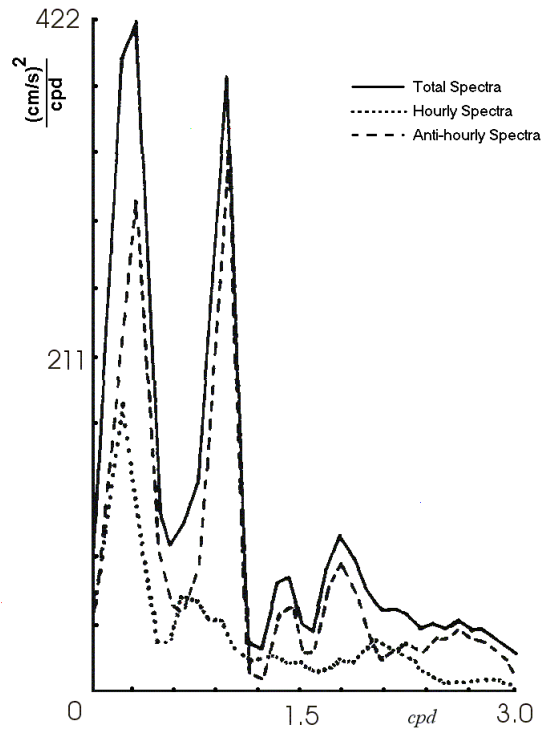


Figure 3b. Current rotary spectra of PST 40 m, (Mesquita et al., 76a)

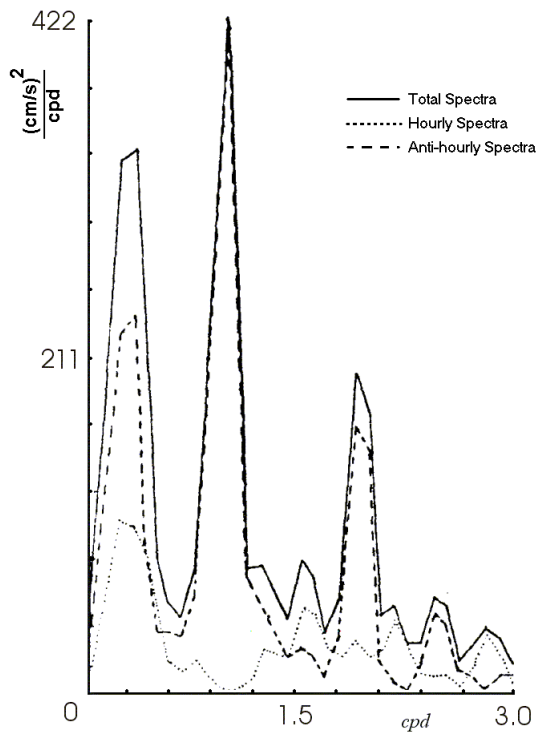


Figure 3c. Current rotary spectra of PRJ 0 m, (Leite, 1983)

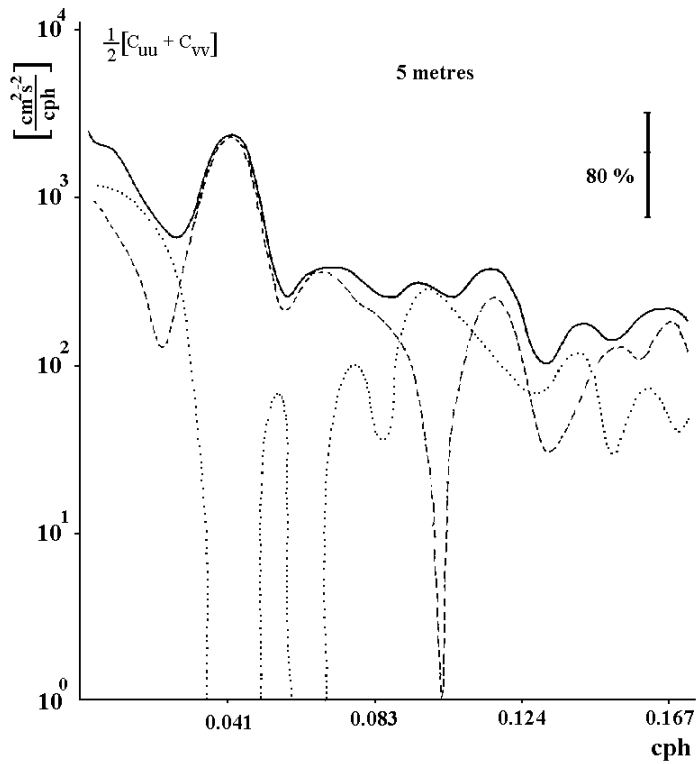


Figure 3c. Current rotary spectra of PRJ 40 m, (Leite, 1983)

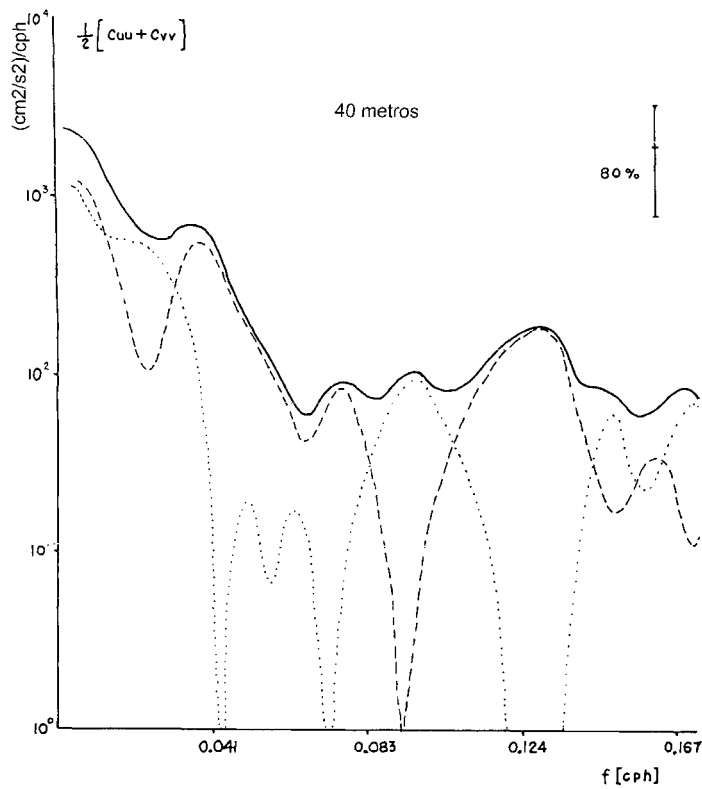


Figure 3c. Current rotary spectra of PRJ 90 m, (Leite, 1983)

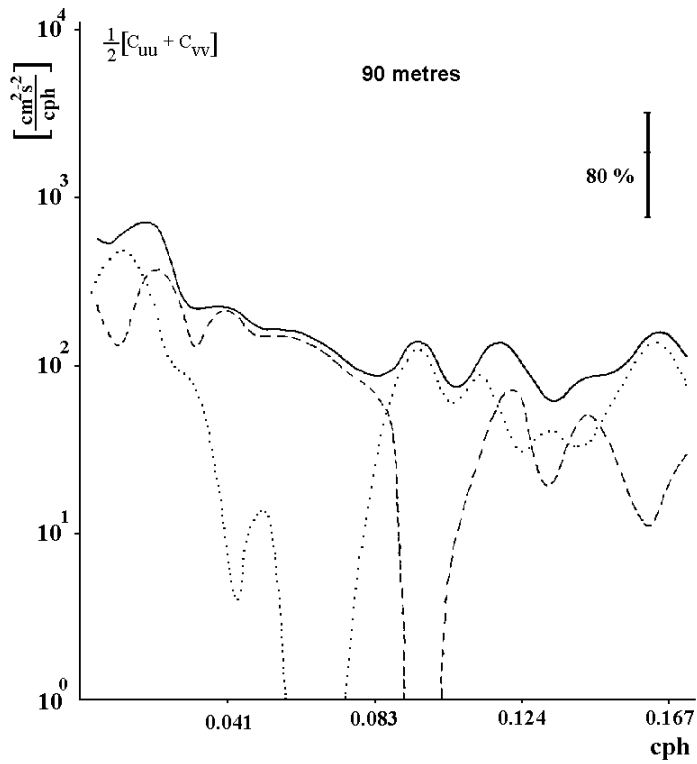


Figure 4. Schematic distribution of surface current in the Southeastern Brazilian Shelf, (Mesquita, 83 & Mesquita & Leite, 86)

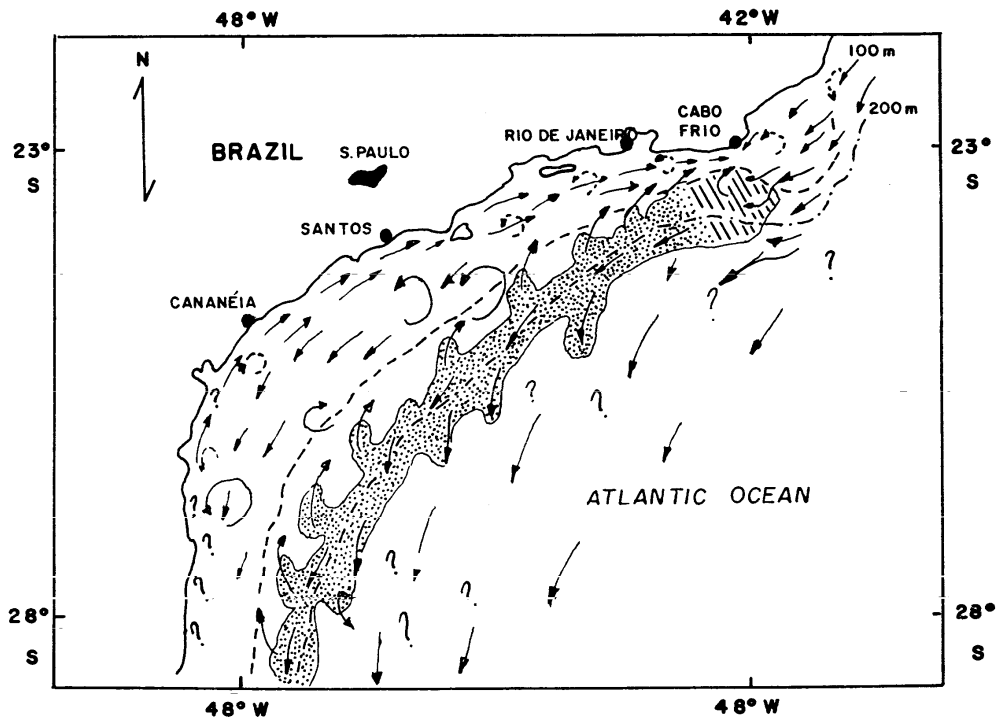


Figure 5a. Progressive vector of wind measurements in PPR, (Mesquita et al., 89)

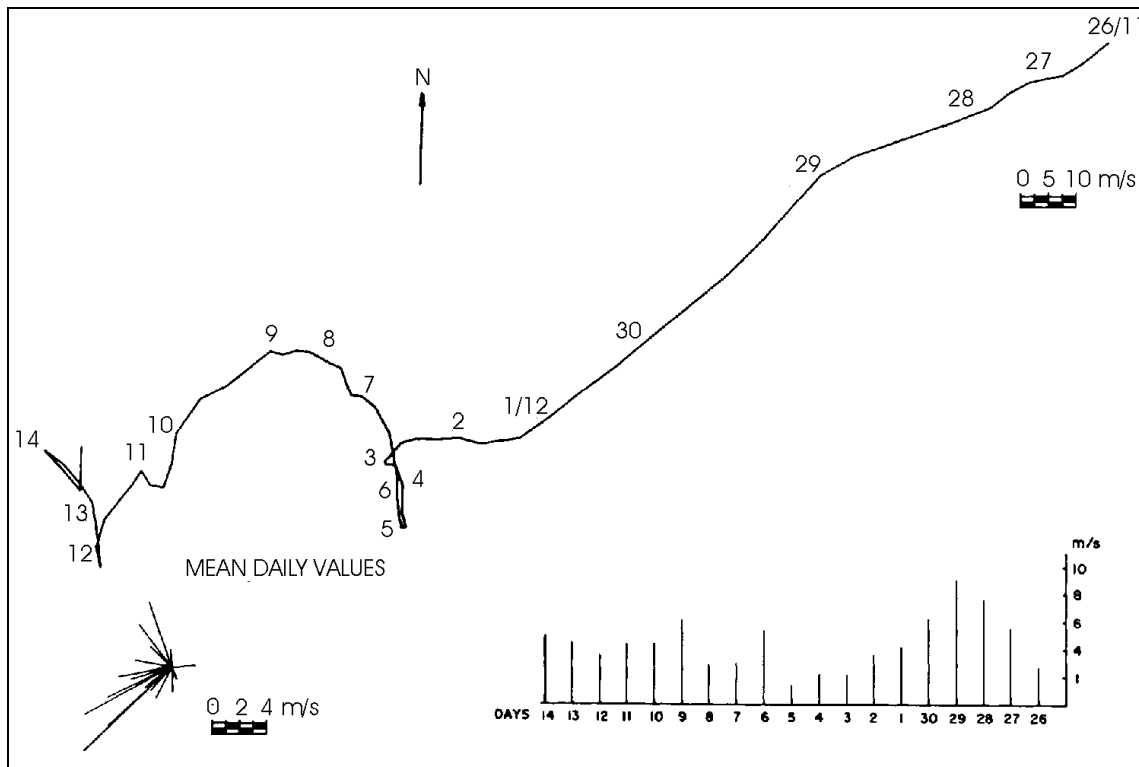


Figure 5b. Progressive vector of current measurements in PPR – 5 m, (Mesquita et al., 89)

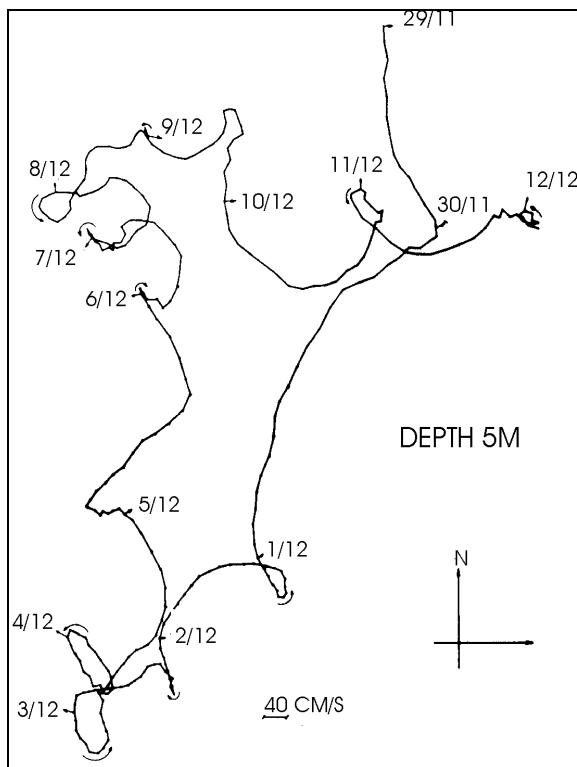


Figure 5c. Progressive vector of current measurements in PPR – 40 m, (Mesquita et al., 89)

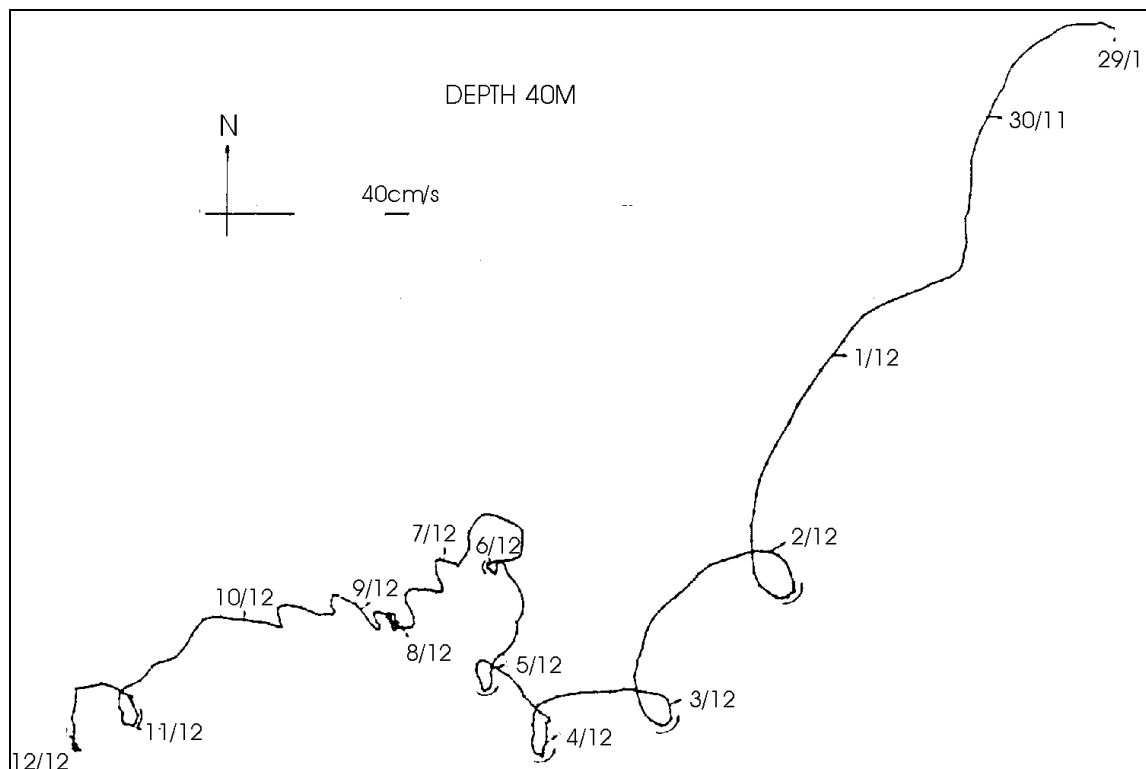


Figure 5d. Progressive vector of current measurements in PPR – 60 m, (Mesquita et al., 89)

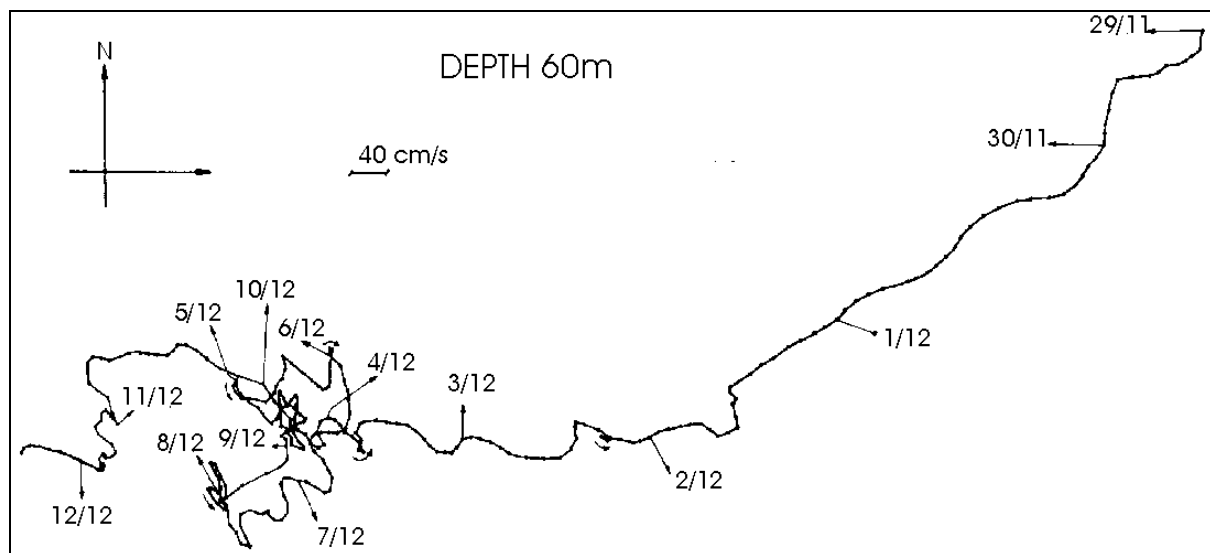
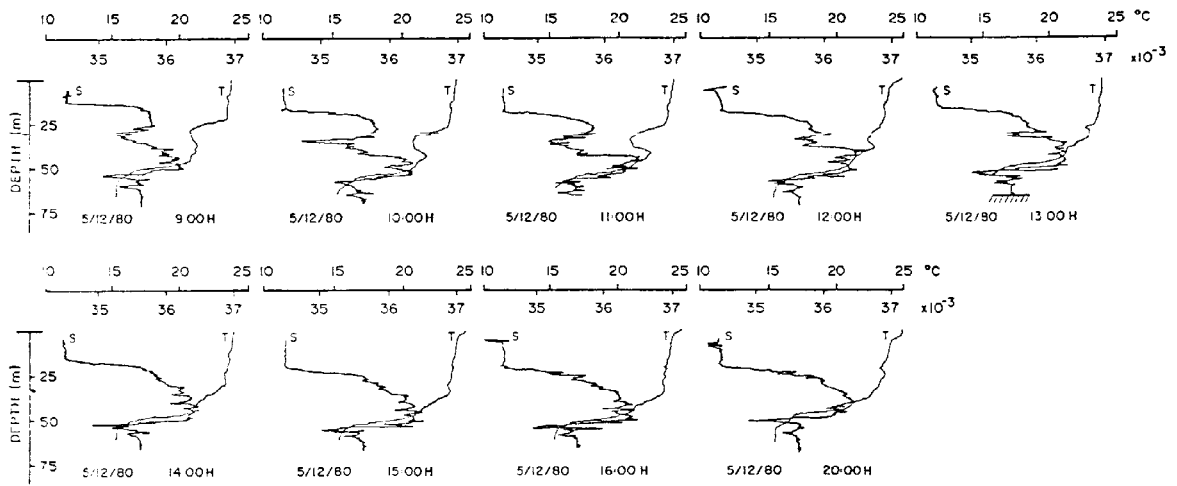


Figure 6. Temperature and salinity vertical profiles of PPR, (Mesquita et al., 89)



**An evaluation of the sea level observing
network in the western Indian Ocean**

M. Odido
Kenya Marine & Fisheries Research Institute
P.O. Box 81651
Mombasa, Kenya

Julius Francis
Institute of Marine Sciences
P.O. Box 668
Zanzibar, Tanzania

The earliest sea level records from the Western Indian Ocean coasts and islands are from Durban (1926), Mombasa (1932), and Port Louis (1942). However, there is evidence that the Port Louis and Port Elizabeth stations were installed earlier than the dates for which data is available from them (1920's and 1937 respectively). In subsequent years gauges have been installed at all the major ports in the region. These, however, seem to have operated well for rather short spans of time.

The early 1960's saw a marked increase in the number of stations submitting data to international centres. This was the period that the International Indian Ocean Expedition was on. In the 1970's the number of gauges operational began reducing again until mid-1985 when the TOGA experiment was launched at around the same time with the Global Sea Level Observing System (GLOSS). Since then there has been a consistent improvement in quality of data generated by the various established centres, and also an increase in the number of operational gauges.

GLOSS STATIONS IN THE WIO REGION

The GLOSS Implementation Plan identified 23 stations in the region:

- 1) Djibouti (DJIBOUTI)
- 2-3) Hafun, Mogadishu (SOMALIA)
- 4) Mombasa (KENYA)
- 5-6) Zanzibar, Mtwara (TANZANIA)
- 7-8) Port Victoria, Aldabra (SEYCHELLES)
- 9-10) Pemba, Inhambane (MOZAMBIQUE)
- 11)-15) Dzaoudzi, Pointes des Galets, Crozet, Kerguelen, St. Paul (FRANCE)
- 16)-17) Nosy Be, Fort Dauphin (MADAGASCAR)
- 18)-20) Port Louis, Agalega, Rodrigues (MAURITIUS)
- 21)-23) Durban, Marion Island, Port Elizabeth (SOUTH AFRICA)

The GLOSS Implementation Plan of 1997, categorises most of the tide gauges into three groups: GLOSS-LTT, GLOSS-ALT and GLOSS-OC.

The GLOSS-LTT consists of gauges with at least 40 or 60 years of data. None of the WIO gauges meet this condition. Nevertheless, some of the gauges with medium length records (i.e. typically 20-30 years) from the region have also been included in this category. These are Simon Bay, Port Elizabeth, Durban, Nosy-be, Port Louis, Mombasa.

The GLOSS-ALT consists of gauges selected based on the following criteria:

- Representative of the nearby deep ocean variability;
- geographic coverage;
- provision of GPS and Doppler Orbitography and Radiopositioning Integrated by Satellite (DORIS).

For the WIO region, only Port Louis in Mauritius belong to this group, as it does meet some of the conditions.

The GLOSS-OC comprised of tide gauges which can be used for ocean circulation studies in: across narrow straits, wider "straits", "choke points" and basin-sections; and along polar coastline, particularly that of Antarctica. None of the gauges in the WIO region could be used for that purpose as these features are none existence in the region.

The International Sea Level Workshop held in Hawaii, USA in 1997 identified a number of tide gauges from the region that could be used for the studies on Indian Ocean Monsoons – seasonal to decadal variability. This include Mombasa, Zanzibar, Rodrigues, Port Louis and Port Victoria.

OTHER SITES IDENTIFIED FOR SEA LEVEL STATIONS

In addition to these, a regional workshop on 'Causes and Consequences of Sea level changes on the Western Indian Ocean Coasts and Islands' held in Mombasa, Kenya in 1991, and the reports of national experts who were identified to evaluate the status of sea level observation in their respective countries recommended the following extra gauges of regional or national importance.

- 1) Kismayo (SOMALIA)
- 2-5) Kiunga, Lamu, Malindi, Shimoni (KENYA)
- 6-8) Tanga, Dar es Salaam, Pemba (TANZANIA)
- 9-16) Maputo, Beira, Nacala, Quelimane, Angoche, Chinde, Mocimbe de Praia, Vilanculo (MOZAMBIQUE)
- 17-20) Majunga, Toliara, Morondova, Manakara (MADAGASCAR)
- 21) Moroni (COMOROS)
- 22-26) Farquhar, Praslin, Bird Island, Amirantes, Coevity (SEYCHELLES)

South Africa did not participate in the workshop, but the following stations have been in operation on South African Indian Ocean coastline and could also be included in the list:

- 27-30) Mossel Bay, Knysna, East London, Richards Bay (SOUTH AFRICA)

This makes a total of 50 stations to serve all interests (national, regional and international).

Installation and operation of sea level stations

The number of operational stations has risen progressively from a low point of one in 1968 to the current 20. By the beginning of 1985, when the GLOSS proposal was adopted, only five of the stations in the network were operational: Zanzibar, Dzaoudzi, Pointe des Galets, Durban and Port Elizabeth.

The situation as at the end of 1998 was as follows:

24 INSTALLED AND OPERATIONAL STATIONS:

These included:

13 GLOSS stations: Mombasa, Zanzibar, Port Victoria, Port Louis, Rodrigues, Pemba (Mozambique), Nosy Be, Fort Dauphin, Port Elizabeth, Durban, Kerguelen, Crozet and St. Paul.

11 Non-GLOSS stations: Lamu, Dar es Salaam, Pointe La Rue, Maputo, Beira, Nacala, Pemba, Mossel Bay, Knysna, East London and Richards Bay.

31 NON OPERATIONAL STATIONS:

10 GLOSS stations: Djibouti, Hafun, Mogadishu, Mtwara, Aldabra, Inhambane, Dzaoudzi, Pointes des Galets, Agalega, Marion Island.

21 Non-GLOSS: Kismayo, Kiunga, Malindi, Shimoni, Tanga, Pemba (Tanzania), Quelimane, Angoche, Chinde, Mocimba de Praia, Vilanculo, Majunga, Toliara, Morondova, Manakara, Moroni, Praslin, Farquhar, Bird Island, Amirantes, Coevity.

The gauges installed at Agalega have been washed away twice by cyclones. It may therefore require special technology to install a gauge at this site. The same applies to Aldabra.

Most of the early stations were installed as part of harbour development activity. The institutions, which maintained the gauges initially were therefore mainly, harbour authorities. This included the South African Railways and Harbours Corporation, and the East African Railways and Harbours Corporation. In some instances the quality and volumes of data deteriorated once sufficient data for reasonable predictions had been collected. Other organizations like IHP and SHOM and ORSTOM also installed some of the sea level stations.

The Munro float, or Kent float gauges were initially the most popular gauges in the English speaking countries, whereas OTT R16 was more popular in the other countries (Mozambique, Madagascar, Reunion-France).

In mid 1980's the University of Hawaii (UH) replaced several of the Munro's with Leopold Stevens (float). These too were analogue gauges using batteries. The stations sent the charts, together with tide staff readings to UH for digitizing. The Leopold Stevens gauges were in turn replaced after a short time with Fischer and Porter (float) gauges. The need for frequent replacement of charts and batteries were two shortcomings of the LS and FP gauges. Where the stations are not checked frequently, or the chart gets finished over a weekend several days of data could be lost. Charts were not available locally and had to be shipped in from UH. These were at times lost while being mailed to UH. This led to loss of data of up to six months since in most cases the processing of the data was not done locally.

The stations that were installed by UH have since been upgraded to Hander Encoder. The batteries were replaced with solar panels, while real-time transmission of data via satellite was also incorporated in some of the stations. The data is also stored on site on the encoder's memory, as well as on diskette.

The South African stations were changed from KENT to LEA, which were not very successful. They were then all changed to SRD Acoustic gauges 1996, after less than a year of operation. There are plans to install float gauges at all the stations to operate side-by-side with the SRDs.

Madagascar, Mozambique and Reunion still operate the OTT R16.

Transmission of data to local/international centres

The mode of transmission of data to the local/international centres varies depending on the station. Most of the stations installed by UH transmit data hourly to the UHSLC. The staff readings and a diskette with the data are also sent by mail to Hawaii on a monthly basis.

The data from the South African stations are transferred to the national data centre weekly via modem/telephone.

The other stations operational in the region still use charts, which have to be changed and sent to the national centre for digitizing. Poor communication with outlying stations means that there is a delay in data delivery, and even in identifying problems with the instruments.

CONTRIBUTING FACTORS TO NON-OPERATION OF STATIONS

The following are some of the problems that lead to sea level stations not being operational or delivering poor quality data:

- Marine growth blocking tide well orifice (e.g. Pte des Galets)
- Marine growth covering pneumatic sensors under water (e.g. Old Lamu)
- Tide wells knocked by boats/ships (e.g. Tulear, Dar es Salaam)
- Construction at harbour leading to removal of equipment/benchmarks (e.g. Mombasa, Port Victoria, Tulear)
- Incorrect installation of gauges (e.g. Pemba-Tanzania)
- Hostile environment (cyclones etc) (e.g. Agalega, Aldabra)
- Shortage of consumables (charts, batteries)

Recommendations

1. The priority need is to develop and strengthen institutional linkages between the national organisations with an interest in sea level data collection and processing. This includes: hydrographic and surveying departments, marine research institutions, meteorological organisations, universities, and port and harbour authorities. This will enable the optimal use of available capacity for production of a continuous time series of quality data.
2. Concerted efforts should be made to ensure that the installation of the sea level network in the region is completed, with priority being given to stations of global and regional importance. The GLOSS Group of Experts should explore the means to activate/install gauges in Somalia.
3. Basic tools should be provided to tide gauge technicians to enable them perform minor repairs and maintenance checks.
4. The institutions operating the stations should ensure regular levelling (at least once a year) of the tide gauge benchmarks. Expertise available locally (at national level) should be explored before resorting to external expertise for this. Records should be maintained of the levelling, and benchmark changes.
5. Available capacity for collection, processing and analysis of sea level data should be strengthened through: i) refresher courses and workshops to introduce new technologies and techniques, and ii) short-term attachments and on-site training for technicians and scientists.
6. National Oceanographic Data centres in the region should archive copies of all data collected at stations in their respective countries.
7. There is a need for real-time transmission of data for all global and regional stations, and weekly transfers (or longest delay of one month) from national stations.

8. Measurements of additional parameters at tide gauge locations are necessary, especially atmospheric pressure, atmospheric temperature, winds, water temperature, and salinity.
9. It is important to have GPS stations at key locations in the region. Data from operational GPS stations should be available, and training on GPS/Sea level data linkages be provided to local experts.
10. Efforts must be made to collect historical data available in analogue format. These should be digitized, quality controlled and archived in the NODCs.
11. Regional Group of Experts should be created to stimulate and direct oceanographic research, and especially to address the analysis and interpretation of data collected in the region from global programmes such as TOGA and WOCE. The group of experts should be established within the framework of WIOMSA.
12. A follow-up regional workshop on sea level changes should be organized. This time the theme should be broadened to cover other aspects of physical oceanography (Ocean Processes and Climate).

The resources available for research, particularly physical sciences, have continued to dwindle. Due to this, and the fact that most of the data collected during the TOGA and WOCE experiment in the Western Indian Ocean have not been analyzed, priority should be given to analysis of these data to generate information that could be useful to the region.

REFERENCES

- GCOS-GOOS-ICPO (1998). International Sea Level Workshop-Workshop Report, 10-11 June 1997, Honolulu, Hawaii, USA.
- Neilan R., Van Scoy P.A., and Woodworth. P.A. (1997) Proceedings of Workshop on Methods for Monitoring of Sea level, March 17-18 1997, Pasadena, California USA
- UNESCO (1988) IOC Regional Committee for the Co-operative Investigation in the North and Central Western Indian Ocean: Second Session. 7-11 December 1987 Arusha, Tanzania. *Intergovernmental Oceanographic Commission. Reports of Governing and Major Subsidiary Bodies*
- UNESCO (1990) Global Sea Level Observing System (GLOSS) Implementation Plan. *Intergovernmental Oceanographic Commission Technical Series no.35*
- UNESCO (1993) IOC Regional Committee for the Co-operative Investigation in the North and Central Western Indian Ocean: Third Session. 14-18 December 1992 Vacoas, Mauritius. *Intergovernmental Oceanographic Commission. Reports of Governing and Major Subsidiary Bodies*
- UNESCO (1994) IOC-UNEP-WMO-SAREC Planning Workshop on an Intergrated Approach to Coastal Erosion, Sea Level Changes and their Impacts 17-21 January 1994 Zanzibar, United Republic of Tanzania. *Intergovernmental Oceanographic Commission Workshop Report no.96*
- UNESCO (1994) IOC-UNEP-WMO-SAREC Planning Workshop on an Intergrated Approach to Coastal Erosion, Sea Level Changes and their Impacts: Submitted Papers: 1. Coastal Erosion 17-21 January 1994 Zanzibar, United Republic of Tanzania. *Intergovernmental Oceanographic Commission Workshop Report no.96-Supplement 1*

UNESCO (1994) IOC-UNEP-WMO-SAREC Planning Workshop on an Intergrated Approach to Coastal Erosion, Sea Level Changes and their Impacts: Submitted Papers: 2. Sea Level 17-21 January 1994 Zanzibar, United Republic of Tanzania. *Intergovernmental Oceanographic Commission Workshop Report no.96-Supplement 2*

UNESCO (1997) IOC Regional Committee for the Co-operative Investigation in the North and Central Western Indian Ocean: Fourth Session. 6-10 May 1997 Mombasa, Kenya. *Intergovernmental Oceanographic Commission. Reports of Governing and Major Subsidiary Bodies*

UNESCO (1991) IOC-SAREC-KMFRI Regional Workshop on Causes and Consequences of Sea – Level Changes on the Western Indian Ocean Coasts and Islands, 24-28 June 1991. *Intergovernmental Oceanographic Commission Workshop Report no.77*

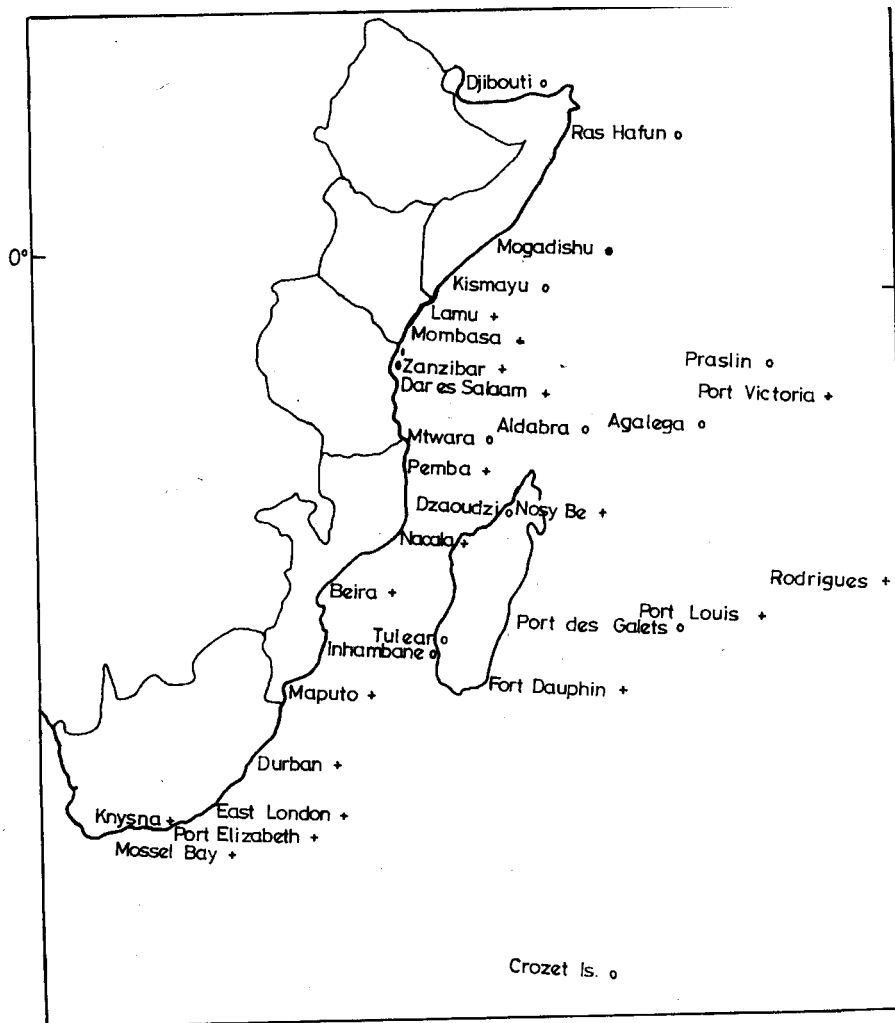


Figure 1 : Sea level Stations in the Western Indian Ocean

- + Operational
- o Non operational

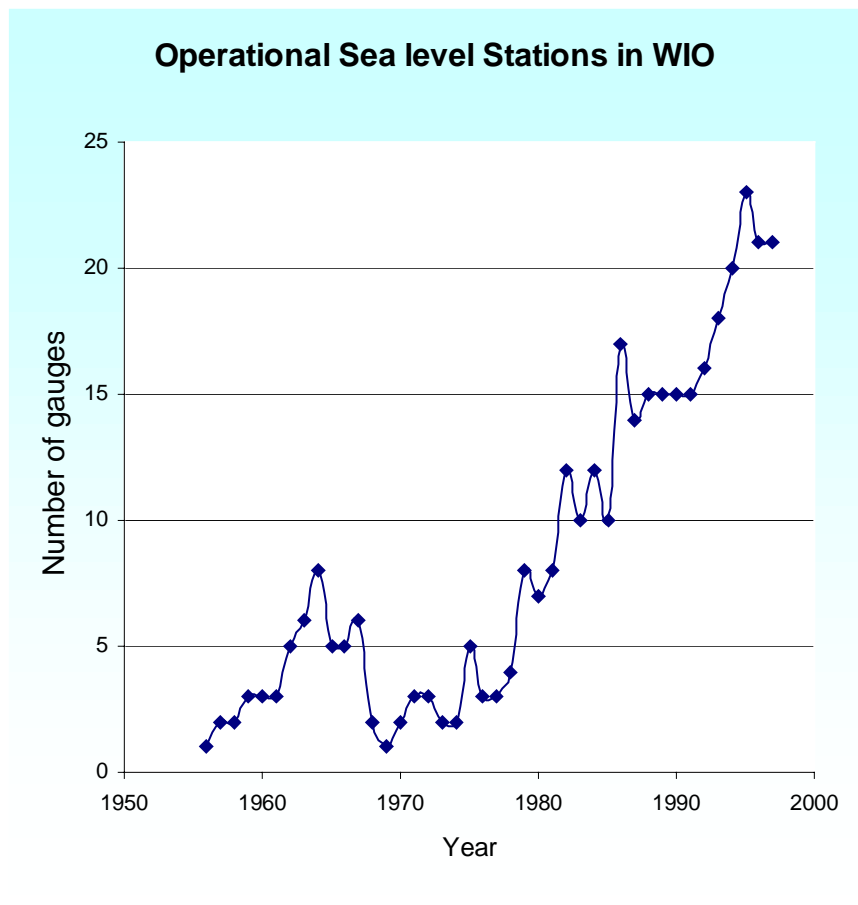


Figure 2: Number of Operational Stations per year from 1956 to 1998

Table 1: Organizations that have installed gauges in the region.

ORGANIZATION	GAUGES INSTALLED
University of Hawaii	OPERATIONAL: <i>Lamu, Mombasa, Zanzibar, Pointe La Rue, Port Louis, and Rodrigues (Port Mathurin)</i> NON-OPERATIONAL: <i>Mogadishu, Kismayo, Dar es Salaam, Praslin and Agalega.</i>
Tanzania Harbours Authority (THA)	<i>Dar es Salaam</i>
Brigade Hydrographique et Topographique des Seychelles (BHTS)	<i>Port Victoria</i>
Instituto Nacional de Hidrografia e Navegacao (INAHINA)	<i>Maputo, Inhambane, Beira, Nacala, Pemba</i>
Foiben Taosarintanin'i Madagasikara (FTM) - Institute for Geography and Hydrography	<i>Nosy Be, Toliara, Taolagrano</i>
Hydrographic Office - South African Navy	<i>Mossel Bay, Knysna, East London, Durban, Port Elizabeth, Richards Bay</i>

In addition to these, several gauges have been installed to collect data at various locations over a limited span of time by private companies, and international organizations both local and foreign. The information from most of these equipment is not available in the public domain.

Table 2: Organizations operating and maintaining sea level stations

ORGANIZATION	GAUGES INSTALLED
Kenya Marine & Fisheries Research Institute	<i>Lamu and Mombasa</i>
Tanzania Harbours Authority (THA)	<i>Dar es Salaam</i>
Commission for Land & Environment: Zanzibar	<i>Zanzibar</i>
Brigade Hydrographique et Topographique des Seychelles (BHTS)	<i>Port Victoria</i>
Seychelles Meteorological Services	<i>Pte La Rue</i>
Mauritius Meteorological Services	<i>Port Louis and Rodrigues</i>
Instituto Nacional de Hidrografia e Navegacao (INAHINA)	<i>Maputo, Inhambane, Beira, Nacala, Pemba</i>
Centre National de Recherches Oceanographiques	<i>Nosy Be, Taolograno</i>
Foiben Taosarintanin'i Madagasikara (FTM) - Institute for Geography and Hydrography	<i>Toliara</i>
Hydrographic Office - South African Navy	<i>Mossel Bay, Knysna, East London, Durban, Port Elizabeth, Richards Bay</i>

These institutions also have the capacity to level the benchmarks as the station.

The University of Hawaii continues to provide assistance in the maintenance of gauges that they installed. Once every 2-3 years a field engineer is sent round to service the gauges, level benchmarks and replace or upgrade stations where necessary.

Report on the proposal for establishment of sea level observing network and storm surge prediction system in the northern Indian Ocean

K. Somasundar and B.N. Krishnamurthy

Department of Ocean Development, CGO Complex, Lodhi Road, New Delhi-110 003

Background

Some of the common concerns of coastal states in the northern Indian Ocean region are impacts caused by tropical cyclones and rises in mean sea level. Countries such as India, Bangladesh, Maldives, Myanmar, Sri Lanka are most vulnerable to tropical cyclones/storms. The surges associated with tropical storms, coupled with high tides in the northern Indian Ocean, cause a great deal of damage to life and property in the coastal areas. Further, increases in sea level due to global warming have potential long-term implications on economic development in those countries. In order to prepare the nations to face such effects, it is important to develop a predictive system for cyclones for these countries through regional and international cooperation. Systematic and reliable data on sea level is one of the prerequisites for development of a predictive system on storm surges.

It may be noted that the countries bordering the Bay of Bengal and the Arabian Sea are mostly developing countries with a per capita income of about 300 dollars in some of the countries. Further, these coastal countries are vulnerable to severe natural calamities such as tropical cyclones, storm surges, rises in mean sea level. On average about 6-10 depressions or cyclones form every year in the region. Available records indicate that about 150 major storm surges occurred in the Bay of Bengal, across eastern India, Bangladesh, Sri Lanka and Myanmar, during the last 200 years (Fig. 1). The maximum number of storm surges occurred in Bangladesh and India and resulted in a great loss of life and property. The number of storms forming in the Bay of Bengal is much higher than that of the Arabian Sea.

The economy of these countries also depends primarily on annual agriculture production, which in turn is controlled by the rainfall associated with monsoons and cyclones that occur in the northern Indian Ocean. Fishing in the coastal waters is one of the major activities contributing to the economy of these countries, in addition to providing employment to millions of fishermen. It is well known that the continental shelf of the Bay of Bengal and the Arabian Sea are potential sources for hydrocarbon, which is being exploited in some of these countries. Since the transportation of goods for export and import of material is largely by sea, shipping and ports play a vital role in the trade and economy of these countries. In order to exploit the resources from the ocean in a sustainable way and to derive benefits effectively, it is important to understand the ocean-atmospheric processes that occur at different time scales.

Since storm surges are a common problem for most of the countries, it is proposed to have a regional cooperation in setting up a system for forecasting in the region. To accomplish this, a project proposal on storm surges was prepared jointly by IOC-WMO-IHP to seek financial assistance from international agencies. A project proposal was prepared by IOCINDIO office at DOD for setting up of sea level observing system and circulated among the member states of IOCINDIO seeking their views and willingness to participate in the project.

The importance of systematic and accurate measurements of sea level are two fold; firstly, to understand the variation in the mean sea level (MSL) primarily caused due to global warming, and secondly, for studies of ocean circulation and its variability. Knowledge of coastal and deep oceanic processes are important for understanding and predicting the climate changes and assisting various maritime activities such as fisheries, off-shore oil spill modeling, economic shipping routes, ports and off-shore development.

The second potential application of reliable long-term tidal data is to derive information on the ocean circulation, particularly in the Bay of Bengal and the Arabian Sea, where the oceanographic

processes are highly variable both in terms of space and time scales. It is known that the oceanographic and meteorological data in this region are rather sparse compared to the Atlantic and Pacific. Although sea level heights can be derived from radar altimeters such as TOPEX/POSEIDON, real-time observed tidal data is required for validation of satellite data. With this objective, a Cell for Monitoring and Analysis (CMAS) has been established at Survey of India, Dehradun, India, under the auspices of the IOC-UNEP-WMO Pilot Activity. This activity will be addressed in detail by Dr. Satish Shetye, NIO, Goa, in a separate report submitted to GLOSS-VI. These studies would contribute to climate prediction studies and other developmental activities in the coastal region. From all the above it can be stated that there is a need to strengthen collection, archival and analysis of long-term tidal data and dissemination to national and international user communities.

Although the measurements of sea level appear to be simple, the actual determination of global sea level is a complex and laborious task involving analysis of decades of high quality data and modeling. In addition to increases in the volume of the water, factors that would contribute to the variations in the sea level are geotectonic activity or uplift, reduction in sediment load reaching the delta and compaction of soil. Considering the importance of these studies, India, with the cooperation of IOC, has made some efforts to promote sea-level studies at national, regional and international levels. The various activities undertaken by the department are described in the following sections.

National efforts

Although the tidal measurements in India using conventional methods dates back to beginning of the century, a concerted effort for measurement of systematic, scientific, accurate collection, archival and analysis of sea level data was made only recently. In order to assess the variation of MSL due to global climate changes, a national project “Sea Level Monitoring and Modeling (SELMAM)” was begun in 1992 by DOD. The Survey of India (SOI) is the nodal agency executing the SELMAM project of DOD.

Tide Gauges

The programme envisages: (i) establishment of a set of accurately measuring modern tide gauges, (ii) generation of micro level coastal area maps, and (iii) development of predictive models for the assessment of the effect of variations in MSL on the coastal areas. The project envisaged establishment of a set of 10 modern tide gauges called Float Type Digital Gauge (FTDG) for continuous recording of diurnal tides in the ports of India, viz. Porbunder, Mumbai, Marmugoa, Kavarratti, Cochin, Chennai, Visakhapatnam, Paradip, Tuticorin and Machilipatnam. Of these, installation of 8 tide gauges have been completed so far and efforts are underway for commissioning of the remaining 2 tide gauges at Machilipatnam and Tuticorin. In addition, three acoustic tide gauges, one each at Chennai, Marmugoa and Port Blair, have also been commissioned for comparison of tidal measurements made by different gauges. A National Tidal Data Centre (NTDC) is set up at Survey of India, Dehradun, for processing, analysis and dissemination.

Modeling

Besides acquiring tidal data along the coast of India, a separate project has been launched to determine processes governing the variability of de-tided sea level. The possible processes contributing to sea level variability to be addressed are storms in the Bay of Bengal and extreme events in the Lakshadweep coral islands in the Arabian Sea. The primary objectives of the project are to identify relationship between de-tided sea level and coastal currents and low frequency coastal waters along the east and west coast of India and to develop numerical models capable of realistic simulation of tidal circulation on the continental shelf of the Bay of Bengal and Arabian Sea. Based on the tidal data (monthly mean) collected along the Indian coast, a numerical model has been constructed to examine the circulation in the Northern Indian Ocean. The data provided a wide range of reasons to study sea level variability along the coast of India on a wide range of temporal scales varying from hours to decades. These studies reveal that the passage of Kelvin and tropical Rossby waves is

recorded in the monthly-mean sea level data. Further, effects of salinity changes on sea level variations are very prominent, which require investigation.

Coastal maps

For assessment of the extent of inundation of the coastal areas due to surges associated with storms, it is important to have coastal maps of the region. Considering this, the Department of Ocean Development and Department of Science and Technology has undertaken a project for the development of fine resolution contour maps for the entire coast of India. The maps would be digitized for use in mathematical models. Under the project, coastal maps on 1:25,000 scale with an accuracy of 0.5 m will be prepared. Currently, coastal maps along the east coast of India between Machilipatnam and Nellore, which are the most cyclone prone areas, have been prepared. Efforts are under way to prepare maps for the entire coast of India up to the coast of Bangladesh.

Regional efforts

During November 1996 the IOC convened the second session of IOCINDIO at Goa, India, which was hosted by the Department of Ocean Development. The meeting was preceded by a Regional Workshop on Global Ocean Observing System (GOOS) Capacity building, which was primarily aimed at identifying various programmes of common interest to the member countries and to take a stock of facilities available in the member states. Based on the outcome of the Regional Workshop, a set of programmes has been recommended by the IOCINDIO-II for implementation. Subsequently, the XIX session of the IOC Assembly held in July 1997 endorsed the recommendations of the IOCINDIO-II through a Resolution. The workshops/training programmes are (i) Storm surge forecasting, (ii) Tropical ocean and climate, (iii) Integrated coastal studies including coastal marine pollution, (iv) Coral reef monitoring and (v) Oil-spill monitoring in the Persian Gulf. Of these, two workshops (ii & v) on Tropical Ocean and Climate and Oil Spill Modeling in Persian Gulf have already been conducted and a workshop on storm surge forecasting is scheduled for October 1999. The programmes proposed to be undertaken in this region include (i) Sea level monitoring, (ii) Storm surge forecasting and (iii) Coral reef monitoring. The various efforts by IOCINDIO for the establishment of programmes (i& ii) are described as follows:

Indian Ocean sea level observing network

The coastal states of the countries in the IOCINDIO region are prone to tropical cyclones which cause great deal of inundation in the low lying areas of the countries. Since most of these countries are dependent on agriculture any flooding of coastal waters would greatly affect the economy of these countries.

In November 1996 the IOCINDIO-II meeting identified several areas relating to marine science for regional cooperation. One of the issues discussed during the meeting was the establishment of a regional sea level programme for the IOCINDIO region. The Second Session of IOC Regional Committee for the Central Indian Ocean (IOCINDIO-II) recommended that all countries in the region should undertake modernization of the existing tide gauges, establish new gauges if necessary and improve capabilities on sea-level analysis. The meeting also proposed setting up a regional sea level network with about 40 tide gauges covering the central Indian Ocean for acquisition of high quality data.

With India being the Chair for the IOCINDIO, efforts were initiated to formulate a project proposal for the establishment of a tide gauge network in the northern Indian Ocean. Accordingly, a draft project proposal for the establishment of a network of tide gauge was prepared and circulated among the 19 member states of IOCINDIO region. The proposal envisages setting up a set of 40 tide gauges in the member countries of IOCINDIO region for long-term continuous monitoring of sea level in the Indian Ocean region. The programme consists of two components; firstly, installation of tide

gauges and networking, and secondly, maintenance, operation, analysis and modeling of the data. The suggested locations of tide gauges stations in various countries are given in Table 1.

The member states were requested to examine the report and indicate -

- i) Willingness of their Govt. for participating in the project;
- ii) Provide the number of tide gauges and their locations;
- iii) Nominate a coordinator.

Based on the response from the member states, a sub-regional proposal was prepared for implementation of the project in Bangladesh, Iran, Iraq, Sri Lanka and India at an estimated cost of US\$174,000. The proposal is for installation, operation and maintenance of seven tide gauges at locations suggested by member states of IOCINDIO. It is expected the entire work including procurement, installation of gauges and providing training to personnel would be completed over a period of one year. It is proposed that member states would meet a partial expenditure of the project of US\$49,000 and remaining cost of US\$125,000 would be met from the IOC.

Bangladesh: Bangladesh has agreed to participate in this programme and suggested a location for the installation of an acoustic tide gauge either at Mongla Port Area near Hiron Point or at Kuakata near Patuakhali. The operation and maintenance of the tide gauge and data management will be the responsibility of the Bangladesh Inland Water Transport Authority (BIWTA). The Director of BIWTA has agreed to be a member of the Coordination Committee of Regional Sea Level Centre (RSLC).

Iraq: Installation of one tide gauge at FAO port, the northernmost tip of Arabian Sea. Marine Science Centre of University of Basrah will be responsible for implementation of the project. The Department of Physical Oceanography of the centre will be the focal point.

Islamic Republic of Iran: Iran has agreed to participate in the programme and proposes to install three tide gauges on the Oman coast. Iranian National Centre for oceanography in Tehran will be responsible for implementing the project.

Sri Lanka: Sri Lanka has expressed willingness to have two tide gauges, one at Kalpitya on the west coast and another at Karinda on the east coast. The National Aquatic Resources Agency (NARA), Crow Island, Mattakuliya, Colombo will be responsible.

The objectives of the networking sea level programme are:

- To set up a sea level network with about 6 modern tide gauges that would generate high precision data;
- To organize a training programme for the scientists from Bangladesh, Iran, Iraq and Sri Lanka in data archival, analysis and dissemination;
- To link the stations with the IOC-GLOSS stations.

Implementation of the programme

Besides the installation and maintenance of tide gauges, it is also important to process and check the quality of the sea-level data at national and regional levels for assessing the relative sea level changes. In order to achieve this objective, networking of the tide gauges proposed to be installed in the three countries of IOCINDIO region is necessary. It is proposed to establish one National Sea Level Centre (NSLC) in each member state, which will be linked to GLOSS network. The details of the action plan and mode of implementation is given in the Annex.

Responsibilities Of National Sea-Level Centre (NSLC)

- The responsibility of NSLC includes periodical maintenance of tide gauges, calibration, collection, quality check and submission of sea level data GLOSS;
- After applying the quality check and initial processing of the data, the hourly, daily and monthly data sets are prepared and archived in a standard;
- The persons employed under NSLC will be trained in operation and maintenance of the tide gauges;
- To provide assistance and local hospitality during commissioning of the tide gauges in the respective countries.

In order to confirm the participation from the member countries and obtain firm commitments, a regional workshop is being organized on Storm Surge in Delhi inviting the countries of IOCINDIO region. One of the objectives of the workshop is to discuss the importance of the sea level measurement in the development of a storm surge model required for operation in this region.

Storm surge disaster reduction for the northern Indian Ocean

Storm surges, normally associated with tropical cyclones in the northern Indian Ocean, cause great havoc to life and properties, particularly in the coastal areas of the IOCINDIO region in Bangladesh, Myanmar, Pakistan, Thailand, Maldives, Sri Lanka, and India. A significant number of tropical cyclones occur in the Bay of Bengal causing a great deal of devastation while crossing the coasts of adjacent countries such as Bangladesh and India. Due to high astronomical tides in these areas, the surges associated with storm surges cause enormous damage to the coastal areas of these countries. However, the frequency of cyclone formation in the Arabian Sea is relatively much lower than that of the Bay of Bengal with a probable ratio of 1:4. The most dangerous coastal floods occur when peak surges coincide with high tides. The major factors contributing to disastrous surges in the Bay of Bengal, especially in Bangladesh, are (i) shallow coastal waters, (ii) convergence of the Bay, (iii) high astronomical tides, (iv) thickly populated low-lying islands and (v) complex coastline with innumerable number of inlets.

The benefits of a storm surge prediction system are quite significant for the countries of northern Indian Ocean. Studies indicate that the ratio of cost/benefit of weather warning system is on the order of 1:55 to 1:127. In order to minimize the loss of life and property by storm surges, it is important to have an accurate forecast of landfall for a tropical cyclone as well as the intensity of the storm. Considering the importance of these studies, particularly for countries in the northern Indian Ocean where most of the member states are developing countries, there is a need for regional cooperation. UNCED Agenda 21 calls for cooperation among international agencies in the implementation of projects.

Recognizing the importance of the storm surge prediction system, the World Meteorological Organization (WMO) and the Intergovernmental Oceanographic Commission of UNESCO have developed a comprehensive project proposal on the storm surges in the northern Indian Ocean. Under the project, a reliable storm surge prediction system duly supported by oceanographic, meteorological and communication components would be developed in the region. The project would also strengthen links among national meteorological, hydrological, marine services and disaster management organizations. The key component of the proposal is capacity building and human resources development through workshops and seminars. The total estimated cost of the project is US\$45.4 million, out of which US\$33.5 million is expected as external assistance and US\$11.9 million as national contributions.

The primary objectives of the project are to save lives, reduce damages and encourage sustainable development of low-lying coastal regions in the northern Indian Ocean where the storm surges occur most frequently; i.e., the Bay of Bengal and the Arabian Sea. The project envisages establishment of infrastructure for forecasting of storms and providing training to technical persons from these countries with respect to the prediction, simulation and evaluation of storm surges associated with the occurrence of tropical cyclones in the Bay of Bengal and Arabian Sea. The

fundamental requirements to make the project operational are (i) systematic real-time meteorological, hydrological, and oceanographic observations, (ii) development of cyclone models for forecasting and reducing the uncertainties in cyclone landfall timing and location and (iii) improved communication facilities and evolution of a response mechanism among organizations for disaster prevention and preparedness measures.

In order to provide forecasts it is proposed to establish various systems in the countries of region for acquiring the met-ocean parameters through national and international resources; i.e., surface and upper weather stations, upper air stations, automatic weather stations (AWS), high gust anemometers, ship data, weather radars, water level recorders, tide gauge networks and deep sea meteorological buoys. In addition, communication systems for dissemination of information among countries through Global Telecommunication System (i.e., Karachi-New Delhi to 2400 bhs) via satellite and satellite receiving equipment will be installed in six countries, which are Bangladesh, Maldives, Myanmar, Pakistan, Oman, and Sri Lanka. A Regional Computer Network (RCN) responsible for the installation and operation of storm surge models and Analyzing Forecasting Data Processing (AFDPS) would be commissioned with international efforts. For understanding the past events of tropical cyclones, which is required for hindcast, it is important to collect and compile of information of storm surge data by preparing cyclone dossiers. It is proposed to set up a Data Archival Centre in the region linking the existing meteorological oceanographic and hydrological data management facilities. In addition to generation and dissemination of information to coastal communities through the setting up of a warning system, community participation and risk zone mapping are equally essential for the mitigation of surge effects.

The important elements of the project are capacity building and human resource development, through which eventually the countries in the region would be self-sufficient in the storm surge problem by the end of the project. The activities envisaged under this, mostly through international resources, are on-the-job training in Doppler Radar, deep-sea meteorological buoy networks, tide gauge networks, surge height measurements and RCN.

The member states are to be responsible for the implementation of the project as far as possible within the existing infrastructure. The implementation should be undertaken under the general direction of participating member countries with technical assistance from international agencies (i.e., WMO, IOC, IHP) and appointed experts. A monitoring committee with representatives from the member states, UN agencies and the funding institutes would be constituted for periodic review of the project and to provide advice for implementation of the project. The project director will be responsible for overall coordination and implementation of the project. The director will be assisted by an administrative officer, a technological manager and a scientist in charge. The project advisor will provide overall scientific advice to the director who is appointed by the participating countries in consultation with the heads of UN agencies concerned.

In order to assess the present level of knowledge for the prediction of storm surges in the region, a regional IOCINDIO workshop is planned to be held in Delhi in October 1999. Following the workshops, a regional meeting of the members of the countries of the region is scheduled for October 1999 to discuss the Northern Indian Storm Surge Project proposal.

The meeting would deliberate and decide on the following:

- Acceptance of the project proposal with amendment, if necessary
- Identification of the funding agencies and extent of international funding
- Role and responsibility of the member countries, including financial contribution to programme implementations, plans, and programme management system.

Conclusion

Although the response is very slow from the member states, the IOCINDIO has been striving to establish a project entitled 'Sea Level Observing Network System' (IOSLON) to acquire systematic and accurate measurements on sea level variations in this region. The purpose of this proposal is to obtain willingness from the member states to cooperate and support the implementation of this programme as this could be achieved only through regional cooperation.

References

Project proposal on Storm Surge reduction for the Northern part of the Indian Ocean, February 1998
by IOC, WMO, UNESCO

The Science of Climate Change, 1995 by J.T. Houghton, L.G. Meira Filho, B.A. Callander, N. Harris,
A. Kattenberg and K. Maskell - Cambridge University. U.K.

Project proposal on Indian Ocean Sea Level Network prepared by IOCINDIO office at DOD in 1998.

The need for a regional sea level data base

A. ADEKOYA

*Nigerian Institute for Oceanography and Marine Research
P.M.B. 12729 Victoria Island, Lagos Nigeria*

ABSTRACT

The proposal for the formation of the African GLOSS Network brought about the need for the Regional Sea Level Data Base (RSLDB). This will call for data links for the tide gauges and necessary transmission. The method in which the data will be transmitted will depend very much on the time response required and the distance involved.

The need for Regional Sea Level Data Base (RSLDB) includes: (i) essential quality control of all local sea level station and data centres, (ii) archiving of long term historical sea level data set, (iii) having at least a subset of country raw data available for studies and scientific uses, and (iv) increasing the catalogue of data yearly.

A comprehensive Regional Data Base for the coastal zone will probably be made up of a number of National Sub-regional centres with appropriate network facilities to enable input and retrieval from centralized sources, and output to related activities of global uses.

The Data Base will be established as an African Regional Data Center for Sea Level and its responsibility will include; collection, publication, distribution of data, analysis and interpretation of this data. However, hardware and software should be made available for storing, retrieving, accessing and processing the data.

Data can easily be transmitted routinely from a regional base over computer networks (via web site) and electronic mail across the Internet. It is certain that this data base will definitely enhance the activities of African GLOSS Sea Level Data Networks since two centres already are in existence in the Sub Region, namely South Africa and Western Indian Ocean Group.

**Atlantic Ocean tsunami hazards : Call for an
Intra-Americas sea tsunami system**

G. Maul

*Florida Institute of Technology
150 West University Boulevard
Melbourne FL 32901 USA*

Tsunami events have been recorded in Atlantic Ocean since antiquity, and by Europeans in the Intra-Americas Sea (Gulf of Mexico, Caribbean Sea, Bahamas, and Guianas) since the 16th century. These events are both local in origin and from distant sources, but occur at the rate of several severe occurrences per century. The great Lisbon earthquake of 1755 for example created 6 and 7 meter-high teletsunami waves in the Lesser Antilles. In the last 150 years, tsunamis have been the cause of more deaths in the Caribbean (369 (- 1,790 persons by some reports) than in Alaska (121), Hawaii (275), or the US West Coast (18). Although there have been deadly tsunamis in the Intra-Americas Sea this century (1918: 42 persons, 1946: 100 persons), it is the event of 1867 in St. Croix, US Virgin Islands, that is most reminiscent of the 1998 occurrence in Papua New Guinea.

Preventing a major disaster was the focus of a May 1996 scientific meeting, initiated in 1995 by the IOC and hosted by the University of the Virgin Islands on St. John. In June 1997 a public workshop was held at the University of Puerto Rico at Mayaguez. At Mayaguez, there were approximately 150 concerned citizens of the region, civil defense and government officials, scientists, and tsunami warning experts, both local and from abroad. In July 1997 the US Head of State was formally informed of recommendations made at the Mayaguez workshop. It focused on four mitigation measures: education, warning, management, and research. It is important to note that the US Federal "Tsunami Hazard Mitigation Implementation Plan" (April 1996) has no Atlantic component.

The Intra-Americas Sea clearly should have a tsunami element integrated into the regional Global Ocean Observing System (GOOS). Indeed, calling for the creation of an Atlantic Tsunami Warning Centre would not be inappropriate.

**Elements of a tsunami warning system for
the Intra-Americas sea**

G. Maul

*Florida Institute of Technology
150 West University Boulevard
Melbourne FL 32901 USA*

D. Martin

*NOAA National Ocean Survey
1305 East-West Highway
Silver Spring MD 20910 USA*

At a series of workshops (Barbados, 1995; St. John, 1996; Puerto Rico, 1997; Miami, 1998) the case has been made for significant tsunami hazards in the Intra-Americas Sea (Gulf of Mexico, Caribbean Sea, Bahamas, and Guianas). For example, since the great 1867 US Virgin Islands earthquake and 9 meter-high tsunami, the population density of the region has increased 10-fold, infrastructure development has progressed without a notable natural hazards component, and governments seem to be oblivious to the risk. Accordingly, four essentials comprise the proposed Intra-Americas Sea Tsunami Hazards System: Education, Warning, Management, and Research.

The first order of business is to better educate the populace through public information, K-12 student indoctrination, video and other multi-media products, workshops, and popular press articles. The warning component should capitalize on the recently established CPACC (Caribbean Planning for Climate Change) sea-level/weather GOES-reporting network, on existing seismic and meteorological reporting and warning systems, and on active participation with the ICG/ITSU (International Coordination Group for the Tsunami Warning System in the Pacific). Management issues include: integration with other natural hazards warning systems; exploration for funds; local warning and evacuation; search and rescue; fire suppression; emergency medical services; damage assessment; inter- and intra-governmental coordination; and, damage and hazard analysis. Research needs are: improved resolution bottom relief data; travel time maps for population centres; earthquake magnitude / depth thresholds; tsunami wave arrival amplitude estimation; potential for Kick'em Jenny and Soufriere (Montserrat) eruption; tsunami and earthquake history improvements; fault locations, activity, and tsunamigenic mechanisms; inundation maps; GPS stations for crustal motion monitoring; and loss estimation studies, amongst others.

**Tide gauge network in the Republica Oriental
del Uruguay: Current state and future
perspectives**

E. Forbes

*Div. Oceanografía Física – Servicio de Oceanografía
Hidrografía y Meteorología de la Armada (SOHMA)
Casilla de Correos 15209
Montevideo, R.O. del URUGUAY*

ABSTRACT

The Oceanographic, Hydrographic and Meteorological Service of the Navy (SOHMA), since its creation in the year 1935, carries out observations of tidal heights. At the present time it operates a tidal network with fifteen stations; this network participates in the PSMSL program with five stations and in the GLOSS program with one station. Since 1987, SOHMA, jointly with the Uruguayan Antarctic Institute (IAU), carries out during the Antarctic summers a tidal program at the Scientific Antarctic Base “ARTIGAS”, and since 1998 with the intention of being a permanent station. Presently, SOHMA is involved with programs whose main objectives are the strengthening of the operational network, the training in operation and analysis of the data, and support of coastal zone management. At the same time, there exist interest in improving relationship with regional and international programs.

INTRODUCTION

One of the most important precepts of SOHMA is to offer security to mariners, so one of the activities is to observe the level of the sea and maintain a tidal station network along the whole Uruguayan coast. The biggest contributions have been the support to nautical charts, the determination of the tidal fundamental planes, the annual publication of tide tables; as well as support for naval operations and private activities, and also scientific contributions.

Current state

SOHMA’s Physical Oceanography Division has two graduated oceanographers, a student, an administrative and a field operator. The graduated oceanographers are not in physical oceanography because in Uruguay this discipline is not dictated; one of them carried out international post-graduate courses in topics related to physical and coastal oceanography, especially to tides.

The main effort is directed to tides; the maintenance of the network, digitizing tidal records, obtaining the data, entering it into the database and doing quality controls, which implies a daily and continuous task. In 1983 the Division experienced a technical and scientific invigoration resulting in the publication of the “TABLAS DE MAREAS” (Tide Tables) since 1988 and on the Internet (<http://www.armada.gub.uy/dimat/sohma/predic.htm>) since 1997. A more active participation in the PSMSL and GLOSS programs was also possible, and scientific contributions on tide high height anomalies and sea level rise (among others) were conducted.

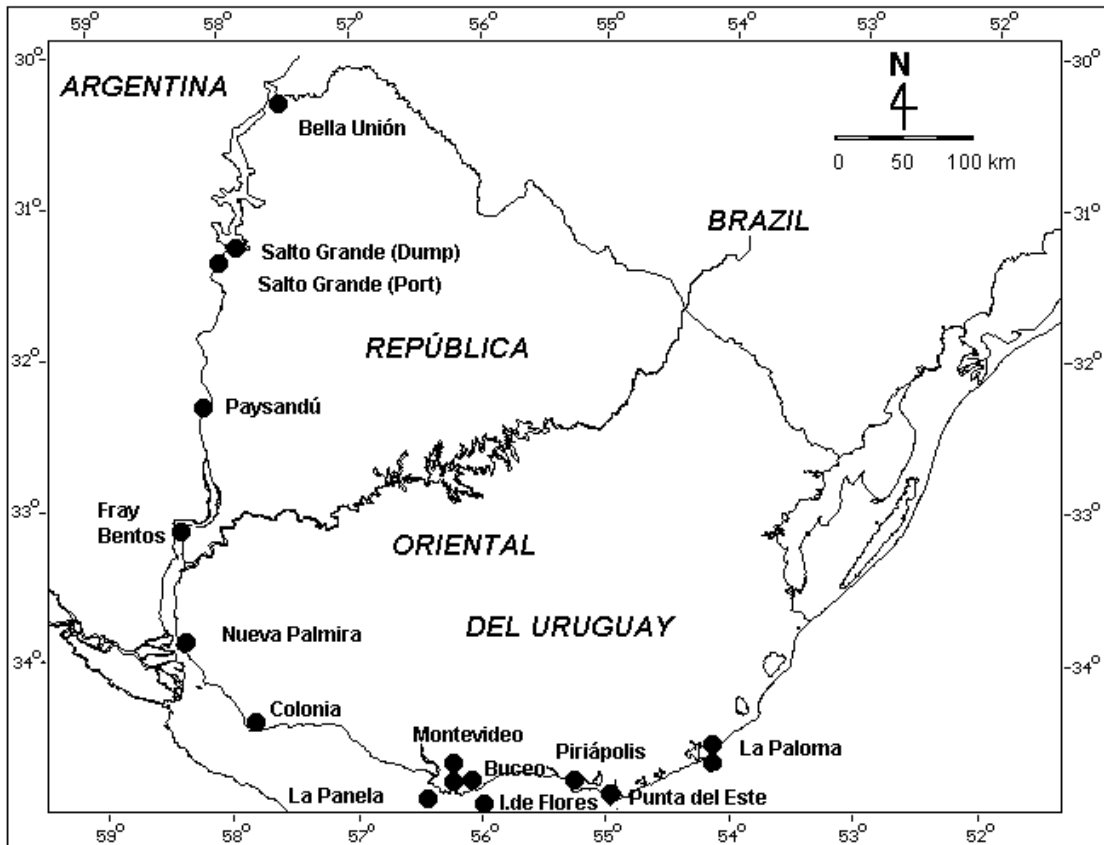


Figure 1 : Tide gauge network.

The tidal network is composed of fifteen stations (Table 1, Figure 1); presently the equipment is reduced and some stations are inoperative due to lack of instruments and budget for repair and maintenance.

TABLE 1 - The Uruguayan Tidal Network.

LOCATION	STATION	PSMSL #	GLOSS #
Uruguay River	Bella Unión		
	Salto Grande (Dump)		
	Salto Grande (Port)		
	Paysandú		
	Fray Bentos	870007	
	Nueva Palmira		
Río de la Plata	Colonia	870001	
	La Panela		
	Montevideo	870011	300
	Buceo		
	Isla de Flores		
	Piriápolis		
Atlantic Ocean	Punta del Este	870021	
	La Paloma	870031	
Antarctica	BCA Artigas		

Along the Uruguay River all the stations are operating and data is obtained through hourly readings of tide poles; data is sent monthly to SOHMA. Fray Bentos Station is part of the PSMSL

program but has not contributed data since 1990 because it is strongly influenced by the discharge of Salto Grande Hydroelectric Dam.

Río de la Plata is an area of great economic importance with a continuously growing coastal population and marine traffic. Shallow depths with channels and banks and great salinity variability characterize it. The Colonia and Montevideo stations belong to PSMSL program, while Montevideo station belongs to GLOSS program.

In the Atlantic Ocean there are two stations, both belonging to the PSMSL network. Punta del Este is located at the main Uruguayan tourist resort, and La Paloma Station is on a fishing port with a navy base where there exists a project to develop the Uruguayan deep-water port.

In 1987, in agreement with the Uruguayan Antarctic Institute, SOHMA began to carry out tidal observations during the Antarctic summers at the Antarctic Scientific Base “ARTIGAS” (King George Island), contributing information on the nautical and terrestrial cartography, among others. In January 1998 a new stage of the project began with the objective of maintaining a permanent station.

Table 2.- Current SOHMA´s projects.

PROJECT	SPONSOR	OTHER PARTICIPANTS
EcoPlata III: “Support to the Integrated Coastal Zone Management of Río de la Plata”.	IRDC (Canada) UNDP MVOTMA	University of the Republic (Faculty of Sciences and Faculty of Social Sciences), National Institute of Fishing, Ministry of Housing, Territorial Regulation and Environment, Dalhousie University, Acadia Estuarine Centre, and Bedford Institute of Oceanography.
Environmental Protección of the Río de la Plata and its Maritime Front: “Contamination Control and Prevention and habitat restoration”	PNUD-GEF	CTMFM/CARP.
Secure sailing corridors	European Comunity Trieste Academy	
Environmental aspects of the secure sailing corridors	BID	

Future perspectives

SOHMA participates in several national projects that are in different stages of execution (Table 2). We have also been carrying out activities in the Coastal GOOS “QUIJOTE” Pilot Project, encouraging the integration of local coastal stations to a regional network.

An expected result of these present and future activities is the invigoration of the operational tidal network, mainly those belonging to PSMSL and GLOSS. A study of the possibilities of real time data acquisition should be implemented.

Conclusions

The training of SOHMA's scientific staff is a real necessity, and this training can be achieved as much through the participation in courses organised by the GLOSS (or others) as by receiving scientific investigators and technical advisers at SOHMA. Also, there exists the necessity to incorporate instruments for the operational invigoration of the network, and to carry out an implementation analysis of real-time data acquisition by receiving information from other institutions and programs. We think that this is the way for the reduction of the operating costs and to achieve a greater efficiency.

**A multi-data approach to assess the spatio-temporal variability of the
Ivorio-Ghanaian coastal upwelling**

A. Aman
Université de Cocody
UFR SSMT 22 BP 582
Abidjan 22
Côte d’Ivoire

H. Demarcq
IRD-HEA, Centre de Montpellier
BP 5045 Montpellier Cedex

ABSTRACT

The Gulf of Guinea is mainly characterized by the presence of seasonal or permanent coastal upwelling. The sea surface temperature is currently used to quantify this upwelling. An approach based on five days of satellite observations and on daily in situ measurement is used to produce a monthly climatology with good precision compared to Reynolds’s result. A Coastal Upwelling Index (CUI) based on in situ measurement is then produced to analyze the dynamics of the upwelling on the western and eastern sides of the Ivorian coast. The time series associated with the ratio of major upwelling to minor upwelling shows that the intensity of the minor upwellings is more variable on the eastern side than on the western side of Côte d’Ivoire. However, these indices derived from SST measurements are not sufficient to describe absolutely the rise of the thermocline during the upwelling season. A combination of satellite data, coastal and ship SST, and tidal files can contribute significantly to understand this important and complex phenomenon that takes place seasonally along the coast of Côte d’Ivoire and Ghana.

INTRODUCTION

In the Guinea Gulf region, the ocean dynamics are mainly linked to the seasonal presence of the Guinea current, the equatorial upwelling and to the coastal upwelling along the Côte d’Ivoire and Ghana coasts (Ingham, 1970; Morlière, 1970; Collin et al., 1993). The upwelling that occurs in this coastal area, especially off Côte d’Ivoire and Ghana, has been actively studied since the early 1960s. Two upwelling seasons, major and minor, have been identified. These two upwelling events have two main centers, creating an important spatial and temporal heterogeneity in the Ivorio-Ghanaian coastal marine ecosystem. These upwellings observed off Côte d’Ivoire and Ghana are rather peculiar because the mechanisms causing the upwelling are due to complex interactions between several processes. Off the Côte d’Ivoire and Ghana ecosystem, the wind intensity remains below 5 m/s, but the value of the upwelling index is similar to values observed on other eastern boundaries. As the cooling cannot be totally related to the wind intensity, analysis of sea temperatures has been the main approach to qualitatively access the upwelling.

Côte d’Ivoire and Ghana have a very good coastal sampling of SST. A comparatively smaller coastal sampling SST may be obtained by ship of opportunity meteorological data (called “SHIP” data), at lower space and time scales. Finally, the images disseminated by Meteosat provide very good complementary information on the spatial structure of these coastal upwellings despite the small number of cloudless images available.

The remote sensing benefit

The SST reconstruction over the Guinea Gulf based on Meteosat images is very limited by the quasi-permanent cloudiness associated with the high water vapor content of the atmosphere. However, Meteosat series provide a very high time frequency of images for a spatial resolution of 5 km. This is

used to process daily synthesis images of radiative temperature. This processing minimizes the atmospheric absorption (Demarcq and Citeau, 1995). Previous studies based on Meteosat data allowed a quantification of the upwelling off Senegal and Mauritania (Demarcq and Citeau, 1995) and the localization of the surface cooling off Côte d'Ivoire and Ghana (Aman and Fofana, 1995).

SHIP RECORDS AND COASTAL OCEANOGRAPHIC MEASUREMENTS

Despite of the high observation frequency, the SST images computed from meteorological satellites do not supply information on a regular temporal basis on the Guinea Gulf. The high cloud cover makes impossible a direct observation of the upwelling structure. So the SST data provided by merchant ships and the coastal stations constitute an opportunity to analyze precisely the temporal dynamics of the coastal upwelling. Two data sources are available for that.

The first data source used in this study is based on nearshore SST provided at six coastal stations located along the open Ivorian gulf from Tabou to Assinie and at six other stations in Ghana from Axim to Keta. The measurements are performed since 1977 for Côte d'Ivoire and since 1985 for Ghana. Compared to the ship data, the regular sampling of these stations supply a precise absolute value of the zonal SST gradient.

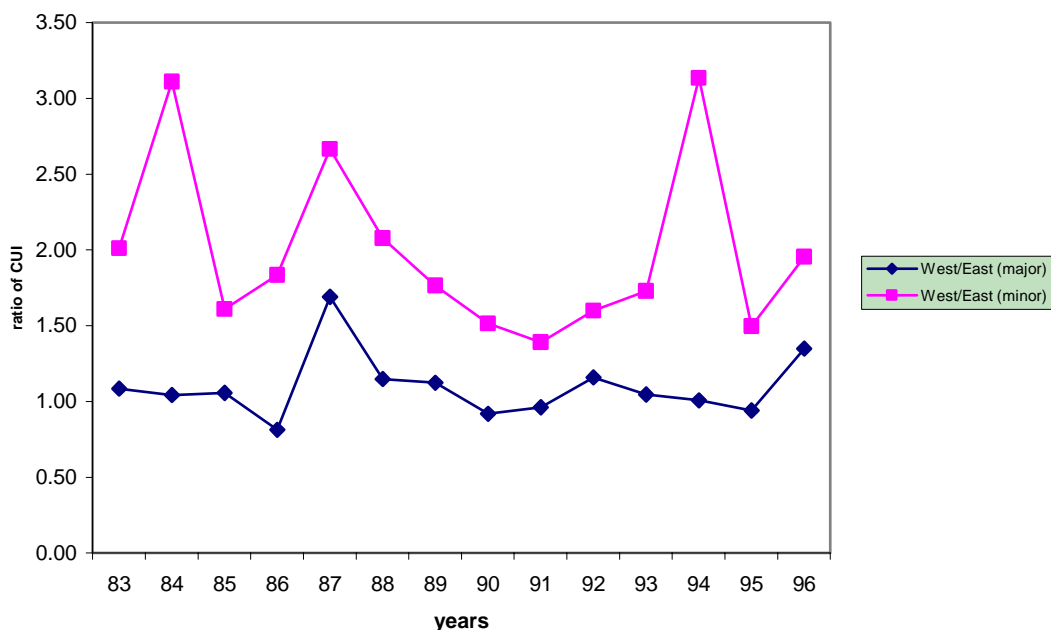
The ship of opportunity data disseminated by GTS in the "SHIP" meteorological messages (including SST, air temperature, etc.) and synthesized in the COADS database are rather convenient for this study, providing an adequate density of SST measurements in the Gulf of Guinea at a more regional scale. The spatial coverage of the ship data is not particularly appropriate to supply precisely information on coastal upwelling. Nevertheless, a very averaged spatial description of the upwelling extent may be obtained, and approximately 25000 records are compiled for the 1984-1997 period for each upwelling season.

An improvement of the upwelling index based on the coastal measurements (Arfi et al., 1991) is carried out. The coastal upwelling index is computed from the shoreline bucket samples by considering the temperatures less than 26°C and the length (days) of that occurrence.

SST computed from merchant ships and coastal data indicate a bimodal curve with a slight drop in temperature in February and deep cooling from July to September (Ingham, 1970). In this way, two upwelling seasons are determined:

- minor upwelling from January to March
- major upwelling from July to September.

figure 1: ratio of major CUI in West to East and of minor CUI in West to East



The integration of satellite, SHIP and coastal data has been used to create a monthly climatology. A specific processing including the three available sources of SST is used to build a monthly blended SST climatology that supplies useful information on the mean seasonal cycle of the upwellings and their associated spatial structure (Demarcq and Aman, 1998).

Coastal upwelling index time series

A threshold equal to 26°C is used to compute the Coastal Upwelling Index (CUI). Four coastal stations have been selected: two in the western side (Tabou an San Pedro) and the two others are located in the eastern side (Abidjan and Assinie). The CUI is carried out as follows:

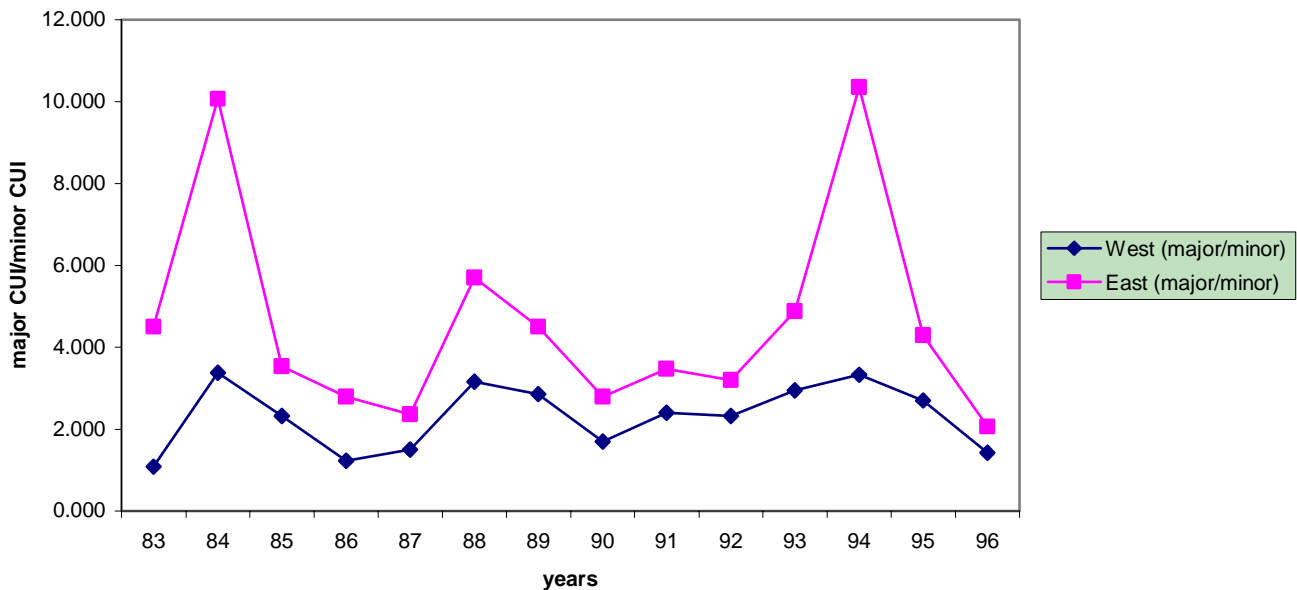
t_j represents daily temperature. k is the number of fortnights during the minor or the major upwelling

$$CUI = \frac{1}{k} \sum_{j=1}^n (28 - t_j)$$

for t_j less than 28°C. CUI=0 for t_j greater than or equal to 28°C.

The CUI time series shows that the intensity of the minor upwelling is greater than it appears when using the SST derived from ships. As mentioned by some authors (Pezennec and Koranteng, 1998; Aman and Fofana, 1998), the CUI is higher on the western side than on the eastern side off Côte d'Ivoire during the minor upwelling (Fig. 1). The ratio of the CUI time series represented by west/east shows that the variability of the upwelling intensity is globally induced by the annual variability of the minor upwelling index (Fig. 1). However there is no significant trend of the intensification of the major and minor upwelling during the last fifteen years as mentioned by Pezennec and Bard (1992). Except for 1987, the CUI relative to the major upwelling is quasi-constant during the period 1983 – 1996 from the west to east sides off Côte d'Ivoire. The fluctuations of the global CUI are created by the variability of the minor upwelling observed on the east side (Fig. 2). Even though the difference between the two upwelling seasons seems quite important, it can be observed that the minor upwelling off Côte d'Ivoire could be as important as the major upwelling. For example, the 1986, 1987 and 1990 minor upwelling seasons were characterized by high intensities in West Côte d'Ivoire as indicated by Figure 2.

figure 2: ratio of major CUI to minor CUI in West and East Côte d'Ivoire



Interest for the sea level measurement

Historical sea level data recorded during the period 1967-1978 have been used by Verstraete (1985) to analyze the annual upwelling signal off Abidjan and fluctuation of the mean sea level. The results of his study based on sea level files established the cycle of the mean sea level in association with the annual upwelling that is observed off Abidjan. Verstraete noticed also that the drop of the sea level takes place one month before the beginning of the decrease of the sea surface temperature along the coastline.

Cury and Roy (1998) show that there is an intensification of the minor upwelling during the last 20 years. However, the significant change is relative to the west side off Côte d'Ivoire (Tabou, San Pedro). The surface cooling is generally well localized on Meteosat images on the west side and moves to the east side during the minor upwelling (Aman and Fofana, 1995). A combination of satellite data, coastal and ship SST and tidal files can contribute to understand this important and complex phenomenon. The use of the tide gauge measurements in both Abidjan (east side) and San Pedro (west side) will contribute significantly to supplementing the understanding of this local but important upwelling system.

Conclusion and perspective

The infrared imagery disseminated by the European Meteosat satellite is of the utmost importance for the study of seasonal cycle of the Ivorio-Ghanaian coastal upwellings and their spatial structure despite severe atmospheric limitations. The integration of complementary in situ data supplied by ships of opportunity and coastal measurements improve considerably a monthly climatology based on SST. Moreover, these in situ measurements allowed us to study the spatial dynamics of the Coastal Upwelling Index (west side and east side). The fluctuation of the global CUI is essentially caused by spatio-temporal dynamics of the minor upwelling. The importance of the minor upwelling observed particularly in the west side off Côte d'Ivoire since the 1980s requires us to vary the method of investigation. The addition of tidal gauge data, for example, will contribute significantly to supplementing the understanding of this local but important upwelling system. Adapted from Verstraete, the use of the tide gauge measurements from San Pedro and Abidjan (Côte d'Ivoire) and Takoradi (Ghana) will be necessary for a more comprehensive understanding of this coastal upwelling system.

References

- Aman A. and Fofana S.; 1998. Spatial dynamics of the upwelling off Côte d'Ivoire. Colloques et séminaires, Orstom Editions, pp.139-147.
- Aman, A.; Fofana, S. 1995; Coastal sea surface temperature as detected by Meteosat satellite and received at the University of Abidjan; Acts of DUSRU meeting, Coloques et Séminaires, Orstom Editions, pp 52-59.
- Arfi, R.; Pezenec, O.; Cissoko, S.; Mensah, M.A.; 1991. Variations spatiale et temporelle de la résurgence ivoiro-ghanéenne. Cury, Ph., Editeur Scientifique. Pêcheries ouest-africaines-Orstom Editions 1991, pp 162-172.
- Collin, C. Gallardo, Y. Chuchla, R., and Cissoko, S.; 1993; Environnements climatique et océanographiques sur le plateau continental de Côte d'Ivoire. Environnement et Ressources Aquatiques de Côte d'Ivoire; Tome I – Le milieu marin. Orstom Editions; pp 75-110.
- Demarcq, H.; Citeau, J.; 1995. Sea surface temperature retrieval in tropical area with Meteosat: the case of Senegalese coastal upwelling. *Int. J. Remote Sensing*. 16(8):1371-1395.
- Ingham, M.C.; 1970; Coastal upwelling in the northwestern Gulf of Guinea. *Bull. Mar. Sci.* 1970; 20:2-34.
- Morlière, A.; 1970. Les saisons marines devant Abidjan. Doc. Scient. Centre Rech. Océanograph. Abidjan. 1(2): 1-15.
- Pezenec, O.; Koranteng, K.; 1998. Changes in the dynamics and biology of small pelagic fisheries off Côte d'Ivoire and Ghana: the ecological puzzle. In colloques et séminaires, Orstom Editions, pp. 329-341.
- Pezenec O.; Bard, F.X.; 1992. Importance écologique de la petite saison d'upwelling ivoiro-ghanéenne et changements dans la pêche de sardinella aurita. *Aquatic Living Resources* 5:249-259.
- Verstraete, J.M.; 1985. Contre-courants équatoriaux et variations saisonnières du contenu thermique et du niveau moyen de l'Atlantique tropical Est.

Sea-level fluctuations as an index of upwelling

*G. Brundrit and H. Waldron
University of Cape Town
South Africa*

The setting for this study is the southern sector of the Benguela upwelling system, the location of a fishing industry important to the economy of the west coast of South Africa. Features that make these shelf seas of interest to oceanographers include the cold inshore waters with upwelling centres constrained to the coast and the warm offshore oceanic waters with their embedded large Agulhas Rings of tropical Indian Ocean water. This spatial variability is complemented by temporal fluctuations imposed by local winds and the poleward passage of coastal trapped waves to form a pulsed system with an event-scale of perhaps one week.

On this event scale, sea level is just one of the variables that can be used as a proxy for upwelling. Integrating over the temporal and spatial scales sustains relationships between the variables of the physical environment of the wind driven shelf circulation. Even to the interannual scales and decadal scales, strong winds, high cumulative sea level fluctuations and cool temperatures occur together.

In general, physical factors tend to dominate marine ecosystem function, particularly so for matched time and space scales when enhanced boom and bust responses are found. Then any predictive ability for physical events can be carried into the ecosystem function and there are prospects for extending forecasts from the physical environment into the realm of living marine resources. The key link is the significant negative relationship between SST and the supply of nitrate to the surface in upwelled water. The nitrate supply fuels a short food chain through primary productivity and zooplankton to shoal fish such as anchovy and sardine. Each upwelling event brings nitrate to the surface; the stronger the event the greater the nitrate supply. From the sum of all the events in each June to May year, the cumulative nitrate supply gives annual estimates of potential new production for the years of the eighties for the southern Benguela.

The magnitudes of the potential new production are reasonable. However for the interannual variability there is a crucial test. Is there any relation between the estimates of annual new production and the estimates of fish biomass obtained acoustically by the regulative authority? The result agrees with the Optimal Environmental Window hypothesis of Cury and Roy (1980), which says that both too much and too little upwelling are detrimental to the fishery. A subjective positioning of the OEW suggests that upwelling events that result in potential new production of between 54 and 61 Mt of carbon per year will maximise the anchovy biomass. Less strong upwelling does not provide enough food, whilst very strong upwelling disrupts the food chain. If this OEW relationship is robust, an estimate of biomass can be obtained from the cumulative upwelling events up to May of each year, which is six months before results from the acoustic survey used for setting the annual quota. Such advance notice can be of considerable value to the fishing industry regulators.

**Non-linear tidal analysis: Transferring
energy from the astronomical tide to the
mean sea level**

Eduardo Marone
Centro de Estudos do Mar
UFPR – Brazil

Abstract

With the development of new time series analysis methodologies it is now possible to assess other physical processes that are part of the sea level signal. All the classical methodologies used to analyse sea level records are based in linear and stationary mixed models (stochastic). In that sense, the spectral estimators are convergent to the true spectral constituents only if the time series are stationary, continuous, differentiable, convergent and linear. It is also well known that the sea level signal is not necessarily a phenomenon that fits those criteria. Relative sea level rise (or drop) is a non-stationary processes and thus not convergent. On the other hand, the full hydrodynamic equations governing the tidal dynamics show clear non-linear terms (advective and frictional). The astronomic tidal potential has harmonic forcing, thus, the resulting sea level signal, after interacting with the solid and atmospheric boundaries, responds to this forcing in linear and non-linear ways, with the non-linear or shallow water tidal constituents being the commonly known “output” on the non-linear domain. Those non-linear interactions are well explained in mathematical models where the second and third order interaction can be represented through cosine (or sine) products whose arguments include those frequencies that are interacting to produce non-linear tidal constituents. The frequency that results from those processes can be obtained from the summation or difference between the astronomical harmonic components. In the theory of the generation of non-linear tidal constituents, much effort was made to explain the appearance of tidal energy in frequencies that do not correspond to astronomical forcing. Less attention was paid to the energy transference from astronomical frequencies to the mean sea level, which has a zero frequency. If we consider any given frequency interacting in a non-linear second order way with itself, it is common to pay attention to the resulting non-linear signal that has twice the original frequency value. On the other hand, the difference, i.e. the zero frequency or the mean sea level, was not so well studied. Using bispectral analysis applied to hourly sea level data it is possible to see that significant tidal energy is transferred to the mean sea level. Through more adequate mathematical tools it is possible to obtain clear evidence that the non-linear energy transference from harmonic constituents to the mean sea level is important. This effect needs to be considered in a global perspective to clarify how advective and frictional long-term changes could result in sea level changes through non-linear energy transference. To do that, the mathematical tools need to be extended in order to allow for the analysis of long records, which is the only way to search for changes in the non-linear behaviour of the mean sea level.

Introduction

Modern tidal analysis is based on several time series analysis methodologies. Virtually all these established methodologies rest on two fundamental assumptions: the series is *stationary* (or can be reduced to one by a simple transformation) and conform to a *linear* model. The first assumption means that the main statistical properties of the series remain *constant over time*. Meanwhile, the second one means that the values of the observed series can be represented as *linear combination* of past and present values of *independent and/or strictly random* series (Priestley, 1989). The harmonic representation of the sea level conforms to this concept. This model, known as a mixed spectrum model (Priestley, 1981), could be expressed as:

$$\zeta(t) = \sum_i A_i \cos(\omega_i t + \phi_i) + \varepsilon_t$$

Where $\zeta(t)$ is the observed sea level at instant t , ε_t is a white noise and the summation of harmonic terms consists in the tidal components' amplitudes A_i , frequencies ω_i and phases ϕ_i .

This conceptual model has two limitations that were not well studied until recent times:

- (i) It is a linear and stationary model.
- (ii) It supposes that the entire non-harmonic signal could be well represented as white noise.

Needless to say, both these assumptions are mathematical idealisations that, in some cases, may be valid only as approximations to the real world.

Limitation (ii) has consequences on the accuracy of the tidal estimates, but despite several works dealing with those uncertainties (Cartwright and Amin, 1988; Franco and Rock, op. cit.; Gutiérrez et al., 1981; Mosetti, F. et al., 1985; Mosetti, R., 1983; Zetler et al., 1979; etc.) they were always considered not important enough to modify the final results or to mask the physics behind the data and results (when classical tidal analysis methods were well applied, of course). Even if it is not completely true that these errors are not negligible (Marone et al., 1997), the result of the use of these methodologies gave the opportunity to advance in several fields of the oceanography. The tidal analysis methods and their calculated tidal constants worked fine until the arrival of very sophisticated numerical models and satellite altimetry that require very fine and well adjusted tidal estimates, which are not possible to obtain with the classical methods due to the above listed limitations.

In that sense, limitation (i) seems to be more important because of a well known fact: *sea level is neither stationary nor linear*. A reasonable improvement would be to represent the sea level under a non-linear multi-spectral model (Marone, 1994), as:

$$\begin{aligned} \zeta(t) = & \sum A_i \cos(\omega_i t + \phi_i) + \sum \sum A_i \cos(\omega_i t + \phi_i) A_j \cos(\omega_j t + \phi_j) \\ & + \sum \sum \sum A_i \cos(\omega_i t + \phi_i) A_j \cos(\omega_j t + \phi_j) A_k \cos(\omega_k t + \phi_k) + \\ & \vdots \\ & + \varepsilon_t \end{aligned}$$

This is known as the poly-spectral model (Priestley, op. cit).

BISPECTRAL APPROACH

There are as yet no easy computing algorithms, as the FFT was in the past, to estimate poly or multi spectra of any degree as the above equation represents, but recent developments gave us the tools to estimate bispectra, i.e. the second order non-linear terms of the multi spectral representation (Suba Rao & Gabr, 1988, Marone et al., op. cit.). In that sense, it is a step forward, especially when one thinks that many non-linear phenomena are of the second order in marine physics.

Non-linear effects, in the hydrodynamic equations, are related with advective and frictional terms (non-linear terms). Friction, for instance, is represented as being proportional to $\mathbf{u}|\mathbf{u}|$, where \mathbf{u} are oscillating currents. Then, we will have product of cos (or sin) between different tidal frequencies as:

$$\cos(\alpha) \cos(\beta) = 1/2 \cos(\alpha + \beta) + 1/2 \cos(\alpha - \beta),$$

That could be expanded, calling $\alpha = \omega_1 t$ and $\beta = \omega_2 t$ and using the trigonometric relationships, as:

$$\begin{aligned} & [\cos(\omega_1 t) + \cos(\omega_2 t)] + \{[\cos^2(\omega_1 t) + \cos^2(\omega_2 t)] + [\cos(\omega_1 t) \cos(\omega_2 t)]\} \\ & = 2 \cos(\omega_0 t) + \cos(\omega_1 t) + \cos(\omega_2 t) + 1/2 [\cos(\omega_3 t)] + 1/2 [\cos(\omega_4 t)] + [\cos(\omega_5 t)] \end{aligned}$$

where

$$\omega_0 = 0 = (\omega_1 - \omega_1) = (\omega_2 - \omega_2), \omega_3 = 2\omega_1, \omega_4 = 2\omega_2 \text{ and } \omega_5 = (\omega_1 + \omega_2).$$

As can be observed, one of the resulting frequencies is zero, i.e., corresponding to the mean sea level. It means that energy from astronomical tidal frequencies could be transferred to the mean sea level by non-linear effects.

Using adequate mathematical tools (non-linear spectral estimators, Suba Rao et al., op. cit.) it is possible to obtain the spectral density of non-linear second order interactions, which modifies the total amount of energy at the mean sea level frequency (zero), thus modifying the mean sea level itself. Following this advancement it is now possible to assess other physical processes that are part of the sea level signal, separating also the linear from the non-linear spectral energy (Marone, 1996).

SOME RESULTS

Through the use of bispectral analysis applied to hourly sea level data it is possible to observe that significant tidal energy is transferred to the mean sea level. Hourly sea level data obtained in Ingeniero White, Argentina, separated by season, were analysed using bispectral analysis (among others not shown for brevity). The respective bispectra, plotted in Figure 1, show that the bispectral density has maxima at different crossing frequencies (both that are non-linearly interacting), and also that seasonal variation on the non-linear interaction are important. As can be verified, there is clear evidence of the non-linear energy transference from harmonic constituents to the mean sea level, because most interactions are between the same frequencies.

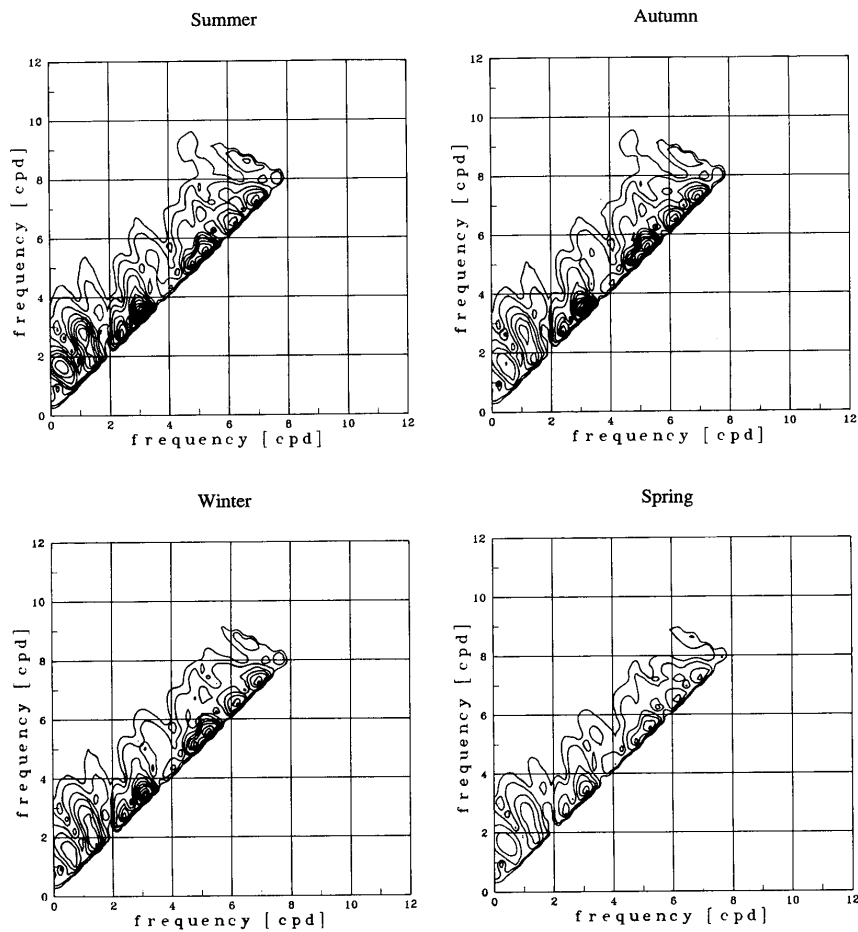


Figure 1. Seasonal bispectral normalised density function plot. Second order non-linear combination between frequencies (horizontal and vertical axes) produce energy accumulation in different frequencies combinations, as indicated by isolines nuclei.

An approximate quantification of the bispectral density function contribution of each tidal band to other frequencies (Table 1), shows that mean sea level receives as much energy as almost all the other tidal bands (except eight-diurnal). This energy seems to be mainly transferred by non-linear effects from the semi-diurnal band.

Table 1. Normalised bispectral density function $\{[(h \text{ cm}^2)^{1/2}]10^3\}$. Seasonal maxima and main tidal band interacting to produce the respective maxima for Ingeniero White, Argentina (hourly seasonal sea level data). (nD indicates the nth diurnal band)

Normalised bispectral density function and the main source (tidal band)								
Tidal Band	Summer	Main Source	Autumn	Main Source	Winter	Main Source	Spring	Main Source
Mean sea level	11	2D	6.2	2D	6	2D	5.3	2D
Long period	15	2D	8.5	2D	8	2D	7.5	2D
Diurnal	14	3D	11	2D	12	2D	7.5	3D
Semidiurnal	8.5	3D	15	3D	6.4	3D	8.1	3D
Terdiurnal	29	3D	27	3D	23	3D	13	3D
Fourth-diurnal	6.7	4D	7.4	4D	7.2	4D	4.1	4D
Fifth-diurnal	17	5D	18	5D	19	5D	9.1	5D
Sixth-diurnal	13	6D	15	6D	13	6D	7.4	6D
Seventh-diurnal	13	7D	14	7D	13	7D	7.0	7D
Eighth-diurnal	3.3	8D	3.6	8D	3.5	8D	1.1	8D

These effects need to be considered in a global perspective to clarify how advective and frictional long-term changes could result in sea level changes through non-linear energy transference. Mathematical tools need to be extended in order to allow for the analysis of long records, which is the only way to search for changes in the non-linear behaviour of the mean sea level.

Miscellaneous

Other work related to mean sea level studies, which is being carried out by the Marine Physics Lab of the CEM-UFPR, is in connection with the new Brazilian Program of Mean Sea Level, which decentralised the digitisation and processing of the sea level records, formerly by the Brazilian Navy, to local universities. In that sense, we are now processing the tidal data obtained at the Paranaguá Bay, and very soon we will be able to present the new results. On the other hand, we are planning to change the old tidal gauges, now operating in Paranaguá, with new automatic gauges that are also linked with a Coastal GOOS Pilot Project. High accuracy DGPS techniques are also being used to occupy the tidal stations. All three permanent operational tidal gauges are being fixed with high precision DGPS. The most important work is related with the reoccupation of the Imbituba tidal station (not yet permanently) using automatic tidal gauges in the site of the old (abandoned) tidal station, simultaneously with earth tides and gravimetric tidal studies and DGPS positioning. The importance of these studies can be clearly understood by mentioning that the Imbituba tidal station and related benchmark is used as the official Brazilian Vertical Datum origin. This station was abandoned when the Imbituba harbour was privatized, and the old tidal gauge deactivated. More accurate values for the geoid reference are now available for that location. The use of numerical tidal modelling to simulate the coastal dynamics in different geological ages (under different sea levels) is another work that should be mentioned.

Acknowledgment

This work was finished during an Associate Visit at the International Centre for Theoretical Physics, Trieste, Italy.

References

- Cartwright D.E. and Amin, M.; 1988: *The variances of tidal harmonics*. Dt. hydrogr. Z., **39**, 235-253.
- Franco A.S. and Rock N.J.; 1974: *Comparative accuracy of Fourier tidal analysis employing different time spans with reference to a Doodson analysis*. Ciência e Cultura, **26**, 498-507.
- Gutiérrez A., Mosetti F and Purga N.; 1981: *On the indetermination of the tidal harmonic constants*. Nuovo Cim., **4C**, 563-575.
- Marone E. and Mesquita A.R.; 1994: *On non-linear analysis of tidal observations*. Continental Self Research, 14(6), 557-588.
- Marone E.; 1996: "Radiational Tides" as nonlinear effects: bispectral interpretation. Continental Self Research, 16(8), 1117-1126.
- Mosetti F. and Purga N.; 1985: *Some question about the reliability of the analysis of tides and related phenomena*. Boll. Geof. Teor. Appl., **3**, 219-253.
- Mosetti R.; 1983: *A Kalman filter estimate of the tidal harmonic constants*. Nuovo Cim., **6C**, 445-452.
- Munk W.H. and Cartwright D.E.; 1966: *Tidal spectroscopy and prediction*. Phil. Trans. Roy. Soc. A, **1105**, 533-581.
- Priestley M. B.; 1981: *Spectral analysis and time series*. Academic Press, London. 890 pp.
- Priestley M. B.; 1989: *Non-linear and non-stationary time series analysis*. Academic Press, London. 237 pp.
- Suba Rao T. and Gabr M.M.; 1988: *The estimation of bispectral density function and the detection of periodicities in a signal*. Jour. of Multivariate Analysis, **27**(2), 457-477.
- Zetler B.D., Cartwright D.E. and Berkman S.; 1979: *Some comparison of response and harmonic tide predictions*. Int. hydrogr. Rev., **56**, 105-115.

Sea level changes in the Black Sea (1923-1997)

V. Belokopytov and Y. Goryachkin
Marine Hydrophysical Institute, 2, Kapitanskaya St,
Sevastopol, 335000, Ukraine

During its geologic history the Black Sea, like other parts of the ocean, has undergone large changes of sea level. The most spectacular changes were connected with regressions and transgressions, for example, at the Upper Pleistocene Period (17,000 to 6,000 years ago), when the rate of sea level rising was about 90 cm per century, and the Holocene period (beginning 6,000 years ago), when the increasing of sea level has been 10 to 40 cm per century. Moreover, the Black Sea repeatedly was separated from the ocean and existed as a lake. Studies of the Black Sea benches has shown that over the last 4,000 years the Black Sea level was at least as low as two times than the contemporary level. Observations of sea level in the Black Sea started in the middle of the last century, but regular ones have been carried out only since 1873.

The Black Sea is an internal sea connected with the Mediterranean through the system of Turkish straits. Since the straits are rather narrow and shallow the Black Sea is one of the most isolated seas in the world. It leads to the effective weakening of tidal oscillations penetrating from the Atlantic and Mediterranean, diluting the sea and the crucial role of the fresh water budget in sea level peculiarities. The general picture of the sea level spatial distribution shows a permanent elevation zone along the coastline and a lowered area in the central deep part of the basin. Mesoscale variability manifests itself in numerous eddies both moving and stationary on the background of steady cyclonic circulation.

Despite tidal oscillations that are negligible in the Black Sea, temporal short-term variability comprises a significant part of total sea level variability, especially in shelf areas such as Odessa where wind-induced phenomena prevail and sometimes reach 2-3 m. In locations close to continental slope such as Sebastopol or Tuapse, short-term oscillations usually do not exceed 20 cm.

Monthly time-series reveal a well-developed annual cycle with magnitude 20-40 cm (Fig. 2a). The mean sea level march has its maximum in June and minimum in October (Fig. 2b). Main constituents of the annual cycle are fresh water input (FWI), steric and atmospheric pressure effects. They have mutual phase shifts and can act as oppositely directed forces. The steric effect has its maximum in August when FWI has its minimum. On the whole FWI exceeds by about two times the steric and barometric effects. The main components of the FWI (Fig. 2c) are river runoff and evaporation. Their annual marches coincide very closely. Precipitation has a smaller magnitude and only modifies the resulting FWI curve.

The mean range of year-to-year sea level oscillations is similar to seasonal and short-term variations. If we infiltrate prevailing frequencies of 2-3, 5-6 and 11-12 years, then the long time series can be broken down into the two periods: before the 1920s of this century and after the 1920s (Fig. 3). The first period could be characterized as stable with slight lowering of sea level. After the 1920s there is a positive trend with a mean rate 2.8 mm per year (from 2.0 in Tuapse and 3.4 in Evpatoriya). If we accept existing estimates of tectonic movements of the whole Black Sea as a subsidence with rate 0.7-1.1 mm per year, then we can conclude that two thirds of the sea level rise in this century is due to an increase of water volume (sea signal).

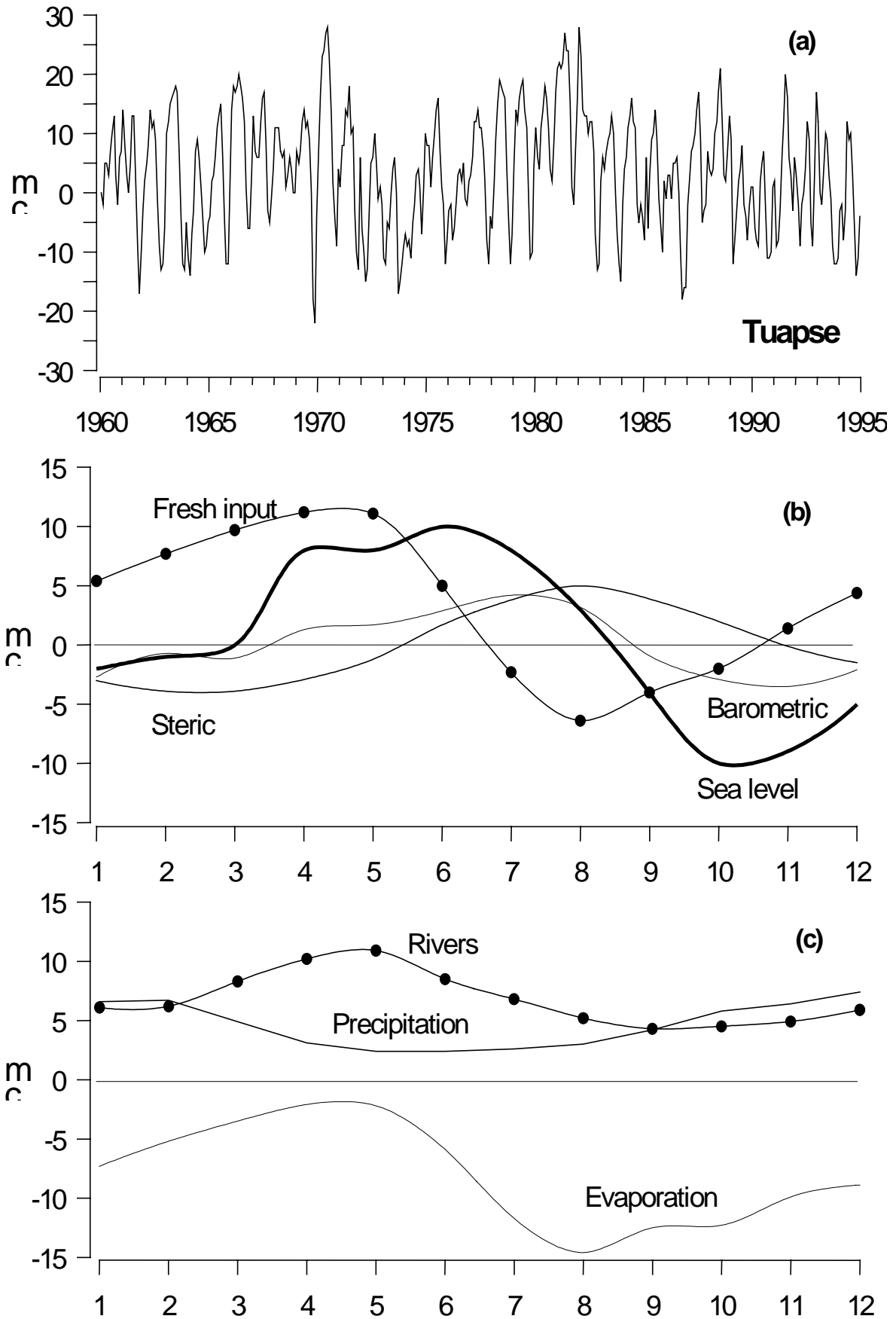


Fig. 2 (a) Monthly sea level time-series in Tuapse; (b) Sea level seasonal cycle in the Black Sea
(c) Components of the fresh water input

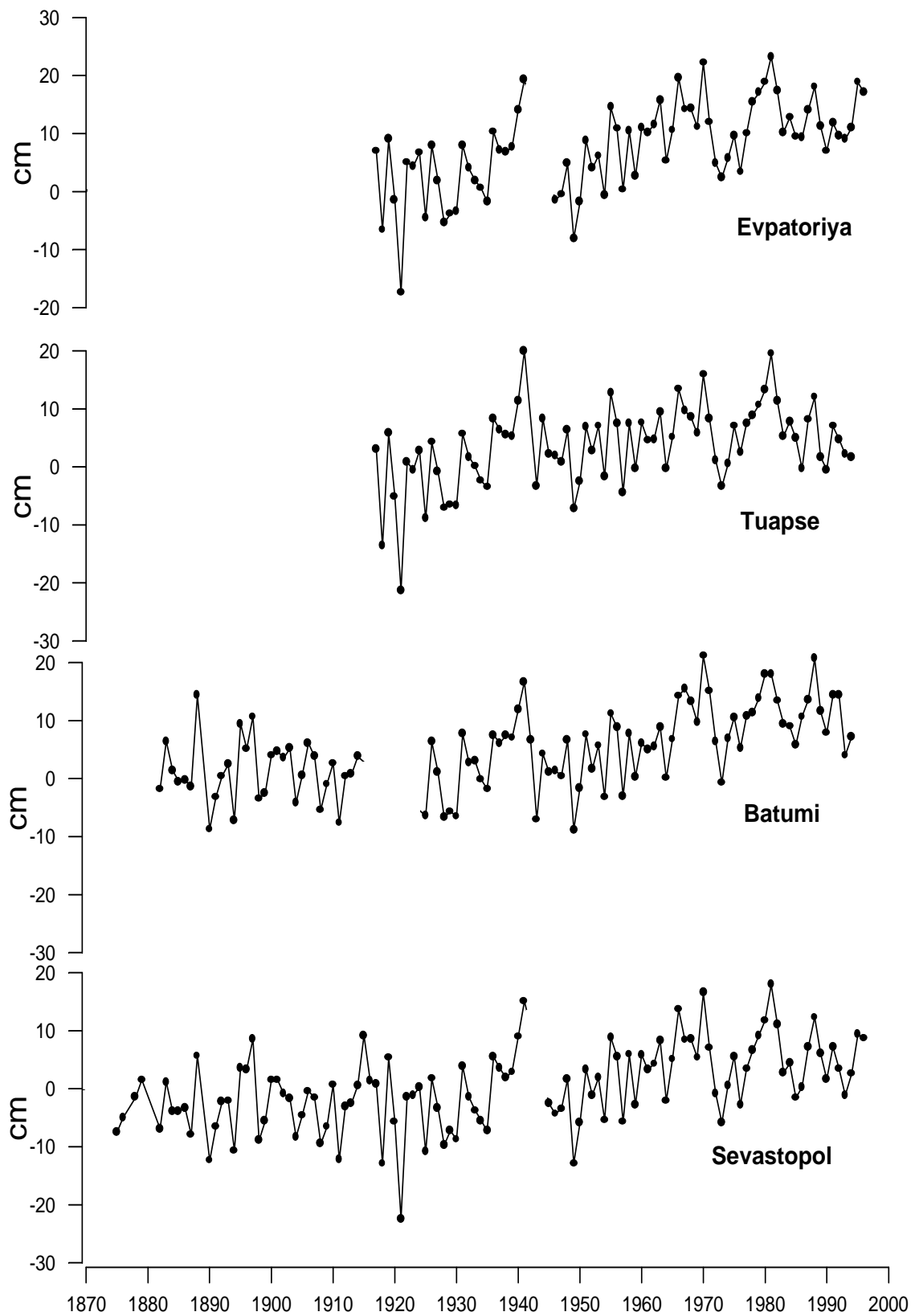


Fig. 3 Yearly sea level time-series along northern and eastern coast of the Black Sea (reference zero is the long-term mean in Sevastopol)

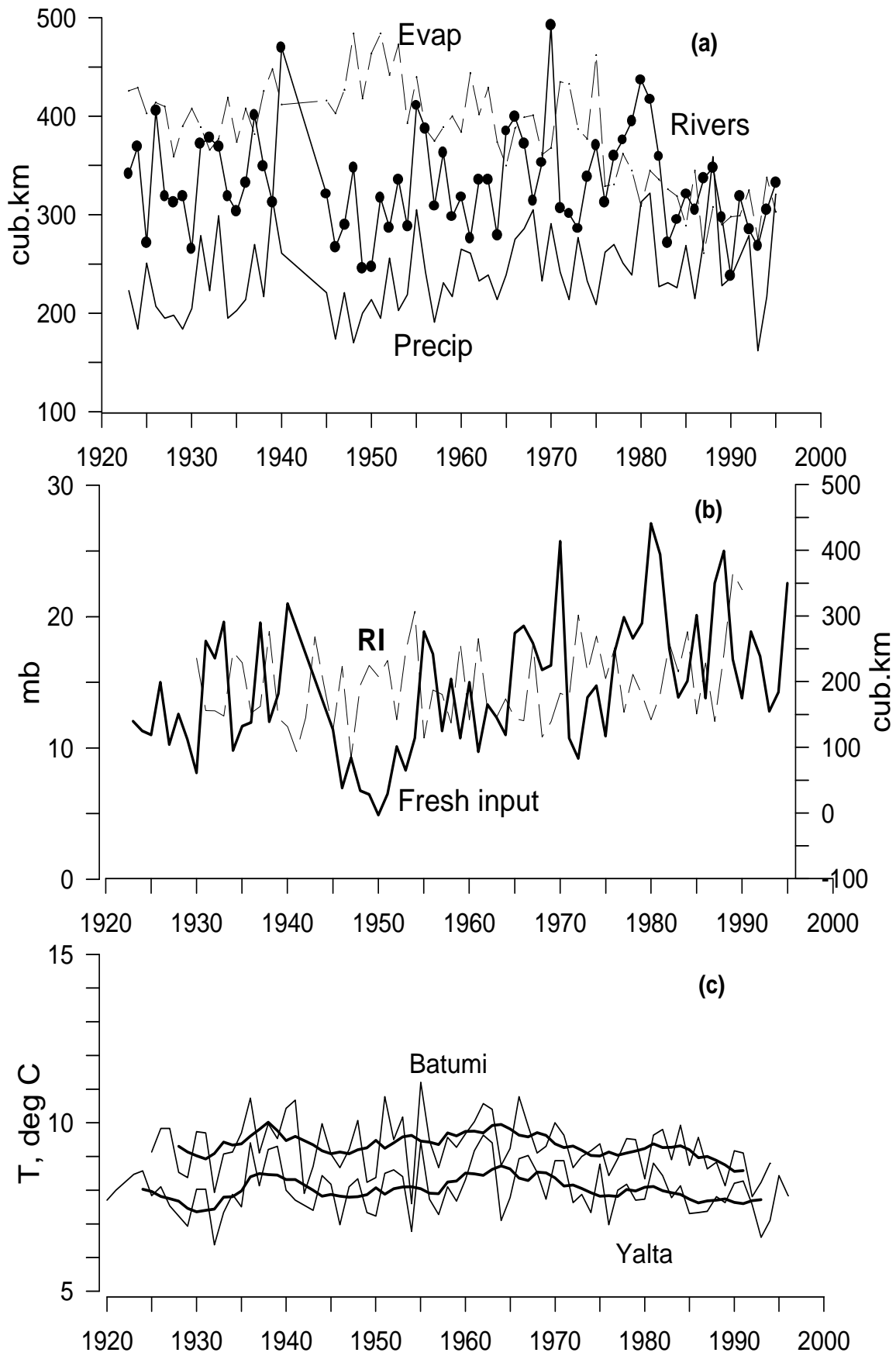


Fig. 4 (a) Yearly components of fresh water input; (b) Fresh water input and Rossby index; (c) winter averaged SST time-series

Interannual and decadal sea level variability closely correlate with FWI variability on the same scales. The mean trends of the FWI components are assessed as 1.5 cubic km per year for river runoff, 1.6 cubic km per year for precipitation and –3 cubic km per year for evaporation for last 40-year period (Fig. 4a). That is, there was a tendency toward the growth of river runoff and precipitation, accompanied by a considerable reduction of evaporation. In turn, the FWI is connected with processes of large-scale atmospheric circulation, especially over the North Atlantic and Europe. It is quite evident, for example, from comparison of the Rossby index (RI) and FWI time-series (Fig. 4b), where significant negative correlation exists. Such a connection is explained by the changing of large-scale atmospheric patterns. In periods of high RI cyclone paths shift to the North of Europe and the Black Sea river catchments gain less precipitation, and when the RI is low more cyclones pass through Black Sea region bringing moisture and increasing runoff.

The steric effect, or thermal expansion factor due to global warming, is not so evident in the Black Sea as in some other parts of world ocean. Sea surface temperature (SST) trends in summer are not significant or have different signs from site to site. Winter SST time-series manifest more clear and coherent tendencies (Fig. 4c). There is warming up to the 1960s and then cooling up to now. Similar trends also exist in the case of temperature in the core of the Cold Intermediate Layer in which renewal occurs in cold winters. A decrease of 1°C is revealed over the last 30 years in this water mass as well on surface time-series.

Despite the existing trends of the FWI, it hardly causes the sea level rise observed in the Black Sea. Usually excess of water in the Black Sea is balanced by the Bosphorus flow into the Sea of Marmora. The most evident cause is eustatic rise of ocean level and assessments of the Mediterranean sea level rise (2.5 mm per year) correspond to the Black Sea estimates.

**MedGLOSS pilot network of sea level monitoring in
Mediterranean and Black Seas : Present and future activities**

D. Rosen

*Israel Oceanographic & Limnological Research
National Institute of Oceanography
Tel Shikmona, Haifa 31080, Israel*

Background

Presently, a worldwide eustatic sea-level rise due to the “greenhouse effect” has been forecasted by the WMO/UNEP Intergovernmental Panel on Climate Change (IPCC). Those are due to global warming, leading to water volume expansion as the major component and ice cap melting as the secondary one. However, the report authors also recognized that regional sea-level rise may differ significantly from the globally averaged sea-level rise forecasts, in particular due to tectonic movements, meaning that relative sea-level changes may be as important or even more than those of the absolute sea-level.

Recognizing the importance of the subject for the region, as well as its capability to serve as a model for the world-wide processes, the IOC and the Commission Internationale pour l'Exploration Scientifique de la mer Méditerranée (CIESM), have agreed in 1996 to jointly cooperate in the study of this important subject by establishing a long-term monitoring network system for systematic sea-level measurements in the Mediterranean and Black Seas. The system, named MedGLOSS (Mediterranean regional subsystem of the Global Sea Level Observing System), a monitoring network system for systematic measurements in the Mediterranean and Black Seas, is being developed by applying basic GLOSS requirements and methodology, aiming to provide high-quality standardized data, which can then be directly applied for the various regional and world-wide studies.

A preliminary expert workshop on MedGLOSS was held jointly by CIESM and IOC at CIESM headquarters in Monaco in February 1996. In the summer of 1996 a Memorandum of Understanding was signed between IOC and CIESM (by Prof. Frederic Briand - Director General of CIESM, , and Dr. Gunnar Kullenberg – Executive Secretary of IOC), establishing also a Joint Group of Experts on the MedGLOSS programme, composed of Prof. Suzanna Zerbini (Italy), Mr. Pierre-Yves Le Traon (France), Cdr. M. Emin Ayhan (Turkey) and Mr. Dov S. Rosen (Israel). Later on Dov Rosen was appointed chairman of this group. Following the recommendations of the Joint Group of Experts on MedGLOSS, at their 1st session on 20-21 January 1997 at the IOC/UNESCO headquarters in Paris, it was decided to start MedGLOSS by launching a pilot network monitoring system. The Joint Group of Experts noted that the IOC Black Sea Regional Committee at its First Session (September 1996) had recommended to initiate a Black Sea sea-level monitoring programme in association with GLOSS, with emphasis on coastal regions subject to flooding and sea-level rise impact.

The pilot network was initially planned to include some 27 stations in 13 countries which have expressed their interest in joining this international research network. Inclusion of additional stations/countries to the pilot phase by other countries could be considered if they answered the requirements of the pilot stations. Details were provided in the summary document on MedGLOSS prepared by the author in February 1997. The pilot network was intended to become operational and provide initial useful results during 1998, to serve as a model to all countries along the coasts of the Mediterranean and Black Seas, with respect to the attributes and gains expected by all Mediterranean and Black Seas countries joining the MedGLOSS. The pilot network consists of the five GLOSS sea-level monitoring stations available in the basin area, and a limited number of sea-level monitoring stations located in countries which expressed their interest in joining MedGLOSS. The pilot plan called for a minimum of two visits of 3-5 days GPS missions and absolute gravimetry at all selected sites, of which a limited number were planned to become permanent GPS stations. The sea-level stations should provide hourly sea-level and atmospheric pressure data daily, via near real-time monitoring, communication and presentation system. The preliminary outcome of the data processing

and applications were planned to be presented at the CIESM Congress in Dubrovnik which took place in June 1998, with the intention to invite at that time all Mediterranean and Black Seas bordering countries to join the MedGLOSS network.

Progress of pilot network set-up

During 1997 contacts were established with the 13 countries listed in Table 1 attached here. Later on requests from two more countries (Romania and Georgia) for joining the MedGLOSS pilot network were received. In June 1997 a joint IOC-CIESM training workshop on sea-level observations and analysis for the countries of the Mediterranean and Black Seas was held at the Proudman Oceanographic Observatory in UK. It included trainees from Algeria, Bulgaria, Croatia, Egypt, Morocco, Romania, Turkey and Ukraine which enjoyed the lectures of a number of invited experts and of POL experts. The writer presented the trainees with the MedGLOSS programme and established direct contacts with the participants. An additional course in accurate benchmark leveling for sea-level reference and plate tectonics movements detection was held under the leadership of Prof. Suzanna Zerbini in Kos, Greece.

Following these workshops, the writer presented an update of the needs of the various countries which expressed interest in joining MedGLOSS. All resumed to some way or another in requesting some financial support. On the basis of the status of the various stations selected for the pilot stage, it was estimated that a sum of about \$300,000 will be needed to cover the cost of upgrading some of the sea-level monitoring stations and especially for the combined GPS/accurate gravimetry missions. It became clear that the IOC and CIESM can not provide so large funds, so an effort was done by Suzanna Zerbini and Dov Rosen to prepare proposals for funding from European research programmes in fall 1997 and winter 1998. These however unsuccessful as the time schedule for the submission of the proposals could not be met due to lack of partners from Egypt or Tunisia in one proposal with Italy and Israel, or too late arrival of another final proposal for submission (with United Kingdom, Israel, Ukraine and Georgia).

At the CIESM Congress held in Croatia in June 1998, the importance of MedGLOSS was again reaffirmed, and CIESM commitment to MedGLOSS was reconfirmed. CIESM decided to support the upgrading of 4 sea-level stations in 4 member countries, namely Romania, Croatia, Egypt and Tunisia which were considered of higher priority in provision of sea-level data at regions lacking any digital stations for near-real time data transfer. Matching for the measurement of the benchmarks by accurate GPS and gravimetry were expected to be provided by IOC, but so far these were not received. However, with the recent occupation of the IOC position held in the past by Dr. Albert Tolkatchev by Dr. Thorkild Aarup, Programme Specialist it is expected that IOC once again will join forces with CIESM in the advancement of MedGLOSS, including provision of funds. The countries adhering to the MedGLOSS pilot network, have been requested to commit themselves for long-term maintenance of the sea-level stations, for submission of the near-real time sea-level and atmospheric pressure data to the temporary MedGLOSS centers established at Israel Oceanographic and Limnological Research, National Institute of Oceanography (sea-level verification and redistribution), the satellite sea-level monitoring station of the Collecte-Localisation-Satellite (CLS), Direction de l'Océanographie Spatiale in Toulouse, France as well as to the PSMSL in UK and at the University of Bologna for GPS Sea-Level Bench Marks data.

After contacts with the Tunisian authorities, it was decided by them that Tunisia will setup on its own funds a sea-level station according to the MedGLOSS standards. At present time it is yet not clear when its integration in the MedGLOSS pilot network will be effected. Consequently, CIESM decided to install the equipment of the available sea-level station to Malta. Official commitments to join MedGLOSS pilot network (including data transmission and long-term maintenance and operation) have been received from Romania, Croatia and Malta, while the ones from Egypt are yet to be received, although positive expression to join was given.

Conclusions

The integration of MedGLOSS near-real time sea-level ground true data with the Mediterranean Forecasting System (MFS) has been recognized at the Malta workshop in December 1997. It will be used for providing the ellipsoid to geoid corrections in the sea-level real time satellite elevations measurements, without which the flow gradients fed to the oceanographic numerical models run in these basins may be wrongly determined. It is hoped that the end of the millenium will become a time pivot point in the progress of MedGLOSS. The recent confirmation of the increased rate of melting of the ice cover over Greenland published in Nature this February and the hot 90's period with the climax in 1998 (so far, perhaps jointly by El-Nino and global warming) show that MedGLOSS is becoming a very important means of knowledge and tool for decision making in regards to long term planning in the marine environment and at the coasts of the Mediterranean and Black Seas (particularly in the southern part of the Mediterranean and certain parts of the Black Sea, which seem that could be potentially more affected by sea-level rise). Hence, continued support by CIESM and IOC and the countries joining MedGLOSS should be given high priority and adequate support.

Table 1 : List of selected stations for the MedGLOSS pilot network

Station No.	Station Name	State	Present status	Past Data Since	Sea Level Sensor Type	Digital Data	GPS plans for monitoring
1	Gibraltar	U.K.	GLOSS	1961			fix
2	Alicante	Spain		1916			fix
3	Palma	Spain		1964			fix
4	Marseille	France	GLOSS	1885			fix
5	Genoa	Italy		1884			fix
6	Naples	Italy		1899			fix
7	Catania	Italy		1960			fix
8	Brindisi	Italy					fix
9	Trieste	Italy		1905			fix
10	Split	Croatia		1954			fix
11	Dubrovnik	Croatia		1956			fix
12	Preveza	Greece		1975	Float		fix
13	Kalamata	Greece		1936	Float		fix
14	Piraeuss	Greece		1933	Float		fix
15	Soudhas	Greece		1973	Float		fix
16	Rodhos	Greece		1981	Float		fix
17	Burgas	Bulgaria					fix
18	Katsively	Ukraine					fix
19	Tuapse	Russia	GLOSS	1917			fix
20	Erdek	Turkey		1985	Float		fix
21	Mentes	Turkey		1986	Float		fix
22	Bodrum	Turkey		1986	Float		fix
23	Antalya	Turkey		1986	Float		fix
24	Hadera	Israel	GLOSS	1993 (1958)	Pressure	yes	fix
25	Alexandria	Egypt		1958			fix
26	Mellieha Bay	Malta		1993	Pressure		fix
27	Ceuta	Spain	GLOSS	1944			fix
new	Constanta	Romanie		1933	float		fix
new	Bizerte ?	Tunisia		?			fix

Additional countries and sea-level stations are welcome to join MedGLOSS

**Ascension Island: a central Atlantic node for
sea level and geodesy**

*P. Axe
CCMS-Proudman Oceanographic Laboratory
Bidston Observatory
Prenton, Wirral, CH43 7RA, U.K.*

ABSTRACT

For altimeter calibration studies, it is recommended to use tide gauges that have low levels of residual variance between the altimeter and the tide gauge. This excludes sites with large levels of wind and wave setup, generally restricting choice of sites to tropical regions.

Since April 1983, sea level has been measured at Ascension Island, by tide gauges in Clarence Bay (until 1995) and English Bay (since May 1993). These data are collected as part of the Proudman Oceanographic Laboratory's ACCLAIM program (Spencer et al., 1993), and have been used to study harmonic constants (Cartwright et al., 1988) and departures from the local inverse barometer model (Woodworth et al., 1995). These measurements can be related to the reference ellipsoid through the International GPS Service station (ASC1) on the island. PRARE (Precise Rate and Range-rate Equipment), and DORIS (Doppler Orbitography and Radio-positioning Integrated by Satellite) contribute to precise orbit positioning for the ERS-2 and TOPEX/Poseidon satellites respectively. The use of tide gauge data integrated with GPS will allow precise altimeter comparison with observed sea levels over the long term. Complementing these island based measurements, the nearby PIRATA mooring 'GAVOTTE' at 10° S, 10° W provides temperature and salinity data down to 500 m, allowing an assessment of baroclinic influences on measured sea level.

INTRODUCTION

Ascension (7.92° S, 14.42° W) is a volcanic island in the equatorial Atlantic. The first tide gauge was installed at Clarence Bay in April 1983, as part of the Proudman Oceanographic Laboratory's (POL) 'ACCLAIM' (Antarctic Circumpolar Current sea Levels by Altimetry and Island Measurements) programme, described by Spencer et al. (1993). This tide gauge consisted of a sea bed mounted pressure recorder, and data were used in Cartwright et al.'s (1988) study of Atlantic tides, and in Woodworth et al.'s (1995) study of the inverse barometer effect. This gauge was operated until January 1995. In May 1993, a new tide gauge was installed at English Bay. This gauge is a POL 'B-gauge' (Woodworth et al., 1996) so has precise datum control, and is suitable for long term trend as well as higher frequency (for example harmonic analysis) studies. These high frequency data is available via ftp from POL at <http://bisag.nbi.ac.uk/pub/woce/acclaim/phase2>.

Geodetic measurements have been available from the IGS GPS station at the US air force base on the island since April 1996. Daily solutions are available via ftp from, for example, the JPL and SOPAC web sites. In addition to GPS, a PRARE system, for tracking ERS-2 is operated by POL on the north west of the island. This provides precise fixing of satellite position and velocity, for improved orbit modelling. This in turn improves the altimeter-based estimate of sea level. On the eastern side of the island, a DORIS beacon is operated by CNES (Centre National des Etudes Spatiales) for tracking Spot and TOPEX/Poseidon satellites. Geodetic levelling between these instruments and the tide gauge allows the sea level data to be included in the same geocentric reference frame as satellite altimetry measurements. Figure 1 shows a map of the island, and the location of these instruments.

The waters off Ascension are stratified, with a surface mixed layer depth of 60 m. It has long been suspected that internal tides, for example, might affect the sea surface elevations measured at the island. Since 1997, the PIRATA (Pilot Research Array for the Tropical Atlantic) project has been installing ATLAS (Autonomous Temperature Line Acquisition System) moorings in the tropical

Atlantic. This is a collaborative international contribution to CLIVAR-GOALS and GOOS from research teams in Brazil, France and the United States. The PIRATA implementation plan is available from http://www.ifremer.fr/orstom/pirata/infos_us.html. Two PIRATA moorings have been deployed in the vicinity of Ascension. The GAVOTTE mooring at 10° S, 10° W has been operational since September 1997, while the VALSE mooring was deployed in January 1999. Both moorings consist of thermistors at the surface and down to depth of 500 m. Conductivity sensors are fitted at depths of 1, 20, 40 and 120 m.

SEA LEVEL AND GEODESY

Sea level was calculated from the B-gauge pressure measurements using the method described in Woodworth et al. (1996). These 15 minute values were filtered to hourly (using the filter described in Pugh, 1987), and then to daily values using the Doodson X0 filter. Data were harmonically analysed to remove seasonal (annual and semi-annual) terms.

The daily means, least squares fitted annual and semi-annual harmonic components, and the monthly averaged residuals are shown in Figure 2. Mean sea level based on this analysis is 5.6 cm below B-gauge datum (May 1993). A linear trend based on this short record indicates a rate of change of mean sea level of +7 mm/yr. Variance in the non-tidal component of the recorded sea level is low - typically contributing less than 2% of the total record variance. This compares with a value of 15% at a higher latitude site such as Tristan da Cunha.

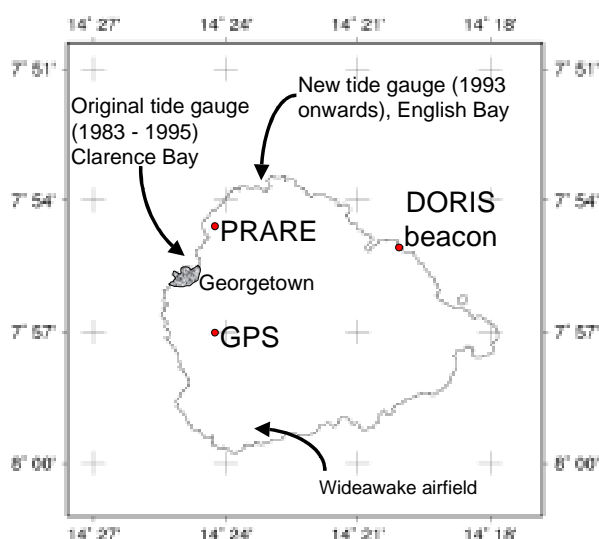


Figure 1 Ascension (Wideawake) Island, showing locations of equipment

Altimetry estimates of sea surface height were collated from TOPEX and Poseidon ascending and descending orbit tracks closest to the island. Data were reduced to an arbitrary datum (the median level of the tide gauge record). The daily mean values obtained from the altimeters by this method are shown in the 2nd panel of Figure 2. Altimeter and tide gauge data appear to be in good agreement (rms differences between daily means of approximately 3.5 cm).

Analysis of the IGS station data by JPL gave station co-ordinates and velocity estimates from April 1996. Estimates of the local vertical movement indicate a subsidence of 3 mm/yr. Assuming that the GPS site does not move relative to the tide gauge benchmark, the estimate of the absolute sea level change is +4 mm/year.

Estimates of horizontal land movements based on the IGS station record¹ indicate a 12.5 mm/yr motion, on a bearing of 336°. This is similar to estimates based on PRARE observations, and also from the NUVEL-1A plate motion model (De Mets et al., 1994). Estimates based on the DORIS beacon observations are not yet available.

DYNAMIC HEIGHTS

Dynamic heights were calculated using data from the PIRATA mooring GAVOTTE. The specific volume anomaly was integrated between the surface and 500 db. Where salinity data was

¹ These data are available from <http://sideshow.jpl.nasa.gov/mbh/all/ASC1.gif>.

unavailable (i.e. prior to November 1999, and also below 120 m depth) annual mean values were taken from Levitus (1994).

The dynamic height difference is plotted in Figure 2. Due to sensor failure between 98 and day 309, 1998, the record length is too short to compare with the tidal residual signal, to see how baroclinic changes around Ascension contribute to the observed sea level signal.

CONCLUSION

Ascension Island is equipped with a range of satellite tracking and geodetic instrumentation and contributes to the definition of international reference frames. The low residual variance in the sea level signal, and the presence of satellite tracking and GPS equipment make it an ideal site for altimeter calibration. The rugged terrain of the island does make levelling between instruments difficult however. Particular effort needs to be put into overcoming this problem, perhaps by the installation of a second (perhaps single frequency) GPS at the tide gauge to describe relative movements between this site and the IGS station. The deployment of ATLAS moorings in the PIRATA project will allow the better understanding of the influence of baroclinic motions on the observed sea levels.

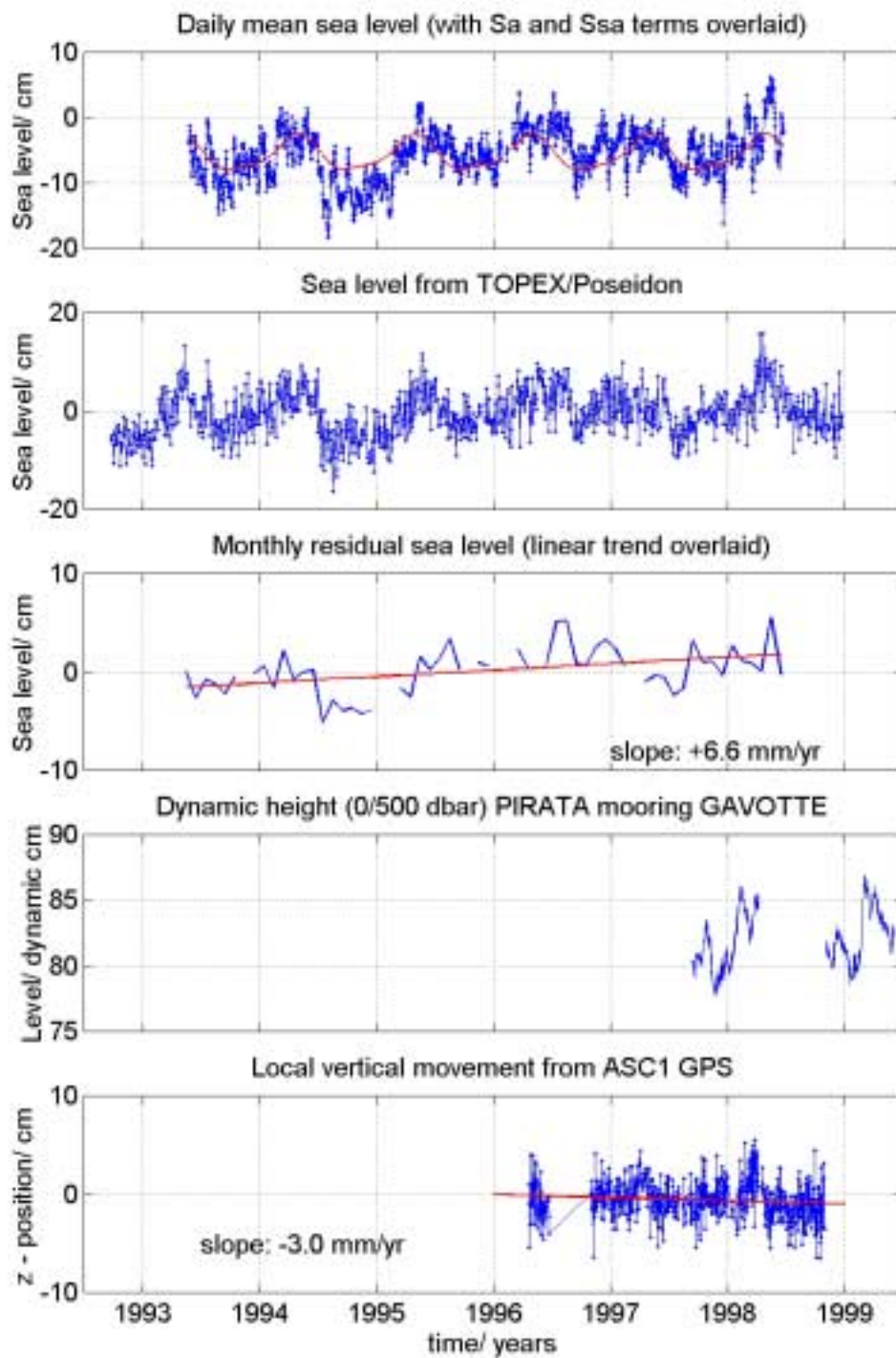


Figure 2 Time series of sea level related data from, or around, Ascension Island. Top panel is sea level relative to May 1993 datum, from the B-gauge in English Bay. Below that is sea level from TOPEX/Poseidon, from the closest passes, and reduced to a median datum. Next plot is monthly residuals (S_a and S_{sa} terms removed) calculated from the B-gauge data. Below this is dynamic height, between the 0 and 500 dbar levels, calculated from the PIRATA mooring at 10° S, 10° W. Final plot shows estimates of local vertical movement based on GPS solutions for the IGS station ASC1, calculated by JPL.

REFERENCES

- Cartwright D.E., R. Spencer, J.M. Vassie, and P.L. Woodworth, 1989, The tides of the Atlantic Ocean, 60°N to 30°S, Philosophical Transactions of the Royal Society of London volume 324, number 1581, pp 513-563,
- DeMets, C., R. G. Gordon, D. F. Argus, and S. Stein, Effect of recent revisions to the geomagnetic reversal time scale on estimate of current plate motions, Geophys. Res. Lett., vol. 21, no. 20, 2191-2194, 1994
- Pugh D.T., 1987, Tides, surges and mean sea level: A handbook for engineers and scientists, pub by Wiley, 471p
- Spencer R., P.R. Foden, C. McGarry, A.J. Harrison, J.M. Vassie, T.F. Baker, M.J. Smithson, S.A. Harangozo and P.L. Woodworth, 1993, The ACCLAIM programme in the South Atlantic and Southern Oceans, International Hydrographic Review, volume 70(1), pp 7-21
- Woodworth P.L., S.A. Windle and J.M. Vassie, 1995, Departures from the local inverse barometer model at periods of 5 days in the central South Atlantic, Journal of Geophysical Research, volume 100, C9, pp 18,281 - 18,290
- Woodworth P.L., J.M. Vassie, R. Spencer and D.E. Smith, 1996, Precise datum control for pressure tide gauges, Marine Geodesy, 19:1-20

Absolute calibration and verification of multiple radar altimeters

C.K. Shum, M.E. Parke
Civil and Environmental Engineering and Geodetic Science
The Ohio State University
2070 Neil Av., Columbus, Ohio 43210, USA

Doug Martin
Center for Operational Oceanographic Products and Services
National Oceanic and Atmospheric Administration
1315 East-West Highway
Silver Spring, Maryland 20910-2857, USA

Abstract

Satellite radar altimeter (RA) represents the only current technique capable of monitoring global sea level change with a temporal scale of days and a spatial scale of 100 km or longer. The use of island tide gauge measurements for the monitoring of the drift in TOPEX/POSEIDON (T/P) altimetric sea level measurements with an accuracy approaching 1 mm/yr has been demonstrated [Mitchum, 1998]. This paper addresses the potential use of multiple absolute RA calibration sites and the associated technical issues to monitor radar altimeter instrument, media and correction drifts using GPS buoys. Preliminary results using GPS buoy campaigns for absolute calibration of TOPEX Side B altimeter are presented.

Introduction

The ability to accurately measure global sea level variations is critical for global climate change studies, both in its present state and towards its prediction. The determination of the 21st century sea level rise, with published rate of 2-3 mm/yr, primarily used coastal and island tide gauges and correcting the postglacial rebound effect [e.g., Peltier, 1988]. Satellite observations are unique in their ability to measure sea level change with the appropriate spatial and temporal resolutions. Contemporary satellite radar altimeter (RA) represents the only current technique capable of monitoring global ($\pm 81^\circ$ latitude) sea level change with a temporal scale of days and a spatial scale of 100 km or longer. The primary limitations in the use of satellite radar altimeters for the accurate monitoring of global sea level variations include (1) their relatively short data record (<15 years of different altimeter mission data) as compared to century data span for some of the tide gauges, (2) the relative "complex" measurement system which requires various instrument, media and geophysical corrections to be known to reduce RA data to sea level measurements; thus representing a stringent requirement to monitor or model the measurement error at the 1 mm/yr level, (3) the necessity to "link" different RA instruments with the needed accuracy to enable the establishment of a long sea level measurement time series, and (4) the potential sampling errors associated with spatial and temporal coverage of RAs.

The use of island tide gauge measurements (~40 WOCE gauges) for the monitoring of the drift in sea level measurements inferred from satellite radar altimeter (TOPEX/POSEIDON) data has been demonstrated with an accuracy of approximately 1 mm/yr [Mitchum, 1998, Chambers et al., 1998]. The current limitations of this technique include the lack of accurate tide gauge vertical datum control and the lack of geographical coverage [Mitchum, 1997]. The planned 30 globally distributed tide gauge network would minimize the geographical coverage problem and would enable the altimetric sea level drift to be monitored with an accuracy of less than 1 mm/yr [Mitchum, 1997]. Another limitation is that this technique is excellent in the monitoring of the combined "drift" of altimetric sea level measurements, however not necessarily be able to monitor the drifts of each of the corrections needed to reduce RA data to sea level measurements. In theory, absolute RA calibration sites represent one technique that can potentially have the ability to monitor the RA drift in an "absolute" sense. For

example, GPS limb-sounding techniques and upward looking in situ radiometers represent independent measurements capable of potentially measuring altimetric media corrections (ionosphere and wet troposphere corrections) and provide one component of the sea level measurement error budget. However, the current operating absolute calibration sites are only a handful (i.e., Harvest Platform, Burnie, English Channel, etc), and cannot achieve the accuracy of relative altimetric sea level measurement drift monitoring using global tide gauges (i.e., the Mitchum [1998] technique). In addition, a number of limiting error sources currently inhibit the calibration accuracy to achieve the 1 mm/yr level, including the inaccurate modeling of the sea surface gradient correction due to the fact that the altimetric ground track does not pass directly over tide gauges at absolute calibration sites.

In this paper, we present preliminary results for the feasibility of operating absolute calibration sites and use the GPS-buoy techniques to minimize the sea surface gradient error and its potential to translate the tide gauge sea level data to geocentric measurements for long-term calibration.

Absolute RA calibration sites and GPS-buoy campaigns for TOPEX calibration

The current operational and planned absolute RA calibration sites include Harvest, Burnie, English Channel, and Baltic Sea (operating), and Corsica, Catalunya, Gulf of Mexico, Lake Erie, North Sea and New Caledonia (planned). The planned Gulf of Mexico site is near an offshore oil platform owned by Unical/Spirit Energy Oil Co. The location of the calibration site is near an altimeter "triple" crossover point (i.e., the altimeter ground tracks from TOPEX/POSEIDON, ERS-2, and GFO-1 intersecting approximately within a few kms). The Spirit Energy offshore platform is about 3-5 km from the triple crossover point. The anticipated instrumentation include fiducial GPS receiver on the platform, the Next Generation Water Level Measurement System (NGWLMS) tide gauge (built by Gary Jeffrey of Texas A&M at Corpus Christi), and an autonomous GPS buoy at the triple crossover point. The planned absolute RA site is located in Lake Erie near the Ohio State University F.T. Stone Laboratory on the Gibraltar Island. The site is located near a TOPEX/POSEIDON or Jason descending track and near a NOAA tide gauge.

The GPS-buoy campaigns conducted in Lake Michigan is in part to prepare for the establishment and operation of the two planned absolute RA calibration sites. There are a number of technical issues associated with the use of GPS-buoys to autonomously measure accurate sea level measurements for the specific application of radar altimeter calibration. They include: (1) difficulty of accurate kinematic solutions of vertical GPS (receiver) location (i.e., sea level change) using reference station longer than 30 km, (2) hardware design involving communication (radio modem capability), robust data transfer, power supply, the ability to sense water level and attitude of the buoy (tilt-meter), and (3) other typical error sources such as multi-path (when buoys are near a platform) and waves and shape of domes.

The GPS-buoy campaigns were conducted to support the calibration and verification of two new altimeters: the TOPEX Side B (TSB) and GFO-1 altimeters. The campaigns were conducted in Lake Michigan; and in Catalunya off the coast of Spain, during March 1999. During the campaigns, fiducial GPS sites were occupied to take 1-second GPS data for coincide with the GPS buoy data acquisition. The altimeter passes in Lake Michigan are at 1999/3/30/22:59:44 UTC for TOPEX Side B pass, and at 1999/3/24 16:18:6 UTC for the GFO pass. Fig. 1 shows the preliminary results of the TSB radar altimeter calibration, i.e., GPS water level kinematic solution comparing with altimeter measurement of lake level during T/P overflight. The GPS kinematic solution was obtained using KARS (authored by Gerry Mader) software system. The altimeter bias estimated is 3.1 ± 10 cm. Although the conservative estimate uncertainty at 10 cm is about an order of magnitude from the needed calibration accuracy of 1 cm, it is anticipated that a portion of the error budget is variable error and can be reduced by more samples (e.g., 100) of calibration passes.

GPS buoy surveys were also conducted to "link" T/P altimeter measurement with a NOAA tide gauge (20 km away), Holland West, located in Holland, Michigan, in Lake Michigan. That is, water level measurements obtained by GPS-buoys at the tide gauge and underneath the altimeter track

during March 1999, were used to estimate the offset between the closest T/P altimeter measured lake level height and the tide gauge datum. Fig. 2 shows the resulting comparison or calibration of T/P historic measurement from 1993 to 1999 using time series of water level from the Holland West tide gauge. This preliminary analysis shows the potential of “calibrating” altimeter using existing tide gauges by “linking” the reference datum of the tide gauge and the altimeter measured surface.

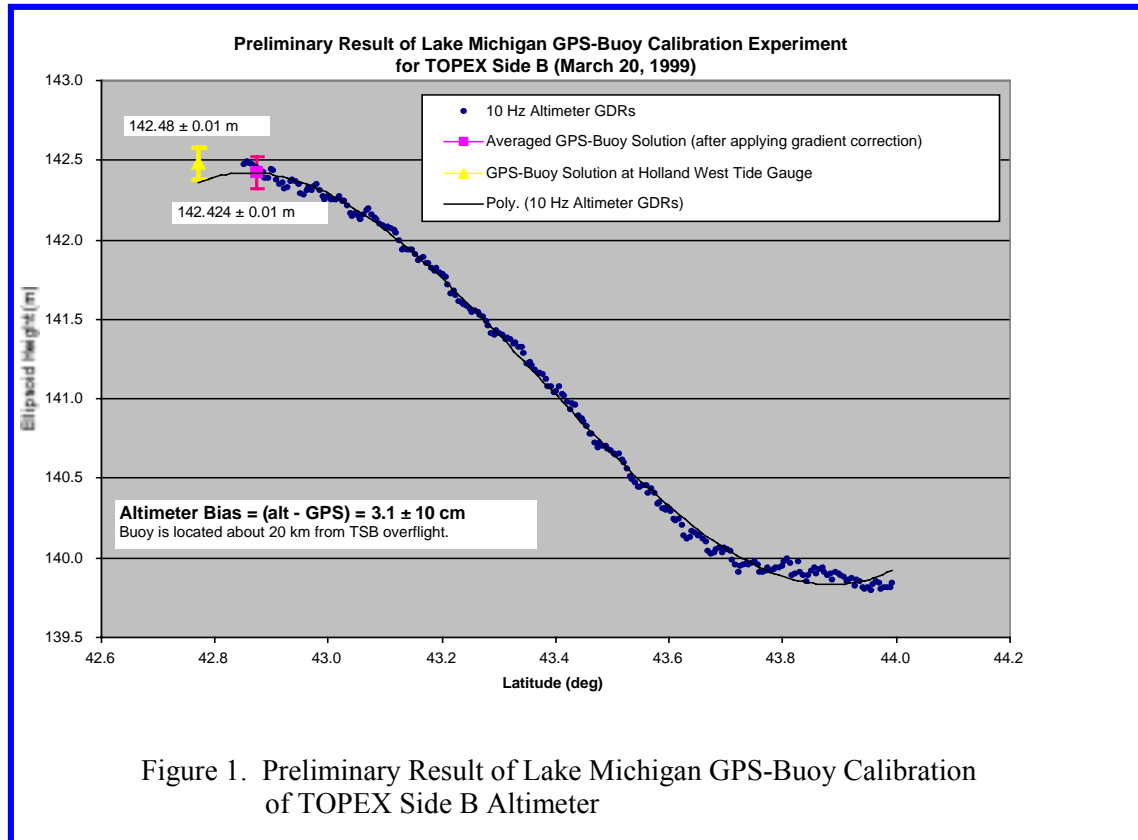
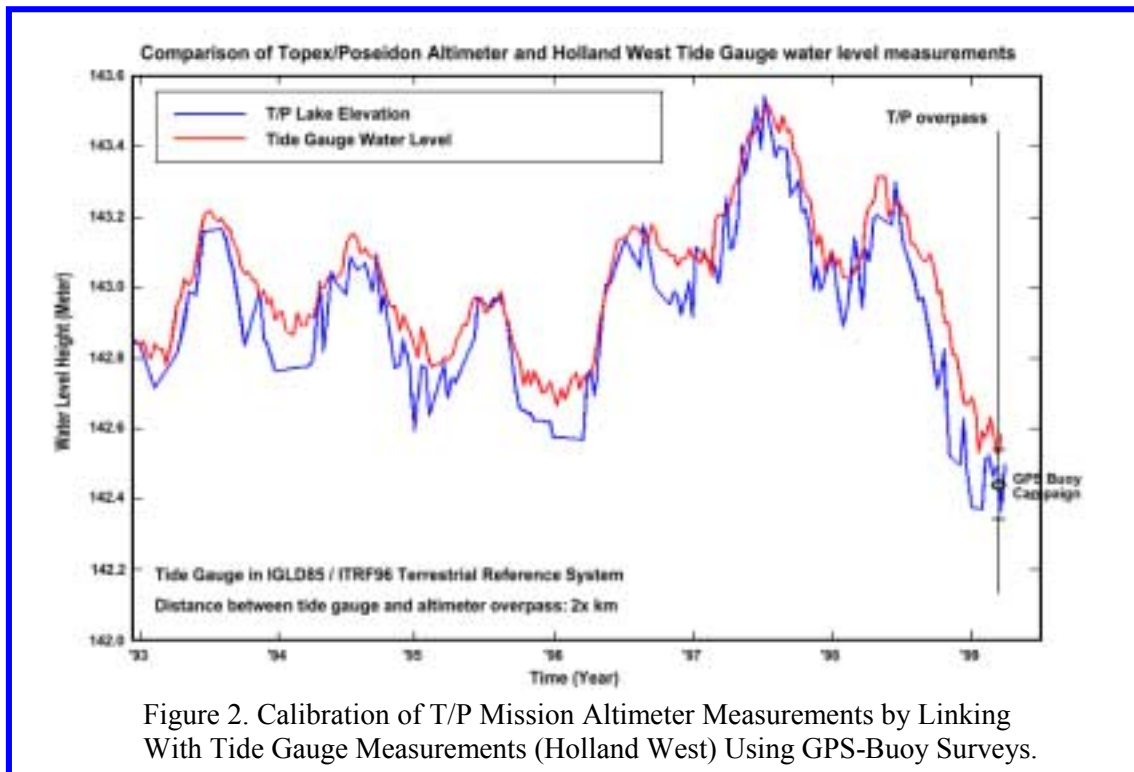


Figure 1. Preliminary Result of Lake Michigan GPS-Buoy Calibration of TOPEX Side B Altimeter



Conclusions

The potential use of multiple absolute radar altimeter calibration sites and the associated technical issues to monitor radar altimeter instrument, media and correction drifts using GPS buoys is discussed. The GPS-buoy campaigns conducted in Lake Michigan for absolute calibration of TOPEX Side B altimeter is in part to prepare for the establishment and operation of the two planned absolute RA calibration sites in Lake Erie and in the Gulf of Mexico. Preliminary results using GPS buoy campaigns for absolute calibration of TOPEX Side B altimeter show that one calibration sample has a conservative error estimate of about 10 cm. However, it is anticipated that the accuracy can be significantly improved with more measuring samples, and by averaging calibration measurements from other absolute calibration sites.

References

- Chambers, D. P., J. C. Ries, C. K. Shum, and B. D. Tapley, On the use of tide gauges to determine altimeter drift, *J. Geophys. Res.*, 103 (C6), 12885-12890, 1998.
- Mitchum, G., A tide gauge network for altimeter calibration, IGS-PSMSL Workshop, JPL, Pasadena, CA, 1997.
- Mitchum, G., Monitoring the stability of satellite altimeters with tide gauges, *Jl. of Atmospheric and Oceanic Technology*, 15(3), June 1998.
- Peltier, W. R., Global sea level and Earth rotation, *Science*, 240, 895-901, 1988.

Density and residual tidal circulation and related mean sea level of the Barents Sea

*S.K.Popov, G.F.Safronov, O.I.Zilberstein, O.V.Tikhonova and O.A.Verbitskaya
Hydrometeorological Research Center of Russia, Bol.Predtechensky per., 9-13,
123242 Moscow, Russia; e-mail: infomar@orc.ru*

Introduction

Nowadays the definition of constant currents and mean sea level is of great practical significance due to exploiting mineral resources in coastal zones. A number of factors make computation of these characteristics difficult. In the first place, it is variability of coastline and bottom relief. In the second place, it is adjoining ocean and sea areas influence on the currents structure through the open boundaries. In the third place, it is the interaction of the atmosphere and the ocean and rivers outflows. This problem can be presented at various levels of complexity. When dealing with the most complete formulation of tidal and surge level variations, related changes of temperature and salinity and also heat and mass exchange at the sea surface should be taken into account. To decide the complete prognostic setting for currents, temperature and salinity fields requires a computer with high performance [Oey et al., 1985].

Simpler models are often used to obtain non-periodic quasi-steady components of currents velocities and mean sea level. These models are based on a diagnostic approach where the density field is to be extracted from observations and is not to be determined in the study. The simplest version of the diagnostic approach is the dynamic method. It should be noted that the application of this method for shallow coastal zones is very doubtful because in this case, in contrast to deep ocean areas, it is impossible to choose the level of no motion (reference depth, at which the steady current is considered negligible). The diagnostic method removes the dynamic method imperfection. Current fields are determined from the complete system of equations, the wind influence on the sea surface is taken into account and the density field is extracted from observations. The major difficulty of using this method is in the fact that we have to have reliable and qualitative information on density at every level since the accuracy of the currents obtained depends on the quality of the density field [Sarkisyan et al., 1986].

Prognostic models including density field determination are the most comprehensive. In this case the density field is specified only on the entrance boundaries and are calculated in the domain. In comparison with the diagnostic approach less input data is needed, but we should have detailed information on heat and salinity flows at the sea surface.

So to define characteristics of mean (monthly, seasonal) density and currents fields the method of hydrodynamic adjustment is used. This combines the diagnostic and prognostic approaches [Sarkisyan et al., 1986]. As initial conditions for the prognostic model we use the currents fields with high frequency noise and fields of temperature and salinity extracted from observations and obtained from the diagnostic model and then averaged by time and space. The computation of temperature, salinity and current velocity stops after a short time of quick field adjustment during which the noise in averaged temperature and salinity fields is neutralized. The time of quick field adjustment is defined from the temporal variation of kinetic energy. It has a sharp decrease of kinetic energy followed by slower changes (see, for example, Fig.1). As experience shows, more adjusted fields typical for prognostic models are obtained when the kinetic energy changes slowly. The calculations stop at the moment when the kinetic energy decreases sharply. The aim of the adjustment is to obtain smoother quasi-steady and approximately adjusted fields of currents, temperature and salinity, and during this process the fields of temperature and salinity are required to not differ greatly from the data observed.

The method of hydrodynamic adjustment is often used to obtain mean climate fields of density and currents. For the Barents Sea the monthly [Bulushev and Sidorova, 1994] and seasonal [Semenov,

Chvilev, 1996] mean sea circulation was obtained by this method. In the above mentioned articles 3-D hydrodynamic models with the rigid lid condition on the surface were used. Contrary to those articles, the present article presents results of simulating the complete circulation by the 3-D model with a free surface, which allows taking into account surface gravity waves.

3D baroclinic model with free surface for the computation of steady and variable currents (storm surge and tide)

Equations

In Cartesian coordinates, and with the approximations of hydrostatics and f-plane, the system of equations for free surface liquid motion has the following form [Oey et al., 1985, Arkhipov, Popov, 1996]:

$$\frac{\partial u}{\partial x} + \frac{\partial v}{\partial y} + \frac{\partial w}{\partial z} = 0, \quad (1)$$

$$\frac{\partial u}{\partial t} + \frac{\partial}{\partial x} u^2 + \frac{\partial}{\partial y} vu + \frac{\partial}{\partial z} wu - fv = -g \frac{\partial \zeta}{\partial x} - \frac{1}{\rho_0} \frac{\partial p_s}{\partial x} + N_h \left(\frac{\partial^2 u}{\partial x^2} + \frac{\partial^2 u}{\partial y^2} \right) + N_z \frac{\partial^2 u}{\partial z^2}, \quad (2)$$

$$\frac{\partial v}{\partial t} + \frac{\partial}{\partial x} v^2 + \frac{\partial}{\partial y} wv + fu = -g \frac{\partial \zeta}{\partial y} - \frac{1}{\rho_0} \frac{\partial p_s}{\partial y} + N_h \left(\frac{\partial^2 v}{\partial x^2} + \frac{\partial^2 v}{\partial y^2} \right) + N_z \frac{\partial^2 v}{\partial z^2}, \quad (3)$$

$$\frac{\partial \rho}{\partial t} + \frac{\partial}{\partial x} u \rho + \frac{\partial}{\partial y} v \rho + \frac{\partial}{\partial z} w \rho = K_z \frac{\partial^2 \rho}{\partial z^2}. \quad (4)$$

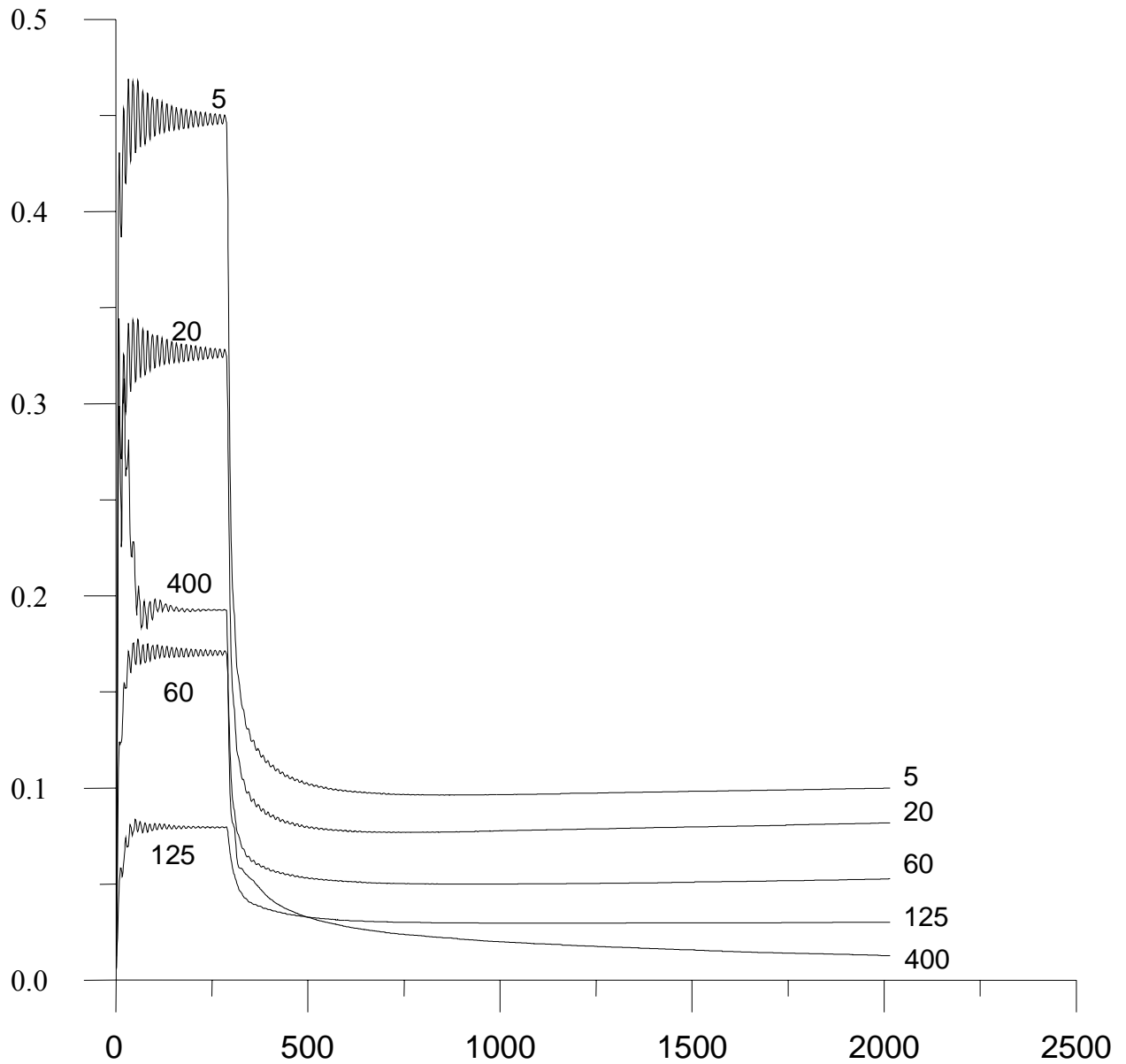


Fig. 1. The temporal variation of averaged kinetic energy at different horizons for August in the Barents Sea. Diagnostic time is 12 days. Adjustment time is 12 days. The total time of the calculations is equal to 84 days. Time (the X axis) is in hours, energy (the Y axis) is in J/m^3 . Figures near lines mark horizons in m.

The coordinate system origin coincides with the undisturbed sea surface, z is directed vertically upwards, and x and y are directed to the east and the north, respectively. The following notation is used: f is the Coriolis parameter, p is pressure, ρ stands for density and ρ_0 is its reference value, u, v, w are current speed components parallel to x, y, z , respectively, and g denotes the acceleration of gravity.

Pressure can be expressed as follows using the hydrostatic relation:

$$p = \int_z^{\zeta} \rho g dz = \rho_0 \zeta + \int_z^{\zeta} \rho g dz = \rho_0 g \zeta + p_s, \quad (5)$$

where ζ is deviation of free surface from its undisturbed position,

$$p_s = \int_z^0 \rho g dz.$$

N_h, N_z denote coefficients of horizontal and vertical turbulent viscosity, and K_z stands for the coefficient of vertical turbulent diffusion.

Boundary conditions

Wind stress components, kinematics condition and buoyancy flux were specified at the sea surface as:

$$N_z \frac{\partial u}{\partial z} = 0, N_z \frac{\partial v}{\partial z} = 0, \frac{\partial \zeta}{\partial t} + u \frac{\partial \zeta}{\partial x} + v \frac{\partial \zeta}{\partial y} = w, K_z \frac{\partial \rho}{\partial z} = 0. \quad (6)$$

At the bottom the frictional force was specified, and was assumed to be quadratic. In addition to that a kinematics condition was set describing the flow over the bottom relief, and lack of buoyancy vertical flux was prescribed:

$$N_z \frac{\partial u}{\partial z} = \tau_{bx}, N_z \frac{\partial v}{\partial z} = \tau_{by}, u \frac{\partial H}{\partial x} + v \frac{\partial H}{\partial y} = w, K_z \frac{\partial \rho}{\partial z} = 0. \quad (7)$$

where

τ_{bx} - bottom friction stress

$$(\tau_{bx}, \tau_{by}) = (\alpha u_b |\vec{U}_b|, \alpha v_b |\vec{U}_b|), \quad (8)$$

\vec{U}_b – current speed near the bottom, bottom friction coefficient $\alpha = 2,5 \cdot 10^{-3}$.

Finite difference scheme

A rectangular grid x_i, y_j, z_k is specified and the whole domain is represented as a set of grid boxes. Lateral boundaries coincide with vertical planes passing through the grid nodes. The upper boundary of the grid boxes changes in time while the lower boundary is fixed, being determined by the bottom relief. The vertical step varies from surface to the bottom. The number of layers is determined by the overall depth and changes from one (when the upper and lower layers coincide) up to n .

To approximate the equations with respect to time we use a semi-implicit staggered grid. Current speed components are determined at even time steps, while density and sea level correspond to odd time steps. The terms expressing vertical turbulent viscosity and diffusion are approximated

implicitly thus avoiding a limitation on a time step, which would have been valid for an explicit scheme:

$$\Delta t \leq \Delta z^2 / 2N_z. \quad (9)$$

The most severe limitation on the time step results from the explicit approximation of the terms that are responsible for the description of the propagation of long gravity waves:

$$\Delta t \leq \Delta x / (2gH)^{1/2}. \quad (10)$$

Velocities u , v , w are specified at the edges of boxes while density and level are specified at the central points of the boxes. This means that we use a C-grid (see [Mesinger, Arakawa, 1976]). To obtain a spatial approximation we used an integration-interpolation method (see [Samarsky, 1989]). The initial equations were integrated over the boxes, continuous functions were replaced with their discrete analogs, and fluxes across box boundaries were expressed by corresponding finite difference approximations. In the result, the following set of finite-difference equations was obtained:

Continuity equation:

$$\begin{aligned} & \delta_k \cdot (\zeta^{n+3} - \zeta^{n+1})_{i+1/2, j+1/2} / \Delta t + \left(\sigma_{i+1}^{n+1} \cdot u_{i+1}^{n+2} - \sigma_i^{n+1} \cdot u_i^{n+2} \right)_{j+1/2, k+1/2} / \Delta x + \\ & \left(\sigma_{j+1}^{n+1} \cdot v_{j+1}^{n+2} - \sigma_j^{n+1} \cdot v_j^{n+2} \right)_{i+1/2, k+1/2} / \Delta y + \left(\omega_{k+1}^{n+2} - \omega_k^{n+2} \right)_{i+1/2, j+1/2} = 0. \end{aligned} \quad (11)$$

Equation for u-component:

$$\begin{aligned} & \left(\sigma^{n+1} u^{n+2} - \sigma^{n+1} u^n \right)_{i, j+1/2, k+1/2} / \Delta t + \left(\sigma_{i+1/2}^{n+1} \bar{u}_{i+1/2}^n u_{a,i}^n - \sigma_{i-1/2}^{n+1} \bar{u}_{i-1/2}^n u_{b,i}^n \right)_{j+1/2, k+1/2} / \Delta x + \\ & \left(\sigma_{j+1}^{n+1} \bar{v}_{j+1}^n u_{c, j+1/2}^n - \sigma_j^{n+1} \bar{v}_j^n u_{d, j+1/2}^n \right)_{i, k+1/2} / \Delta y + \left(\bar{\omega}_k^n u_{e, k+1/2}^n - \bar{\omega}_{k+1}^n u_{f, k+1/2}^n \right)_{i, j+1/2} = \\ & = \sigma_{i, j+1/2, k+1/2}^{n+1} \cdot [-g \cdot (\zeta_{i+1/2}^{n+1} - \zeta_{i-1/2}^{n+1})_{j+1/2} / \Delta x - (P_{s, i+1/2}^{n+1} - P_{s, i-1/2}^{n+1})_{j+1/2} / \Delta x + f \cdot \bar{v}_{i, j+1/2}^n \\ & + N_h \cdot (u_{i+1} - 2u_i + u_{i-1})_{j+1/2}^n / \Delta x^2 + N_h \cdot (u_{j+3/2} - 2u_{j+1/2} + u_{j-1/2})_i^n / \Delta y^2]_{k+1/2} \\ & + (\tau_{xk}^{n+2} - \tau_{xk+1}^{n+2})_{i, j+1/2}. \end{aligned} \quad (12)$$

Equation for v-component:

$$\begin{aligned} & \left(\sigma^{n+1} v^{n+2} - \sigma^{n+1} v^n \right)_{i+1/2, j, k+1/2} / \Delta t + \left(\sigma_{i+1}^{n+1} \bar{u}_{i+1}^n v_{a, i+1/2}^n - \sigma_i^{n+1} \bar{u}_i^n v_{b, i+1/2}^n \right)_{j, k+1/2} / \Delta x + \\ & \left(\sigma_{j+1/2}^{n+1} \bar{v}_{j+1/2}^n v_{c, j}^n - \sigma_{j-1/2}^{n+1} \bar{v}_{j-1/2}^n v_{d, j}^n \right)_{i+1/2, k+1/2} / \Delta y + \\ & \left(\bar{\omega}_k^n v_{e, k+1/2}^n - \bar{\omega}_{k+1}^n v_{f, k+1/2}^n \right)_{i+1/2, j} = \\ & = \sigma_{i+1/2, j, k+1/2}^{n+1} \cdot [-g \cdot (\zeta_{j+1/2}^{n+1} - \zeta_{j-1/2}^{n+1})_{i+1/2} / \Delta y + (P_{s, j+1/2}^{n+1} - P_{s, j-1/2}^{n+1})_{i+1/2} / \Delta y - f \cdot \bar{u}_{i+1/2, j}^n + \\ & + N_h \cdot (v_{i+3/2} - 2v_{i+1/2} + v_{i-1/2})_j^n / \Delta x^2 + N_h \cdot (v_{j+1} - 2v_j + v_{j-1})_{i+1/2}^n / \Delta y^2]_{k+1/2} \\ & + (\tau_{y, k}^{n+2} - \tau_{y, k+1}^{n+2})_{i+1/2, j}. \end{aligned} \quad (13)$$

Equation for density:

$$\begin{aligned}
 & (\sigma^{n+3} \rho^{n+3} - \sigma^{n+1} \rho^{n+1})_{i+1/2, j+1/2, k+1/2} / \Delta t + (\sigma_{i+1}^{n+1} u_{i+1}^{n+2} \rho_{a, i+1/2}^{n+1} - \sigma_i^{n+1} u_i^{n+2} \rho_{b, i+1/2}^{n+1})_{j+1/2, k+1/2} / \Delta x + \\
 & (\sigma_{j+1}^{n+1} v_{j+1}^{n+2} \rho_{c, j+1/2}^{n+1} - \sigma_j^{n+1} v_j^{n+2} \rho_{d, j+1/2}^{n+1})_{i+1/2, k+1/2} / \Delta y + (\omega_k^{n+2} \rho_{e, k+1/2}^{n+3} - \omega_{k+1}^{n+2} \rho_{f, k+1/2}^{n+3})_{i+1/2, j+1/2} = \quad (14) \\
 & K_{z, k} (\rho_{k+1/2}^{n+3} - \rho_{k-1/2}^{n+3})_{i+1/2, j+1/2} / \Delta \sigma_k - K_{z, k+1} (\rho_{k+3/2}^{n+3} - \rho_{k+1/2}^{n+3})_{i+1/2, j+1/2} / \Delta \sigma_{k+1}.
 \end{aligned}$$

In finite difference equations (11-14) the following notations are used:

$$\begin{aligned}
 & \delta_k = 1, k = 0; \delta_k = 0, k = 1, \dots, B-1; \omega_k = w_k, k = 1, \dots, B-1; \omega_0 = 0, \omega_B = 0; \\
 & \sigma_{k+1/2} = z_k - z_{k+1}, k = 1, \dots, B-2; \sigma_{1/2} = \zeta - z_1, \sigma_{B-1/2} = z_{B-1} + H; \\
 & (\tau_{xk}, \tau_{y, k}) = N_{zk} \left(\frac{u_{k+1/2} - u_{k-1/2}}{\sigma_k}, \frac{v_{k+1/2} - v_{k-1/2}}{\sigma_k} \right); \sigma_k = (\sigma_{k+1/2} - \sigma_{k-1/2}) / 2, k = 1, \dots, B-1 \\
 & (\tau_{Bx}, \tau_{By}) = \alpha \left| \bar{U}_B \right|^n (u_B, v_B)^{n+2}; \\
 & i = 1, \dots, M \quad j = 1, \dots, N
 \end{aligned}$$

The bar over a letter means an average value over two neighbouring points, i.e.:

$$\bar{u}_{i+1/2} = (u_{i+1} + u_i) / 2,$$

while the $\bar{\bar{}}$ denotes an average value over four neighbouring points:

$$\bar{\bar{v}}_{i, j+1/2, k+1/2} = (v_{i-1/2, j, k+1/2} + v_{i+1/2, j, k+1/2} + v_{i-1/2, j+1, k+1/2} + v_{i+1/2, j+1, k+1/2}) / 4.$$

The nonlinear terms in the equations for velocities and density terms with indexes a, b, c, d, e, f depend on the sign of velocity at the box edge and are determined using a conservative upstream scheme (see [Roache, 1972]):

$$\begin{aligned}
 & \rho_{a, i+1/2} = \rho_{i+1/2}, \quad u_{i+1} \geq 0; \quad \rho_{a, i+1/2} = \rho_{i+3/2}, \quad u_{i+1} \leq 0; \\
 & \rho_{b, i+1/2} = \rho_{i+1/2}, \quad u_i \leq 0; \quad \rho_{b, i+1/2} = \rho_{i-1/2}, \quad u_i \geq 0.
 \end{aligned}$$

Vertical variations of vertical diffusion coefficient are taken into account using the following parameterization [Backhaus, Hainbucher, 1987; Ryabinin, Zilberstein, 1996]

$$N_z = k_{\min} + k_0 k_s, \quad (15)$$

where $k_{\min} = 25 \text{ cm} / \text{s}^2$ is the minimum value of N_z and

$$k_0 = kH \left| \bar{U}_i \right|, \quad (16)$$

where H is the depth, $\left| \bar{U}_i \right|$ is vertically averaged over (i-th layer) absolute value of current speed k is nondimensional turbulent coefficient named after Bowden (see [Bowden, Hamilton, 1975]). It is set equal to $2.7 \cdot 10^{-3}$ according to [Fang, Ichiye, 1983]. In the case of stratificated liquid

$$k_s = (1 + \sigma \text{Ri}_i)^{-p}, \quad (17)$$

Ri_i is Richardson coefficient in the i-th layer, σ and p are the constants equal to 7 and 0.25, respectively. In the above presented scheme the vertical turbulent viscosity depends on dynamic

factors (average velocity U_i in the every layer) and stratification (Richardson coefficient in the i-th layer).

Bottom friction law is specified to be quadratic (8), because vertical resolution of the finite difference scheme is not fine enough to explicitly simulate thin bottom boundary layer.

The time step is equal to 240 s for the coarse grid while the mesh size is 15 nautical miles. For the fine grid the time and spatial steps are 120 s and 6 nautical miles accordingly.

When simulating tides in the Barents Sea as the liquid boundary condition we use the temporal variation of tidal level resulted by the harmonic constants and presented as a sum of the fixed number of tidal components

$$\zeta(x, y, t)|_{\Gamma_2} = \sum_{i=1}^n R_i A_i(x, y) \cos[\sigma_i t + \psi_{oi} - g_i(x, y)], \quad (18)$$

where $A_i(x, y)$ and $g_i(x, y)$ are harmonic constants represented amplitude and phase of the i-th tidal component, σ_i - angular velocity of the i-th tidal component; ψ_{oi} and R_i are initial phase and nodal factor determined from the astronomic data at the moment of the beginning and the middle of the calculations respectively [Duvanin, 1960].

Harmonic constants are determined from the sea level observations made in a fixed number of stations on the liquid boundary and then interpolated to its nodes. In the both models we use the condition of no flow across the solid boundaries. In the model of the whole Barents Sea the bottom friction law is assumed (8).

GENERAL DESCRIPTION OF THE BARENTS SEA CIRCULATION

Tides play a prominent role in circulation of the Barents Sea and dominate summary level variations. At the same time the general circulation of the sea, which acts as a background for tidal motions, is characterized by the presence of steady currents caused by mass exchange at the open boundaries of the sea and by irregularities of the sea water density.

Steady currents are usually calculated using dynamic method, which assumes that current field is fully adjusted to the density field (above a conventionally defined reference depth, at which the steady current is considered negligible). Therefore quasi-steady circulation of the Barents Sea is seen a sum of density-relation currents, which are calculated using multi-year temperature and salinity data.

In the Atlas of Arctic [1985] a scheme for surface currents is given, which was calculated by dynamic method in the Murmansk Branch of the AARI basing on data available in the Murmansk Branch of the Roshdyromet. One can see there several features:

- cold currents namely Coastal current of the Franz-Josef Land, Barents (Eastern Spitzbergen) current, Suidcap current, Medvezhinskoe current, Persey (South-Western) current, Central current and Litke current;

- warm currents namely Southern Spitsbergen current, Nordkap current, Northern, Central and Southern (Coastal) Branches of the Nordkap current, Murmansk current, Murmansk Coastal current, Canin current, Kolguev-Pechora current, Novaya Zemlya current with its Coastal and Western and Eastern branches;

- and river outflow currents namely Belomorskoe and Pechora currents.

Steady currents in the central Barents Sea are not strong and speeds vary from 2 to 5 cm/s. There is a slight intensification of motions in the Medvezhinskoe and Suidcap currents, in the Franz-Josef Land Coastal current, up to 8-13 cm/s.

In the southeastern part of the Barents Sea the circulation is governed by the Murmansk Coastal Current. One branch of this current transforms into the Canin Current that flows to the North of Kolguev Island, and the other part joins the Belomorskoe river outflow current and flows around the southern part of Kolguev Island. Somewhere to NW of the Kolguev Island the Murmansk current joins the Kolguev-Pechora current, which flows around the southern tip of the Kolguev Island. The Murmansk Current joins the Kolguev-Pechora Current in some area to the NE of the Kolguev Island, and the latter current flows around the southwestern coast of the Novaya Zemlya and turns to the NE, becoming parallel to the coast of the island. Around the south coast of the Novaya Zemlya there is the Litke Current that flows from the Kara Gate Strait. To the south of it there is the Pechora River outflow current. Velocities of all these currents generally do not exceed 8-10 cm/s and decrease to 2-4 cm/s at the 25 m depth.

Monthly mean patterns of the quasi-steady circulation were computed from the free surface model for August and February. The August circulation is of interest in that during this month the sea is ice-free. The vertical structure is characterized by the existence of a seasonal thermocline and halocline that are generated by summer heating of the upper water layers and by a decrease in the salinity due to ice melting. The thermocline is completely destroyed during February, which therefore represents a good mark for the evaluation of seasonal changes of the circulation.

The computation was made using the monthly mean density field obtained from observations. The density was represented on a one degree grid with standard levels. The data was prepared in the Centre of Oceanographic Data at the World Data Center Obninsk (WDC B). Only the currents generated under the action of density variations and transports of mass across the open boundaries were the subject of that simulation.

The major problem in the simulation of currents in the Barents Sea is related to specification of open boundary condition. Non-periodic components of current speed should be specified for the use of a 3-D model. Of course, the integral transports should comply with the vertical current profile [Blumberg, Mellor, 1983]. To simulate density distribution for such parts of the open boundary where there is an inflow of waters into the basin one has to know density along such parts of the open boundary. Also we have to know density and integral transports for regions where there is a river outflow to the sea.

Of special importance for the hydrological regime of the Barents Sea is the correct description of its western open boundary. Monthly mean transports across this section calculated using the dynamic approach are equal to about 2000 cubic km for August, while for February it is approximately 1300 cubic km. The main inflow takes place between Cape Nordkap and Bear Island. The same approach gives an estimate of total transport at the northern boundary around 2000 cubic km per year, while across the northeastern boundary the total outflow is of order of 4000 cubic km per year. Averaged (over the section) speeds were equal to 0.5 cm/s for the western boundary, and 0.1 cm/s for the northern and northeastern boundaries.

The circulation of the Barents Sea was simulated on a 15 nm grid. Maximum depth was 400 m, the time step was equal to 180 s and the following coefficients were used:

$$K_z=5 \cdot 10^{-4} \text{ m}^2/\text{s}, N_h=5 \cdot 10^3 \text{ m}^2/\text{s}$$

where N_z is specified by (15). The adjustment time is determined from the averaged kinetic energy temporal variation (Fig. 1). Figures containing variations of kinetic energy averaged by time at the different depth show that process of quick adjustment between density and current fields stops approximately 12 days after the computation begins.

The visual analysis of the results after 12 and 72 days adaptation shows that current fields only become smoother. It is interesting that in [Bulushev and Sidorova, 1994] the adjustment time for monthly mean circulation simulation was defined to be 7 days and in the study of seasonal mean circulation in the Barents Sea [Semenov, Chvilev, 1996] the adjustment time was set to 10 days.

For the computations aimed at achievement of adjustment of the current speed to the density field, we obtained monthly mean circulation for August and February. The simulation revealed overall cyclonic rotation of general circulation and confirmed the existence of major currents in the region. Overall circulation patterns at the surface (density currents only) for August and February are shown in Figs 2 and 4. Figs. 3 and 5 contain the density-related circulation at 150 m depth for August and February. The adjustment time is more than 12 days. It follows from these figures that while entering the Barents Sea the Nordcape Current separates into two branches. The first one, the northern branch, forms the Murmansk Current, while the other one forms the Coastal Murmansk Current. Further on the Murmansk Coastal Current goes off the coast, turns to the east, and then transforms into the Kanin and Kolguev-Pechora Currents. The Murmansk Current turns to the northeast and passes to the Novaya Zemlya Current that forms the eastern part of the cyclonic gyre. Its northern boundary is made of the Central and South-Western Currents. Well seen is the Medvezhinskoe Current, which closes the central gyre at its western side. One can also trace South - Spitzbergen and Suidcap Currents close to the edge of the domain considered. Well seen also is the Belomorskoe River Outflow Current, which naturally goes out of the White Sea.

The general structure of currents at 100 m depth coincides with that on the surface, but with the overall range of current speed being correspondingly smaller. Currents change with depth very little and most of them are uniform in the upper 100-m layer. Many of them have a barotropic nature.

Circulation at the level of 150 m (see Figs. 3, 5) is different from that at the surface. Northward branch of the Nordkap Current is observed in the center of the sea.

On the basis of the density-relation current calculations one can draw a conclusion that currents generated by density gradients are stable during the whole year and are homogeneous with depth. Some decrease of velocity with depth takes place in bottom layers because of the more homogeneous density field and due to bottom friction. Currents are more intense in August than in February. This may be related to greater total inflow across the western boundary in August than in February. The typical speed of the density-related current is small and equals approximately 5 cm/s at the surface, 3 cm/s at the 50 m level and 2 cm/s at the 150 m level. In the central part of the Barents Sea density-related current speeds are nearly constant with depth and are equal approximately to 1.5 cm/s in August and 0.8 cm/s in February.

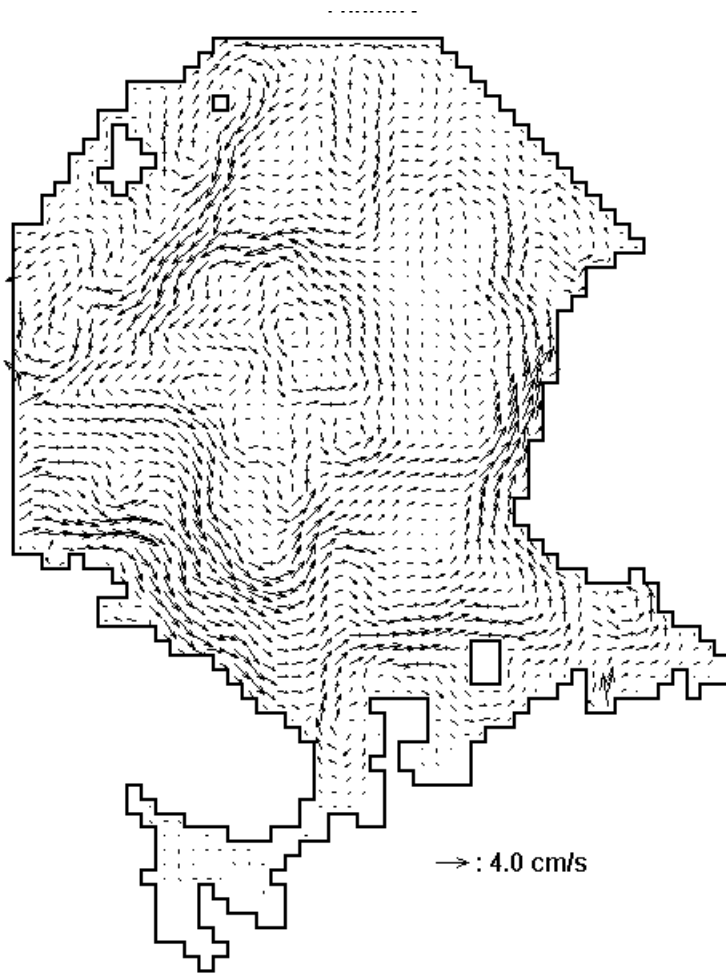


Fig. 2. Multi-year mean fields of density-related currents at the surface of the Barents Sea for August.

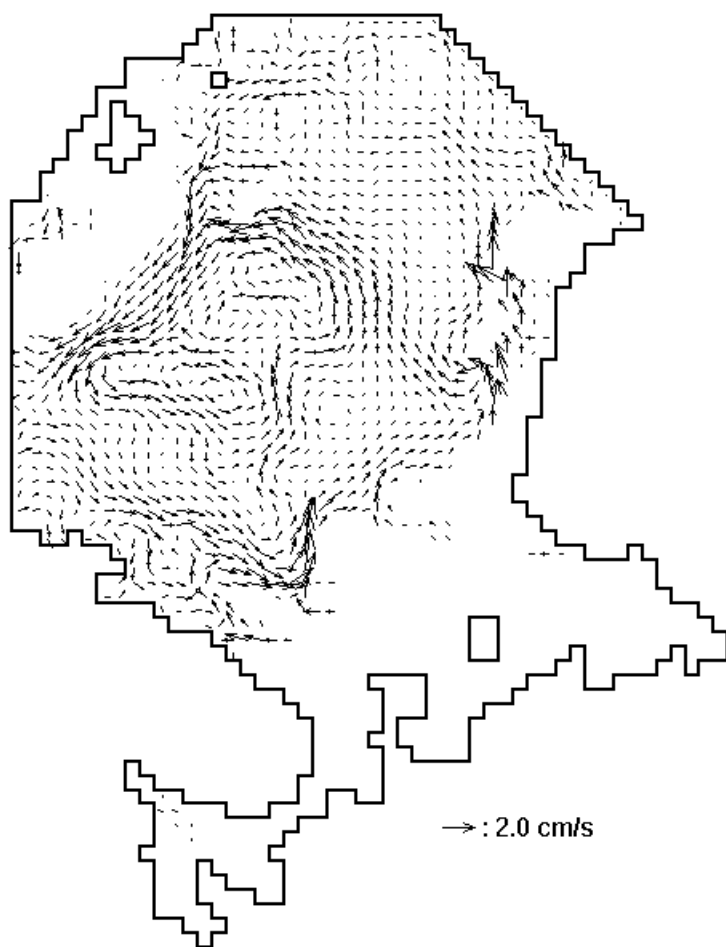


Fig. 3. Multi-year mean fields of density-related currents at depth 150 m in the Barents Sea for August.

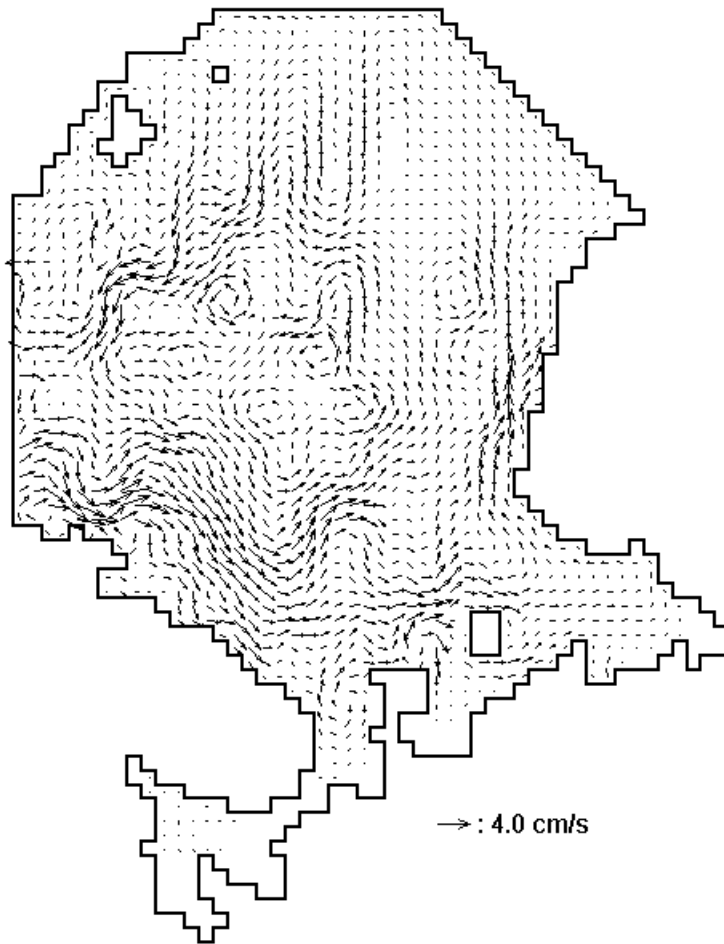


Fig. 4. Multi-year mean fields of density-related currents at the surface of the Barents Sea for February.

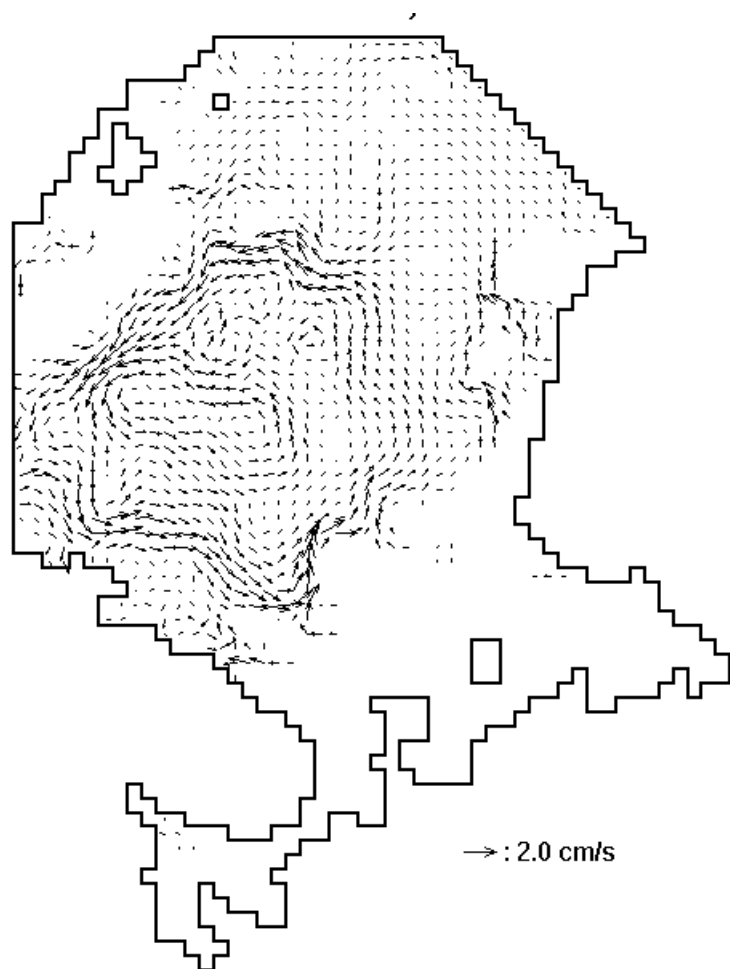


Fig. 5. Multi-year mean fields of density-related currents at depth 150 m in the Barents Sea for February.

Figs. 6 and 7 contain the multi-year mean sea level deviation from the conventionally defined reference level in the Barents Sea in August and February. These fields show the specific character of the density-related circulation given in Figs. 2 and 4. The deviations are positive in the shelf of the southwestern part of the Barents Sea, along the Kolsky shore, at the Spitsbergen shallow water zone and negative in the central deep part of the Barents Sea. The maximum slopes of the mean sea level are along the Kolsky shore and in the area of the Murmansk Coastal Current.

For the ice-free period and for winter months the circulation (with account of the adjustment between fields of current and density) and the multi-year mean sea level in the southeastern part of the Barents Sea were computed (see Figs. 8, 9, 10 and 11). Seasonal variability of the current system is determined by annual variability of atmospheric and sea ice-hydrological processes.

The density gradients generate the circulation. In summer months the waters in the southeastern part of the Barents Sea are characterized by strong stratification of the upper layer and by a very shallow pycnocline. The primary factor in the summer density decrease is the salinity variation. Spreading of the river flood wave results in the formation of a vast area of brackish water, which achieves its peak in July. An additional salinity decrease during that season is generated by ice melting and a larger inflow of the White Sea waters. From August to November (when river flow is smaller than during spring months and mixing processes become stronger) the salinity and density values increase, and their horizontal and vertical gradients become smoother.

The calculated current field for August is similar to the one given in the Atlas of Arctic [1985] for the ice-free period (July-September). Before the start of autumn the circulation intensity achieves its annual maximum and the Belomorskoe Current and the Litke Current are easily seen. The Pechora Current and the southeastern branch of the Kolguev-Pechora Current exist in the southeastern part of the area of interest.

Maximum speeds of the stationary density-related currents are observed in the area of maximum density gradients where they reach 6-8 cm/s, which is in good agreement with those obtained through the dynamic method (see Fig. 8).

Figures 10 and 11 show the monthly mean sea level deviation from the conventionally defined reference level for the ice-free (August) and winter (February) periods in the southeastern part of the Barents Sea. These deviations are the greatest in the whole area of the density changes, i.e. near the shore of the Pechora Sea. Fig. 10 is in good agreement with the density-related current field (see Fig. 8).

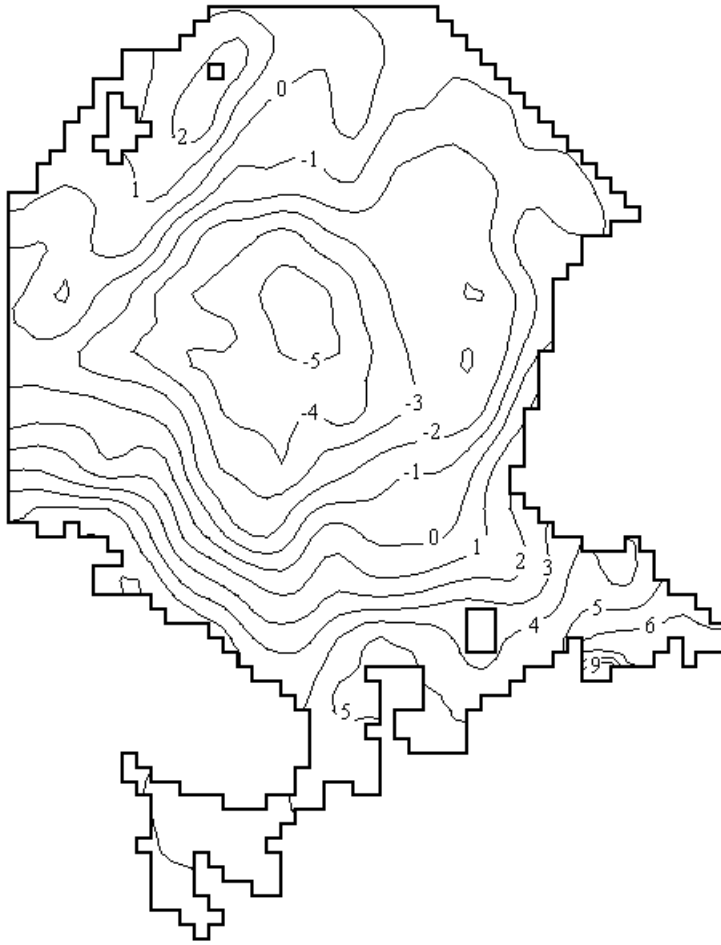


Fig. 6. Multi-year mean sea level of the Barents Sea for August.

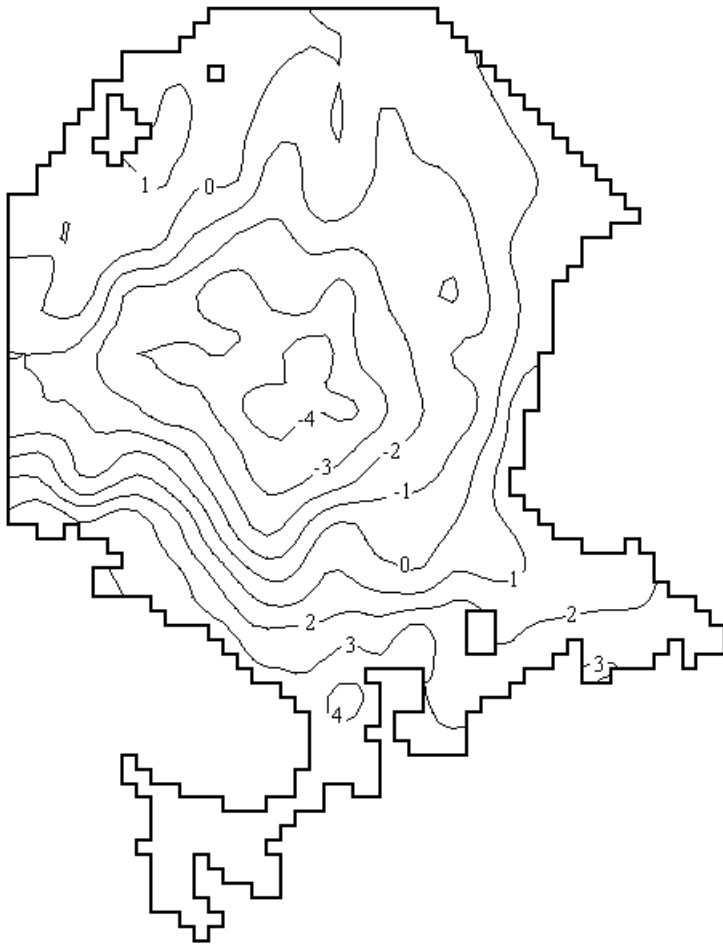


Fig. 7. Multi-year mean sea level of the Barents Sea for February.

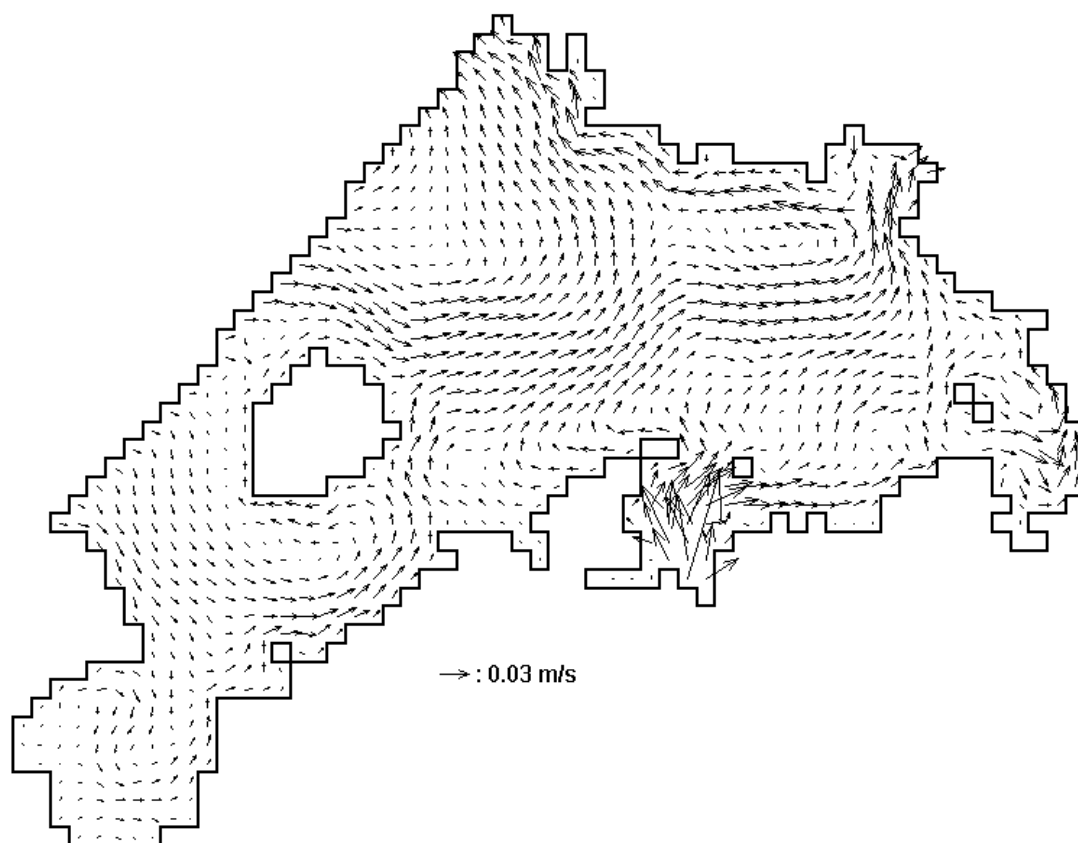


Fig. 8. Multi-year mean fields of density-related currents at the surface in the south-eastern part of the Barents Sea for August.

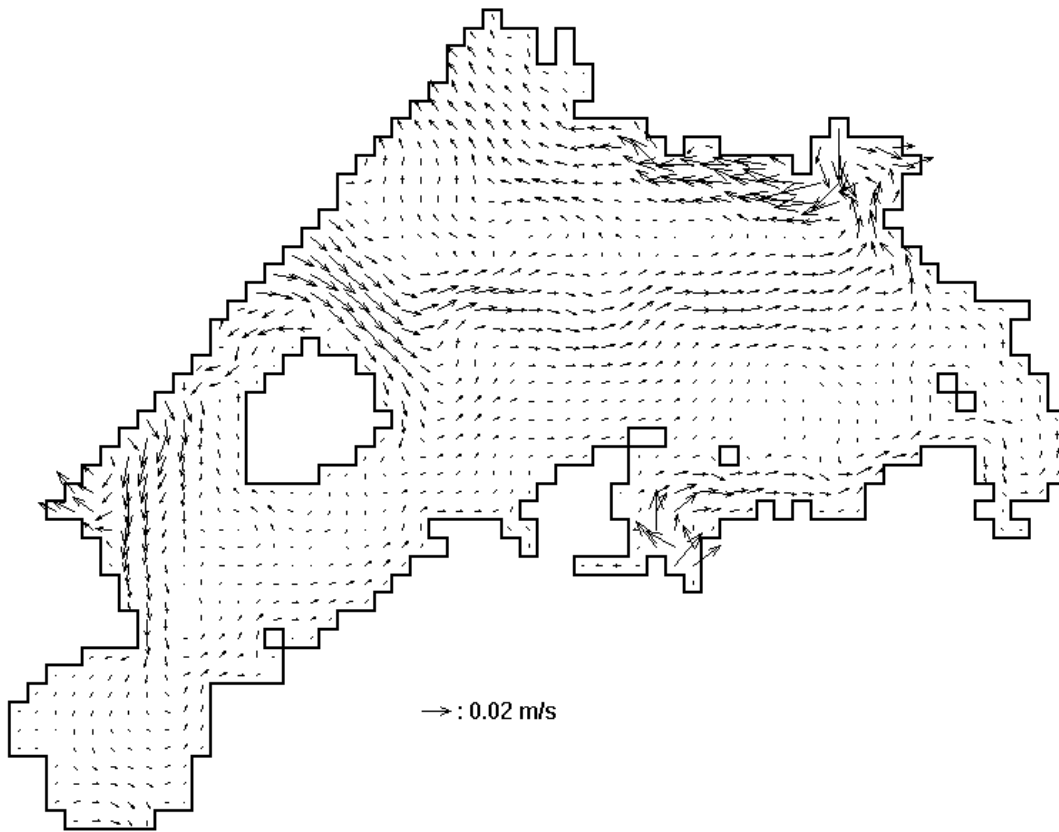


Fig. 9. Multi-year mean fields of density-related currents at the surface in the south-eastern part of the Barents Sea for February.

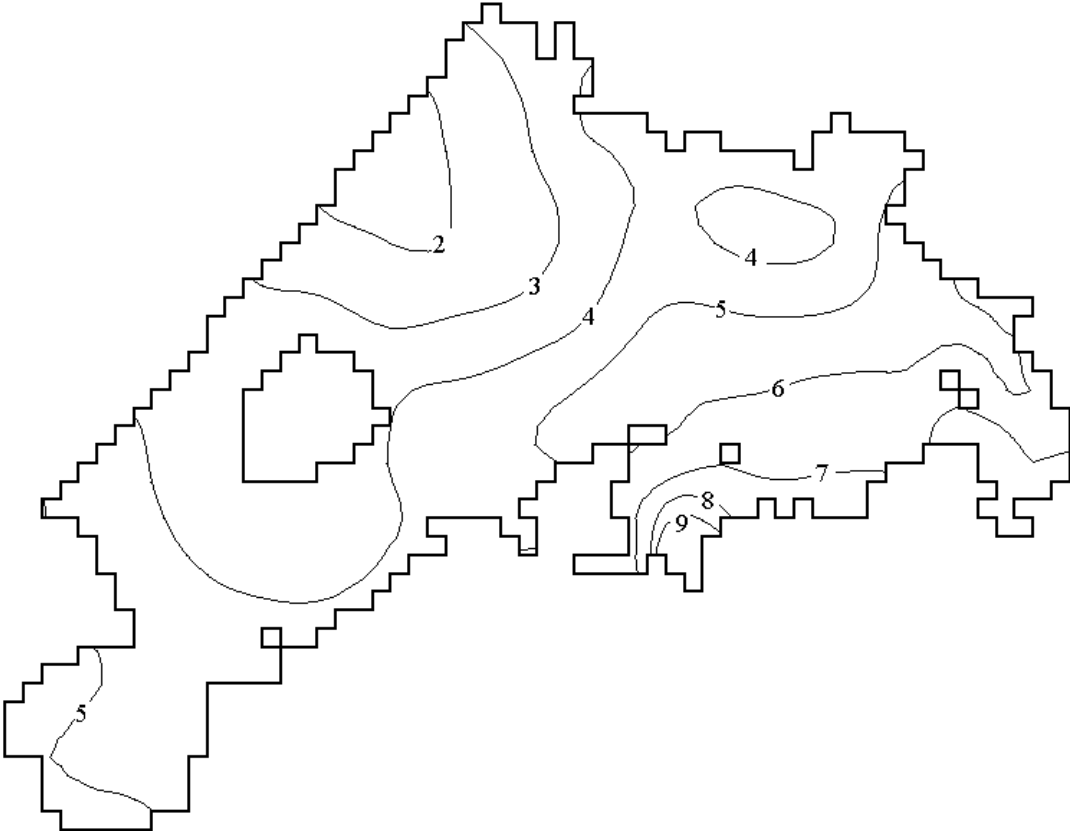


Fig. 10. Multi-year mean sea level of the south-eastern part of the Barents Sea for August.

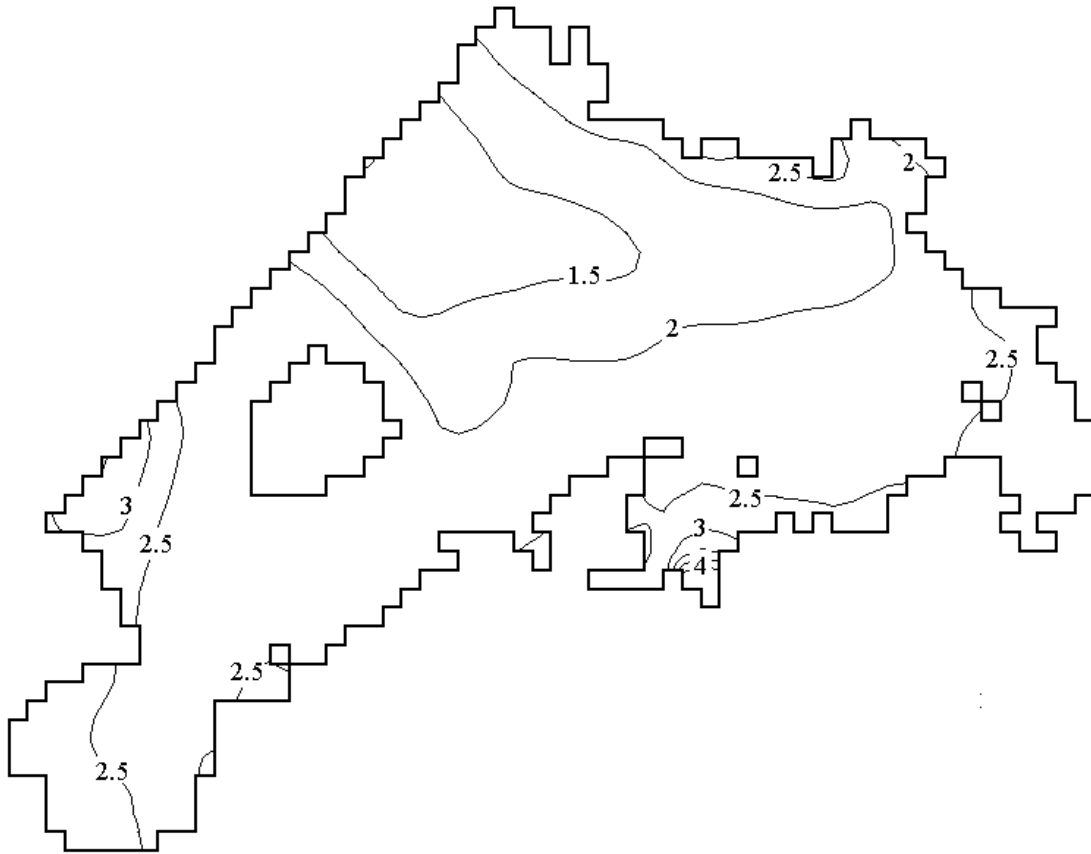


Fig. 11. Multi-year mean sea level of the south-eastern part of the Barents Sea for February.

Figures 12 and 13 show the Eulerian residual tidal circulation generated by M_2 in the whole Barents Sea and in its southeastern part. Figures 14 and 15 show Eulerian residual tidal mean sea level throughout the Barents Sea as a whole and in its southwestern part. The figures show that the Eulerian residual currents are weak. One can see its considerable increase in the shelf zone of the southeastern part of the Barents Sea, in the Crater of the White Sea, near Spitzbergen, the Franz-Josef Land where these values vary from 4 to 7 cm/s. This fact is also noted in [Gjevik et al., 1994]. In the Cheshskaja Guba and near Kanin Nos Island the value of the Eulerian residual tidal level is approximately equal to 10-12 cm. The residual tidal level value reaches its maximum in the Cheshkaja Guba (15 cm), in the Crater of the White Sea (30 cm) and in the Pechora Sea (9 cm). In the rest of the southwestern part of the Barents Sea the residual tidal level values do not exceed 1-2 cm.

Conclusions

In the whole southeastern part of the Barents Sea, the baroclinic transport caused by the density irregularity and the residual tidal circulation goes from the west to east with outflow through the Kara Gate Strait. However, the stationary currents do not effectively influence the water dynamics in this region, contributing less than 10% of the overall currents generated by tides and atmospheric disturbance. But the contribution of the density-related outflows and residual tidal circulations in the mean sea level values of the southeastern part of the Barents Sea and the whole sea is considerable. This fact corresponds well with the multi-year level observations made at the shore stations. For example, the maximum value from the multi-year mean level at station Poljarnoe (the Kolsky Peninsula) from 1936 to 1990, Bely Nos from 1958 to 1990 and the Vajgach Island is 7.68 cm and the computed value is 7 cm (see Figs. 14, 15 and 6, 10). Results of hydrodynamic modeling also confirm the tendency of decreasing the sea level from the west to the east, from the Kolsky shore to the Vajgach Island and from the Kolguev Island to the top of the Hajpudyrskaja Guba.

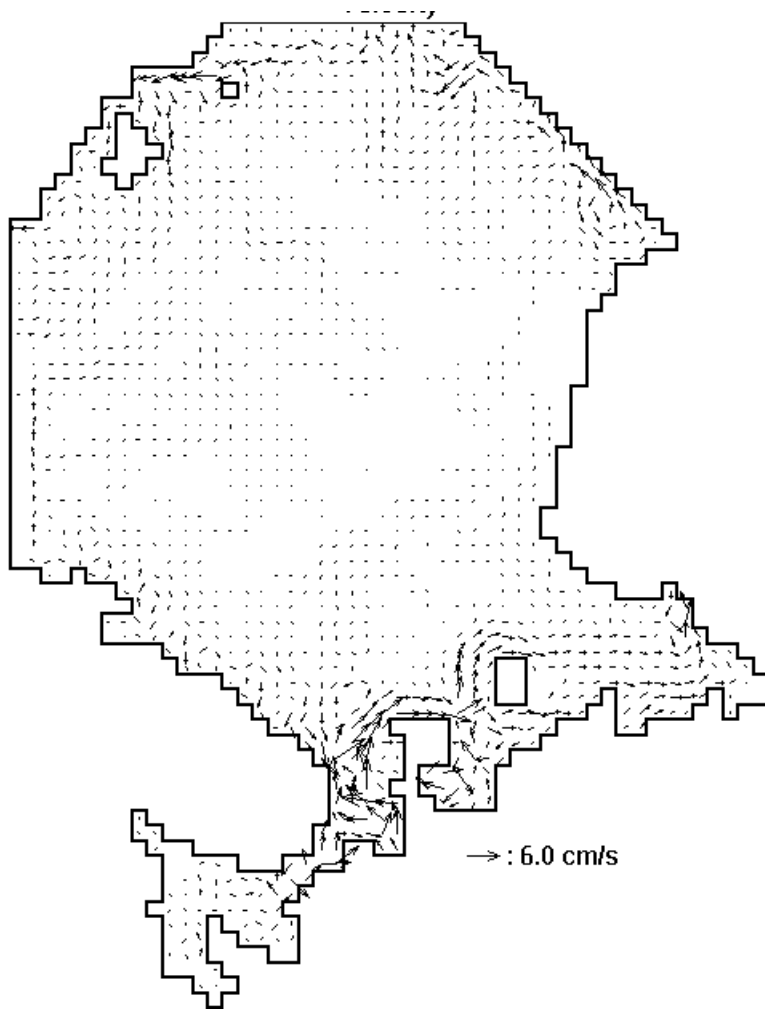


Fig. 12. Eulerian residual surface currents generated by the wave M_2 in the Barents Sea.

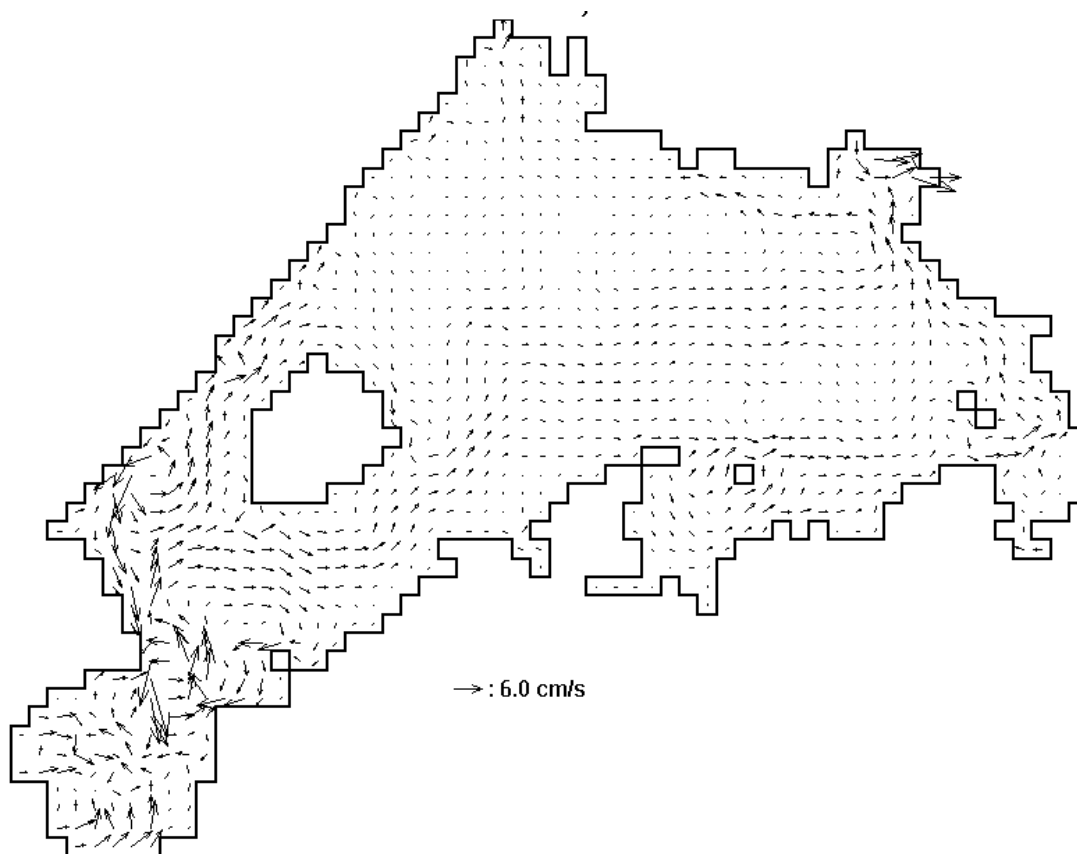


Fig. 13. Eulerian residual surface currents generated by the wave M_2 in the south-eastern part of the Barents Sea.

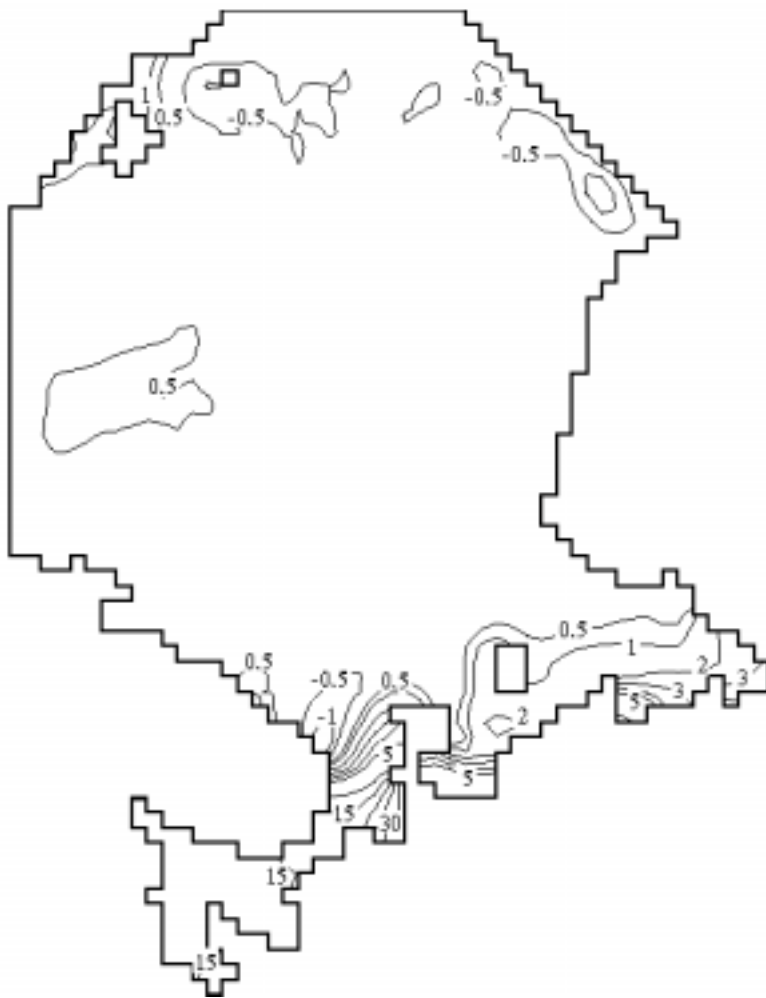


Fig. 14. Eulerian residual sea level generated by the wave M_2 in the Barents Sea.

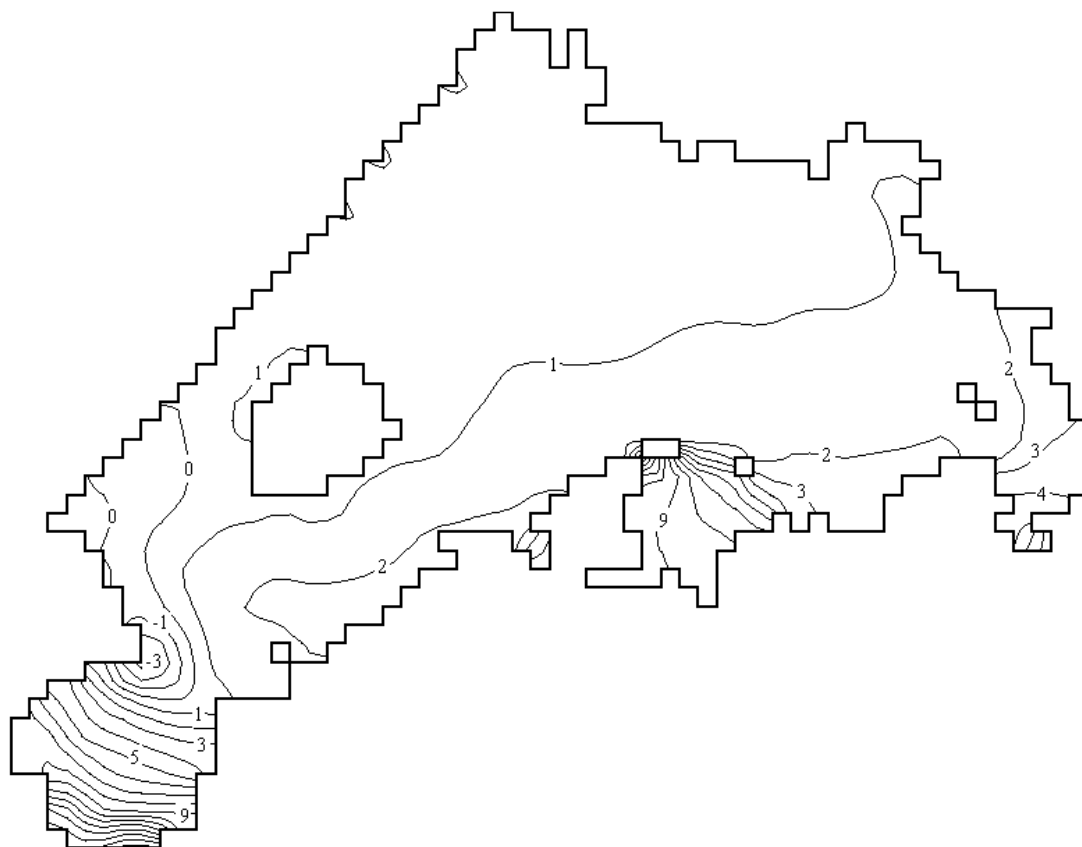


Fig. 15. Eulerian residual sea level generated by the wave M_2 in the south-eastern part of the Barents Sea.

References

- Arkhipov, B.V., Popov, S.K., 1996. Modelling of Currents in the South-Eastern Region of the Barents Sea. *Oceanology*, vol.36, N6, pp. 805-873 (in Russian).
- Atlas of Arctic, 1985. Publisher of the Main Office of Geodesy and Chartography. Moscow, 204 pp (in Russia).
- Backhaus, J.O. and D. Hainbucher, 1987. A finite difference general circulation model for shelf sea and its application to low frequency variability on the north European shelf. – Three - Dimensional models of Marine and Estuarine Dynamics., edited by J.C.J. Nihoul and B.M. Jamart, Elsevier, Amsterdam, pp. 221-244.
- Blumderg, A.F., Mellor, G.L., 1983. Diagnostic and Prognostic Numerical Circulation Studies of the South Atlantic Right. *J. Geophys. Res.*, vol.88, No. C8, pp. 4579-4592.
- Bowden, K.F. and P. Hamilton, 1975. Some experiments with a numerical model of circulation and mixing in a tidal estuary. *Estuar. Coast. Mar. Sci.*, vol. 3, pp. 281-301.
- Bulushev, M.G and A.N. Sidorova, 1994. Calculation of Monthly Mean Circulation in the Barents Sea. *Meteorology and Hydrology*, N4, pp. 78-87. (in Russian).
- Duvanin, A.I., 1960. Tides in the Sea. *Hydrometeoizdat*, Leningrad, 390 pp. (in Russian).
- Fang, G and T. Ichiye, 1983. On the vertical structure of tidal currents in a homogeneous sea. *Geophys. J. Roy. Astr. Soc.*, pp. 65-82.
- Gjevik, E. Nost, and T. Straume, 1994. Model simulations of the tides in the Barents Sea. *J. Geophys. Res.*, vol. 99, No. C2, pp. 3337-3350.
- Mesinger, F., Arakawa, A., 1976. Numerical methods used in atmospheric models. *GAPR, WMO-ICSU*, vol. 1, N 17, 65 pp.
- Oey, L.Y, Mellor G.L., Hires, R.I., 1985. A three-dimensional simulation of the Hudson-Raritan estuary. Part 1. Description of the model and model simulation. *J. Phys. Oceanogr.*, vol. 15, N 11, pp. 1676-1692.
- Roach, P.J., 1972. *Computational fluid dynamics*. Hermosa Publishers, Albuquerque, New Mexico, 434 pp.
- Ryabinin, V.E., Zilberstein, O.I., 1996. Numerical prediction of storm surges – a review. In: *Storm Surges Report*. N 33, WMO/TD – N 779, pp.1-62.
- Samarskiy, A.A., 1989. *Theory of difference schemes.*, Nauka, Moscow, 616 pp. (in Russian).
- Sarkisyan, A.S., Demin, Ju.L., Brechovsky, A.L., Shahanova, T.V., 1986. Methods and results of simulating circulation in the World Ocean. *Hydrometeoizdat*, Leningrad, (in Russian).
- Semenov, G.A., Chvilev, S.V., 1996. Numerical simulation interannual variability of the circulation in the Barents Sea in summer. *Oceanology*, vol. 36, N4, pp.498-511. (in Russian).

In this Series, entitled

Reports of Meetings of Experts and Equivalent Bodies, which was initiated in 1984 and which is published in English only, unless otherwise specified, the reports of the following meetings have already been issued:

1. Third Meeting of the Central Editorial Board for the Geological/Geophysical Atlases of the Atlantic and Pacific Oceans
2. Fourth Meeting of the Central Editorial Board for the Geological/Geophysical Atlases of the Atlantic and Pacific Oceans S. Fourth Session of the Joint IOC-WMO-CCPS Working Group on the Investigations of 'El Niño' (**Also printed in Spanish**)
4. First Session of the IOC-FAO Guiding Group of Experts on the Programme of Ocean Science in Relation to Living Resources
5. First Session of the IOC-UN(OETB) Guiding Group of Experts on the Programme of Ocean Science in Relation to Non-Living Resources
6. First Session of the Editorial Board for the International Bathymetric Chart of the Mediterranean and Overlay Sheets
7. First Session of the Joint CCOP(SOPAC)-IOC Working Group on South Pacific Tectonics and Resources
8. First Session of the IODE Group of Experts on Marine Information Management
9. Tenth Session of the Joint CCOP-IOC Working Group on Post-IDOE Studies in East Asian Tectonics and Resources
10. Sixth Session of the IOC-UNEP Group of Experts on Methods, Standards and Intercalibration
11. First Session of the IOC Consultative Group on Ocean Mapping (**Also printed in French and Spanish**)
12. Joint 100-WMO Meeting for Implementation of IGOSS XBT Ships-of-Opportunity Programmes
13. Second Session of the Joint CCOP/SOPAC-IOC Working Group on South Pacific Tectonics and Resources
14. Third Session of the Group of Experts on Format Development
15. Eleventh Session of the Joint CCOP-IOC Working Group on Post-IDOE Studies of South-East Asian Tectonics and Resources
16. Second Session of the IOC Editorial Board for the International Bathymetric Chart of the Mediterranean and Overlay Sheets
17. Seventh Session of the IOC-UNEP Group of Experts on Methods, Standards and Intercalibration
18. Second Session of the IOC Group of Experts on Effects of Pollutants
19. Primera Reunión del Comité Editorial de la COI para la Carta Batimétrica Internacional del Mar Caribe y Parte del Océano Pacífico frente a Centroamérica (**Spanish only**)
20. Third Session of the Joint CCOP/SOPAC-IOC Working Group on South Pacific Tectonics and Resources
21. Twelfth Session of the Joint CCOP-IOC Working Group on Post-IDOE Studies of South-East Asian Tectonics and Resources
22. Second Session of the IODE Group of Experts on Marine Information Management
23. First Session of the IOC Group of Experts on Marine Geology and Geophysics in the Western Pacific
24. Second Session of the IOC-UN(OETB) Guiding Group of Experts on the Programme of Ocean Science in Relation to Non-Living Resources (**Also printed in French and Spanish**)
25. Third Session of the IOC Group of Experts on Effects of Pollutants
26. Eighth Session of the IOC-UNEP Group of Experts on Methods, Standards and Intercalibration
27. Eleventh Session of the Joint IOC-IHO Guiding Committee for the General Bathymetric Chart of the Oceans (**Also printed in French**)
28. Second Session of the IOC-FAO Guiding Group of Experts on the Programme of Ocean Science in Relation to Living Resources
29. First Session of the IOC-IAEA-UNEP Group of Experts on Standards and Reference Materials
30. First Session of the IOC-ARIBE Group of Experts on Recruitment in Tropical Coastal Demersal Communities (**Also printed in Spanish**)
31. Second IOC-WMO Meeting for Implementation of IGOSS XBT Ship-of-Opportunity Programmes
32. Thirteenth Session of the Joint CCOP-IOC Working Group on Post-IDOE Studies of East Asia Tectonics and Resources
33. Second Session of the IOC Task Team on the Global Sea-Level Observing System
34. Third Session of the IOC Editorial Board for the International Bathymetric Chart of the Mediterranean and Overlay Sheets
35. Fourth Session of the IOC-UNEP-IMO Group of Experts on Effects of Pollutants
36. First Consultative Meeting on RNODCs and Climate Data Services
37. Second Joint IOC-WMO Meeting of Experts on IGOSS-IODE Data Flow
38. Fourth Session of the Joint CCOP/SOPAC-IOC Working Group on South Pacific Tectonics and Resources
39. Fourth Session of the IODE Group of Experts on Technical Aspects of Data Exchange
40. Fourteenth Session of the Joint CCOP-IOC Working Group on Post-IDOE Studies of East Asian Tectonics and Resources
41. Third Session of the IOC Consultative Group on Ocean Mapping
42. Sixth Session of the Joint IOC-WMO-CCPS Working Group on the Investigations of 'El Niño' (**Also printed in Spanish**)
43. First Session of the IOC Editorial Board for the International Bathymetric Chart of the Western Indian Ocean
44. Third Session of the IOC-UN(OALOS) Guiding Group of Experts on the Programme of Ocean Science in Relation to Non-Living Resources
45. Ninth Session of the IOC-UNEP Group of Experts on Methods, Standards and Intercalibration
46. Second Session of the IOC Editorial Board for the International Bathymetric Chart of the Caribbean Sea and the Gulf of Mexico
47. First Session of the IOC Editorial Board for the International Bathymetric Chart of the Western Indian Ocean
48. Twelfth Session of the Joint IOC-IHO Guiding Committee for the General Bathymetric Chart of the Oceans
49. Fifteenth Session of the Joint CCOP-IOC Working Group on Post-IDOE Studies of East Asian Tectonics and Resources
50. Third Joint IOC-WMO Meeting for Implementation of IGOSS XBT Ship-of-Opportunity Programmes
51. First Session of the IOC Group of Experts on the Global Sea-Level Observing System
52. Fourth Session of the IOC Editorial Board for the International Bathymetric Chart of the Mediterranean
53. First Session of the IOC Editorial Board for the International Chart of the Central Eastern Atlantic (**Also printed in French**)
54. Third Session of the IOC Editorial Board for the International Bathymetric Chart of the Caribbean Sea and the Gulf of Mexico (**Also printed in Spanish**)
55. Fifth Session of the IOC-UNEP-IMO Group of Experts on Effects of Pollutants
56. Second Session of the IOC Editorial Board for the International Bathymetric Chart of the Western Indian Ocean
57. First Meeting of the IOC *ad hoc* Group of Experts on Ocean Mapping in the WESTPAC Area
58. Fourth Session of the IOC Consultative Group on Ocean Mapping

59. Second Session of the IOC-WMO/IGOSS Group of Experts on Operations and Technical Applications
60. Second Session of the IOC Group of Experts on the Global Sea-Level Observing System
61. UNEP-IOC-WMO Meeting of Experts on Long-Term Global Monitoring System of Coastal and Near-Shore Phenomena Related to Climate Change
62. Third Session of the IOC-FAO Group of Experts on the Programme of Ocean Science in Relation to Living Resources
63. Second Session of the IOC-IAEA-UNEP Group of Experts on Standards and Reference Materials
64. Joint Meeting of the Group of Experts on Pollutants and the Group of Experts on Methods, Standards and Intercalibration
65. First Meeting of the Working Group on Oceanographic Co-operation in the ROPME Sea Area
66. Fifth Session of the Editorial Board for the International Bathymetric and its Geological/Geophysical Series
67. Thirteenth Session of the IOC-IHO Joint Guiding Committee for the General Bathymetric Chart of the Oceans (**Also printed in French**)
68. International Meeting of Scientific and Technical Experts on Climate Change and Oceans
69. UNEP-IOC-WMO-IUCN Meeting of Experts on a Long-Term Global Monitoring System
70. Fourth Joint IOC-WMO Meeting for Implementation of IGOSS XBT Ship-of-Opportunity Programmes
71. ROPME-IOC Meeting of the Steering Committee on Oceanographic Co-operation in the ROPME Sea Area
72. Seventh Session of the Joint IOC-WMO-CPPS Working Group on the Investigations of 'El Niño' (**Spanish only**)
73. Fourth Session of the IOC Editorial Board for the International Bathymetric Chart of the Caribbean Sea and the Gulf of Mexico (**Also printed in Spanish**)
74. UNEP-IOC-ASPEI Global Task Team on the Implications of Climate Change on Coral Reefs
75. Third Session of the IODE Group of Experts on Marine Information Management
76. Fifth Session of the IODE Group of Experts on Technical Aspects of Data Exchange
77. ROPME-IOC Meeting of the Steering Committee for the Integrated Project Plan for the Coastal and Marine Environment of the ROPME Sea Area
78. Third Session of the IOC Group of Experts on the Global Sea-level Observing System
79. Third Session of the IOC-IAEA-UNEP Group of Experts on Standards and Reference Materials
80. Fourteenth Session of the Joint IOC-IHO Guiding Committee for the General Bathymetric Chart of the Oceans
81. Fifth Joint IOG-WMO Meeting for Implementation of IGOSS XBT Ship-of-Opportunity Programmes
82. Second Meeting of the UNEP-IOC-ASPEI Global Task Team on the Implications of climate Change on Coral Reefs
83. Seventh Session of the JSC Ocean Observing System Development Panel
84. Fourth Session of the IODE Group of Experts on Marine Information Management
85. Sixth Session of the IOC Editorial Board for the International Bathymetric chart of the Mediterranean and its Geological/Geophysical Series
86. Fourth Session of the Joint IOC-JGOFS Panel on Carbon Dioxide
87. First Session of the IOC Editorial Board for the International Bathymetric Chart of the Western Pacific
88. Eighth Session of the JSC Ocean Observing System Development Panel
89. Ninth Session of the JSC Ocean Observing System Development Panel
90. Sixth Session of the IODE Group of Experts on Technical Aspects of Data Exchange
91. First Session of the IOC-FAO Group of Experts on OSLR for the IOCINCWIO Region
92. Fifth Session of the Joint IOC-JGOFS CO₂ Advisory Panel Meeting
93. Tenth Session of the JSC Ocean Observing System Development Panel
94. First Session of the Joint CMM-IGOSS-IODE Sub-group on Ocean Satellites and Remote Sensing
95. Third Session of the IOC Editorial Board for the International Chart of the Western Indian Ocean
96. Fourth Session of the IOC Group of Experts on the Global Sea Level Observing System
97. Joint Meeting of GEMSI and GEEP Core Groups
98. First Session of the Joint Scientific and Technical Committee for Global Ocean Observing System
99. Second International Meeting of Scientific and Technical Experts on Climate Change and the Oceans
100. First Meeting of the Officers of the Editorial Board for the International Bathymetric Chart of the Western Pacific
101. Fifth Session of the IOC Editorial Board for the International Bathymetric Chart of the Caribbean Sea and the Gulf of Mexico
102. Second Session of the Joint Scientific and Technical Committee for Global Ocean Observing System
103. Fifteenth Session of the Joint IOC-IHO Committee for the General Bathymetric Chart of the Oceans
104. Fifth Session of the IOC Consultative Group on Ocean Mapping
105. Fifth Session of the IODE Group of Experts on Marine Information Management
106. IOC-NOAA *Ad hoc* Consultation on Marine Biodiversity
107. Sixth Joint IOC-WMO Meeting for Implementation of IGOSS XBT Ship-of-Opportunity Programmes
108. Third Session of the Health of the Oceans (HOTO) Panel of the Joint Scientific and Technical Committee for GLOSS
109. Second Session of the Strategy Subcommittee (SSC) of the IOC-WMO-UNEP Intergovernmental Committee for the Global Ocean Observing System
110. Third Session of the Joint Scientific and Technical Committee for Global Ocean Observing System
111. First Session of the Joint GCOS-GOOS-WCRP Ocean Observations Panel for Climate
112. Sixth Session of the Joint IOC-JGOFS CO₂ Advisory Panel Meeting
113. First Meeting of the IOC/WESTPAC Co-ordinating Committee for the North-East Asian Regional - Global Ocean Observing System (NEAR-GOOS)
114. Eighth Session of the Joint IOC-WMO-CPPS Working Group on the Investigations of "El Niño" (**Spanish only**)
116. Second Session of the IOC Editorial Board of the International Bathymetric Chart of the Central Eastern Atlantic (**Also printed in French**)
116. Tenth Session of the Off ices Committee for the Joint IOC-IHO General Bathymetric Chart of the Oceans (GEBCO), USA, 1996
117. IOC Group of Experts on the Global Sea Level Observing System (GLOSS), Fifth Session, USA, 1997
118. Joint Scientific Technical Committee for Global Ocean Observing System (J-GOOS), Fourth Session, USA, 1997
199. First Session of the Joint 100-WMO IGOSS Ship-of-Opportunity Programme Implementation Panel, South Africa, 1997
120. Report of Ocean Climate Time-Series Workshop, Joint GCOS-GOOS-WCRP Ocean Observations Panel for Climate, USA, 1997

121. IOC/WESTPAC Co-ordinating Committee for the North-East Asian Regional Global Ocean Observing System (NEAR-GOOS), Second Session, Thailand, 1997
122. First Session of the IOC-IUCN-NOAA *Ad hoc* Consultative Meeting on Large Marine Ecosystems (LME), France, 1997
123. Second Session of the Joint GCOS-GOOS-WCRP Ocean Observations Panel for Climate (OOPC), South Africa, 1997
124. Sixth Session of the IOC Editorial Board for the International Bathymetric Chart of the Caribbean Sea and the Gulf of Mexico, Colombia, 1996 (**also printed in Spanish**)
125. Seventh Session of the IODE Group of Experts on Technical Aspects of Data Exchange, Ireland, 1997
126. IOC-WMO-UNEP-ICSU Coastal Panel of the Global Ocean Observing System (GOOS), First Session, France, 1997
127. Second Session of the IOC-IUCN-NOAA Consultative Meeting on Large Marine Ecosystems (LME), France, 1998
128. Sixth Session of the IOC Consultative Group on Ocean Mapping (CGOM), Monaco, 1997
129. Sixth Session of the Tropical Atmosphere - Ocean Array (TAO) Implementation Panel, United Kingdom, 1997
130. First Session of the IOC-WMO-UNEP-ICSU Steering Committee of the Global Ocean Observing System (GOOS), France, 1998
131. Fourth Session of the Health of the Oceans (HOTO) Panel of the Global Ocean Observing System (GOOS), Singapore, 1997
132. Sixteenth Session of the Joint IOC-IHO Guiding Committee for the General Bathymetric Chart of the Oceans (GEBCO), United Kingdom, 1997
133. First Session of the IOC-WMO-UNEP-ICSU-FAO Living Marine Resources Panel of the Global Ocean Observing System (GOOS), France, 1998
134. Fourth Session of the IOC Editorial Board for the International Bathymetric Chart of the Western Indian Ocean (IOC/EB-IBCWIOW3), South Africa, 1997
135. Third Session of the Joint GCOS-GOOS-WCRP Ocean Observations Panel for Climate (OOPC), France, 1998
136. Seventh Session of the Joint IOC-JGOFS CO2 Advisory Panel Meeting, Germany, 1997
137. Implementation of Global Ocean Observations for GOOS/GCOS, First Session, Australia, 1998
138. Implementation of Global Ocean Observations for GOOS/GCOS, Second Session, France, 1998
139. Second Session of the IOC-WMO-UNEP-ICSU Coastal Panel of the Global Ocean Observing System (GOOS), Brazil, 1998
140. Third Session of IOC/WESTPAC Co-ordinating Committee for the North-East Asian Regional - Global Ocean Observing System (NEAR-GOOS), China, 1998
141. Ninth Session of the Joint IOC-WMO-CPPS Working Group on the Investigations of 'El Niño', Ecuador, 1998 (**Spanish only**)
142. Seventh Session of the IOC Editorial Board for the International Bathymetric Chart of the Mediterranean and its Geological/Geophysical Series, Croatia, 1998
143. Seventh Session of the Tropical Atmosphere-Ocean Array (TAO) Implementation Panel, Abidjan, Côte d'Ivoire, 1998
144. Sixth Session of the IODE Group of Experts on Marine Information Management (GEMIM), USA, 1999
145. Second Session of the IOC-WMO-UNEP-ICSU Steering Committee of the Global Ocean Observing System (GOOS), China, 1999
146. Third Session of the IOC-WMO-UNEP-ICSU Coastal Panel of the Global Ocean Observing System (GOOS), Ghana, 1999
147. Fourth Session of the GCOS-GOOS-WCRP Ocean Observations Panel for Climate (OOPC); Fourth Session of the WCRP CLIVAR Upper Ocean Panel (UOP); Special Joint Session of OOPC and UOP, USA, 1999
148. Second Session of the IOC-WMO-UNEP-ICSU-FAO Living Marine Resources Panel of the Global Ocean Observing System (GOOS), France, 1999
149. Eighth Session of the Joint IOC-JGOFS CO2 Advisory Panel Meeting, Japan, 1999
150. Fourth Session of the IOC/WESTPAC Co-ordinating Committee for the North-East Asian Regional – Global Ocean Observing System (NEAR-GOOS), Japan, 1999
151. Seventh Session of the IOC Consultative Group on Ocean Mapping (CGOM), Monaco, 1999
152. Sixth Session of the IOC Group of Experts on the Global Sea level Observing System (GLOSS), France, 1999
153. Seventeenth Session of the Joint IOC-IHO Guiding Committee for the General Bathymetric Chart of the Oceans (GEBCO), Canada, 1999
154. Comité Editorial de la COI para la Carta Batimétrica Internacional del Mar Caribe y el Golfo de Mexico (IBCCA), Septima Reunión, Mexico, 1998
IOC Editorial Board for the International Bathymetric Chart of the Caribbean Sea and the Gulf of Mexico (IBCCA), Seventh Session, Mexico, 1998
155. Initial Global Ocean Observing System (GOOS) Commitments Meeting, IOC-WMO-UNEP-ICSU/Impl-III/3, France, 1999
156. First Session of the *ad hoc* Advisory Group for IOCARIBE-GOOS, Venezuela, 1999 (**also printed in Spanish**)
157. Fourth Session of the IOC-WMO-UNEP-ICSU Coastal Panel of the Global Ocean Observing System (GOOS), China, 1999
158. Eighth Session of the IOC Editorial Board for the International Bathymetric Chart of the Mediterranean and its Geological/Geophysical Series, Russian Federation, 1999
159. Third Session of the IOC-WMO-UNEP-ICSU-FAO Living Marine Resources Panel of the Global Ocean Observing System (GOOS), Chile, 1999
160. Fourth Session of the IOC-WMO-UNEP-ICSU-FAO Living Marine Resources Panel of the Global Ocean Observing System (GOOS). Hawaii, 2000
161. Eighth Session of the IODE Group of Experts on Technical Aspects of Data Exchange, USA, 2000
162. Third Session of the IOC-IUCN-NOAA Consultative Meeting on Large Marine Ecosystems (LME), France, 2000
163. Fifth Session of the IOC-WMO-UNEP-ICSU Coastal Panel of the Global Ocean Observing System (GOOS), Poland, 2000
164. Second Session of the IOC-WMO-UNEP-ICSU Steering Committee of the Global Ocean Observing System (GOOS), France, 2000